Investigation of Brain Response in Canadian Armed Forces Volunteers Subjected to Recoil Force from Firing Long-Range Rifles Using Instrumented Mouthguards and Finite Element Head Model

by

Tanvi Seeburrun

A thesis

presented to the University of Waterloo

in fulfillment of the

thesis requirement for the degree of

Master of Applied Science

in

Mechanical and Mechatronics Engineering

Waterloo, Ontario, Canada, 2024

© Tanvi Seeburrun 2024

Author's Declaration

This thesis consists of material all of which I authored or co-authored: see Statement of Contributions included in the thesis. This is a true copy of the thesis, including any required final revisions, as accepted by my examiners.

I understand that my thesis may be made electronically available to the public.

Statement of Contributions

Some of the material in this thesis has been published in a journal article:

"Assessment of brain response in operators subject to recoil force from firing long-range rifles." Seeburrun Tanvi, Bustamante Michael C., Hartlen Devon C., Azar Austin, Ouellet Simon, Cronin Duane S. Frontiers in Bioengineering and Biotechnology, 2024 (Accepted).

DOI: 10.3389/fbioe.2024.1352387.

TS: Writing–original draft, Writing–review and editing, Formal Analysis, Investigation, Methodology, Visualization.

MB: Writing–review and editing, Mentoring, Validation.

DH: Methodology, Writing–review and editing, Software.

AA: Writing–review and editing, Data curation.

SO: Writing–review and editing, Conceptualization, Project administration, Resources.

DC: Supervision, Writing–review and editing, Conceptualization, Funding acquisition, Project administration, Resources.

All human volunteer experiments and measurements in this study were conducted by researchers at the Valcartier Research Centre, a division of Defense Research and Development Canada (DRDC), under the ethics approval granted by the DRDC Human Research Ethics Committee (HREC-2021-009).

Abstract

Mild traumatic brain injury (mTBI) may be caused by occupational hazards military personnel encounter, such as falls, shocks, exposure to blast overpressure events, and recoil from weapon firing. The repeated exposure of Canadian Armed Forces (CAF) members to sub-concussive events during the course of their service may lead to a significant reduction in quality of life. Symptoms may include headaches, difficulty concentrating, and noise sensitivity, impacting how personnel complete their duties and causing chronic health issues. CAF members have reported experiencing symptoms of mTBI, and some studies have associated these symptoms with repeated firing of long-range rifles. However, there is limited physical data on head response resulting from rifle recoil and different rifle configurations.

The objectives of this study were to quantify head kinematics for volunteers, assess the head response using kinematic-based metrics, and assess brain response using a detailed finite element head model. Measurements of head motion were recorded in a group of military volunteers using instrumented mouthguards while firing long-range rifles. The head kinematics were then used as inputs in a finite element head model to calculate the brain strains for each firing event and assessed using common response metrics and a Cumulative Strain Volume (CSV) measure to quantify brain deformation resulting from head acceleration.

The measured head kinematics and predicted brain deformation among CAF volunteers were lower than those associated with acute injury. The study highlighted the corpus callosum as the primary site of higher strains in the brain, consistent with previous research on head response to acceleration events. Brain deformation was primarily associated with angular velocity rather than linear acceleration. Comparative analysis between different rifle calibers revealed higher values of head kinematics associated with increased rifle caliber, owing to the higher level of energy. The CSV method identified statistically significant differences between rifle configurations and reductions in brain deformation with a recoil mitigation system (RMS), offering a potential solution to reduce long-term symptoms from firing long-range rifles. The results of this study offer important information about the magnitude of kinematics and strains that volunteers experience when firing long-range rifles.

Acknowledgments

I want to express my gratitude to my supervisor, Dr. Duane Cronin, for their unwavering support, for providing numerous opportunities for me to participate in conferences, and for helping me publish my research. I also want to thank my mentor, Mike Bustamante, for their continuous support, guidance, and patience with all my questions.

I would like to acknowledge the funding received from Defence Research and Development Canada, Valcartier Research Centre, the Natural Sciences and Engineering Research Council of Canada, Kapsul, and Voxel.AI. This research was made possible, in part, thanks to funding from the Canada Research Chairs Program.

I would like to acknowledge the Global Human Body Model Consortium for the use of the HBM, and the Digital Research Alliance of Canada for computational resources.

I would like to gratefully acknowledge the volunteers who participated in this study.

A big thank you to all the members of the IMMC lab for being an amazing team.

Finally, I would like to express my heartfelt gratitude to my family for their continued support and encouragement throughout this journey. I am especially grateful to my dad, whose guidance, wisdom, and belief in me have been a constant source of strength. Thank you, Dad, for always being my greatest supporter and inspiration.

Table of Contents

Author's Declaration ii

Statement of Contributions iii

Abstract iv

Acknowledgments v

List of Figures ix

List of Tables xvi

1 Introduction 1

1.1 Motivation for research 1

1.2 Approach 3

2 Background 5

2.1 Anatomy 6

2.1.1 Anatomic Planes and Co-ordinate System 6

2.1.2 Head Anatomy 8

2.2 Types of Head Injuries 14

2.3 Injury Mechanisms 16

2.4 Experimental Data Related to Head Response 19

2.4.1 Nahum et al.'s Linear Impact Experiment 20

2.4.2 Hardy et al.'s NDT Experiment 20

2.4.3 Alshareef et al.'s Sonomicrometry Experiment 21

2.5 Impact Sensing Devices 21

2.6 Head Injury Metrics 27

2.6.1 Kinematic-Based Injury Metrics 28

2.6.2 FE Models 37

2.6.3 Tissue-Based Metrics 42

2.6.4 Boundary Condition for Isolated Head Model 48

2.7 Subconcussive Head Exposures 50

2.7.1 Subconcussive Head Exposures in Sports 50

2.7.2 Subconcussive Head Exposures in Military 51

3 Methods 53

3.1 Experimental Data Collection 55

3.1.1 Datasets Overview 55

3.1.2 Experimental Set Up 56

3.1.3 Mouthguard Data Collection 58
3.2 Post-processing 59
3.2.1 Post-Processing for "Good Captures" 59
3.2.2 Post-Processing for "Late Captures" 63
3.3 Head Model Set Up 63
3.4 Metrics for Brain Response Comparison 65
3.5 Comparison of Metrics 69
4 Results 72
4.1 Comparison of Head Kinematics Between Different Rifles and Volunteers 72
4.1.1 Head Kinematic Results for Dataset 1: May 2021 72
4.1.2 Head Kinematic Results for Dataset 2: May 2022 75
4.1.3 Summary of Head Kinematic Results from Datasets 1 and 2 78
4.2 Kinematic-based Metric Results 79
4.2.1 Comparison of HIC_{15} Between Different Rifles and Volunteers 79
4.2.2 Summary of HIC_{15} Results from Datasets 1 and 2 87
4.2.3 Comparison of BrIC Between Different Rifles and Volunteers 89
4.2.4 Summary of BrIC Results from Datasets 1 and 2 97
4.3 Strain-based Metrics Results 99
4.3.1 Comparison of MPS_{95} Between Different Rifles and Volunteers 99
4.3.2 Summary of MPS_{95} Results from Datasets 1 and 2 108
4.3.3 Comparison of CSV Curves of the Whole Brain Between Different Rifles and Volunteers 110
4.3.4 Summary of CSV Results for the Whole Brain from Datasets 1 and 2 119
4.3.5 Comparison of CSV Curves of Eight Brain Regions Between Different Rifles and Volunteers 120
4.3.6 Summary of CSV Results for the Eight Brain Regions from Datasets 1 and 2 131
4.4 Rotational vs Linear Head Motion Results 131
4.4.1 Study 1: Linear Acceleration vs Angular Velocity 132
4.4.2 Study 2: Directional Dependence 136
5 Discussion 140
5.1 Head Kinematics Resulting from Rifle Discharge 141
5.2 Kinematic-Based Injury Metrics 143
5.3 Strain-Based Metrics for Whole Brain Response 145
5.4 Strain-Based Response of Individual Brain Regions 148

5.5 Linear Acceleration vs Angular Velocity Contribution to Brain Response 149
5.6 Limitations 150
6 Conclusion **152**
Letters of Copyright Permission **156**
References **188**
Appendix **206**
Appendix A: Head Kinematics 206
Appendix B: HIC_{15} 213
Appendix C: BrIC 230
Appendix D: MPS_{95} 247
Appendix E: A_{CSV} 265
Appendix F: Individual Brain Regions 283

List of Figures

Figure 1: Anatomical planes and directions for the human body. Adapted from Anatomical Planes by CFCF, 2014, Wikimedia Commons (https://commons.wikimedia.org/wiki/File:Anatomical_Planes.svg). CC BY-SA 3.0. 7

Figure 2: The SAE coordinate system used in the GHBMC model. 8

Figure 3: The adult skull consisting of (i) the neurocranium and (ii) the viscerocranium. (i) The neurocranium is adapted from Cranial bones by Edoarado, 2014, Wikimedia Commons (https://commons.wikimedia.org/wiki/File:Cranial_bones_en_v2.svg). CC0 1.0 Universal Public Domain Dedication. (ii) The viscerocranium is adapted from Facial skeleton by Own Work, 2015, Wikimedia Commons (https://commons.wikimedia.org/wiki/File:Facial_skeleton_-_en.svg). CC0 1.0 Universal Public Domain Dedication. 9

Figure 4A: The cranial meninges from Meninges by Mysid, n.d., Wikimedia Commons (https://commons.wikimedia.org/wiki/File:Meninges-en.svg). CC BY-SA 3.0……10

Figure 4B: The Circle of Wilis from Circle of WillisN by OpenStax, 2016, Wikimedia Commons (https://commons.wikimedia.org/wiki/File:1314_Circle_of_WillisN.jpg). CC BY 4.0. 11

Figure 5: The cerebrum, cerebellum, midbrain, pons, and medulla oblongata from Trauma Biomechanics (p. 88), by K. Schmitt, P.F. Niederer, D.S. Cronin, B. Morrison III, M.H. Muser, F. Walz, 2019, Springer Cham. Copyright 2019 by Springer Nature Switzerland AG 2019. Reprinted with permission. 12

Figure 6: Gyrus vs sulcus from Gyrus sulcus by Albert Kok, 2007, Wikimedia Commons (https://commons.wikimedia.org/wiki/File:Gyrus_sulcus.png). CC0 1.0 Universal Public Domain Dedication. 12

Figure 7: The Falx Cerebri and Tentorium Cerebelli from Basic Finite Element Method as Applied to Injury Biomechanics (p. 475), by H. Mao, n.d., Mara E. Conner. Copyright 2018 by Elsevier Inc. Reprinted with permission. 13

Figure 8: Description from Goodwin - Drawing Coronal and sagittal section of the brain - English labels by Cindy Seiwert and Goodwin University, n.d., ANATOMYTOOL (https://anatomytool.org/content/goodwin-drawing-coronal-and-sagittal-section-brain-english-labels). CC BY-NC-SA. 14

Figure 9: Types of head injuries adapted from Trauma Biomechanics (p. 89), by K. Schmitt, P.F. Niederer, D.S. Cronin, B. Morrison III, M.H. Muser, F. Walz, n.d., Springer Cham. Copyright 2019 by Springer Nature Switzerland AG 2019. Adapted with permission. 14

Figure 10: The Wayne State tolerance curve from Basic Finite Element Method as Applied to Injury Biomechanics (p. 480), by H. Mao, n.d., Mara E. Conner. Copyright 2018 by Elsevier Inc. Reprinted with permission. 18

Figure 11: The (i) Stanford's customized mouthguard, (ii) Stanford's boil-and-bite mouthguard, (iii) Prevent Biometrics' customized mouthguard, (iv) Prevent Biometrics' boil-and-bite mouthguard, and (v) Sports & Wellbeing Analytics' customized mouthguard. Adapted from "Validation and Comparison of Instrumented Mouthguards for Measuring Head Kinematics and Assessing Brain Deformation in Football Impacts" by Liu, Y., Domel, A.G., Yousefsani, S.A. et al.,2020, Ann Biomed Eng., Volume 48, pages 2580–2598 (https://doi.org/10.1007/s10439-020-02629-3). Copyright 2020 by Biomedical Engineering Society. Adapted with permission. 26

Figure 12: (i) The GHBMC M50 full human body model and (ii) the GHBMC M50 head and neck model. 40

Figure 13: The isolated GHBMC M50 head model (without neck region)..... 41

Figure 14: (a) The volunteer fired the long-range rifle. (b) Head kinematics data, including linear acceleration and angular velocity, were collected using instrumented mouthguards. (c) The head kinematics were then used as inputs to an isolated GHBMC 50^{th} percentile head model. (c) Strains were extracted from the head model to quantify brain deformation. 54

Figure 15: Overview of datasets collected during experimental trials at DRDC 56

Figure 16: Volunteer in prone position..... 57

Figure 17: The data is collected in the (a) mouthguard coordinate system and transformed to the (b) SAE J211 coordinate system 60

Figure 18: Head kinematics data transformed from mouthguard to head CoG 63

Figure 19: Mid-sectioned view of the isolated GHBMC 50^{th} percentile male head model..... 64

Figure 20: The 8 regions (referred to as the whole brain when grouped together) in the GHBMC 50^{th} percentile male head model..... 65

Figure 21: The process to generate the cumulative-strain curve. Note that in this exemplar case, we are assuming that the region consists of 5 elements with Element ID 1 to 5. (a) First, the maximum principal strain (MPS_1 to MPS_5) and initial volume (VOL_1 to VOL_5) of every element in the specified region are extracted. (b) The volume fraction for each element (VF_1 to VF_5) within the region is computed. (c) The elements are then arranged in ascending order based on their MPS values. (d) The percentage volume is calculated by subtracting the volume fraction of each element from that of the volume of the region in the preceding row, starting with 100% as the initial volume. 67

Figure 22: An exemplar CSV curve with Maximum Principal Strain (MPS) on the x-axis and Cumulative % Volume of a region on the y-axis. (a) As an example, the CSV curve can be interpreted as 40% of the region's volume experiencing an MPS of at least 0.035. (b) The curve decreases as less and less of the region's volume experiences high strains..... 68

Figure 23: The area under a CSV curve referred to as A_{CSV} 69

Figure 24: The head kinematics for Volunteer 1 (from Dataset 1: May 2021), including (i) linear acceleration in X, (ii) linear acceleration in Y, (iii) linear acceleration in Z, (iv) angular velocity in X, (v) angular velocity in Y and (vi) angular velocity in Z for all the shots fired using Rifles A, B, and C. Note that the designation in brackets represents the features of each rifle; for example Rifle A (X .50) indicates that Rifle A has Chassis X and is a .50 caliber rifle. 73

Figure 25: The head kinematics of Volunteers 1, 2, and 3 (from Dataset 1: May 2021) firing Rifle C, including (i) linear acceleration in X, (ii) linear acceleration in Y, (iii) linear acceleration in Z, (iv) angular velocity in X, (v) angular velocity in Y and (vi) angular velocity in Z. 74

Figure 26: The head kinematics for Volunteer 8 (from Dataset 2: May 2022), including (i) linear acceleration in X, (ii) linear acceleration in Y, (iii) linear acceleration in Z, (iv) angular velocity in X, (v) angular velocity in Y and (vi) angular velocity in Z for all the shots fired using Rifles D and E. Note that the designation in brackets represents the features of each rifle; for example Rifle D (.338) indicates that Rifle D is a .338 caliber rifle. 75

Figure 27: The head kinematics for Volunteer 4 (from Dataset 2: May 2022), including (i) linear acceleration in X, (ii) linear acceleration in Y, (iii) linear acceleration in Z, (iv) angular velocity in X, (v) angular velocity in Y and (vi) angular velocity in Z for all the shots fired using Rifles D and E. Note that the designation in brackets represents the features of each rifle; for example Rifle D (.338) indicates that Rifle D is .338 caliber rifle. 76

Figure 28: The (i) X, (ii) Y, (iii) Z angular velocity signals of all volunteers from Dataset 2 firing Rifle D. The (iv) X, (v) Y, (vi) Z angular velocity signals of all volunteers from Dataset 2 firing Rifle E. 77

Figure 29: Mean HIC_{15} and variation of the three rifles for (i) Volunteer 1, (ii) Volunteer 2, and (iii) Volunteer 3 (Dataset 1: May 2021). * = statistically significant difference detected between rifles. CV = coefficient of variation. Number of shots for Volunteer 1 (Rifles A:4, B:4, C:4), Volunteer 2 (Rifles A:2, B:4, C:4) and Volunteer 3 (Rifles A:3, B:3, C:3). 81

Figure 30: Mean HIC_{15} and variation of the three volunteers for (i) Rifle A, (ii) Rifle B, and (iii) Rifle C (Dataset 1: May 2021). CV = coefficient of variation. Number of shots for Volunteer 1 (Rifles A:4, B:4, C:4), Volunteer 2 (Rifles A:2, B:4, C:4) and Volunteer 3 (Rifles A:3, B:3, C:3). 83

Figure 31: Mean HIC_{15} and variation of the two rifles for (i) Volunteer 4, (ii) Volunteer 5, (iii) Volunteer 6, (iv) Volunteer 7, (v) Volunteer 8 (Dataset 2: May 2022). *= statistically significant difference detected between rifles. CV = coefficient of variation. Number of shots for Volunteer 4 (Rifles D:36, E:11), Volunteer 5 (Rifles D:2, E:15), Volunteer 6 (Rifles D:33, E:6), Volunteer 7 (Rifles D:8, E:18) and Volunteer 8 (Rifles D:5, E:10). 85

Figure 32: Mean HIC_{15} and variation of the five volunteers for (i) Rifle D and (ii) Rifle E (Dataset 2: May 2022). Number of shots for Volunteer 1 (Rifles A:4, B:4, C:4), Volunteer 2 (Rifles A:2, B:4, C:4) and Volunteer 3 (Rifles A:3, B:3, C:3). 86

Figure 33: Mean BrIC and variation of the three rifles for (i) Volunteer 1, (ii) Volunteer 2, and (iii) Volunteer 3 (Dataset 1: May 2021). * = statistically significant difference detected between rifles. CV = coefficient of variation. Number of shots for Volunteer 1 (Rifle s A:4, B:4, C:4), Volunteer 2 (Rifles A:2, B:4, C:4) and Volunteer 3 (Rifles A:3, B:3, C:3). 90

Figure 34: Mean BrIC and variation of the three volunteers for (i) Rifle A, (ii) Rifle B, and (iii) Rifle C (Dataset 1: May 2021). *= statistically significant difference detected between volunteers. CV=coefficient of variation. Number of shots for Volunteer 1 (Rifle s A:4, B:4, C:4), Volunteer 2 (Rifles A:2, B:4, C:4) and Volunteer 3 (Rifles A:3, B:3, C:3). 92

Figure 35: Mean BrIC and variation of the two rifles for (i) Volunteer 4, (ii) Volunteer 5, (iii) Volunteer 6, (iv) Volunteer 7, (v) Volunteer 8 (Dataset 2: May 2022). *= statistically significant difference detected between rifles. CV = coefficient of variation. Number of shots for Volunteer 4 (Rifles D:36, E:11), Volunteer 5 (Rifles D:2, E:15), Volunteer 6 (Rifles D:33, E:6), Volunteer 7 (Rifles D:8, E:18) and Volunteer 8(Rifles D:5, E:10). 94

Figure 36: Mean BrIC and variation of the five volunteers for (i) Rifle D and (ii) Rifle E (Dataset 2: May 2022). *= statistically significant difference detected between rifles. CV = coefficient of variation. Number of shots for Volunteer 1 (Rifles A:4, B:4, C:4), Volunteer 2 (Rifles A:2, B:4, C:4) and Volunteer 3 (Rifles A:3, B:3, C:3). 96

Figure 37: Mean MPS_{95} and variation of the three rifles for (i) Volunteer 1, (ii) Volunteer 2, and (iii) Volunteer 3 (Dataset 1: May 2021). * = statistically significant difference detected between rifles. CV = coefficient of variation. Number of shots for Volunteer 1 (Rifles A:4, B:4, C:4), Volunteer 2 (Rifles A:2, B:4, C:4) and Volunteer 3 (Rifles A:3, B:3, C:3). 101

Figure 38: Mean MPS_{95} and variation of the three volunteers for (i) Rifle A, (ii) Rifle B, and (iii) Rifle C (Dataset 1: May 2021). * = statistically significant difference detected between volunteers. CV = coefficient of variation. Number of shots for Volunteer 1 (Rifles A:4, B:4, C:4), Volunteer 2 (Rifles A:2, B:4, C:4) and Volunteer 3 (Rifles A:3, B:3, C:3). 103

Figure 39: Mean MPS_{95} and variation of the two rifles for (i) Volunteer 4, (ii) Volunteer 5, (iii) Volunteer 6, (iv) Volunteer 7, (v) Volunteer 8 (Dataset 2: May 2022). *= statistically significant difference detected between rifles. CV=coefficient of variation. Number of shots for Volunteer 4 (Rifles D:36, E:11), Volunteer 5 (Rifles D:2, E:15), Volunteer 6 (Rifles D:33, E:6), Volunteer 7 (Rifles D:8, E:18) and Volunteer 8 (Rifles D:5, E:10). 105

Figure 40: Mean MPS_{95} and variation of the five volunteers for (i) Rifle D and (ii) Rifle E (Dataset 2: May 2022). *= statistically significant difference detected between rifles. CV=coefficient of variation. Number of shots for Volunteer 1 (Rifles A:4, B:4, C:4), Volunteer 2 (Rifles A:2, B:4, C:4) and Volunteer 3 (Rifles A:3, B:3, C:3). 107

Figure 41: Cumulative strain-volume curves, mean A_{CSV} and variation of the three rifles for (i,iv) Volunteer 1, (ii,v) Volunteer 2, (iii,vi) Volunteer 3 (Dataset 1: May 2021). * = statistically significant difference detected between rifles. CV = coefficient of variation. Number of shots for

Volunteer 1 (Rifles A:4, B:4, C:4), Volunteer 2 (Rifles A:2, B:4, C:4) and Volunteer 3 (Rifles A:3, B:3, C:3). 111

Figure 42: Cumulative strain-volume curves, mean A_{CSV} and variation for each shot across the three volunteers for (i,iv) Rifle A, (ii,v) Rifle B, (iii,vi) Rifle C (Dataset 1: May 2021). * = statistically significant difference detected between volunteers. CV = coefficient of variation. Number of shots for Volunteer 1 (Rifles A:4, B:4, C:4), Volunteer 2 (Rifles A:2, B:4, C:4) and Volunteer 3 (Rifles A:3, B:3, C:3). 113

Figure 43: Cumulative strain-volume curves for each shot across the two rifles for (i) Volunteer 4, (ii) Volunteer 5, (iii) Volunteer 6, (iv) Volunteer 7, (v) Volunteer 8 (Dataset 2: May 2022). *= statistically significant difference detected between rifles. CV=coefficient of variation. Number of shots for Volunteer 4 (Rifles D:36, E:11), Volunteer 5 (Rifles D:2, E:15), Volunteer 6 (Rifles D:33, E:6), Volunteer 7 (Rifles D:8, E:18) and Volunteer 8(Rifles D:5, E:10). 115

Figure 44: Mean A_{CSV} and variation across the two rifles for (i) Volunteer 4, (ii) Volunteer 5, (iii) Volunteer 6, (iv) Volunteer 7, (v) Volunteer 8 (Dataset 2: May 2022). *= statistically significant difference detected between rifles. CV=coefficient of variation. Number of shots for Volunteer 4 (Rifles D:36, E:11), Volunteer 5 (Rifles D:2, E:15), Volunteer 6 (Rifles D:33, E:6), Volunteer 7 (Rifles D:8, E:18) and Volunteer 8(Rifles D:5, E:10). 116

Figure 45: Cumulative strain-volume curves, mean A_{CSV} and variation for each shot across all volunteers for (i,iii) Rifle D and (ii,iv) Rifle E (Dataset 2: May 2022). *= statistically significant difference detected between rifles. CV=coefficient of variation. Number of shots for Volunteer 1 (Rifles A:4, B:4, C:4), Volunteer 2 (Rifles A:2, B:4, C:4) and Volunteer 3 (Rifles A:3, B:3, C:3). 118

Figure 46: Mean A_{CSV} of the eight brain regions for (i) Volunteer 1, (ii) Volunteer 2, and (iii) Volunteer 3 (Dataset 1: May 2021), arranged in descending order of A_{CSV} 122

Figure 47: Mean A_{CSV} of the eight brain regions for (i) Rifle A, (ii) Rifle B, and (iii) Rifle C (Dataset 1: May 2021), arranged in descending order of A_{CSV} 124

Figure 48: Mean A_{CSV} and variation across the two rifles for (i) Volunteer 4, (ii) Volunteer 5, (iii) Volunteer 6 (Dataset 2: May 2022). *= statistically significant difference detected between rifles. CV=coefficient of variation. Number of shots for Volunteer 4 (Rifles D:36, E:11), Volunteer 5 (Rifles D:2, E:15), Volunteer 6 (Rifles D:33, E:6), Volunteer 7 (Rifles D:8, E:18) and Volunteer 8(Rifles D:5, E:10). 127

Figure 49: Mean A_{CSV} of the eight brain regions for (i) Volunteer 7, (ii) Volunteer 8 (Dataset 2: May 2022), arranged in descending order of A_{CSV} 128

Figure 50: Mean A_{CSV} of the eight brain regions for (i) Rifle D and (ii) Rifle E, arranged in descending order of A_{CSV} 130

Figure 51: Cumulative strain-volume curves for one shot across the three rifles in Dataset 1 for (i,ii,iii) Volunteer 1, (iv,v,vi) Volunteer 2 and (vii,viii,ix) Volunteer 3 showing the difference

between angular velocity only inputs, linear acceleration only inputs and 6 DOF inputs to the head model 133

Figure 52: Cumulative strain-volume curves for one shot across the two rifles in Dataset 2 for (i,ii) Volunteer 4, (iii,iv) Volunteer 7 and (v,vi) Volunteer 8 showing the difference between angular velocity only inputs, linear acceleration only inputs and 6 DOF inputs to the head model 135

Figure 53: Cumulative strain-volume curves for one shot across the three rifles in Dataset 1 for (i,ii,iii) Volunteer 1, (iv,v,vi) Volunteer 2 and (vii,viii,ix) Volunteer 3 showing the difference between separate angular velocity and linear acceleration inputs to the head model 137

Figure 54: Cumulative strain-volume curves for one shot across the two rifles in Dataset 2 for (i,ii) Volunteer 4, (iii,iv) Volunteer 7 and (v,vi) Volunteer 8 showing the difference between separate angular velocity and linear acceleration inputs to the head model..... 139

Appendix Figure 55: The head kinematics for Volunteer 2 (from Dataset 1: May 2021), including (i) linear acceleration in X, (ii) linear acceleration in Y, (iii) linear acceleration in Z, (iv) angular velocity in X, (v) angular velocity in Y and (vi) angular velocity in Z for all the shots fired using Rifles A, B and C. Note that the designation in brackets represents the features of each Rifle; for example, Rifle A (X .50) indicates that Rifle A has Chassis X and is a 50 caliber rifle. 206

Appendix Figure 56: The head kinematics for Volunteer 3 (from Dataset 1: May 2021), including (i) linear acceleration in X, (ii) linear acceleration in Y, (iii) linear acceleration in Z, (iv) angular velocity in X, (v) angular velocity in Y and (vi) angular velocity in Z for all the shots fired using Rifles A, B and C. Note that the designation in brackets represents the features of each rifle; for example Rifle A (X .50) indicates that Rifle A has Chassis X and is a 50 caliber rifle. 207

Appendix Figure 57: The head kinematics of Volunteers 1,2 and 3 (from Dataset 1: May 2021) firing Rifle A**,** including (i) linear acceleration in X, (ii) linear acceleration in Y, (iii) linear acceleration in Z, (iv) angular velocity in X, (v) angular velocity in Y and (vi) angular velocity in Z. 208

Appendix Figure 58: The head kinematics of Volunteers 1,2 and 3 (from Dataset 1: May 2021) firing Rifle B, including (i) linear acceleration in X, (ii) linear acceleration in Y, (iii) linear acceleration in Z, (iv) angular velocity in X, (v) angular velocity in Y and (vi) angular velocity in Z. 209

Appendix Figure 59: The head kinematics for Volunteer 5 (from Dataset 2: May 2022), including (i) linear acceleration in X, (ii) linear acceleration in Y, (iii) linear acceleration in Z, (iv) angular velocity in X, (v) angular velocity in Y and (vi) angular velocity in Z for all the shots fired using Rifles D and E. Note that the designation in brackets represents the features of each rifle; for example Rifle A (.338) indicates that Rifle D 338 caliber rifle. 210

Appendix Figure 60: The head kinematics for Volunteer 6 (from Dataset 2: May 2022), including (i) linear acceleration in X, (ii) linear acceleration in Y, (iii) linear acceleration in Z, (iv) angular

velocity in X, (v) angular velocity in Y and (vi) angular velocity in Z for all the shots fired using Rifles D, and E. Note that the designation in brackets represents the features of each rifle; for example Rifle A (.338) indicates that Rifle D 338 caliber rifle. 211

Appendix Figure 61: The head kinematics for Volunteer 7 (from Dataset 2: May 2022), including (i) linear acceleration in X, (ii) linear acceleration in Y, (iii) linear acceleration in Z, (iv) angular velocity in X, (v) angular velocity in Y and (vi) angular velocity in Z for all the shots fired using Rifles D and E. Note that the designation in brackets represents the features of each rifle; for example Rifle A (.338) indicates that Rifle D 338 caliber rifle. 212

Appendix Figure 62: Example of CSV file after data processing for one shot by Volunteer 1. The signal has 800 data points, i.e., data is recorded every 0.000625 s. 213

Appendix Figure 63: Example of the resultant linear acceleration plot for one shot of Volunteer 1 213

Appendix Figure 64: Example of calculating the area for every 15 ms interval 214

Appendix Figure 65: Script used to calculate HIC_{15} for each shot 215

List of Tables

Table 1: AIS scale for head injury recreated from [29], [39] 15
Table 2: Examples of Kinematic Metric Thresholds 36
Table 3: List of brain tissues 42
Table 4: Brain tissue material properties [26] 42
Table 5: MPS values from literature 45
Table 6: Weapon platforms and number of shots per volunteer in Dataset 1: May 2021. 57
Table 7: Weapon platforms and number of shots per volunteer in Dataset 2: May 2022. 58
Table 8: Summary of HIC_{15} results from Dataset 1 87
Table 9: Summary of HIC_{15} results from Dataset 2 88
Table 10: Summary of BrIC Results from Dataset 1 97
Table 11: Summary of BrIC Results from Dataset 2 98
Table 12: Summary of MPS_{95} Results from Dataset 1 108
Table 13: Summary of MPS_{95} Results from Dataset 2 109
Table 14: Percentage difference between Rifles A and B and A and C for each brain region in descending order. A more detailed table can be found in Appendix F. 123
Table 15: A_{CSV} values for linear acceleration only and angular velocity only curves 134
Table 16: A_{CSV} values for the separate angular velocity input signal 138
Table 17: Summary of HIC_{15} values in Dataset 1: Volunteers 1,2,3 firing Rifles, A, B, and C 216
Table 18: Summary of HIC_{15} values in Dataset 1: Volunteers 1,2,3 firing Rifles, A, B, and C 217
Table 19: Summary of HIC_{15} values in Dataset 2: Volunteers 4,5 firing Rifles D, E 218
Table 20: Summary of HIC_{15} values in Dataset 2: Volunteer 6 firing Rifles D, E 219
Table 21: Summary of HIC_{15} values in Dataset 2: Volunteers 7,8 firing Rifles D, E 220
Table 22: Summary of HIC_{15} values in Dataset 2: Volunteers 4,5,6,7 and 8 firing Rifle D 220
Table 23: Summary of HIC_{15} values in Dataset 2: Volunteers 4,5,6,7 and 8 firing Rifle E 221
Table 24: One-Way ANOVA for Volunteer 1 222
Table 25: One-Way ANOVA for Volunteer 2 223
Table 26: One-Way ANOVA for Volunteer 3 224
Table 27: One-Way ANOVA for Rifle A 225
Table 28: One-Way ANOVA for Rifle B 225

Table 29: One-Way ANOVA for Rifle C 227
Table 30: t-Test for Volunteer 4 227
Table 31: t-Test for Volunteer 5 227
Table 32: t-Test for Volunteer 6 228
Table 33: t-Test for Volunteer 7 228
Table 34: t-Test for Volunteer 8 229
Table 35: Summary of BrIC values in Dataset 1: Volunteers 1,2,3 firing Rifles A, B, and C 230
Table 36: Summary of BrIC values in Dataset 1: Volunteers 1,2,3 firing Rifles A, B, and C 230
Table 37: Summary of BrIC values in Dataset 2: Volunteers 4,5 firing Rifles D and E 231
Table 38: Summary of BrIC values in Dataset 2: Volunteer 6 firing Rifles D and E 232
Table 39: Summary of BrIC values in Dataset 2: Volunteers 7,8 firing Rifles D and E 233
Table 40: Summary of BrIC values in Dataset 2: Volunteers 4,5,6,7 and 8 firing Rifle D 234
Table 41: Summary of BrIC values in Dataset 2: Volunteers 4,5,6,7 and 8 firing Rifle E 235
Table 42: One-Way ANOVA for Volunteer 1 235
Table 43: One-Way ANOVA for Volunteer 2 236
Table 44: One-Way ANOVA for Volunteer 3 237
Table 45: One-Way ANOVA for Rifle A 238
Table 46: One-Way ANOVA for Rifle B 240
Table 47: One-Way ANOVA for Rifle C 241
Table 48: t-Test for Volunteer 4 242
Table 49: t-Test for Volunteer 5 243
Table 50: t-Test for Volunteer 6 243
Table 51: t-Test for Volunteer 7 243
Table 52: t-Test for Volunteer 8 244
Table 53: One-Way ANOVA for Rifle D 244
Table 54: One-Way ANOVA for Rifle E 245
Table 55: Summary of MPS_{95} values in Dataset 1: Volunteers 1,2,3 firing Rifles A, B, and C 247
Table 56: Summary of MPS_{95} values in Dataset 1: Volunteers 1,2,3 firing Rifles A, B, and C 247
Table 57: Summary of MPS_{95} values in Dataset 2: Volunteers 4,5 firing Rifles D and E 248
Table 58: Summary of MPS_{95} values in Dataset 2: Volunteers 6 firing Rifles D and E 249

Table 59: Summary of MPS_{95} values in Dataset 2: Volunteers 7,8 firing Rifles D and E 250
Table 60: Summary of MPS_{95} values in Dataset 2: Volunteers 4,5,6,7 and 8 firing Rifle D 251
Table 61: Summary of MPS_{95} values in Dataset 2: Volunteers 4,5,6,7 and 8 firing Rifle E 252
Table 62: One-Way ANOVA for Volunteer 1 252
Table 63: One-Way ANOVA for Volunteer 2 254
Table 64: One-Way ANOVA for Volunteer 3 255
Table 65: One-Way ANOVA for Rifle A 255
Table 66: One-Way ANOVA for Rifle B 256
Table 67: One-Way ANOVA for Rifle C 258
Table 68: t-Test for Volunteer 5 259
Table 69: t-Test for Volunteer 6 260
Table 70: t-Test for Volunteer 7 260
Table 71: t-Test for Volunteer 8 260
Table 72: One-Way ANOVA for Rifle D 261
Table 73: One-Way ANOVA for Rifle E 262
Table 74: Summary of area under cumulative strain-volume curves (A_{CSV}) values in Dataset 1: Volunteers 1,2,3 firing Rifles A, B, and C 265
Table 75: Summary of area under cumulative strain-volume curves (A_{CSV}) values in Dataset 1: Volunteers 1,2,3 firing Rifles A, B, and C 265
Table 76: Summary of area under cumulative strain-volume curves (A_{CSV}) values in Dataset 2: Volunteers 4,5 firing Rifles D and E 266
Table 77: Summary of area under cumulative strain-volume curves (A_{CSV}) values in Dataset 2: Volunteers 6 firing Rifles D and E 267
Table 78: Summary of area under cumulative strain-volume curves (A_{CSV}) values in Dataset 2: Volunteers 7,8 firing Rifles D and E 268
Table 79: Summary of MPS_{95} values in Dataset 2: Volunteers 4,5,6,7 and 8 firing Rifle D 269
Table 80: Summary of MPS_{95} values in Dataset 2: Volunteers 4,5,6,7 and 8 firing Rifle E 270
Table 81: One-Way ANOVA for Volunteer 1 270
Table 82: One-Way ANOVA for Volunteer 2 272
Table 83: One-Way ANOVA for Volunteer 3 273
Table 84: One-Way ANOVA for Rifle A 273

Table 85: One-Way ANOVA for Rifle B 275
Table 86: One-Way ANOVA for Rifle C 276
Table 87: t-Test for Volunteer 4 277
Table 88: t-Test for Volunteer 5 278
Table 89: t-Test for Volunteer 6 278
Table 90: t-Test for Volunteer 7 278
Table 91: t-Test for Volunteer 8 279
Table 92: One-Way ANOVA for Rifle D 279
Table 93: One-Way ANOVA for Rifle E 281
Table 94: Mean A_{CSV} of each individual brain region when Volunteers 1,2 and 3 fired Rifle A, B and C 283
Table 95: Mean A_{CSV} of each individual brain region when Volunteers 1,2 and 3 fired Rifle A, B and C 284
Table 96: Mean A_{CSV} of each individual brain region when Volunteers 4,5,6,7 and 8 fired Rifle D and E 285
Table 97: Mean A_{CSV} of each individual brain region when Volunteers 4,5,6,7 and 8 fired Rifle D and E 286

1 Introduction

1.1 Motivation for research

Traumatic brain injury (TBI) encompasses a variety of brain injuries caused by external forces, leading to disrupted brain function [1]. These forces can lead to varying degrees of damage, affecting different brain regions. Damage can be either focal, affecting a single region, or diffuse, affecting multiple regions. TBI can be categorized as penetrating or non-penetrating [2], [3]. Penetrating TBI, also called open TBI, occurs when a foreign object (e.g., projectile or bone fragment) passes through the skull and damages the brain tissue. Non-penetrating TBI, also known as closed or blunt TBI, can occur as a result of a direct or an indirect impact to the head, causing the brain to deform and generating damage in the tissue, which in turn affects brain function.

Mild traumatic brain injury (mTBI), often termed “concussion,” falls under the category of non-penetrating TBIs and can occur due to various incidents such as falls, motor vehicle accidents, sports-related activities (e.g., football, boxing, hockey), violence, and military engagements and training [2]. Besides imposing a substantial health burden, mTBI also carries a significant societal and economic burden, and it can hinder an affected individual's ability to resume their previous or expected roles and responsibilities within their family, social life, and occupation. Over 69 million new TBI cases are reported annually worldwide, and more than 80% are classified as mTBI [4]. The European Union estimates 2.5 million TBI cases annually, while the United States records approximately 3.5 million [4]. In Ontario, Canada, the annual concussion rate average is 147 815 [5]. It is worth noting that many mTBI cases go unreported, potentially raising the actual incidence. One of the challenges associated with mTBI lies in its broad definition, which tends to hinder the development of preventative strategies and diagnostic tools. The classification of mTBI has historically relied on qualitative symptoms or the cause of the injury. Typical symptoms include brief loss of orientation, loss of consciousness lasting between 0 and 30 minutes, post-injury seizures, lethargy, vomiting, headaches, dizziness, and irritability [1], [6].

Various qualitative and quantitative tools have been used to assess the occurrence and severity of mTBI. The Glasgow Coma Scale (GCS) is one such example [7]. GCS is a widely used objective

measure that evaluates impaired consciousness by assessing eye-opening, motor response, and verbal response [8]. Scores range from 3 to 15, with lower scores indicating more severe head injuries (e.g., 3-5 indicating no responsiveness) and higher scores indicating mild head injuries (e.g., 13-15 indicating suitable responsiveness across all assessed aspects). Other methods for indicating injury severity include the Russell Posttraumatic Amnesia (PTA) scale [9], which measures the time taken for an injured person to return to a conscious or responsive state, as well as symptom-based questionnaires like the Sports Concussion Assessment Tool (SCAT) [10]. Another example involves quantifying the time to follow commands, with a value of less than or equal to 20 minutes indicating a mild head injury [11]. mTBI is increasingly gaining recognition as a significant public health concern due to its potential to lead to adverse cognitive, behavioral, and psychological consequences [12].

One approach to address challenges in understanding mTBI is investigating the mechanical causes of TBIs and developing preventive measures. This calls for a detailed examination of the causative factors to establish preventive protocols and create more effective safety systems. Advanced finite element human body models (HBMs) are emerging as a promising method to assess brain tissue response, offering insights into brain deformation and injury risk. For example, several research studies have used Finite Element (FE) models to examine the response of the brain to impact [13], [14], [15], [16]. These studies collect kinematic data during head impacts identified as concussions, often occurring in injury-prone environments (e.g., soccer, football, and boxing), and reconstruct these scenarios using computational models. The aim is to establish criteria and thresholds for different types of head injuries.

Recent research has now also linked mTBI symptoms, ranging from headaches, fatigue, sensitivity to noise, dizziness, and loss of consciousness, to more severe manifestations like the delayed onset of long-term neurological damage, including chronic traumatic encephalopathy (CTE), Alzheimer's disease, and Parkinson's disease, with repetitive sub-concussive exposures [17], [18], [19], [20]. Such neurological impairments have been observed in military populations due to repeated exposures from various sources of low-level blast waves [21], [22], [23] and, more recently, from the repeated firing of 0.50 caliber rifles (an example of a long-range rifle) [24]. More specifically, members of the Canadian Armed Forces (CAF), referred to as operators

hereafter, have reported experiencing chronic mTBI symptoms from firing these long-range rifles [24].

While the majority of research has primarily concentrated on the correlation between the blast characteristics (overpressure) resulting from firing 0.50 caliber rifles and mTBI, it is crucial to recognize that when firing a long-range rifle, recoil forces are transferred via the shoulder and neck to the head, resulting in head accelerations. Furthermore, operators frequently equip their rifles with suppressors, which have been shown to reduce the transmission of the muzzle blast toward the operator [25], but in some cases increase the recoil forces. Hence, there is a need to understand the relationship between repeated exposure to rifle recoil and brain injury, which in turn will allow for the implementation of preventive measures to mitigate long-term adverse consequences.

1.2 Approach

This research seeks to quantify the brain response of operators when firing long-range rifles using an advanced finite element head model (FE HM). To achieve this goal, head kinematics data (accelerations and angular velocities) of CAF volunteers exposed to rifle recoil during regular training exercises were collected by project partners using instrumented mouthguards. The first task involved analyzing the recorded head kinematics to assess the magnitude and shape of the head kinematic response between the different volunteers and rifle configurations. The experimental head kinematics were then inputted to the Global Human Body Models Consortium (GHBMC) 50^{th} percentile male FE HM [26].

The HM was used to recreate the experiments and assess deformation in the brain that may be associated with repetitive exposure to recoil forces. In addition to traditional kinematic-based injury prediction metrics, tissue-level deformation was assessed in eight different brain regions, some of which have been previously associated with concussion [27]. This workflow (instrumented mouthguards to FE model) provides a unique opportunity to gain insight into this population's magnitudes of head kinematics. These findings mark an initial stride towards research aimed at informing training procedures and establishing exposure limits for members of the CAF. The effect of a recoil mitigation system (RMS) was also evaluated. Such measures are

crucial to ensuring safety and mitigating any potential long-term effects stemming from occupational exposures to recoil forces.

2 Background

Over the span of several decades, extensive research has been conducted to understand the incidence and causes of traumatic brain injuries (TBIs), an important step for developing effective strategies to prevent and mitigate such injuries. This research encompasses various applications, for example, developing protective headgear, establishing standards and protocols for head protection, and improving the design of safety systems for motor vehicles. These efforts, as aptly described by Meaney et al., form a "natural research cycle" that begins with identifying locations of severe injuries and discerning changes in injury patterns over time [28]. Then, these injury scenarios are replicated in a laboratory setting to establish the correlation between physical factors and resulting injuries. As this knowledge evolves into advanced protective technologies, one research cycle concludes, and another begins, dedicating itself to addressing the most significant injuries in the population [28]. The previous cycle has already produced advancements in protective headgear and passive safety systems, particularly concerning moderate and severe brain injuries. For instance, all new vehicles incorporate restraint systems like seat belts and airbags aimed at reducing the possibility of head impact with interior parts of the vehicle, such as the steering assembly or dashboard [29].

Present efforts are now predominantly focused on mild TBI, affecting both civilians and military personnel [28]. It should be noted that the primary mechanical response of the brain to different types of loading (e.g., impacts, impulsive forces, and blast events) depends on factors such as the geometry and material characteristics of the brain and skull [28], [29]. Additionally, each instance of TBI unfolds under distinct conditions, posing a significant challenge: developing a universally applicable methodology to consolidate diverse mechanical factors linked to each injury and predict when such injuries are likely to occur in the general population. So far, the most effective method for understanding TBIs involves defining external mechanical loads during injurious situations. Brain models, whether physical, analytical, or computational, are then employed to estimate how these forces translate into strains and stresses within the brain tissues [28]. Tolerance criteria specific to tissues are then used to identify brain regions likely affected through injury by externally applied forces.

Studies indicate that the incidence of mTBI is at least 10 times more frequent than moderate and severe TBIs [30], [31]. Comparisons between the prevalence of long-term impairments in mTBI patients and other medical conditions are especially alarming. For instance, approximately 225,000 new patients each year suffer from lasting deficits due to mTBI, equivalent to the combined annual diagnoses of breast cancer, multiple sclerosis, and traumatic spinal cord injuries [32]. The emergence of mTBI in the military population further emphasizes the urgent need for effective long-term treatments and preventive measures [28], [30], [31], [32].

Currently, there are no clinical solutions to reverse the initial brain damage caused by mTBIs completely. However, the biomechanical community can play a crucial role in reducing the occurrence of mTBIs and preventing further injuries after an initial incident. To achieve such goals, it is essential to have a deeper understanding of the mechanisms of TBI, particularly mTBI. Such knowledge provides a scientific foundation for developing advanced protective devices, improving diagnostic and prognostic tools, and creating innovative therapeutic methods. The following section provides essential background information to facilitate a comprehensive understanding of the study presented in this thesis.

2.1 Anatomy

This section will provide a brief overview of the anatomic planes and head anatomy.

2.1.1 Anatomic Planes and Co-ordinate System

The anatomical position refers to a standard configuration in which a person stands upright, with their head, feet, and palms facing forward (Figure 1), as described by [36]. This baseline posture is essential as it provides a consistent framework for describing human anatomy, regardless of the individual's specific posture at any given moment. The three orthogonal planes in this position include the frontal (or coronal), transverse (or axial), and sagittal (or median) planes (Figure 1).

The frontal plane is vertically oriented, segmenting the body into anterior and posterior sections. The sagittal plane, which is also vertically oriented, bisects the body into mirror-image left and

right halves. In contrast, the transverse plane is horizontally aligned, dividing the body into upper and lower portions.

The following definitions should be noted as well: The "superior" direction is upward, towards the head, while "inferior" is downward, towards the feet (for example, the eyes are superior to the nose, and the mouth is inferior to the nose). "Posterior" points to the back, while "anterior" points to the front of the body. "Medial" refers to parts close to the body's center, and "lateral" describes parts away from the body's center, either to the left or right. "Proximal" is used for structures near the center of the body, whereas "distal" is for structures farther away from the body's center (for example the hands are distal compared to the elbow). The Society of Automobile Engineers (SAE) J211 coordinate system (Figure 2) is used in this study where the x and z axes point towards the anterior and inferior directions, respectively.

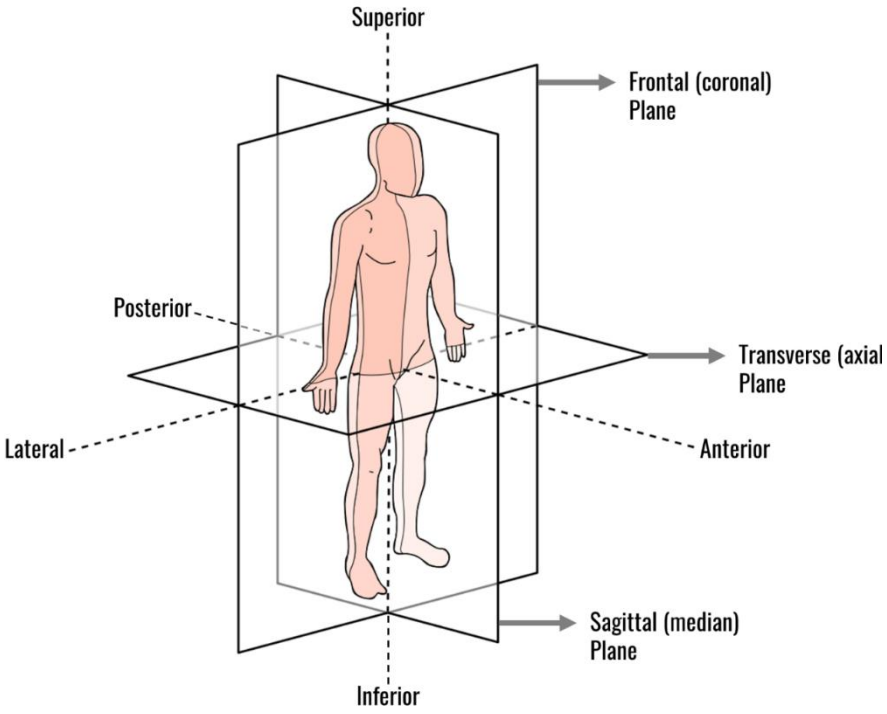


Figure 1: Anatomical planes and directions for the human body. Adapted from Anatomical Planes by CFCF, 2014, Wikimedia Commons (https://commons.wikimedia.org/wiki/File:Anatomical_Planes.svg). CC BY-SA 3.0.

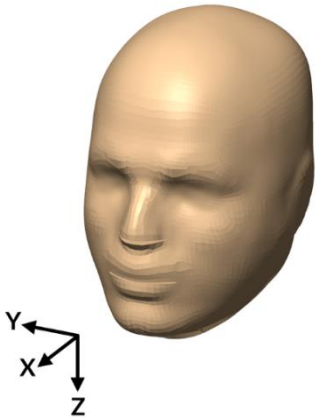


Figure 2: The SAE coordinate system used in the GHBMC model.

2.1.2 Head Anatomy

The human head is a complex and intricate structure, encompassing various layers and components, starting with the scalp, followed by the skull, the meninges, and the central nervous system. Note that the description of the head anatomy in Section 2.1.2 is from [29], [37], [38].

The scalp measures 5 to 7 mm in thickness. It comprises three primary layers: the hair-bearing skin (known as the cutaneous layer), a subcutaneous connective-tissue layer, and a layer consisting of muscle and fascia. Below the scalp is a loose connective-tissue layer, along with a fibrous membrane that envelops the underlying bone, known as the periosteum. These outer three layers of the scalp can move as a single unit, in response to a traction force applied to the scalp.

The adult human skull is a complex structure made up of three layers, including a central layer of porous trabecular bone sandwiched between two outer layers of dense cortical bone. It consists of 22 bones, categorized into the viscerocranium, composed of 14 bones, and the neurocranium, consisting of 8 bones (Figure 3). The viscerocranium forms the facial skeleton, representing the lower and anterior portion of the skull and comprising structures such as the orbits, nasal cavities, and oral cavities. On the other hand, the neurocranium, located in the superior and posterior part of the skull, serves as the protective housing for the brain and its membranous coverings, known as the meninges. The neurocranium is made up of eight irregularly shaped flat bones,

including the frontal, left and right parietal, left and right temporal, occipital, sphenoid, and ethmoid bones (Figure 3). Notably, the sphenoid and ethmoid bones play a crucial role in bridging the connection between the viscerocranium and the anterior skull base. Beneath the neurocranium, a network of openings accommodates arteries, veins, and nerves, with the foramen magnum, which serves as a transition area that facilitates the passage between the spinal cord and the brainstem.

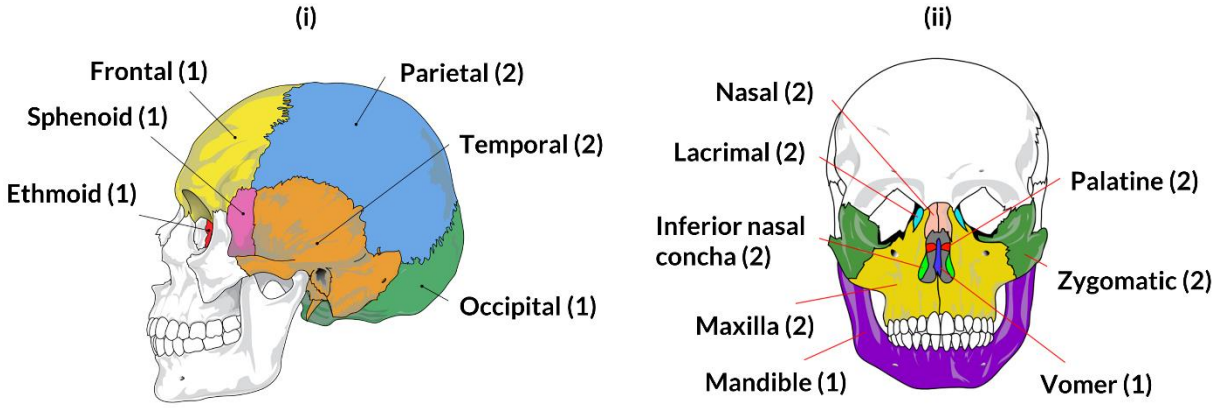


Figure 3: The adult skull consisting of (i) the neurocranium and (ii) the viscerocranium. (i) The neurocranium is adapted from Cranial bones by Edoarado, 2014, Wikimedia Commons (https://commons.wikimedia.org/wiki/File:Cranial_bones_en_v2.svg). CC0 1.0 Universal Public Domain Dedication. (ii) The viscerocranium is adapted from Facial skeleton by Own Work, 2015, Wikimedia Commons (https://commons.wikimedia.org/wiki/File:Facial_skeleton_-_en.svg). CC0 1.0 Universal Public Domain Dedication.

The cranial meninges form a protective system of three connective tissue layers that envelop the brain and spinal cord (Figure 4A). The outermost layer, known as the dura mater, is thick and fibrous, adhering closely to the skull's inner surface. Just beneath it lies the delicate arachnoid mater, separated from the brain and spinal cord by the subarachnoid space, filled with cerebrospinal fluid (CSF). CSF is a clear and colorless fluid with critical roles—it acts as a cushion, shielding the brain and spinal cord from physical shocks, provides buoyancy, allowing the brain to float within the skull, and aids in the transport of nutrients and removal of waste products. An average adult cranial cavity contains approximately 140 mL of CSF. The innermost layer, the pia mater, maintains direct contact with the brain and spinal cord, closely following their contours.

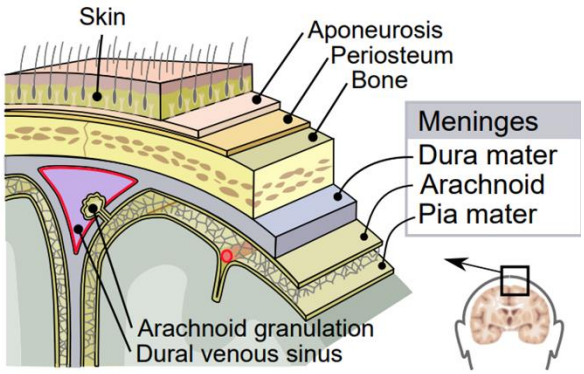


Figure 4A: The cranial meninges from Meninges by Mysid, n.d., Wikimedia Commons (https://commons.wikimedia.org/wiki/File:Meninges-en.svg). CC BY-SA 3.0.

Despite making up only 2% of the body's mass, the brain requires a substantial 20% of the body's total blood supply, highlighting the critical role of the brain's vasculature in sustaining normal function. The primary arteries, such as the internal carotid and vertebral arteries, enter the cranial cavity through the foramen magnum and give rise to various cerebral arteries (Figure 4B). These arteries are intricately connected through vessels like the anterior and posterior communicating arteries, collectively forming a vital structure known as the Circle of Willis. From the Circle of Willis, cortical arteries branch out to provide blood to the brain's surface and deeper regions. Cortical veins also traverse through the subarachnoid space. Bridging veins pass through the dura mater, draining venous blood into the dural sinuses. These sinuses are venous channels located between layers of the dura mater, eventually exiting the cranium through the internal jugular veins. Finally, the scalp receives its blood supply from the internal and external carotid arteries.

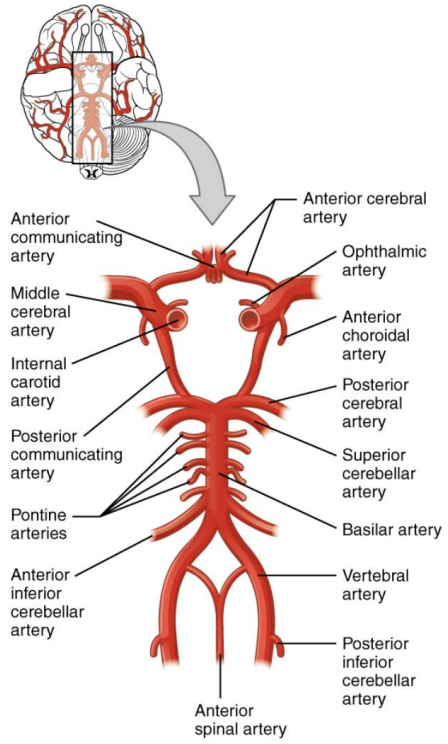


Figure 4B: The Circle of Wilis from Circle of WillisN by OpenStax, 2016, Wikimedia Commons (https://commons.wikimedia.org/wiki/File:1314_Circle_of_WillisN.jpg). CC BY 4.0.

The central nervous system (CNS) is primarily composed of a microscopic network of neurons and supportive tissues. This intricate arrangement includes distinct regions known as gray and white matter. Gray matter consists of nerve-cell bodies concentrated on the brain's surface and deep within its structure, while white matter comprises myelinated nerve-cell processes, also known as axons, forming tracts that connect different parts of the central nervous system. In terms of both structure and function, the brain can be categorized into five components: the cerebrum, cerebellum, midbrain, pons, and medulla oblongata (Figure 5).

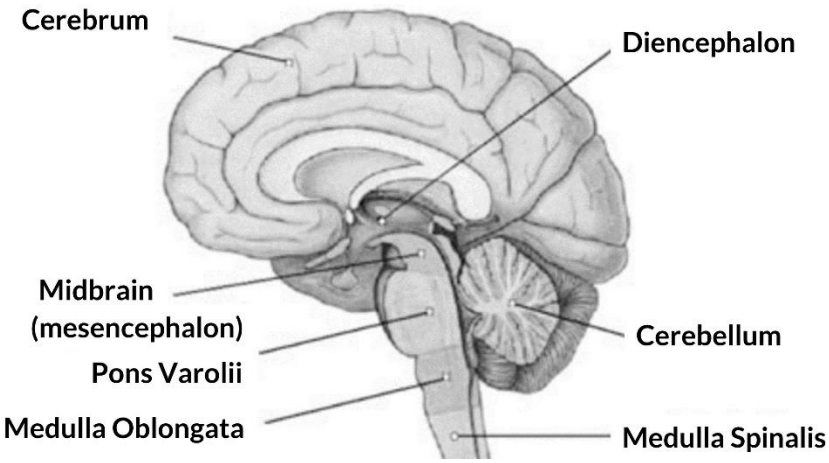


Figure 5: The cerebrum, cerebellum, midbrain, pons, and medulla oblongata from Trauma Biomechanics (p. 88), by K. Schmitt, P.F. Niederer, D.S. Cronin, B. Morrison III, M.H. Muser, F. Walz, 2019, Springer Cham. Copyright 2019 by Springer Nature Switzerland AG 2019. Reprinted with permission.

The cerebrum, the largest part of the brain, is divided into two hemispheres separated by an interhemispheric fissure in the middle. The surface of these cerebral hemispheres features raised structures called gyri and folded structures known as sulci (Figure 6). These gyri and sulci collectively increase the brain's surface area, enabling a higher density of neurons within the cortex, which is crucial for information processing. The pattern of sulci serves as consistent landmarks that divide each cerebral hemisphere into four main parts: the frontal, parietal, temporal, and occipital lobes (Figure 3).

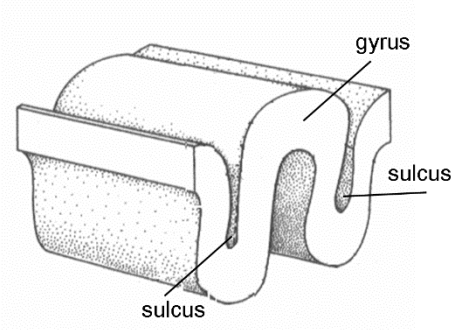


Figure 6: Gyrus vs sulcus from Gyrus sulcus by Albert Kok, 2007, Wikimedia Commons (https://commons.wikimedia.org/wiki/File:Gyrus_sulcus.png). CC0 1.0 Universal Public Domain Dedication.

The meninges extend into a longitudinal fissure known as the falx cerebri (Figure 7). It is a dura infold and serves as a partition between the posterior parts of the cerebral hemispheres. It connects to another dura infolding known as the tentorium cerebelli (Figure 7), which separates the occipital lobes of the cerebrum from the cerebellum. The falx cerebri as well as the tentorium cerebelli are firmly attached to the skull and are much stiffer than the brain tissue. Consequently, these membranes tend to limit movement during extensive motions such as head rotations.

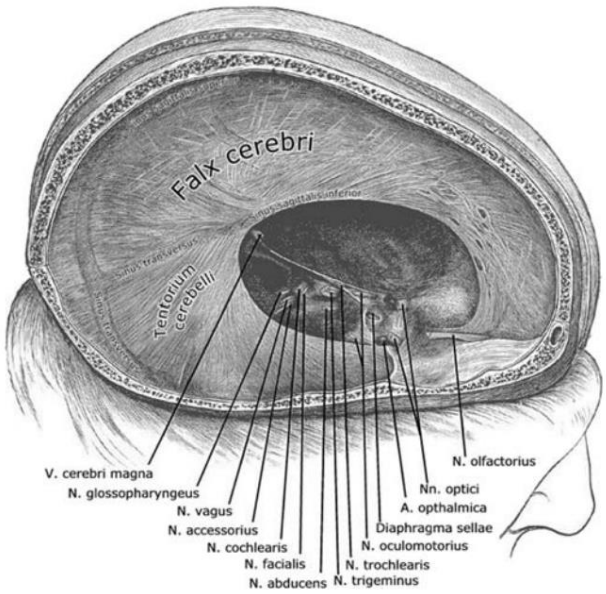


Figure 7: The Falx Cerebri and Tentorium Cerebelli from Basic Finite Element Method as Applied to Injury Biomechanics (p. 475), by H. Mao, n.d., Mara E. Conner. Copyright 2018 by Elsevier Inc. Reprinted with permission.

The two cerebral hemispheres are connected by the corpus callosum, a bundle of white matter, below the longitudinal cerebral fissure (Figure 8*).* Much like the cerebrum, the cerebellum is also divided into two roughly symmetrical hemispheres, separated by the falx cerebelli. Situated in front of the cerebellum is the brainstem, connecting the cerebrum to the spinal cord (Figure 8). The brainstem is composed of the pons, medulla oblongata, and midbrain. Positioned above the brainstem are the thalamus and basal ganglia (Figure 8).

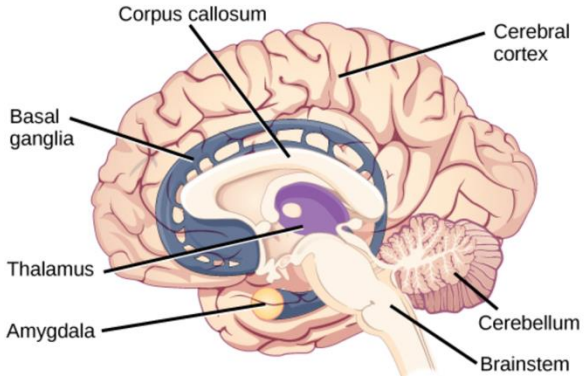


Figure 8: Description from Goodwin - Drawing Coronal and sagittal section of the brain - English labels by Cindy Seiwert and Goodwin University, n.d., ANATOMYTOOL (https://anatomytool.org/content/goodwin-drawing-coronal-and-sagittal-section-brain-english-labels). CC BY-NC-SA.

2.2 Types of Head Injuries

There are many different types of head injuries (Figure 9), and their severity can be assessed using the Abbreviated Injury Scale (AIS) [29], [39], ranging from 1 (minor) to 6 (fatal). This scale considers factors such as the extent of brain structure damage, bleeding, and functional impairment. Lower AIS values correspond to less severe injuries, while higher values indicate more severe and potentially life-threatening head injuries.

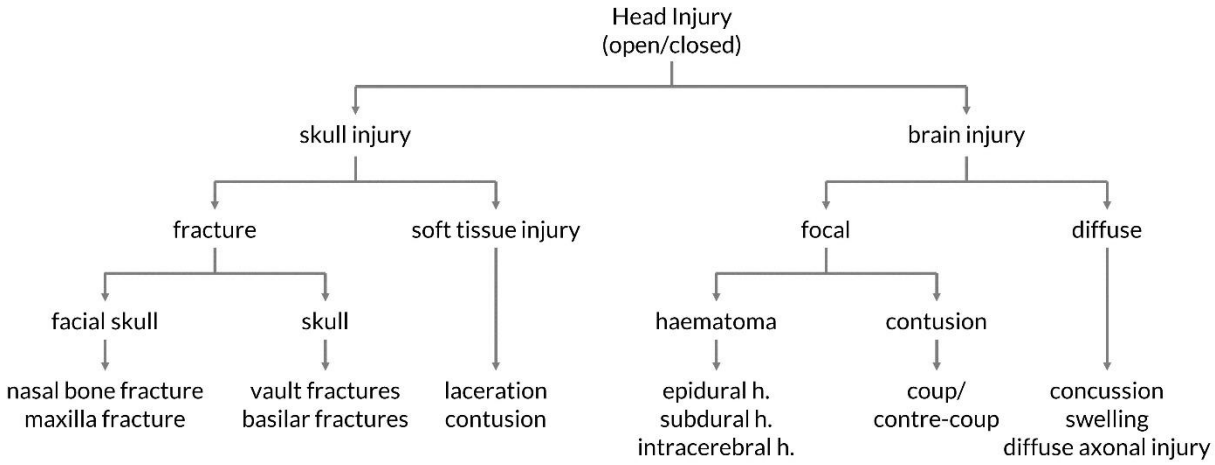


Figure 9: Types of head injuries adapted from Trauma Biomechanics (p. 89), by K. Schmitt, P.F. Niederer, D.S. Cronin, B. Morrison III, M.H. Muser, F. Walz, n.d., Springer Cham. Copyright 2019 by Springer Nature Switzerland AG 2019. Adapted with permission.

Table 1: AIS scale for head injury recreated from [29], [39]

AIS Score	Injury Severity	Description
1	Minor	- Skin/scalp: abrasion, superficial laceration - Face: nose fracture
2	Moderate	- Skin: major avulsion - Vault fracture: simple, undisplaced - Mandible fracture: open, displaced - Maxilla fracture: LeFort I and II
3	Serious (not life-threatening)	- Basilar fracture - Maxilla fracture: LeFort III - Total scalp loss - Single contusion cerebellum
4	Severe (life-threatening but survivable)	- Vault fracture: complex, open with torn, exposed or loss of brain tissue - Small epidural or subdural hematoma
5	Critical (survival uncertain)	- Major penetrating injury (>2 cm) - Brain stem compression - Large epidural or subdural hematoma - Diffuse axonal injury (DAI)
6	Fatal	- Massive destruction of both cranium and brain (crush injury)

Head injuries can be broadly classified into open or closed injuries based on whether the dura mater is affected (open) or not (closed). These injuries can also be subcategorized as either skull or brain injuries. Soft tissue injuries, falling into the skull injury category, often occur in automotive accidents and typically result in contusions and lacerations, which are generally considered minor. Similarly, facial injuries, such as those affecting the eyes or ears, are typically rated as AIS1 or AIS2, signifying their relatively minor nature. On the other hand, more severe head injuries can result from fractures, including fractures of the nasal bone and maxillary fractures. Maxillary fractures are considered more serious and can have AIS grades of up to 3.

Brain injuries can be categorized as focal injuries and diffuse injuries. Focal injuries can take the form of hematomas (bleeding into and around the brain) or contusions (bruising of brain tissue), with contusions being the most observed lesions resulting from head impacts. Contusions generally occur at both the impact site (referred to as coup contusion) and at the site opposite the impact (known as contre-coup contusion).

Three different types of hematomas, known as epidural hematoma, subdural hematoma, and intracerebral hematoma, can be distinguished depending on the site of the bleeding. Epidural hematoma, characterized by bleeding above the dura mater, typically arises due to trauma to the skull and the underlying meningeal vessels. Subdural hematoma refers to the hematoma located beneath the dura mater. Three sources have been identified for subdural hematomas: lacerations of cortical veins and arteries resulting from penetrating injuries, significant contusion-related bleeding into the subdural space, and the rupture of bridging veins connecting the brain's surface to the dural sinuses. Intracerebral hematomas are distinct collections of homogeneous blood within the brain and can be differentiated from contusions using medical imaging.

Diffuse brain injuries range from mild concussions (mTBI) to diffuse white matter injuries. Diffuse axonal injury (DAI) refers to scattered lesions over a widespread area in white matter tracks. Regarding mTBI, as highlighted in the introduction, there is no standardized definition. Various organizations, including the American Congress of Rehabilitation Medicine (ACRM), the Centers for Disease Control and Prevention (CDC), and the World Health Organization (WHO), offer their interpretations of mTBI, each detailing potential symptoms associated with such injuries. Nevertheless, they all share the following criteria: a minimum Glasgow Coma Scale (GCS) score of 13, typically less than a 30-minute period of unconsciousness, less than 24 hours of post-traumatic amnesia, and the absence of abnormal findings on neuroimaging studies [40], [41], [42].

2.3 Injury Mechanisms

Injury mechanisms can be categorized into two classes: injuries resulting from static and dynamic loadings. Schmitt et al. defined static loading as a sustained load lasting for more than 200 ms, during which the head deforms until it reaches maximum deformation, resulting in skull fracture [29]. It is worth noting that this type of loading is relatively rare. Dynamic loading, a more common loading scenario, is further divided into two categories: contact and non-contact loading. When the head directly hits or is hit by an object (contact loading), it can deform, potentially leading to fractures near the impact site (direct fractures) or along the force's

direction (burst fractures). This type of loading can also result in local brain injuries like epidural hematoma or contusion, as well as scalp injuries, rather than fractures [29].

Such focal brain injuries and bruising may also be caused by intracranial compression. This phenomenon is observed when the applied force generates stress waves that traverse through either the skull or the brain. These waves can lead to pressure disparities, characterized by increased pressure at the impact site (coup) and reduced pressure on the opposite side (contre-coup), resulting in intracranial compression. Furthermore, this pressure gradient can induce shear strain within the deep structures of the brain. Brain contusions and the tearing of bridging veins, which can eventually lead to subdural hematoma, can result from the brain moving relative to the skull [29], [37].

In non-contact situations, the head motions are due to inertial forces. Typically, concussive injuries are a result of this inertial loading [32]. During this type of loading two types of motion can happen: translational and rotational motion. Understanding the mechanisms of mTBI is inherently challenging because direct observation of the brain is difficult. As a result, our understanding of how the brain responds during injurious events remains limited. An alternative approach involves measuring the head kinematics during the potentially injurious event and correlating the measurements to subsequent brain injuries.

One such example is the ground-breaking experiments conducted by Dr. Gurdjian and Professor Lissner at Wayne State University. They measured the linear accelerations resulting from dropping human cadavers from different heights to the ground, concurrently investigating head injuries such as skull fractures and brain contusions. Afterward, their team introduced the Wayne State tolerance curve (WSTC) (Figure 10). This curve suggests that the risk of head injury depends on both the duration and magnitude of head linear acceleration. Notably, the curve illustrates that the head can tolerate higher acceleration magnitudes during short impact durations, but it withstands lower magnitudes with prolonged impacts [43], [44], [45].

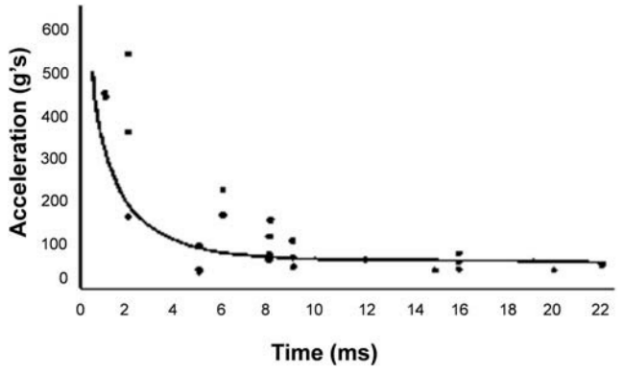


Figure 10: The Wayne State tolerance curve from Basic Finite Element Method as Applied to Injury Biomechanics (p. 480), by H. Mao, n.d., Mara E. Conner. Copyright 2018 by Elsevier Inc. Reprinted with permission.

Researchers have challenged the predominant linear acceleration-based injury mechanisms, emphasizing the significance of rotational acceleration. In a pioneering study by Holbourn (1943), he used simple photoelastic materials to highlight regions of a brain surrogate subjected to high shear strains during rapid rotational motions [46]. This approach shed light on the crucial role of shear strains resulting from angular acceleration of the skull, particularly in the context of concussions. Pudenz and Shelden (1946) corroborated Holbourn's observations by visually examining the surface of animal brains. Their experimental approach involved substituting the upper portion of a monkey's skull with transparent polymer calvarium to observe the deformations of the brain in response to linear acceleration. Additionally, a series of animal experiments demonstrated that head rotation alone, even without linear acceleration, could result in substantial brain damage, such as axonal injury and subdural hematoma [47], [48]. This evidence highlighted that both linear and rotational accelerations have the potential to cause brain damage.

In the 1974 study, Ommaya and Gennarelli introduced the "centripetal theory of concussion" outlining that the skull rotation transmits to the outer surface of the brain, and the inner regions lag behind due to inertial effects, inducing shear strain. This, in turn, leads to axonal damage, resulting in concussion symptoms [48], [49]. In dynamic events where the head rotates about multiple axes, the shearing forces are expected to be more diffuse. As a result, rotational loading is known for causing widespread injuries across the brain. The theory also suggests that the

centripetal progression of axonal disruption is amplified in regions of structural irregularity in the brain, such as the boundaries between white and grey matter. Other studies have also supported the theory of axonal damage or disruption [50], [51].

It is worth noting that numerous numerical studies have delved into brain tissue deformation as a potential indicator of concussion [52], [53], [54], [55]. Changes in intracranial pressure, signaling catastrophic head injuries, were initially linked to alterations in the linear acceleration of the head. However, when looking at brain tissue deformation and, consequently, concussion, the key factor is the rotational motion of the head [56]. This deformation is not solely driven by rotational motion but depends on distinct brain regions and brain tissue material properties [32], [57]. While inducing unconsciousness, a key indicator of severe concussion, through linear acceleration alone is challenging, introducing a rotational component significantly heightens the likelihood of unconsciousness [48]. This can be attributed to the mechanical properties of brain tissue, particularly its high bulk modulus in relation to its low shear modulus [46], rendering the brain susceptible to deformation under shear forces.

Studies have revealed that the tolerance to acceleration is closely tied to the anatomical direction, with coronal rotation causing the most severe injuries [45], [51], [56], [57]. However, it is important to recognize that similar injuries may arise if higher magnitudes of rotational acceleration are applied in other planes of motion. For example, in a review of NFL concussions by Lessley et al., over 50% of concussions during the 2015-2016 NFL season were attributed to impacts on the side of the helmet, inducing motion in the coronal plane [60]. These studies highlight the importance of considering both the directional aspects and the magnitude of linear as well as rotational motion and when assessing mTBI.

2.4 Experimental Data Related to Head Response

Researchers have employed various strategies to understand the response of the brain to mechanical forces. Initially, experiments involving both human and animal models played a crucial role in identifying specific types of mechanical loading associated with severe brain injuries. Over the past decade, computational methods have gained popularity in the study of head injuries, encompassing traumatic brain injuries including mild traumatic brain injuries.

However, ensuring the accuracy of these numerical models requires thorough validation. Researchers commonly employ a combination of experimental and computational tools to establish a clear link between external mechanical input and brain injury. Given the complex structure of the brain, it is not surprising that early efforts to understand its mechanical response and address injuries heavily leaned towards experimental approaches. This section will provide a summary of key experimental work, particularly those instrumental in validating current finite element models.

2.4.1 Nahum et al.'s Linear Impact Experiment

The initial experiments conducted by Nauhm et al. are now widely recognized. In these experiments, a seated cadaver was subjected to an impact from a 5.59 kg cylindrical object moving at a constant velocity of 9.94 m/s. The impact was directed along the mid-sagittal plane of the specimen in an anterior-posterior direction, with the skull rotated 45° to the horizontal in the Frankfort anatomical plane. Intracranial pressure during the impact was measured at five locations using pressure transducers. This pressure data is widely used to validate numerical models. While many models use these results for validation, it is essential to note that validating solely against pressure is insufficient due to the potential extensive range of deformation that can occur without significantly impacting pressure distribution [59]. Therefore, it is prudent to consider Nahum's findings as an initial validation step in the model development process, followed by additional validation against a displacement-based method [28].

2.4.2 Hardy et al.'s NDT Experiment

Hardy et al. conducted pioneering studies, one in 2001 and one in 2007. Both used high-speed biplane X-ray technology and Neutral Density Targets (NDTs) implanted in the brain to quantify PMHS brain motion relative to the skull during various impacts. The experiments involved 45 impacts with velocities ranging from 2.5 to 3.9 m/s. The NDTs, tin granules encased in polystyrene capsules, were tracked using X-ray technology. The arrangement of NDTs differed between the studies: the 2001 investigation employed a columnar arrangement, while the 2007 study used clusters. Both studies assessed responses to impacts inducing linear or combined linear and angular kinematics. The localized motions of the NDTs during impacts in both experiments

generally exhibited loop or figure-of-eight patterns with peak displacements of approximately 5 mm. Results indicated a correlation between brain motion, strain, and the angular speed of the head. Intracranial pressure (ICP) in the parenchyma was measured, revealing a direct correlation between coup pressure and resultant linear acceleration at the center of gravity of the head. Despite conducting tests under varying impact conditions, angular kinematics were not controlled. [60], [61]

2.4.3 Alshareef et al.'s Sonomicrometry Experiment

Hardy et al.'s experiment, although widely recognized, had some limitations. For example, they somewhat neglected the role of rotational motion, which is crucial in understanding concussion. To address this limitation, Alshareef et al. conducted experiments focusing on pure rotational loading of the head using sonomicrometry. This technique, employing ultrasonic pulses to measure dynamic distances between implanted crystals, allowed for the recording of brain motion and represented relative displacement along all three anatomical axes. Unlike sonomicrometry, the biplanar X-ray technique used by Hardy et al. is constrained to two directions due to the inability to place targets at multiple depths, limiting NDT placement to planar columns or regional clusters. In their 2018 study, Alshareef et al. conducted initial testing of crystals in situ with porcine brain tissue [64]. Building on this groundwork, their 2020 investigation replicated the methodology, with 30 sonomicrometry transmitters inserted in the brain and six receivers attached to the skulls of six cadavers [65]. The innovative approach of Alshareef et al. (2018,2020) holds promise for the validation of Finite Element Head models [64],[65].

2.5 Impact Sensing Devices

In the last decade, a novel approach to studying mTBI has emerged, treating injury exposure sources, such as sports fields, as 'passive' biomechanics laboratories [66]. This method involves directly collecting field data to estimate human tolerance to mTBI, facilitated by multiple monitoring technologies. By bypassing approximations in laboratories, this approach provides a direct measure of human tolerance over time. Researchers, particularly in sports, have adopted this strategy, focusing on studying head impacts to ethically gather real-world injury data. The

majority of advances and studies focusing on the understanding of mTBI have been conducted in the sports and automotive fields. Consequently, a significant portion of the forthcoming information and examples will be drawn from these fields. The methodologies, injury criteria, and established findings will be extrapolated to the military context, which is the population under examination in this thesis.

Note that American football is the most commonly studied sport [67]. The rise in this approach is attributed to increasing public awareness of the long-term effects of both concussive and subconcussive injuries. By quantifying the biomechanics of head impacts in athletes, even though these are considered minor injuries compared to earlier experimental work, valuable data is obtained to establish the lower limits for head injury tolerance. An integral component in evaluating the risk of brain injury involves the measurement of in-field kinematics. The primary objective here is to establish a meaningful relationship between external forces, including factors such as acceleration, impact force, and duration, experienced in situations that may pose a risk of injury, and the subsequent mechanical responses exhibited by the brain, which includes factors like stress and strain.

The earlier techniques employed to investigate the mechanical loading of the head during potentially injurious events include video analysis and anthropometric testing device (ATD) reconstructions. An anthropomorphic test device, commonly referred to as a dummy, serves as a precise testing instrument to assess the potential for human injury [29]. These dummies are often used as substitutes for Post-mortem Human Surrogate (PMHS) testing, replicating human responses to impacts, accelerations, deflections, and the forces and moments of inertia associated with injury-causing scenarios. Each dummy is designed to mimic the shape, weight, and movement characteristics of the human body. Equipped with an array of sensors and transducers, the dummy provides crucial measurements of the physical forces exerted on each body part during events that may lead to injury. “Sierra Sam” was the first ATD developed in 1949 for aviation safety testing. Subsequently, in 1977, General Motors introduced the Hybrid III ATD, a model that remains widely used in impact testing.

Some exemplar cases are the studies conducted by Newman et al. and Pellman et al. in the National Football League (NFL) to examine concussions in professional football [68], [69], [70], [71]. They examined recorded concussive impacts from various camera angles, using the video data to reconstruct impact angles, speeds, and player kinematics. This information was then used to replicate impact conditions in the lab with instrumented Hybrid III dummies. However, the findings, including linear and rotational risk curves, were specific to NFL players and not broadly applicable.

Another example is a study by Withnall that used video analysis to examine head impacts in soccer [72]. They looked at 62 cases from FIFA-sanctioned matches, analyzing video footage provided by the FIFA Medical Assessment and Research Centre (F-MARC). The aim was to recognize the diverse body parts involved in striking (such as elbow-to-head) and the corresponding range of speeds. Findings from the research indicated that the upper extremity, followed by the head, were the predominant striking body parts.

While NFL reconstructions offered valuable estimates of concussion biomechanics, their time-consuming nature limits the sample size. Error propagation from translating head kinematics in game videos to laboratory reconstructions has led researchers to turn to head impact sensors in athletes [66]. Despite its extensive application, using ATDs to reconstruct head impacts faces limitations such as lack of bio fidelity, time consuming set ups and high maintenance costs.

The progress in microelectromechanical system (MEMS) inertial sensors have improved the overall capabilities (including accuracy and sensitivity) of the wearable sensor used in sports, making them more valuable tools for studying and understanding head impacts in sports [73]. The wearable sensors typically include accelerometers, measuring linear accelerations, and gyroscopes, measuring rotational kinematics. By instrumenting a large group of participants, researchers could obtain comprehensive data to study situations with and without injuries and understand the occurrence of concussions in various scenarios.

A practical approach for incorporating these sensors involved attaching them to existing athletic headgear, like helmets. As a matter of fact, the head impact telemetry system (HITS) is the most predominant head impact sensor to date [66]. Developed in the early 2000s, over 1.5 million

head impacts were recorded among high school and collegiate football players with this device [74]. Research using HITS has resulted in the creation of concussion risk curves for adult male athletes [75], [76], [77], leading to changes in regulations in different football leagues, such as the NFL [78], in an attempt to reduce injurious impacts. Despite its effectiveness, the HITS system has limitations, including a per-sensor cost exceeding $2000, limiting widespread use and applicability beyond football. Additionally, significant errors may be introduced in the measurements from helmet sensors as they may be displaced during impact [79], [80]. It is worth noting that while much research has centered on football, substantial concussion rates also occur in other sports like ice hockey, lacrosse, and soccer for both men and women.

Recent technological strides have led to various head impact sensors, including instrumented helmets [81], [82], [83], headbands [84], [85], [86], skin patches [87], [88], ear plugs [89], [90] and mouthguards [91], [92], [93], [94]. Using these instrumented equipment allow for the capture of in vivo head impact kinematics, facilitating the differentiation between injurious and non-injurious scenarios.

Apart from HITS, the gForce Tracker (GFT) is another device designed for measuring 6DOF head impact kinematics. This device offers the advantage of easily attaching to the interior of various football helmet styles compared to HITS, providing real-time outputs for linear acceleration, rotational velocity, and impact location for each helmet impact. In a study by Campbell et al. (2016), they assessed the GFT's accuracy by impacting a football helmet attached to a Hybrid III ATD head-neck system using a linear impactor [95]. The study revealed a strong correlation between GFT and Hybrid III ATD peak linear accelerations and rotational velocity measurements. The correction algorithm to predict kinematics at the head CoG was proposed to be tailored to the specific brand of the helmet [93] supported [78].

Another example of a device measuring head kinematics is the X2 X-Patch, a compact microelectromechanical system equipped with a triaxial accelerometer and gyroscope. Worn just behind the ear, either on the right or left mastoid process, the X-Patch has been used in numerous studies to capture kinematic data in various sports, such as male American football [96], [97], [98], female soccer [99], [100], and youth rugby [101]. It samples linear acceleration at

a rate of 1 kHz and angular velocity at 800 Hz. The primary challenge posed by devices like skin patches and even skull caps lie in their limited coupling with the head, caused by the inherent relative motion between the device and the skull, attributed to skin dynamics. Consequently, these devices may not accurately measure head kinematics [88].

In contrast, sensors like the MV1 (MVTrak), in-ear sensors, have been developed specifically to enhance skull coupling. This is achieved through a tailor-made placement within the external ear canal. However, an accuracy assessment conducted by Sandmo et al. (2019) revealed significant random errors in the in-ear sensor when compared to Hybrid III head form measurements [102]. While the sensor effectively distinguished head impacts from other accelerative events in youth soccer, the author cautioned against interpreting absolute values without due care and recommended employing additional verification methods, such as video analysis, to enhance reliability in real-life settings.

Wu et al. (2016) investigated the accuracy of three different sensors under sagittal soccer head impacts ranging from 6 to 13 g [88]. The study involved monitoring fiducial grids using dual high-speed video recording. The participant, a 26-year-old male, wore a custom-fit instrumented mouthguard, a skin patch (specifically, the xPatch Gen2 from X2Biosystems, Inc.) attached to the mastoid process, and an elastic Reebok skull cap. To simulate soccer head impacts, the study used a ball launcher was used to replicate the force of a kicked ball. The sensor-skull coupling was evaluated by measuring the displacement from an ear-canal reference point. The mouthguard, skin patch, and skull cap exhibited displacements around <1mm, 4mm, and 14 mm from the reference point, respectively.

Mouthguard-based sensors, in particular, show promise in providing tighter skull coupling compared to alternative sensor mounting approaches. The ongoing development of recording technologies aims to make these sensors smaller, more affordable, and widely accessible. Instrumented mouthguards offer a practical solution for measuring head impact and understanding concussion biomechanics, prompting numerous companies and institutions to advance their development. This has resulted in various validation studies of the different mouthguards.

For instance, Liu et al. conducted a study using a pneumatic impactor on an HIII test dummy head form replicating American football head impacts [93]. A range of mouthguards were assessed, including Stanford's customized and boil-and-bite versions, Prevent Biometrics' customized and boil-and-bite models, and Sports & Wellbeing Analytics' customized mouthguard (Figure 11). They found that all three mouthguards provided accurate measurements for peak angular acceleration, peak angular velocity, and brain injury criteria values, with mean average errors below 13%, 8%, and 13%, respectively. Specifically, the Prevent Biometrics custom-fit instrumented mouthguard demonstrated mean relative errors of 4.9%, 4.6%, and 2.5% for angular acceleration, angular velocity, and linear acceleration at the HIII head center of gravity. In another study evaluating eight different sensors, Kieffer et al. reported that the Prevent Biometrics instrumented mouthguard outperformed all others in the study [103]. Note that the experiments mentioned in the methods section of this thesis used a customized version of the Prevent Biometrics mouthguard.

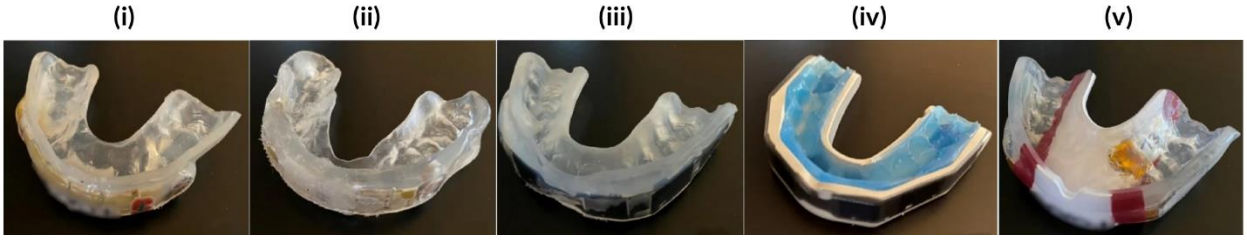


Figure 11: The (i) Stanford's customized mouthguard, (ii) Stanford's boil-and-bite mouthguard, (iii) Prevent Biometrics' customized mouthguard, (iv) Prevent Biometrics' boil-and-bite mouthguard, and (v) Sports & Wellbeing Analytics' customized mouthguard. Adapted from "Validation and Comparison of Instrumented Mouthguards for Measuring Head Kinematics and Assessing Brain Deformation in Football Impacts" by Liu, Y., Domel, A.G., Yousefsani, S.A. et al.,2020, Ann Biomed Eng., Volume 48, pages 2580–2598 (https://doi.org/10.1007/s10439-020-02629-3). Copyright 2020 by Biomedical Engineering Society. Adapted with permission.

With the progression of wearable sensors, ongoing research prioritizes collecting actual human head motion in real-life settings from environments with frequent injury occurrences. An important next step involved integrating these sensor data with computational modeling tools to attain a more holistic understanding of brain injury biomechanics.

2.6 Head Injury Metrics

Accurate injury prediction plays a key role in driving advancements in preventive technologies. When researchers can identify the specific circumstances or conditions that lead to injuries, they can develop targeted technologies and interventions to prevent or minimize their impact. This, in turn, fosters progress in protective gear, safety regulations, and innovative technologies designed to reduce injury risks across various scenarios.

Research has focused on identifying biomechanical metrics, also known as injury criteria, to create injury risk functions. These metrics aim to estimate the probability of injury in distinct loading scenarios, illustrating the connection between physical parameters and resulting injuries. Typically expressed as mathematical expressions or force and/or acceleration thresholds derived from experiments, they represent the maximum load that the body can undergo without experiencing severe injury. For example, an injury risk function could be devised using the peak linear acceleration of the head and establishing a correlation between the acceleration level with the percentage of concussion risk derived from empirical data. Subsequently, an injury risk threshold can be set; for instance, exceeding a particular head acceleration level is associated with a 50% probability of sustaining an mTBI.

The effectiveness of injury metrics becomes evident when we observe a significant reduction in fatal injuries in both sports and automotive contexts. As an example, Cantu et al. conducted a study examining the occurrence and causes of brain injury-related deaths in American football from 1945 to 1999 [104]. During this time frame, 69% of all football-related fatalities occurred as a result of brain injuries. Most of these brain injury-related deaths involved high school football players who sustained a specific type of head injury known as a subdural hematoma while either making a tackle or being tackled during a game [104]. The highest number of brain injury-related deaths happened between 1965 to 1969, but there was a significant decrease in these numbers from 1975 to 1994. This reduction can be attributed to two key safety measures. First, in 1976, a rule change was implemented to prevent initial contact with the head and face during blocking and tackling. Second, the introduction of the National Operating Committee on Standards for Athletic Equipment (NOCSAE) helmet standard played a crucial role. This standard was adopted

by colleges in 1978 and by high schools in 1980. Shortly after NOCSAE's safety standards were implemented, a substantial 74% decrease in fatal head injuries was observed [104].

The safety standards for motor vehicles, referred to as Federal Motor Vehicle Safety Standards (FMVSS), have achieved a remarkable 81% reduction in the fatality rate among motor vehicle occupants [105]. Although these fatalities are not exclusively related to head injuries, they underscore the effectiveness of safety standards in diminishing severe and fatal injuries. It is important to note that a significant proportion of motor vehicle occupant fatalities are attributed to head injuries, which have been mitigated through specific head injury prevention measures outlined in safety standards [106]. As the initial head injury metrics have effectively reduced severe head injuries and fatalities when incorporated into safety standards, current safety efforts are now focused on preventing and minimizing less severe but still significant head injuries such as mTBI.

Head injury metrics are based either on the observed head kinematics during the injurious scenario or on intracranial factors, such as stress and strain in brain tissues. Kinematic metrics are determined from translational, rotational, or a combination of both motions. Tissue-based metrics are developed using finite element models to quantify brain deformation through the intracranial factors [66]. The following section lists examples of kinematic and tissue-based metrics mentioned in literature.

2.6.1 Kinematic-Based Injury Metrics

2.6.1.1 Wayne State Tolerance (WST) Curve

The Wayne State Tolerance (WST) curve is a graph where acceleration is plotted on the y-axis and time on the x-axis. It was derived from just six data points, each representing instances of skull fractures resulting from sagittal impacts on cadavers. This curve suggests a threshold for survivable impacts and indicates that high accelerations are tolerable for short durations, whereas lower accelerations can be endured for longer periods [43], [44], [45]. Criticisms about the WST curve, as summarized by Newman, include the limited number of data points, the definition of acceleration levels, types of instruments, and experimental methods [107].

Moreover, the WST curve did not differentiate between skull fracture and brain damage, and did not consider the impact location as well as impact direction.

2.6.1.2 Severity Index (SI)

Gadd transformed the WSTC into a severity index known as the Gadd Severity Index (GSI) [106].

$$GSI = \int_0^t a(t)^{2.5} dt \qquad \text{Equation 1}$$

where

a_t = linear acceleration at head CoG given in multiples of g (gravitational acceleration)

t = duration of impact event in ms

The exponent of 2.5 in the equation corresponds to the slope of the WSTC when graphed on a log-log scale. Subsequently, Versace [109] adapted the SI to create the Head Injury Criterion (HIC).

2.6.1.3 Head Injury Criterion (HIC)

NHTSA further adapted HIC to its present version (Equation 2). HIC is the maximum area under the resultant linear acceleration-time plot within a specified time frame.

$$HIC = \max\left\{(t_2 - t_1)\left[\frac{1}{t_2 - t_1}\int_{t_1}^{t_2} a(t)dt\right]^{2.5}\right\} \qquad \text{Equation 2}$$

where

$a(t)$ = the resultant linear acceleration (in g)

t_1 and t_2 (in seconds) = timepoints during the acceleration pulse selected such that the value of HIC is maximized. Note that the term (t_2 - t_1) is 15 ms for HIC_{15} and 36 ms for HIC_{36}

NHTSA integrated HIC into FMVSS 208 (a motor vehicle standard) as a criterion, specifying that the time interval (t_2-t_1) should be 36 ms, commonly known as HIC_{36}, with a tolerance level of 1000 for the average stature male. Then, NHTSA also introduced another version of HIC, referred to as

$HIC_{15,}$ where the time interval (t_2-t_1) was shortened to 15 ms, with an adjusted tolerance level of 700 for the 50th percentile male. This was because the injurious points on the WST curve had durations in the range of 13 to 17 ms [64]. Hence, a shorter time limit (15 ms) was suggested. Note that the HIC_{15} value of 700 and the HIC_{36} value of 1000 represented a 31% and 48% probability of an AIS2+ injury [29].

Translational metrics, like HIC, have successfully predicted severe brain injuries [110], yet they display uncertainty and varied thresholds when predicting the risk of milder injuries, such as concussions [73]. The traditional metrics mentioned above have been criticized for only considering translational kinematics and not being injury-specific. Both theoretical and experimental studies have emphasized the importance of rotational head kinematics. Despite the early recognition of the role of rotational kinematics in concussion, the metrics initially formulated and incorporated into standards were solely based on linear acceleration. This limitation stemmed from the small dataset available in the metric development process as well as the challenges associated with measuring rotational kinematics accurately [66], [111].

2.6.1.4 Rotational Velocity and Angular Velocity Threshold

Considering the importance of rotational kinematics, Ommaya proposed concussion thresholds for humans. He suggested an angular velocity threshold of 50 rad/s for short durations impulses (typically less than 20 ms) and a rotational acceleration threshold of 1800 rad/s² for longer durations impulses (typically lasting more than 20 ms), based on primate experiments. In the late 1980s, Margulies et al. further advanced our understanding by establishing a tolerance curve for diffuse axonal injury. Note that concussion can be considered as a milder form of axonal injury. The determined tolerance thresholds for rotational velocity and acceleration ranged from 46.5 to 100 rad/s for short-duration impulses and 7000–16,000 rad/s² for long-duration impulses [112].

2.6.1.5 GAMBIT

In 1986, Newman introduced the “generalized acceleration model for brain injury threshold” (GAMBIT), the first metric to integrate translational and rotational kinematics to assess the risk of brain injury [113]. It draws a parallel to engineering design, where, similar to the relationship

between normal and shear stresses in maximum in-plane shear, GAMBIT connects linear and angular acceleration [114].

$$GAMBIT = \left[\left(\frac{a(t)}{a_c}\right)^n + \left(\frac{\alpha(t)}{\alpha_c}\right)^m\right]^{1/S} \quad \text{Equation 3}$$

where

a_t = linear acceleration

α_t = rotational acceleration

a_c = critical linear acceleration above which severe head injury would occur (set to 250 g based on analysis of automotive accident database) [66]

α_c = critical rotational acceleration above which severe head injury would occur (set to 25 000 rad/s^2 based on analysis of automotive accident database) [66]

n,m,S = empirical constants selected to fit available data

Through an examination of automotive accident data and simulations, it was determined that recommended critical values are 250 g and 25,000 rad/s² for linear acceleration and rotational acceleration respectively [66], [115]. Two options were mentioned for the exponent n,m and s: When all empirical constants are set to 1, translational and rotational components are correlated linearly. When all empirical constants are set to 2, translational and rotational components are correlated with an elliptical function. When the empirical constants are set to 2, a threshold of G = 1 signifies a 50% likelihood of AIS 3+ head injury [66], [70].

2.6.1.6 Head Impact Power (HIP)

Head Impact Power (HIP), another metric integrating both linear and rotational acceleration, was introduced in year 2000 [71]. The underlying premise of HIP is that a particular level of kinetic energy transferred to the head signifies a critical threshold for head injury. The derivation of HIP involved expressing the WSTC in the form of rate of change in kinetic energy.

$$HIP = 4.5a_x \int a_x dt + 4.5a_y \int a_y dt + 4.5a_z \int a_z dt + 0.016\alpha_x \int \alpha_x dt + 0.024\alpha_y \int \alpha_y dt + 0.022\alpha_z \int \alpha_z dt$$

Equation 4

where

a = linear acceleration of head about x, y and z axes

α = rotational acceleration of head about x, y and z axes

Note that the coefficients, equivalent to the mass and moment of inertia for each head axis, are adjustable based on the head's directional sensitivity to impact.

2.6.1.7 Kleiven's Linear Combination (KLC)

Kleiven's linear combination (KLC) was introduced in 2007, a metric that linearly combines HIC and the maximum change in rotational velocity [116]. KLC was one of the proposed injury predictors as it exhibited a high correlation with brain tissue strain observed in finite element simulations of head impacts in American football players [66], [116].

$$KLC = 0.004718\Delta\omega_r + 0.000224HIC$$

Equation 5

where

$\Delta\omega_r$ = maximum change in rotational velocity

HIC = Head Injury Criterion injury metric

2.6.1.8 Principal Component Score (PCS)

In 2008, Greenwald et al. introduced the Principal Component Score (PCS), a metric that integrates four distinct parameters: linear acceleration, rotational acceleration, HIC, and SI [117]. This metric was empirically derived using an extensive dataset obtained from helmet-mounted accelerometers worn by American high school and college football athletes. Over three football seasons, a thorough examination of 289,916 head impacts revealed 17 diagnosed concussions.

PCS was applied to establish relationships between each parameter and the identified concussions.

$$PCS = 10 \times ([0.4718 \times sSI + 0.4742 \times sHIC + 0.4336 \times sa + 0.2164 \times s\alpha\ ] + 2) \quad \text{Equation 6}$$

$$sX = \frac{X - mean[X]}{standard\ deviation\ [X]} \quad \text{Equation 7}$$

where

SI = severity index metric

HIC = head injury criterion metric

a = linear acceleration

α = rotational acceleration

Subsequently, the weighted form of PCS (wPCS) was suggested to account for severity of impacts based on location of impact. The weighting coefficients for each impact location are 1.00 for side, 0.95 for front, 0.62 for back, and 0.48 for top.

2.6.1.9 Combined Probability of Concussion (CP)

Rowson et al. formulated a concussion risk function by examining helmeted impacts in football players. This metric, CP, was derived through the application of multivariate logistic regression, using recorded data to model risk with a combination of linear and rotational accelerations [118].

$$CP = \frac{1}{1 + e^{-(-10.2+4.33x10^{-2}a+8.73x10^{-4}\alpha-9.20x10^{-7}a\alpha)}} \quad \text{Equation 8}$$

where

a = peak linear acceleration during impact

α = peak rotational acceleration during impact

This risk function has been used to assess variations in the protective effectiveness of football helmets, hockey helmets, soccer headgear [119], [120], [121].

2.6.1.10 Power Rotational Head Injury Criterion (PRHIC)

As awareness of the importance of rotation in understanding concussions increased, studies began to focus on rotational metrics as well. For instance, in 2011, Kimpara et al. introduced two rotational-only techniques by modifying HIC. The first, referred to as PRHIC, involves substituting the linear acceleration term of the HIC injury metric with the rotational component of the HIP injury metric [122].

$$PRHIC = \max\left[\frac{1}{t_2 - t_1}\int_{t_1}^{t_2} HIP_{rot}\,dt\right]^{2.5}(t_2 - t_1) \qquad \text{Equation 9}$$

2.6.1.11 Rotational Head Injury Criterion (RIC)

The second rotation metric introduced by Kimpara et al. is RIC. Similar to PRHIC, RIC is obtained by replacing the linear acceleration term in the HIC injury metric with rotational acceleration [122].

$$RIC = \max\left[\frac{1}{t_2 - t_1}\int_{t_1}^{t_2} \alpha(t)\,dt\right]^{2.5}(t_2 - t_1) \qquad \text{Equation 10}$$

2.6.1.12 Brain Injury Criterion (BrIC)

The first iteration of BrIC, introduced by Takhounts et al., incorporated both angular velocity and angular acceleration [123]. This metric was designed with the aim of evaluating the risk of brain injuries, specifically diffuse axonal injury (DAI), in occupant crash tests that might not be detected by the conventional Head Injury Criterion (HIC).

$$BrIC = \frac{\omega_m}{\omega_{cr}} + \frac{\alpha_m}{\alpha_{cr}} \qquad \text{Equation 11}$$

where

ω_m = maximum resultant angular velocity

α_m = maximum resultant angular acceleration

ω_{cr} = critical angular velocity

α_{cr} = critical angular acceleration

In 2013, Takhounts et al. proposed a revision to the original BrIC formula, modifying it to include angular velocity solely. Their investigations indicated that relying on angular velocity alone proved sufficient in predicting FE model strains in both pendulum and occupant crash tests [124]. This updated criterion, denoted by Equation 12, is formulated by assessing the maximum magnitudes of the three orthogonal components of head angular velocity.

$$BrIC = \sqrt{\left(\frac{\omega_x}{\omega_{xcr}}\right)^2 + \left(\frac{\omega_y}{\omega_{ycr}}\right)^2 + \left(\frac{\omega_z}{\omega_{zcr}}\right)^2} \qquad \text{Equation 12}$$

where

ω_x = maximum angular velocity in x axis (rad/s)

ω_y = maximum angular velocity in y axis (rad/s)

ω_z = maximum angular velocity in z axis (rad/s)

ω_{xC} = critical angular velocity in x axis (rad/s) set at 66.30 rad/s

ω_{yC} = critical angular velocity in x axis (rad/s) set at 53.80 rad/s

ω_{zC} = critical angular velocity in x axis (rad/s) set at 41.50 rad/s

In contrast to earlier rotational criteria, BrIC dissects angular velocity into distinct directional components, thereby accounting for variations in injury tolerance based on direction. Note that Gabler et al. demonstrated that BrIC is among the most closely correlated kinematic response metrics with brain deformation [114]. In their study, they established correlations between 15 distinct kinematic response metrics and two tissue-based metrics MPS and CSDM obtained from simulating those impacts using FE head models. The objective was to identify the kinematic response metrics that are most suitable to predict brain response.

2.6.1.13 UBrIC and DAMAGE

Gabler et al. have introduced two kinematic-based metrics, UBrIC and DAMAGE, which aim to predict brain injury severity [125], [126]. They argue that existing metrics have been mostly

derived empirically, and that computational modeling offers potential but often demands significant time and expertise with solvers to provide a quick injury severity assessment. Both metrics are based on the assumption that maximum brain deformation under rotational head motion is similar to deformation from a second-order system under excitation [125]. UBrIC predicts strain-based responses from finite element brain models, using directionally dependent magnitudes of angular velocity and acceleration [125]. On the other hand, DAMAGE predicts maximum brain strain based on three-degree-of-freedom, coupled second-order system equations, using directionally dependent angular acceleration time-histories [126]. In other words, DAMAGE predicts maximum brain strain from triaxial rotational acceleration time histories rather than peak rotational head kinematics. However, the efficacy of UBrIC and DAMAGE hinges on the accuracy of the FE model. Additionally, these metrics predict global MPS, which has historically been correlated with diffuse brain injury. However, the evolving focus of computational mTBI studies now leans towards regional brain strain responses.

2.6.1.14 Examples of Kinematic Metrics Thresholds

Table 2: Examples of Kinematic Metric Thresholds

Metric	Injury	Threshold	References
Average peak linear acceleration	Diagnosed concussion in female ice hockey athletes	43.0g ± 11.5*g*	[128]
	Diagnosed concussion in American football male athletes	112.1g ± 35.4g	[129]
GSI	Diagnosed concussion in American football male athletes	439.3 ± 315.2	[129]
	Life-threatening head injury	1000	[66]
HIC_{15}	31% of AIS2+ injury	700	[29]
	Diagnosed concussion in American football male athletes	321.5 ± 239.4	[129]
	10% risk of concussion	400	[130]
Average peak rotational acceleration	Diagnosed concussion in female ice hockey athletes	4030±1435 rad/s^2	[128]
	Diagnosed concussion in American football male athletes	4253 ± 2287 rad/s^2	[129]
HIP	50% risk of concussion derived from American football impacts	12.79 kW	[71]

2.6.1.15 Shortcomings of Kinematic Metrics

The effectiveness of kinematic-based metrics, such as HIC, in predicting traumatic brain injuries is well-established for severe cases but remains uncertain for milder injuries like concussions [110]. Studies attempting to establish injury risk functions based on head impact data reveal significant variations in concussion risk thresholds. For instance, one study suggests a mere 10% concussion risk at an HIC value of 47 [68], while another identifies an HIC value of 400 for a 10% risk of concussion [130].

Furthermore, kinematic-based metrics, derived from correlations between head kinematics measurements and surrogate outcomes, such as cadaver skull fractures, introduce inherent limitations. These metrics not only oversimplify the complex mechanics of the human brain's response to inertial loads but also rely on assumptions that may not accurately capture real-world scenarios [73]. Additionally, consider controlled cortical impact (CCI) experiments, a classic example of inducing brain damage in a laboratory setting with minimized linear and rotational accelerations. This emphasized a fundamental limitation of using kinematic-based injury metrics in predicting injuries. In scenarios like CCI, where brain damage is induced without substantial accelerations, traditional metrics fail to accurately predict the injuries [37].

2.6.2 FE Models

To address these limitations, recent metrics have been developed using FE models for a more comprehensive understanding, especially in situations where conventional kinematic metrics may fall short. FE models prove invaluable for studying the mechanical response of the brain during impacts. Linear and rotational head movements, along with direct impacts, induce responses at the tissue level in the brain. Even in mild forms, these responses, characterized by strain and stress, can adversely affect brain cells and function. The advantage of FE models lies in their ability to describe these strain/stress reactions. When coupled with tissue-level injury tolerances, these models are valuable for better understanding brain injuries [37].

Additionally, since FE models offer a means to predict tissue strain, they contribute to bypassing the ongoing debate about the relative importance of rotational versus translational acceleration [29] as both kinematic components can be used as inputs to the model. Various institutions

worldwide have developed FE models, and the extensive experimental work, involving physical models and studies with human surrogates and volunteers, generates valuable information essential for validating the accuracy and reliability of these computational models.

Some examples of current state of art finite element head models include KTH, SIMon, THUMS and GHBMC.

2.6.2.1 KTH Head Model

The Kungliga Tekniska Hogskolan (KTH) head model was first developed by Kleiven et al. in 2002 [131], [132]. The most recent version comprises 21,345 elements and includes the skull, facial bones, scalp, cerebrum, cerebellum, dura matter, falx, and a simplified brainstem [52]. Recognizing the inherent nonlinear and viscoelastic properties of biological tissues [133], the KTH head model employs a second-order viscoelastic Ogden model to characterize brain tissue. Furthermore, the latest versions of the model [52], [134] incorporate the anisotropy of white matter. A comparative analysis revealed that the anisotropic version better aligns with experimental data, enhancing the model's fidelity [135]. Validation of the model includes assessments against pressure experiments by Nahum et al. (1977) [136], PMHS tests by Trosseille et al. (1992) [137], and relative motion tests conducted by Hardy et al. (2001) [63]. Numerous studies have used this model [52], [59], [138]. For example, through the application of the KTH model, predictions have been made regarding the maximum axonal strain for reversible injury, estimating it to be 0.07 in the corpus callosum and 0.15 in the brainstem [52].

2.6.2.2 SIMon Head Model

In 2003, Takhounts et al. introduced the Simulated Injury Monitor (SIMon) Finite Element Head Model, designed with relatively simple geometry to adhere to a two-hour runtime constraint [139]. The SIMon FEHM featured a rigid skull, a combined dura-and-cerebrospinal fluid (CSF) layer, a brain, falx cerebri, and bridging veins. However, it did not account for the cerebellum and midbrain. This simplified model, representative of a 50^{th} percentile male, comprised 7852 elements. In 2008, Takhounts et al. subsequently enhanced the SIMon FEHM to focus on studying traumatic brain injuries [140]. This upgraded model incorporated detailed surfaces of the cerebrum, cerebellum, and brainstem, derived from CT scans approximating 50^{th} percentile male

geometries. The mesh expanded to 45,875 elements. The model included key components of the brain such as the cerebrum, cerebellum, brainstem, ventricles, combined CSF and pia arachnoid complex layer, falx, tentorium, and parasagittal blood vessels. The SIMon head model employs a Kelvin-Maxwell linear viscoelastic model characterize brain tissue. Validation of the model includes assessments against pressure experiments by Nahum et al. [136], PMHS tests by Trosseille et al. [137], and relative motion tests conducted by Hardy et al. [63]. This advanced SIMon FEHM demonstrated that a side curtain airbag reduced the potential for brain injury in side impact crashes. The results strongly suggested that angular injury criteria were more predictive of TBI than linear acceleration-based injury criteria.

2.6.2.3 THUMS Head Model

The Total Human Model for Safety (THUMS), a complete human body model, was developed by the Toyota Motor Corporation and Toyota Central Research & Development Laboratories to study detailed injury mechanisms rather than relying on the traditional crash test dummies [141]. Kimpara et al. modified THUMS by isolating the head and neck parts to investigate their biomechanical response during severe frontal impacts [142]. The brain geometry, consisting of the cerebrum, cerebellum, brainstem sagittal sinus, meninges, falx cerebri, tentorium cerebelli and cerebrospinal fluid, was obtained from the NLM Visible Human Project [143]. The resulting model, excluding the neck, comprised 49,579 elements, with a minimum mesh size of 2 mm. THUMS used a linear viscoelastic model to characterize brain tissue and was validated against three sets of brain test data [63], [136], [137].

2.6.2.4 GHBMC Head Model

The GHBMC M50 HBM was developed based on the anatomy of a 26-year-old male subject using computed tomography and magnetic resonance imaging techniques [26]. The development process involved the creation of distinct body region models for the head, neck, upper extremities, thorax, abdomen, and lower extremities, each undergoing independent development and validation before seamless integration into the comprehensive full-body model. The GHBMC head model comprises of 270,552 elements and includes the cerebrum, cerebellum, brainstem, ventricles, bridging veins, cerebrospinal fluid (CSF), skull, facial bones,

meninges, falx, and tentorium. A tied contact algorithm was used between the dura and arachnoid layers, with a linear viscoelastic constitutive model chosen for the brain tissues, CSF and face while other tissues were modeled as linear elastic. Rigorous validation against an array of experimental studies, including assessments by [62], [63], [136], [137], confirms the predictive capabilities of the GHBMC M50 HBM.

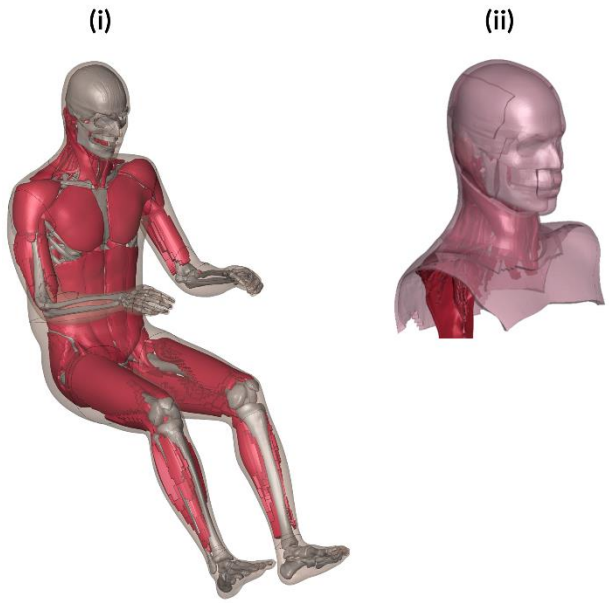


Figure 12: (i) The GHBMC M50 full human body model and (ii) the GHBMC M50 head and neck model.

2.6.2.5 GHBMC Isolated Head Model Validation

In this investigation, the isolated head and brain model was used, extracted from the GHBMC model (v5.0), to examine brain strains efficiently without the added computational time of modeling the entire body. This approach aligns with previous studies, such as David Bruneau's work on investigating brain response in football helmet impacts.

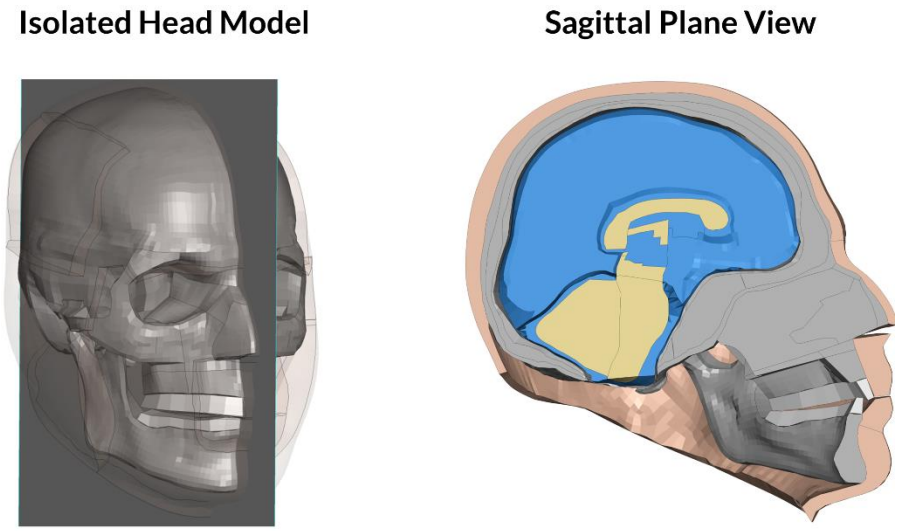


Figure 13: The isolated GHBMC M50 head model (without neck region).

The brain region in the model had a total of 22 components, including the brain tissues, arachnoid, pia matter, falx, tentorium and CSF. The brain tissues had a total mass of 1.16kg and was divided into 8 brain regions (cerebellum, cerebrum gray matter, corpus callosum, thalamus, brainstem midbrain, brainstem, basal ganglia, cerebrum white matter) as listed in Table 3. There were four types of brain material (grey matter, white matter, brain stem and CSF), each with different material properties, assigned to each brain region. The material properties of the brain tissue (listed in Table 4) were determined using values from the literature, as well as testing data from Wayne State University [26]. The corpus callosum of the GHBMC head model was assigned white matter material properties. The following regions: the cerebellum, thalamus, brainstem and basal ganglia on the other hand, were assigned grey matter material properties. Additionally, the outer cerebrum region was assigned grey matter material properties while the inner region was assigned white matter material properties. A Maxwell viscoelastic model (Equation 13) was used to represent the brain tissues and CSF [144]. The meninges, falx and tentorium on the other hand were modelled using an elastic material model [26].

Table 3: List of brain tissues

Brain region	Material	Number of elements	Mass (kg)
Cerebellum	Grey matter	14280	0.123
Cerebrum grey matter	Grey matter	22700	0.491
Thalamus	Grey matter	260	0.012
Basal ganglia	Grey matter	1284	0.026
Brainstem midbrain	Grey matter	504	0.010
Brainstem (pons and medulla)	Grey matter	2280	0.022
Corpus callosum	White matter	980	0.021
Cerebrum white matter	White matter	23340	0.455

Table 4: Brain tissue material properties [26]

Brain Material	Density (kg/m^3)	Bulk Modulus (GPa)	Short-time Shear Modulus (kPa)	Long-time Shear Modulus (kPa)	Decay Constant (β)
Grey matter	1060	2.19	6	1.2	80
White matter	1060	2.19	7.5	1.5	80
CSF	1040	2.19	5	1	80

$$G(t) = G_\infty + (G_0 - G_\infty)e^{-\beta t} \quad \text{Equation 13}$$

where

G_∞ = Long-time shear modulus

G_0 = Short-time shear modulus

β = Decay constant

2.6.3 Tissue-Based Metrics

In computational models, it is important to establish measurable metrics associated with brain injuries. Early research primarily focused on tissue strain as a key indicator, with initial experimental work demonstrating that overstretching could induce significant physiological changes in the tissue. For example, tests on squid giant axons revealed altered depolarization responses during stretching, with neurons failing to fully revert to normal function above a 20%

strain level [145]. These findings, along with additional studies [146], highlighted the potential for physiological dysfunction due to tissue strains, establishing peak tissue strain as a foundational measure for assessing the risk of brain injury.

Researchers are actively working on identifying specific thresholds in brain tissue for concussive injuries using FE modeling, considering them more predictive for concussions than kinematic measures alone [52], [59], [66], [147], [148]. Various finite element-based metrics, such as MPS, CSDM, pressure, stress, and the product of strain and strain rate, have been explored to predict tissue injuries. Typically, kinematic data obtained from in vivo measurements or video reconstructions are used as the boundary conditions for simulation models.

While some studies suggest a link between elevated strain in any brain region and a potential indication of concussion, others argue that specific areas, such as the corpus callosum, may serve as more reliable predictors [53], [54], [59], [149]. However, a consensus is currently lacking regarding the brain region most predictive of concussion. The broader decision on the most effective metric for predicting concussions also remains unresolved, with numerous metrics in the literature, each associated with multiple reported thresholds.

One widely used metric, Maximum Principal Strain (MPS), has consistently been associated with observed concussions [54], [56], [59], [150], [151], [152], [153]. Yet, there is significant variability in proposed thresholds. For example, one study simulated impacts in American football and ice hockey, reporting a mean strain value of 0.28 in the corpus callosum, which aligned with changes in white matter integrity observed through fractional anisotropy in MRI scans [153]. Another study by Hernandez et al. highlighted MPS in the corpus callosum as the most reliable indicator of concussion, with an average strain of 0.3 [59], surpassing findings from [116], who reported a mean strain value of 0.21 in concussed athletes. Patton et al. examined brain tissue deformation in unhelmeted sports, simulating reconstructions of unhelmeted concussion, finding a mean strain value of 0.31 in the corpus callosum in concussion cases and determining a 50% likelihood of concussion above a strain level of 0.15 [53].

In later studies, MPS has been reported as the 95^{th} percentile Maximum Principal Strain (MPS) [127], [154]. This represents the MPS value exceeded by 5% of the elements within a specific

region instead of reporting the maximum (100th percentile) principal strain value. The 95th percentile helps prevent simulation results from being influenced by the response of a single element [127], [154], excluding elements with artificially high strains due to numerical artifacts [154], [155], [156].

Another widely used metric for brain injury assessment is the Cumulative Strain Damage Measure (CSDM) [52], [54], [59], [116], [124], [151], [157]. CSDM calculates the total volume of the region experiencing strain levels beyond a predefined threshold. This threshold is typically set at 0.15 or 0.25 [73]. However, the correlation between CSDM and concussion is not as robust as that observed with MPS [54], [59], [116], [139]. Moreover, CSDM demonstrates high sensitivity to the chosen threshold, with a lack of consensus regarding the specific threshold for strain.

Various studies have explored pressure as an injury predictor. Ward et al. found that intracranial pressures above 235kPa lead to serious brain damage, while pressures below 173kPa are considered non-injurious [136]. In a related study, Zhang et al. used the WSUHIM model to reconstruct 12 head impacts in American football [148]. They observed coup-contre coup behavior and, in cases of concussion, noted an average intracranial coup pressure of 90kPa, correlating strongly with linear acceleration. Zhang et al. also highlighted that higher pressures, as reported by Ward et al., correlate to more severe injuries such as contusions or cerebral cortex hemorrhages, underscoring that pressure alone is not a reliable indicator of concussion.

While less commonly used, other metrics have been explored for predicting concussions. Some studies found a connection between concussion and strain rate, as well as the combination of strain and strain rate [153]. However, these metrics are generally considered less effective predictors compared to Maximum Principal Strain (MPS) [54]. Von-Mises Stress also exhibits promise as a concussion indicator, but exploration remains relatively limited compared to other measures [54]. However, available studies indicate a correlation between Von Mises Stress levels and neurological lesions. In a study by Baumgartner et al., instances of moderate neurological lesions were associated with Von-Mises stresses exceeding 18kPa, posing a 50% risk, while severe brain injury was linked to stresses surpassing 38kPa. These values align closely with the stress

observed in an experiment on head impacts in sheep. A stress of 27kPa was correlated with brain injury [158].

2.6.3.1 Summary

In summary, MPS_{95} is a frequently used metric for assessing deformation-based injury risk, as highlighted by studies such as McAllister et al [14] and Patton et al. [53,54]. This metric demonstrates a stronger association with concussion compared to kinematic metrics, as indicated by research by Hernandez et al. [59]. Nevertheless, there is a lack of consensus regarding the threshold values for MPS_{95} in predicting mTBI/concussions. The current body of literature presents a broad range of reported strains for a concussive head injury, spanning from 0.06 to 0.48 [159], with some examples listed in Table 5.

Table 5: MPS values from literature

Brain Region	Injury Probability	Threshold	References
Whole brain	Median MPS concussed value	0.16	[149]
Grey matter	50% risk	0.26	[116]
Thalamus	50% risk	0.13	[54]
White matter	50% risk	0.26	[54]
Midbrain	Mean concussed value	0.108	[55]
Cerebrum	Median MPS concussed value	0.18	[149]
Cerebellum	Median MPS concussed value	0.09	[149]
Brainstem	Median MPS concussed value	0.14	[149]
Corpus callosum	Median MPS concussed value	0.13	[149]
Corpus callosum	50% risk	0.15	[54]
Corpus callosum	50% risk	0.21	[116]

One limitation of MPS_{95} is that it only represents one maximum strain value, which often can be confined to a specific location or a small volume within the brain. Consequently, this singular metric fails to capture the overall strain distribution throughout the entire brain volume. In this thesis, we use the Cumulative Strain Volume (CSV) metric, a new metric introduced by Rycman

et al. [159], and its step-by-step derivation is outlined in the methods section. The CSV metric is a graph rather than a single value metric and presents an alternative, more comprehensive approach that considers the strain distribution across the entire brain volume without reliance on a predetermined threshold. As such, it offers a more representative measure of brain tissue response.

2.6.3.2 Metric Sensitivity to Brain Region and Impact Direction

Table 5 illustrates the variations in mTBI thresholds across different brain regions. Numerous studies suggest that certain deep inner structures, such as the corpus callosum, thalamus, brainstem, and midbrain, exhibit a higher predictability for concussions compared to other brain regions [53], [54], [55], [59]. Previous research has also emphasized that injuries are more severe when rotation is combined with translational kinematics. Additionally, both animal and computational studies have demonstrated that tolerance to acceleration varies significantly based on the anatomical direction, with coronal rotation being associated with more severe injuries in primates [59]. These studies highlight the significance of directly measuring directional components of rotational acceleration, not solely its magnitude. It is important to bear in mind that these conclusions were drawn from diverse populations and multiple finite element (FE) models. Specifically, Ji et al. highlighted that the anticipated strain for identical kinematic inputs could differ among various FE models [160].

Several studies have investigated strains in the corpus callosum, particularly in the context of mTBI [52], [59]. The corpus callosum plays a pivotal role in various cognitive functions, including perception, speech, orientation, and reaction [161]. Consequently, these cognitive functions are susceptible to impairment in the event of injury. One factor believed to influence the corpus callosum during skull rotation is the falx cerebri. For example, studies using 2D computational models have demonstrated that a softer falx or the absence of a falx may potentially maintain or decrease strains in the corpus callosum [162].

Research conducted by Bayly et al., Feng et al., and Sabet et al. offer further insights into the potential impact of the falx on inducing greater deformation in deep brain structures [163], [164], [165]. These studies used tagged MRI to measure displacements of brain tissues resulting from

both linear and rotational kinematics. Sabet et al. observed the symmetrical and asymmetrical distribution patterns in brain shear strain fields, especially in the case of mild impacts in the coronal plane [164]. This observation suggests that the falx influences neighboring brain tissue during such impacts, leading to strain at those specific locations within the brain.

In their study, Hernandez et al. investigated whether rotations in the coronal and horizontal planes displaces the falx cerebri potentially leading to significant deformation of the corpus callosum [166] . The analysis involved using an FE model to simulate head kinematics of 115 impacts recorded in a sports setting using instrumented mouthguards. The falx cerebri displacement was then correlated with deformation of the corpus callosum. The findings revealed higher mean peak coronal accelerations (8592 rad/s^2) in impacts with mTBI than those without (1412 rad/s^2). Additional findings indicated a strong correlation between coronal acceleration and movement at the center of the falx cerebri, while horizontal acceleration was strongly associated with motion around the periphery of the falx cerebri. The correlation between the corpus callosum and the falx cerebri was further highlighted by the observation that the running the model without the falx cerebri reduced the peak strains in the corpus callosum by half, decreasing from 35% to 17%.

The thalamus, another critical brain region, consistently appears as a key player in concussions, frequently identified in studies as a reliable predictor with the lowest strain threshold [54], [55]. In contrast, strains in the cerebrum grey matter [116] and cerebellum [52], [153], while linked to concussions, do not consistently exhibit the same robust predictive capability as strains in other regions. The brainstem, including the midbrain, also consistently emerges in literature as a factor associated with concussions [52], [160]. It is important to emphasize that relying solely on the head model to predict strains in the lower brainstem may impact the resulting strain values. This is because, in such cases, the brainstem is not integrated with the remainder of the full-body model. However, the use of isolated head models still remains a popular computational approach.

Investigating the direction dependence of injury, a study demonstrated that primate head rotation in the coronal plane, equivalent to human coronal head motion, led to more severe

diffuse axonal injury (DAI) than other planes of head rotation [47]. Finite element (FE) models align with such findings, showing a dependence on impact orientation. In an early brain model (WSUHIM), Zhang et al. observed higher positive pressures in a lateral impact than in a sagittal plane impact [167]. Correspondingly, studies by Patton et al. and Hernandez et al. analyzing kinematics and concussion occurrences in football found that high strains in the corpus callosum and thalamus, as well as coronal angular acceleration, correlated the most with concussion [53,54,59].

Studies consistently indicate that lateral translational impacts to the temporal region are more likely to cause mTBI than anterior or posterior impacts [118], [168]. For example, Rowson et al. noted that 57.9% of concussions in American football occurred on the side of the head (sagittal direction) [118]. Elkin et al.'s investigation of head impacts in helmeted sports also reported a significant increase in strain from lateral impacts [155]. McIntosh et al.'s study on head impacts in rugby suggested that impacts with angular accelerations as low as 1747 rad/s² in the coronal plane may lead to concussion [169].

In summary, the corpus callosum, thalamus, and brainstem midbrain regions appear to have the strongest correlation with concussions. Therefore, it is essential to analyze regional strains when studying mTBI. While MPS is the most commonly used strain metric, there is no consensus on the optimal metric or threshold for mTBI in the modeling approach. Additionally, impact direction, specifically coronal rotation, also correlates with concussion, highlighting the importance of considering this factor in the analysis.

2.6.4 Boundary Condition for Isolated Head Model

Isolated head models are a popular computational approach. For example, in a study by D. Bruneau, the isolated head model was employed to "investigate the biofidelity of the linear impactor helmet test using a contemporary human body model" [170]. This investigation consisted of three studies.

In the first study, D. Bruneau compared head kinematics between the Hybrid III and GHBMC head and neck models (HNM), including an examination of the effect of muscle activation. He reported that the ratings from both the ATD and HNM showed a stronger correlation in the lateral

orientation than in the frontal and rear orientations. All CORA ratings exceeded 0.82 (except Z acceleration) for both bare head and helmeted cases in the lateral orientation. Additionally, the response of the HNM was minimally affected by muscle activation schemes investigated.

In his second study, he explored two approaches to brain deformation: (1) replicating the experimental setup using a helmeted head and neck model and (2) applying the experimental kinematics measured from the ATD experiments to an isolated unhelmeted head model. He then compared whole-brain and regional brain deformation between these two approaches. He reported that in both approaches, the patterns of brain deformation were alike but approach (1) showed consistently higher values of whole brain MPS (averaging 23%) compared to the prescribed kinematics approach. This difference was most pronounced in frontal impacts, where higher angular velocity values were noted.

In a third study, he compared the head and neck model constrained at the First Thoracic (T1) vertebra with an unconstrained Full Human Body Model (FBM). He reported the MPS exhibited a consistent bimodal pattern in both the unconstrained full body and the constrained head and neck. The strain response was similar in the early stages, diverging slightly later, particularly after the occurrence of the two peaks. The predictions for the initial peak of MPS closely resembled those of the constrained HNM, but there was a slight difference in the second peak. The study revealed considerable differences in spine motion, particularly the curvature and T1 motion, between the constrained HNM and unconstrained FBM. The spine of the constrained HNM exhibited significantly more curvature than the FBM, indicating a higher degree of compression. The T1 motion showed substantial differences, with considerably more motion observed in the unconstrained FBM.

Given that the isolated head model has been validated against a head and neck and full body model before, the consistent preservation of the brain deformation pattern observed in study 2, and the significantly reduced computational time, the isolated head model was deemed appropriate for the investigation in this thesis, especially considering the large number of simulations run.

2.7 Subconcussive Head Exposures

Multiple studies have been conducted to understand the biomechanical force of mTBI and reduce its occurrence. Emerging research is now also looking into the potential link between mTBI symptoms and repetitive subconcussive incidents [19], [171], [172].

2.7.1 Subconcussive Head Exposures in Sports

Subconcussion, which can occur as a result of a head impact or rapid head motion that does not immediately lead to a diagnosed concussion [173], is a common occurrence in sports such as hockey and American football. Players often experience multiple impacts during play without immediate symptoms [174]. While individual subconcussive impacts may appear minor, their cumulative effect on an athlete's career could potentially lead to significant implications for neurological health [173].

Neuroimaging studies have played a crucial role in understanding the effects of repetitive sub-concussive head impacts on brain structure and function. Findings from these studies raise concerns about the potential long-term neurological consequences, emphasizing the importance of further research in this area. For example, a longitudinal study by Talavage et al. involved a comprehensive examination of high school football players, incorporating MRI, fMRI, and neurocognitive evaluations at three distinct time points, including pre-season, during the season, and post-season [175]. Remarkably, despite lacking evident signs of concussion, the players exhibited measurable neurophysiological alterations on fMRI studies and cognitive assessments. Notably, those demonstrating functional observed impairment (FOI+) displayed notable changes in fMRI activation during a working memory task, comparable to those diagnosed with a concussion (clinically observed impairment [COI+]). Similarly, a study by Bazarian et al. using diffusion tensor imaging involving nine high school athletes participating in hockey or football alongside six controls found that asymptomatic athletes with multiple subconcussive head impacts exhibited abnormalities in white matter, surpassing that of controls by more than threefold [176].

Autopsy data have revealed that athletes with no history of diagnosed concussions may still have neurodegenerative pathology consistent with chronic traumatic encephalopathy (CTE). This underscores the potential long-term consequences of subconcussive impacts. In 2005, Omalu et al. conducted one of the first studies that linked CTE with repeated mTBI [177]. It is now believed that CTE affects not only American football players but also athletes in other sports like boxing, wrestling, and hockey [173]. Military personnel are also at risk of developing CTE [178]. CTE is a progressive degenerative condition that affects the brain. Patients typically exhibit mood disorders, neuropsychiatric disturbances, and cognitive impairments after a latent period. While conventional brain examination may appear standard, detailed analysis reveals abnormal tau protein deposits indicative of neuronal damage, especially in regions like the neocortex, subcortical areas, and brainstem. Interestingly, a study involving several former professional football players who had no documented history of concussions demonstrated similar neuropathological features consistent with CTE [177], [178]. Such studies show the possibility of subconcussion, where repetitive head impacts may lead to tauopathy and subsequent brain injury, even in the absence of diagnosed concussions.

The emerging understanding of subconcussion highlights the need for comprehensive preventive strategies in sports and other activities prone to repetitive head impacts. Efforts to minimize exposure to subconcussive events are essential to safeguarding the neurological health of athletes and individuals at risk of cumulative head trauma.

2.7.2 Subconcussive Head Exposures in Military

The surge in brain injury studies followed the ground-breaking research by Omalu et al., who identified CTE in professional American football athletes [177]. Subsequent studies corroborated his findings [179], [180], [181], raising concerns about repetitive sub-concussive leading to the increased potential of incurring chronic brain injuries. These injuries can significantly impact an individual's well-being, placing a significant strain on society. In the later stages of CTE, those affected may experience symptoms like depression, cognitive decline, speech impairments, and an increased risk of suicide [182]. This concern also led to an increase in medical research within

the military, initially focusing on blast exposure from improvised explosive devices (IEDs) [183], [184], [185].

The term 'overpressure' describes the pressure exceeding normal atmospheric levels, typically observed in explosive events [186]. Studies have investigated the experiences of 'breachers,' a specific military group regularly exposed to low-level blasts as part of their duties [187]. These exposures, often below the 4-psi threshold for incident overpressure exposure intended to prevent eardrum injury, have been linked to various symptoms, collectively termed 'breacher's brain.' These symptoms, including altered reaction time and headaches, resemble those of clinically diagnosed mTBI. However, current regulations overlook the impact of non-incident components of primary blast exposure on individuals below this threshold [187], [188]. Therefore, further studies are warranted to better understand and address these effects.

Additionally, beyond blast exposure, operational training involving .50 caliber rifle systems has emerged as another source of overpressure exposure for military personnel [189]. Firing such rifles produces consistent overpressure levels exceeding the safety threshold of 4 psi, with variations based on rifle configuration and environmental factors [190]. Innovative solutions like suppressors have been developed to mitigate overpressure, redirecting gases and reducing sound levels [191].

However, it essential to acknowledge that firing .50 caliber rifles also imparts significant movement to the operator’s head due to recoil forces transmitted through the shoulder and neck [192]. The hypothesis is that repeated exposure to these recoil forces during training and active duty poses a potential source of chronic injuries [24], [193]. Such injuries can substantially compromise an individual's quality of life, imposing a considerable burden on society. Despite the extensive exploration of the long-term effects of mTBI in athletes, military personnel still remain an understudied population in this context. Hence, the aim of this thesis is to quantify the impact of recoil forces during the firing of long-range rifles.

3 Methods

The GHBMC 50th percentile male FE model, a contemporary and validated HBM, was used in this study to investigate both the kinematic and tissue-level responses of the brain to rifle recoil. The head kinematics of several volunteers from the Canadian Armed Forces (CAF) as they fired different rifle configurations (Figure 14(a)) were collected using custom instrumented mouthguards (Figure 14(b)). The head model was extracted from the full HBM, referred to as the isolated head model hereafter. The measured head kinematics then served as inputs to an isolated head model (Figure 14(c)). Subsequently, the brain response due to the measured head kinematics resulting from the recoil forces was then quantified using a set of four metrics: Head Injury Criterion (HIC_{15}), Brain Injury Criterion (BrIC), 95th percentile Maximum Principal Strain (MPS_{95}) and Cumulative Strain Volume (CSV) curves (Figure 14(d)). Two of these metrics, HIC_{15} and BrIC, were directly calculated from kinematic measurements, while MPS_{95} and CSV were calculated from the head model simulations. The analysis comprised of three main parts:

1. Evaluating similarities and differences between different rifle configurations fired by volunteers (referred to as 'inter rifle' in the Results section) and between different volunteers firing the same rifle (referred to as 'inter volunteer' in the Results section). This comparison involved analyzing head kinematics graphs and evaluating the mean and coefficient of variation of the four metrics: HIC_{15}, BrIC, MPS_{95}, and CSV.
2. Investigating the response of eight distinct brain regions (cerebellum, cerebrum gray matter, cerebrum white matter, corpus callosum, thalamus, midbrain brainstem, brainstem, and basal ganglia) using the CSV metric to identify any specific brain region experiencing higher strain.
3. Analyzing the area under the CSV curves (A_{CSV}) to explore the influence of angular velocity and linear acceleration on strain outputs.

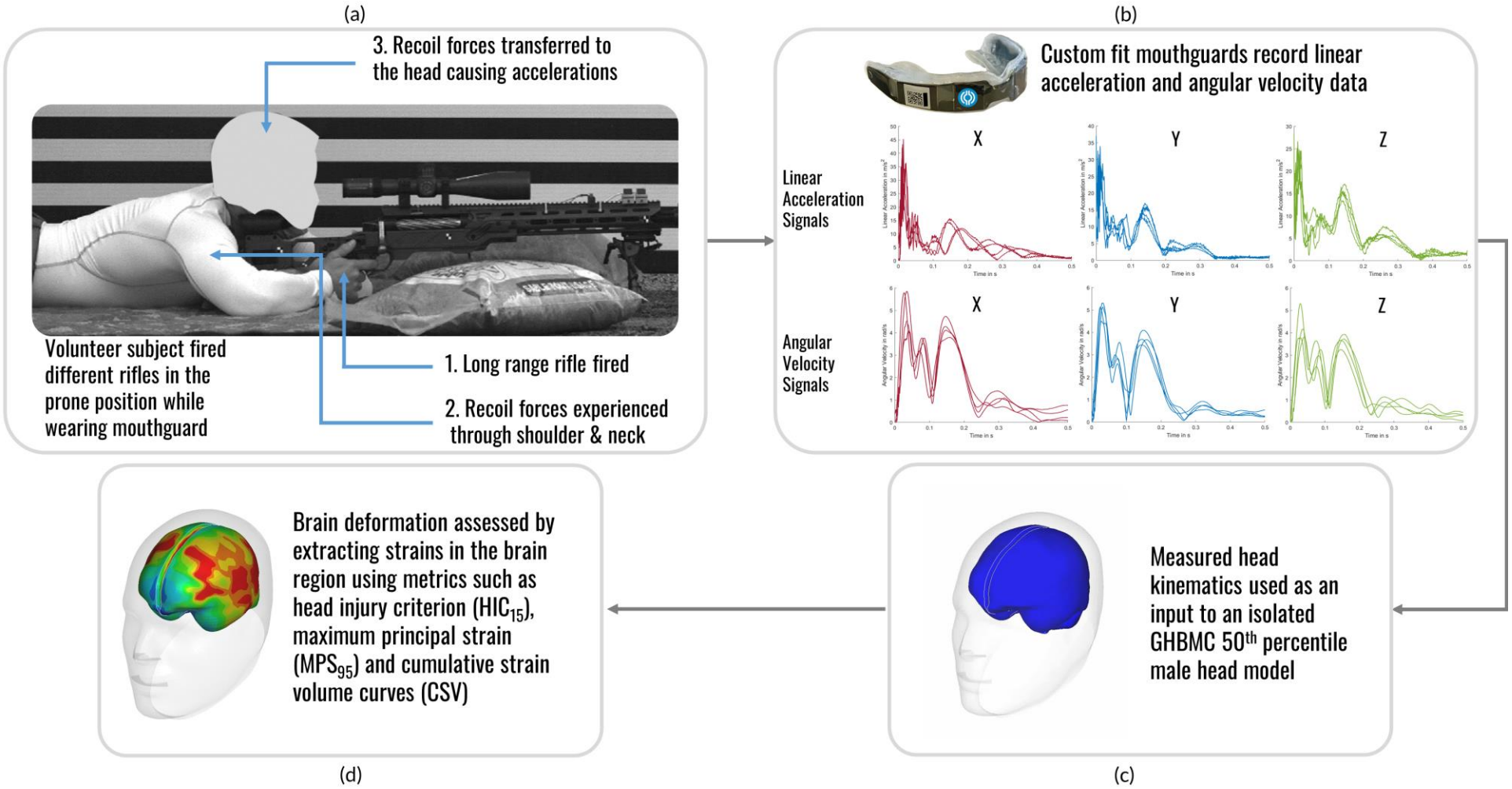


Figure 14: (a) The volunteer fired the long-range rifle. (b) Head kinematics data, including linear acceleration and angular velocity, were collected using instrumented mouthguards. (c) The head kinematics were then used as inputs to an isolated GHBMC 50th percentile head model. (c) Strains were extracted from the head model to quantify brain deformation.

3.1 Experimental Data Collection

3.1.1 Datasets Overview

The researchers at the Valcartier Research Centre, a division of Defense Research and Development Canada (DRDC), conducted all the human volunteer experiments and measurements under the ethics approval granted by the DRDC Human Research Ethics Committee (HREC-2021-009). Ethics approval for secondary analysis of anonymized data from the human volunteer tests was obtained from the University of Waterloo Office of Research Ethics (ORE #44306). Two primary datasets, labeled “Dataset 1: May 2021” and “Dataset 2: May 2022”, were used in this study (Figure 15). Dataset 1: May 2021 involved three volunteers (referred to as Volunteers 1 – 3) from the CAF, while Dataset 2: May 2022 included five volunteers (referred to as Volunteers 4 – 8). It is important to note that the volunteers exhibited varying anthropometrics; however, due to the small sample size and adherence to ethical guidelines preventing subject identification, the specific anthropometrics were not disclosed.

Dataset 1: May 2021 focused on three weapon platforms, Rifles A, B, and C, all of which were .50 caliber, suppressed rifles. Rifles A and B shared the same chassis manufacturer, and Rifle B was additionally equipped with a recoil mitigation system (RMS). In contrast, Rifle C featured a different chassis manufacturer and no RMS. In Dataset 2: May 2022, two weapon platforms, Rifles D and E, were investigated. The chassis manufacturer for these platforms was not provided. Rifles D and E were .338 and .50 caliber rifles, respectively, both suppressed. Note that Rifle E from Dataset 2: May 2022 was the same caliber rifle as the ones in Dataset 1: May 2021. The same type of ammunition was used for all rifles within each dataset.

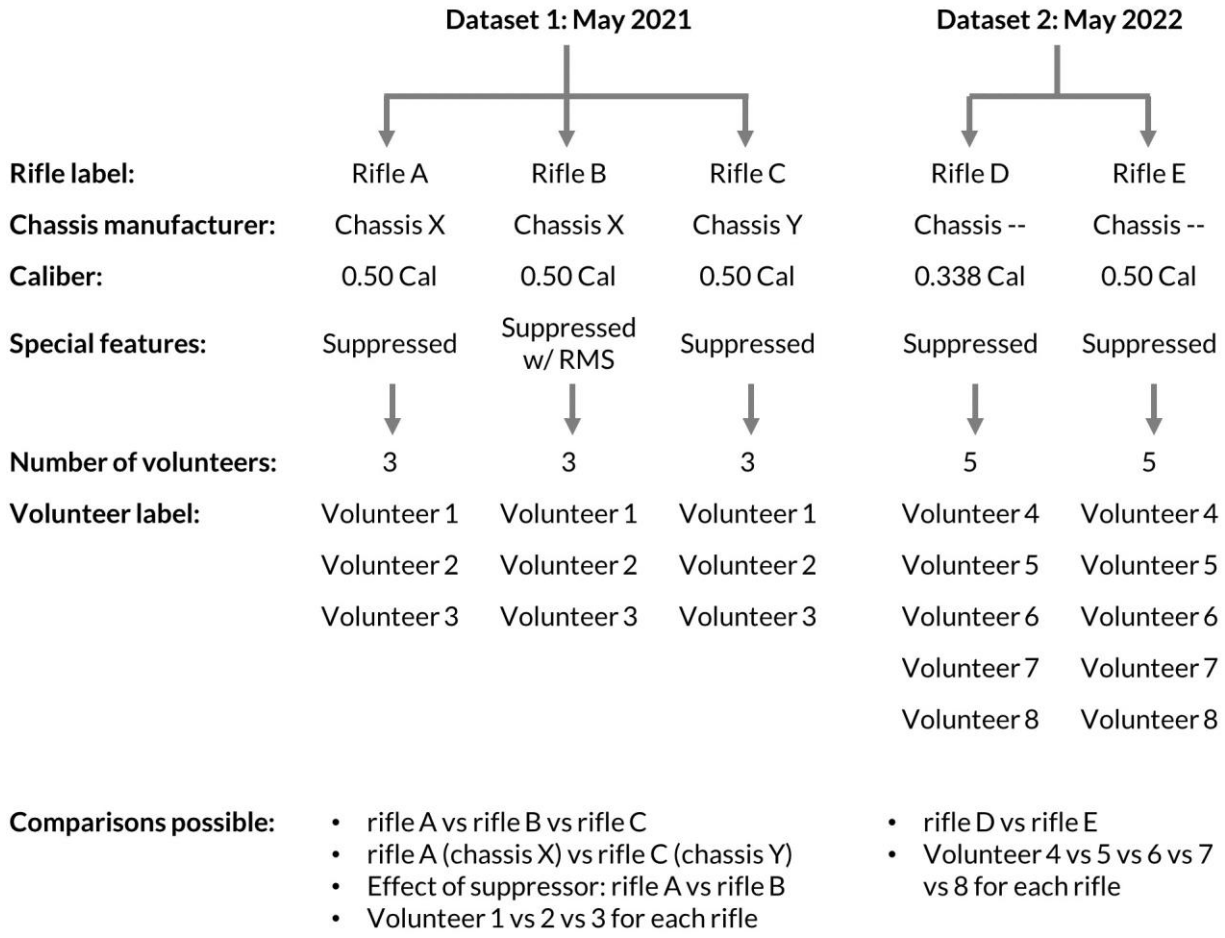


Figure 15: Overview of datasets collected during experimental trials at DRDC

3.1.2 Experimental Set Up

The volunteers, all trained and experienced snipers, fired every round from the prone position and were instructed to maintain their usual posture and routine. The front-end of the rifle was supported on a bipod, with an additional flexible support beneath the buttstock. In the prone position, the volunteers lay on their stomachs behind the rifle, with their cheek placed against the buttstock to facilitate the use of the telescopic sight mounted atop the rifle (Figure 16).

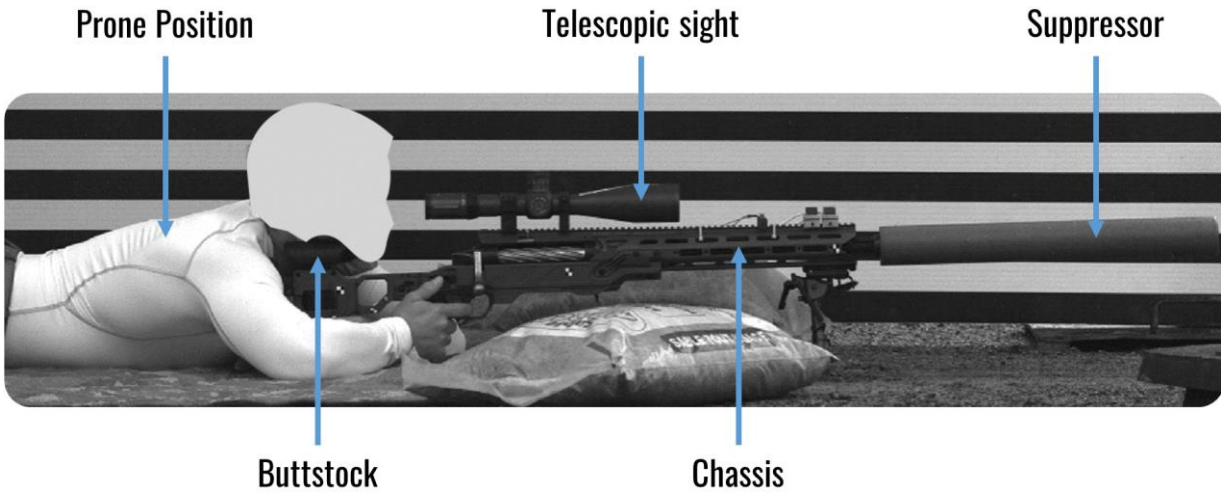


Figure 16: Volunteer in prone position

High-speed videos were acquired at 3000 fps using a high-speed camera (FASTCAN SA-Z, Photron, San Diego). The number of shots per rifle for each volunteer are shown in Tables Table *6* and Table *7*. To minimize the exposure of volunteers, the number of repetitions was kept to a minimum.

Table 6: Weapon platforms and number of shots per volunteer in Dataset 1: May 2021.

Dataset 1: May 2021			
Rifle Configuration	**Number of shots per volunteer per rifle**		
	Volunteer 1	Volunteer 2	Volunteer 3
Rifle A (chassis X, 0.50Cal, Suppressed)	4	2	3
Rifle B (chassis X, 0.50Cal, Suppressed, w/ RMS)	4	4	3
Rifle C (chassis Y, 0.50Cal, Suppressed)	4	4	3
Total number of shots per volunteer	12	10	9
Total number of shots	31		

Two of the four shots fired by Volunteer 2 using Rifle A were considered for the analysis. The remaining two were excluded due to ‘scope bites’, incidents where the volunteer's head unintentionally contacts the telescopic sight, resulting in undesired head accelerations.

Table 7: Weapon platforms and number of shots per volunteer in Dataset 2: May 2022.

Dataset 2: May 2022					
Rifle Configuration	**Number of shots per volunteer per rifle**				
	Volunteer 4	Volunteer 5	Volunteer 6	Volunteer 7	Volunteer 8
Rifle D (0.338Cal, Suppressed)	36	2	33	8	5
Rifle E (0.50Cal, Suppressed)	11	15	6	18	10
Total number of shots per volunteer	47	17	39	26	15
Total number of shots	144				

3.1.3 Mouthguard Data Collection

Head kinematics resulting from recoil forces were recorded using custom-designed instrumented monitoring mouthguards (IMM), v1.5, developed by Prevent Biometrics (USA). The tri-axial linear accelerometer and gyroscope, embedded in the mouthguards, captured linear accelerations and angular velocities across three axes at 1600Hz. Interaction with the mouthguards was facilitated by connecting to an iOS application developed by Prevent Biometrics via Bluetooth. This iOS app granted users the ability to adjust certain experiment parameters, including the trigger threshold for initiating recording and the ability to record using either a low-range accelerometer (0-16g) or a high-range accelerometer (0-200g). For this study, the low-range accelerometer was used to record head kinematics induced by recoil forces. Additionally, a trigger threshold of 2.5 g was applied, capturing 500 ms of data, which included 7.5 ms of pre-trigger data.

When processing the raw mouthguard data, several important factors needed consideration. Firstly, recording commenced once any axis exceeded the user-defined threshold (2.5g), potentially leading to variations in how and when the recordings were triggered depending on the volunteer's initial head position. Secondly, the acceleration detected the influence of gravity that is it consistently measured 1g.

As mentioned above, the mouthguard measured a brief 7.5 ms of pre-trigger data, equivalent to 10-12 data points. This pre-trigger data, representing stationary data, is crucial for post-processing the raw mouthguard data as it enables the computation of the volunteer's head's initial orientation. This orientation, in turn, represents the gravitational components when the head is stationary.

Consequently, the mouthguard data was categorized into shots with stationary pre-trigger data (considered "good captures") and those without (deemed "late captures"). While most processing methods outlined below were similar for both categories, "late captures" required additional data augmentation. Raw mouthguard data was retrieved via the Prevent Biometrics iOS app and transferred to a workstation running MATLAB R2022b or later. Data processing was then conducted using in-house MATLAB scripts developed by DC Hartlen, a doctoral candidate in the IMMC group. Ethics approval for analyzing human volunteer data was obtained from the University of Waterloo Office of Research Ethics (ORE #44306).

3.2 Post-processing

3.2.1 Post-Processing for “Good Captures”

The key steps of raw data processing such that it can be used as inputs into the head model are outlined below.

Step 1: The raw data was converted from bits to physical measurements. The low-range accelerometer had a sensitivity of 208.7 bits/(m/s^2), and the gyroscope had a sensitivity of 16.4 bits/(°/s).

Step 2: The measured data was then transformed from the mouthguard sensor frame of reference (Figure 17 (a)) to the SAE J211 frame of reference (Figure 17 (b)) through a set of three

rotations: a 15° rotation around the x-axis, a 105° rotation around the y-axis, and a 180° rotation around the z-axis, following the right-hand rule and counter clockwise positive conventions for orientation. These rotations adjust for the sensor positions within the mouthguard, the mouthguard's curved shape, and alignment with the volunteer's dental occlusal plane.

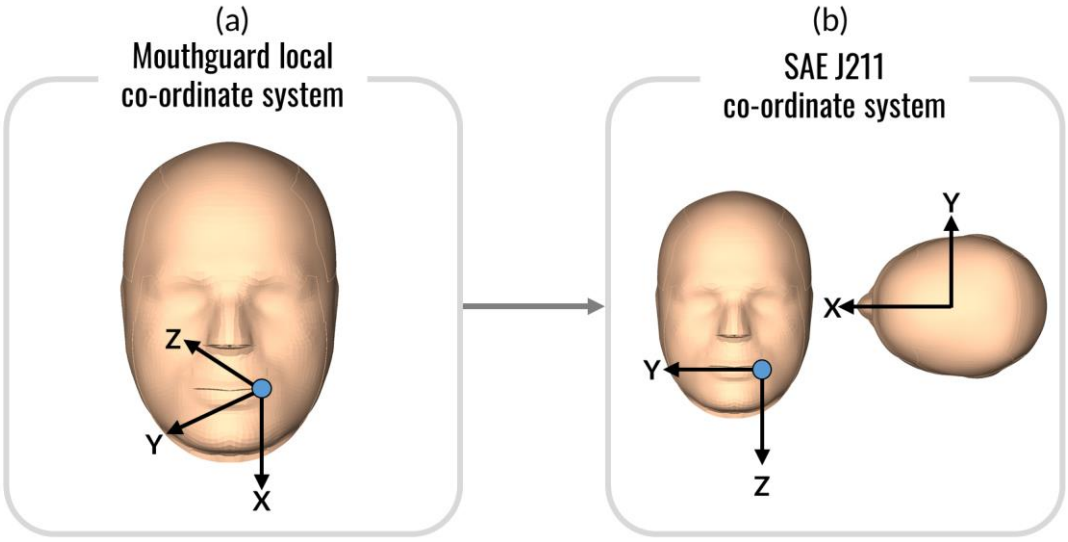


Figure 17: The data is collected in the (a) mouthguard coordinate system and transformed to the (b) SAE J211 coordinate system

Step 3: The acceleration components recorded when the volunteer's head was stationary prior to the recoil event represented the initial orientation of the volunteer's head. Hence, the initial head position for each signal was determined by averaging the pre-trigger data points.

Step 4: Then, the acceleration data was zeroed by subtracting the initial head position determined in step 3 from the signal.

Step 5: Following this adjustment, the linear acceleration and angular velocity measurements were filtered. A fourth-order bandpass Butterworth filter with an upper corner frequency of 500 Hz and a lower corner frequency of 1 Hz was applied to the linear acceleration signals. According to Gellner et al., a 300-500 Hz frequency range effectively eliminates most high-frequency noise while preserving the important linear acceleration and angular velocity signal features when taking measurements at locations other than the center of gravity (CoG) [194].

Summary of Gellner et al. study [194]:

While the SAE J211 recommendations are commonly used to filter kinematic measurements taken at the head CoG, there is a lack of guidance for other locations. Geller et al. introduced a novel methodology for determining the optimal kinematic filtering approach for measurements obtained at locations different from head CoG. Their study involved laboratory head impact tests using a pendulum impactor to replicate on-field scenarios. They collected triaxial linear accelerations at the headform's CoG and both triaxial linear accelerations and angular velocities at the headform's teeth location. Subsequently, they used rigid body motion equations to transform the linear acceleration measured at the teeth location to the headform's CoG.

Various filter combinations were applied to the linear acceleration and angular velocity signals obtained at the teeth location, ranging from 5 Hz to 1650 Hz with 5 Hz increments. Each combination was then compared to the linear acceleration measured at the CoG. Note that the linear acceleration signals at the CoG were filtered using the SAE J211 recommended CFC1000 filter, i.e. with a cut-off frequency of 1650 Hz.

The concept of the novel methodology is that by leveraging the equations of rigid body motion, it becomes possible to transform linear acceleration from one point (e.g. point A on a rigid body) to another point (e.g. the CoG of that body), provided that the body's angular velocity and angular acceleration are known. Thus, the goal in selecting optimal cut-off frequencies for linear acceleration and angular velocity measurements at point A is to minimize the error in the transformation equation output when compared to directly measured linear acceleration at the CoG. They used the peak values of the transformed linear acceleration signals to characterize the transformation error. Through this approach, they identified a cut-off frequency range of 300-500 Hz for linear acceleration and angular velocity signals when conducting measurements at locations other than the CoG.

As previously indicated, the accelerometer registers gravitational force, resulting in a consistent acceleration measurement of 1g, alongside capturing head kinematics. To address this, a lower

corner frequency of 1 Hz was applied to the linear acceleration signals. This adjustment aims to remove the accelerometer drift when the volunteer's head orientation changes during the recoil event, which leads to changes in the measured gravity components. Not filtering out the gravitational component from the acceleration data could lead to non-physical derived quantities. Angular velocity measurements were filtered using a fourth-order low-pass Butterworth filter with a corner frequency of 500Hz to eliminate high-frequency noise. Gellner et al. recommended that linear accelerometer and angular velocity measurements share the same upper corner frequency.

Step 6: After filtering, a rigid body kinematic transformation (Equations Equation 14 and Equation 15) was used to compute the linear acceleration and angular velocity at the CoG of the head for integration into the numerical head model. Angular acceleration alpha was computed by taking the derivative of the measured angular velocity [195]. The parameters of the SG filter were a first-order polynomial and a window size of 7. Angular velocity, the other input to the head model, did not require a kinematic transform.

$$v_H = v_{MG} + \omega \times r \qquad \text{Equation 14}$$

$$a_H = a_{MG} + \alpha \times r + \omega \times (\omega \times r) \qquad \text{Equation 15}$$

where

v_H = linear velocity at head CoG

v_{MG} = measured linear velocity

a_H = linear acceleration at head CoG

a_{MG} = measured linear acceleration

α = angular acceleration

ω = measured angular velocity

r = distance from mouthguard to head CoG of a 50th percentile male head

r = [0.081 −0.013 −0.063] m

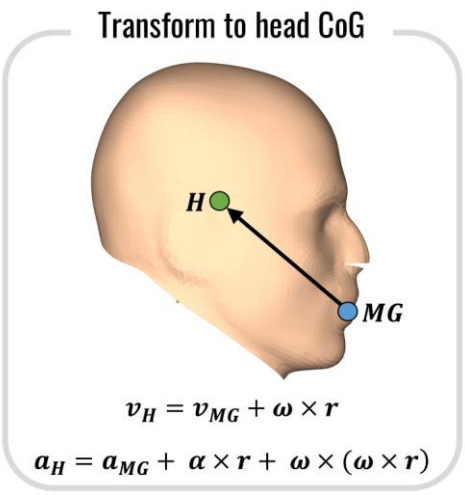


Figure 18: Head kinematics data transformed from mouthguard to head CoG

3.2.2 Post-Processing for "Late Captures"

A methodology similar to that outlined in Section 3.2.1 was employed to process late captures, with only one difference. Given that the pre-trigger data recorded for late captures did not accurately represent the volunteer's stationary head position prior to the recoil event, the stationary head position was inferred based on the average head position from signals considered to be "good captures." Consequently, in step 3 for late captures, the average head position from good captures of the same volunteer was used. All other steps remain the same.

3.3 Head Model Set Up

Following a previously documented approach [156], the processed head kinematics from each round were used as inputs to an isolated GHBMC 50th percentile male head model (version 5) [26]. The head model used in this study (Figure 19) was extracted from the GHBMC 50th percentile male whole-body model at the foramen magnum. The isolated head model also included a small length (34 mm) of the spinal cord. No boundary conditions were imposed on the free end of the spinal cord, allowing for unrestricted movement.

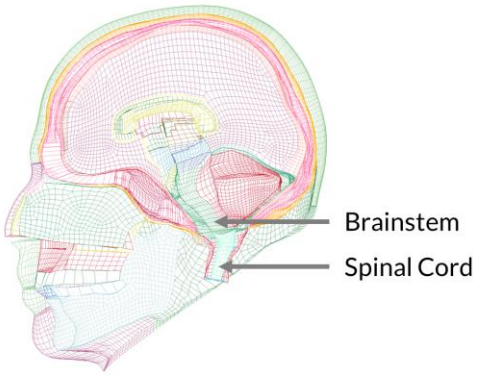


Figure 19: Mid-sectioned view of the isolated GHBMC 50th percentile male head model

The filtered head kinematics, comprising X, Y, Z acceleration signals, and X, Y, Z angular velocity signals, served as inputs for the head model at the head CoG. The CONSTRAINED NODAL RIGID BODIES (CNRB) Dyna command enables the definition of a nodal rigid body by specifying a set of nodes. A CNRB set was created coincident with the nodes of the cranium, along with a node positioned at the CoG of the whole head. Then the prescribed head kinematics were applied using the PRESCRIBED_RIGID_MOTION_ID option in LS-DYNA to the CoG node. Given that the CNRB nodes were coincident with the cranium nodes, hence the cranium effectively mirrored the motion of the CNRB nodes during the prescribed head kinematics. The use of CNRB ensured that the nodes of the skull followed the prescribed motion while maintaining the material properties assigned to the skull in version 5 of the GHBMC head model. The method of prescribing kinematics to a rigid skull has also been employed in previous studies [148], [156], [195]. The kinematics from each individual shot were modeled separately. All models were run on a high-performance computing cluster and solved using LS-DYNA (R9.2 single-precision, ANSYS, Canonsburg). Strain measurements were extracted for both the whole brain and its constituent eight regions (Figure 20). These regions comprise the cerebellum, cerebrum gray matter, cerebrum white matter, corpus callosum, thalamus, midbrain brainstem, brainstem, and basal ganglia.

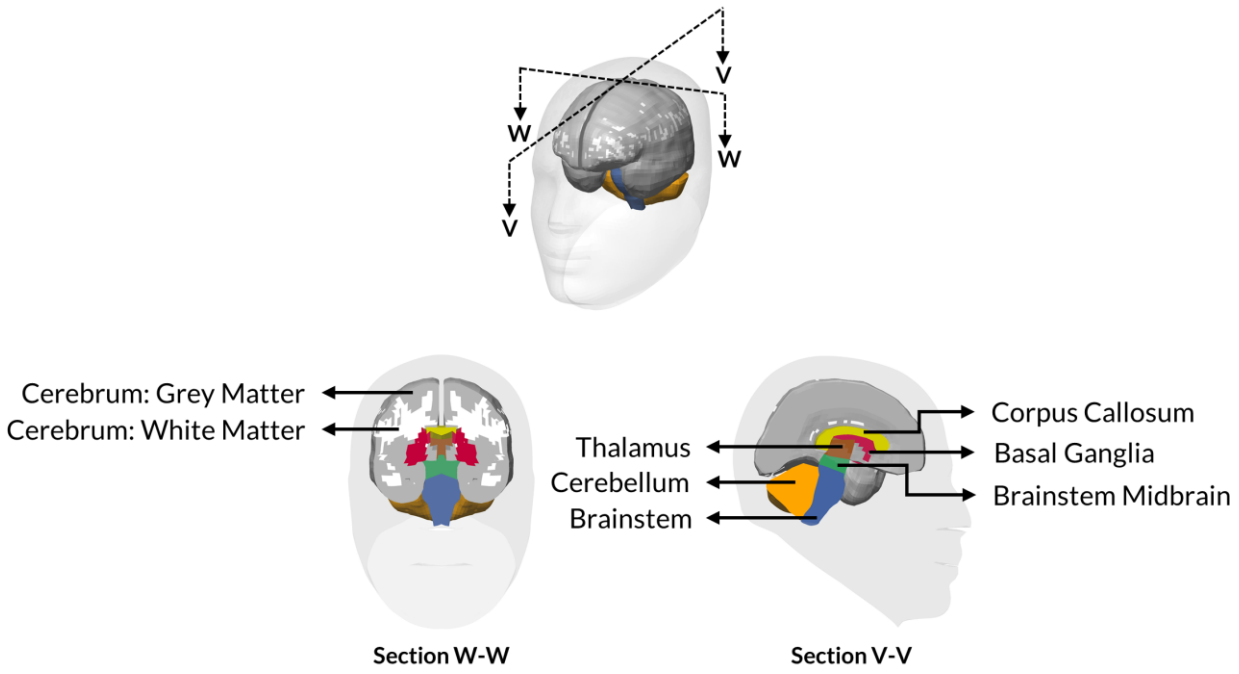


Figure 20: The 8 regions (referred to as the whole brain when grouped together) in the GHBMC 50th percentile male head model

3.4 Metrics for Brain Response Comparison

In analyzing trends among rifles and volunteers, an essential initial step involves establishing a sensitive metric to gauge loading severity accurately. Consequently, four distinct metrics were investigated: HIC_{15} (a linear kinematic-based metric), BrIC (a rotational kinematic-based metric), MPS_{95} (a strain-based metric), and the CSV curve (a recent strain-based metric).

1. The maximum area under the resultant linear acceleration-time plot within a specified 15 ms time frame was determined to compute HIC_{15} as shown by Equation 16.

$$HIC_{15} = max\left\{(t_2 - t_1)\left[\frac{1}{t_2 - t_1}\int_{t_1}^{t_2} a(t)dt\right]^{2.5}\right\} \quad \text{Equation 16} \qquad [29]$$

where,

$a(t)$ = the resultant linear acceleration (in g)

t_1 and t_2 (in seconds) = timepoints during the acceleration pulse selected such that the value of HIC_{15} is maximized. Note that the term (t_2 - t_1) is 15 ms for HIC_{15}.

An example of how HIC_{15} was calculated for a signal is shown in Appendix B.

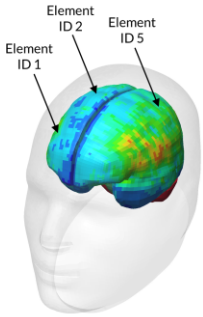
2. Equation 17 was used to compute BrIC. ω_x, ω_y and ω_z and ω_{xC}, ω_{yC} and ω_{zC} refers to the maximum angular velocities (in rad/s) and the critical angular velocities (in rad/s) about the X, Y, Z axes respectively. The following critical values (ω_{xC} = 66.30 rad/s, ω_{xC} = 53.80 rad/s and ω_{xC} = 41.50 rad/s) were used in this study.

$$BrIC = \sqrt{\left(\frac{\omega_x}{\omega_{xC}}\right)^2 + \left(\frac{\omega_y}{\omega_{yC}}\right)^2 + \left(\frac{\omega_z}{\omega_{zC}}\right)^2} \quad \text{Equation 17} \qquad [124]$$

3. The 95th percentile maximum principal strain (MPS_{95}) was used as opposed to the maximum principal strain (i.e. 100th percentile maximum principal strain) to remove elements with artificially high strains as a result of numerical artifacts [154], [155], [156]. MPS_{95} was calculated by first extracting the maximum principal strain measured by each element of the whole brain region during the entire simulation time. MPS_{95} then corresponds to the value remaining after the top 5% of that strain range was removed. Although, MPS_{95} has been widely used to assess brain response, this single value metric is limited as it only represents the maximum strain potentially occurring at one location of the brain.

4. The cumulative strain-volume (CSV) method, on the other hand, primarily functions as an indicator quantifying the amount of strain within specific regions of the brain. A key advantage of CSV is that it does not require a cut-off value (e.g. 95th percentile) and offers a clear representation of the percentage volume of the brain region experiencing a specific magnitude of maximum principal strain (MPS). CSV curves have the cumulative percentage volume of a region on the y-axis and MPS on the x-axis.

To create CSV plots, the procedure involved the extraction of both the maximum principal strain (MPS) and initial volume for every element within a specified brain region throughout the simulation duration (Figure 21(a)). Following this, the volume fraction for each element within the region was computed, by dividing its initial volume with the total region volume (Figure 21(b)). Elements were subsequently arranged in ascending order based on their MPS values (Figure 21(c)). Calculating the percentage volume involved subtracting the volume fraction of each element from that of the volume of the region in the preceding row, starting with 100% as the initial volume (Figure 21(d)). Finally, using the MPS values (Figure 21(a)) and cumulative percentage volume (Figure 21(d)), the CSV curves were constructed.



(a)

Element ID	MPS	Element Volume	(b) Volume Fraction
1	MPS_1	VOL_1	$*VF_1$
2	MPS_2	VOL_2	VF_2
3	MPS_3	VOL_3	VF_3
4	MPS_4	VOL_4	VF_4
5	MPS_5	VOL_5	VF_5

sort

(c) (d)

Element ID	MPS	Volume Fraction	Cumulative Volume
3	MPS_3	VF_3	$\%V_1 = 100\% - VF_3$
5	MPS_5	VF_5	$\%V_2 = \%V_1 - VF_5$
2	MPS_2	VF_2	$\%V_3 = \%V_2 - VF_2$
1	MPS_1	VF_1	$\%V_4 = \%V_3 - VF_1$
4	MPS_4	VF_4	$\%V_5 = \%V_4 - VF_4$

$$*VF_1 = \left(\frac{VOL_1}{total\ volume\ of\ region}\right) \times 100$$

Figure 21: The process to generate the cumulative-strain curve. Note that in this exemplar case, we are assuming that the region consists of 5 elements with Element ID 1 to 5. (a) First, the maximum principal strain (MPS_1 to MPS_5) and initial volume (VOL_1 to VOL_5) of every element in the specified region are extracted. (b) The volume fraction for each element (VF_1 to VF_5) within the region is computed. (c) The elements are then arranged in ascending order based on their MPS values. (d) The percentage volume is calculated by subtracting the volume fraction of each element from that of the volume of the region in the preceding row, starting with 100% as the initial volume.

An exemplar CSV curve for a brain region is shown in Figure 22. The CSV curve (Figure 22(a)) can be interpreted as: 40% of the region experiences an MPS of at least 0.035. Essentially, the CSV curve analyzes how much of the region's volume is subjected to strains beyond a specified level.

For example, 100% of a volume would experience a strain greater than 0 MPS. However, the plot decreases as less and less of the brain volume experiences high strains (Figure 22(b)).

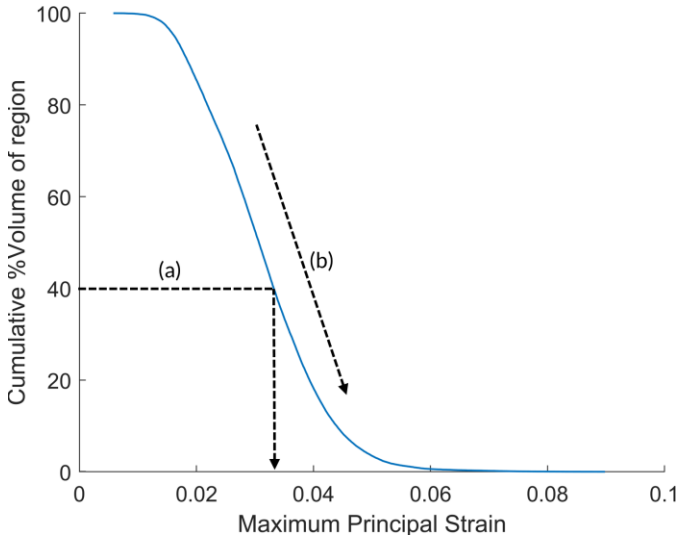


Figure 22: An exemplar CSV curve with Maximum Principal Strain (MPS) on the x-axis and Cumulative % Volume of a region on the y-axis. (a) As an example, the CSV curve can be interpreted as 40% of the region's volume experiencing an MPS of at least 0.035. (b) The curve decreases as less and less of the region's volume experiences high strains.

To generate a single summary value for statistical analysis, CSV plots were integrated with respect to percentage volume(Figure 23). Essentially, this involved calculating the area under the CSV curves bounded by the y-axis (A_{CSV}).

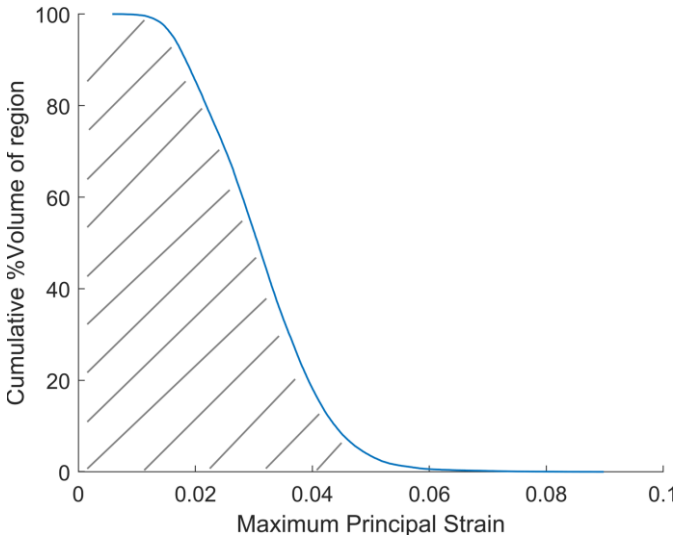


Figure 23: The area under a CSV curve referred to as A_{CSV}

3.5 Comparison of Metrics

Several statistical measures were used to understand the trends between rifles and volunteers, all calculated within Excel. Specifically, the mean, standard deviation, and coefficient of variation (CV) were computed for each group under comparison.

The mean, i.e. the average value of a group, was determined using the "=AVERAGE()" function in Excel.

The standard deviation illustrates the spread of data points around the mean. It indicates the extent of variability within the dataset. A higher standard deviation suggests greater variability, while a lower standard deviation indicates more consistency among the datapoints. The standard deviation of a group was calculated using the "=STDEV.S()" function in Excel.

The CV serves as a normalized measure of dispersion, calculated by dividing the standard deviation by the mean and expressed as a percentage. A lower CV suggests less variability relative to the mean, while a higher CV indicates greater variability. This metric is particularly useful for assessing the relative variability between different groups with either distinct units or significantly different means.

Additionally, a one-way ANOVA was conducted for comparing means across multiple groups, while the t-test was used for comparing means between two groups. All statistical analyses were performed in Excel as well. For instance, a one-way ANOVA with a significance level of α=0.05 was conducted for all four metrics to evaluate differences in brain response among the three rifle configurations (A, B, C) in Dataset 1. Similarly, a t-test (assuming unequal variances) with a significance level of α=0.05 was applied for all four metrics to analyze differences in brain response between the two rifle configurations (D, E) in Dataset 2. If the p-value obtained from the ANOVA or t-Test is below the significance level (α=0.05), it suggests significant differences between at least two of the group means. The functions "t-Test: Two-Sample Assuming Unequal Variances" and "ANOVA: Single Factor" functions in Excel were used for the statistical analysis.

For the ANOVA analysis, if the p-value was below the significance level (α=0.05), it suggested significant differences between at least two of the group means. To find out which group means were statistically different, the Tukey-Kramer post hoc test was manually conducted in Excel following the steps outlined below:

1. The absolute mean difference between each group was calculated
2. The Q critical value was calculated using Equation 18

$$Q\ critical\ value = Q * \sqrt{\frac{S^2_{pooled}}{n}} \qquad \text{Equation 18}$$

where

Q = value from Studentized Range Q Table

S^2_{pooled} = pooled variance across all groups

n = sample size for a given group

   a. The value of Q was obtained from the Studentized Range Q Table based on the number of groups (k) and the degree of freedom (df). Note that df is calculated by subtracting the number of groups (k) from the total number of samples for all groups.

3. To determine which group means were statistically different, the absolute mean difference value between each group was compared to the calculated Q critical value. If the absolute mean difference value was greater than the Q critical value, the difference between the group means was considered statistically significant.

4 Results

Two primary datasets, labeled “Dataset 1: May 2021” and “Dataset 2: May 2022”, were used in this study. Dataset 1: May 2021 involved three volunteers (referred to as Volunteers 1 – 3) and three rifle configurations (Rifles A, B, C), while Dataset 2: May 2022 included five volunteers (referred to as Volunteers 4 – 8) and two rifle configurations (Rifles D, E). Each dataset was collected at different points in time of the project. The study results are presented in the following manner: Section 4.1 compares head kinematic signals for all rifles and volunteers in Datasets 1 and 2. Section 4.2 shows trends in both datasets using kinematic-based metrics, HIC_{15} and BrIC, calculated for all shots in both datasets. The comparison includes observations between rifles (inter-rifle) and between volunteers (inter-volunteer). Section 4.3 shows trends in Datasets 1 and 2 using two strain-based metrics, MPS_{95} and Cumulative Strain Volume (CSV) curves of the whole brain, calculated for all shots in both datasets. The comparison also includes observations between rifles (inter-rifle) and between volunteers (inter-volunteer). CSV curves are also plotted for the eight individual brain regions of the model to investigate if a specific region experiences higher strains. Finally, Section 4.4 examines the relative contributions of linear acceleration and angular velocity on strain outputs using the CSV curves.

4.1 Comparison of Head Kinematics Between Different Rifles and Volunteers

4.1.1 Head Kinematic Results for Dataset 1: May 2021

4.1.1.1 Inter-Rifle Head Kinematic Comparison for Three Rifle Configurations

The recoil forces transferred through the shoulder and neck, resulting from the impact of the rifle's buttstock on the volunteer's shoulder, induced accelerations in the head. The measured head kinematics were filtered, transformed to the head CoG, and then plotted for comparison. Grouping the kinematic traces by rifle (Figure 24 and Appendix Figure 55,Appendix Figure 56) for each volunteer revealed broadly similar features in head linear accelerations and angular velocities. The peak accelerations occurred within the initial 50 ms (0.05 s). While the timing of the initial peak aligned across all three rifles, variations in the magnitudes of linear accelerations and angular velocities were observed, with Rifle C usually exhibiting higher magnitudes, followed

by Rifles A and B. Similar observations were made between rifles for Volunteers 2 and 3 (Appendix Figures 1,2).

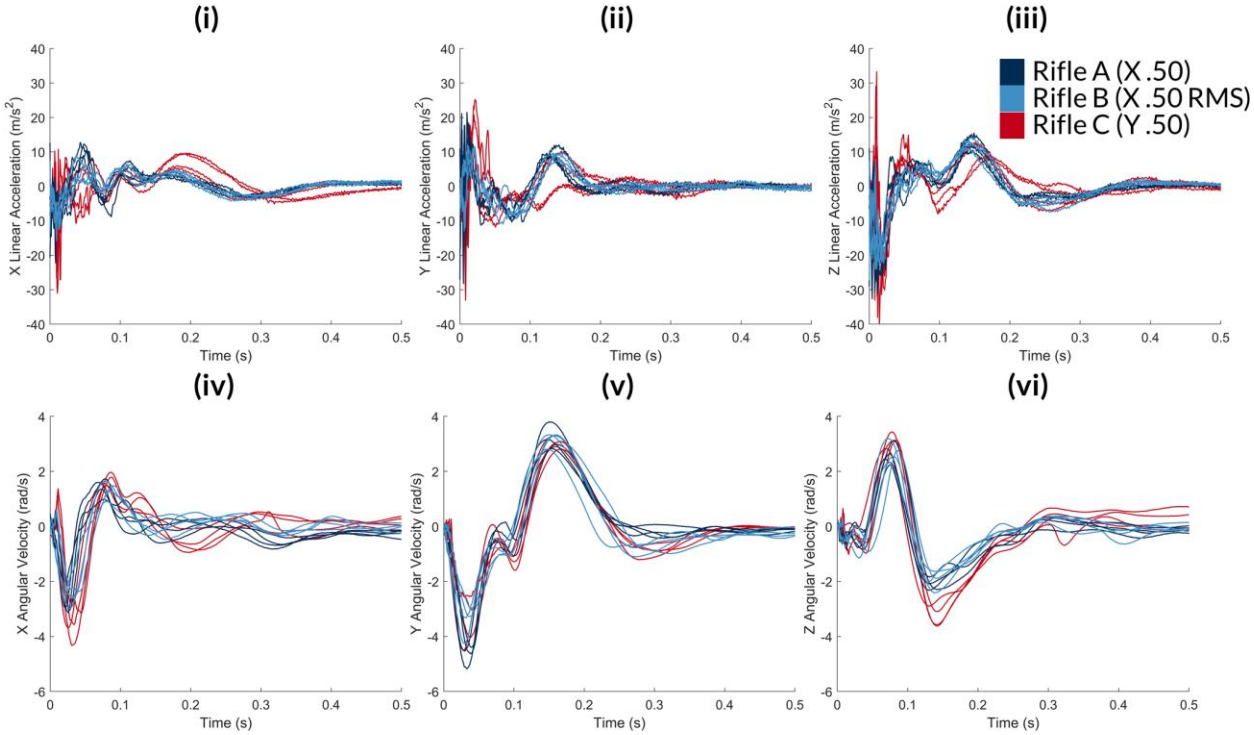


Figure 24: The head kinematics for Volunteer 1 (from Dataset 1: May 2021), including (i) linear acceleration in X, (ii) linear acceleration in Y, (iii) linear acceleration in Z, (iv) angular velocity in X, (v) angular velocity in Y and (vi) angular velocity in Z for all the shots fired using Rifles A, B, and C. Note that the designation in brackets represents the features of each rifle; for example Rifle A (X .50) indicates that Rifle A has Chassis X and is a .50 caliber rifle.

4.1.1.2 Inter-Volunteer Head Kinematic Comparison for Three Volunteers

Slight differences between volunteers were noticed, mainly when grouping the angular velocity curves of each volunteer for every rifle in Dataset 1 (Figure 25 and Appendix Figure 57,Appendix Figure 58). All volunteers in Dataset 1 exhibited coronal rotation (x angular velocity) when firing Rifle C (Figure 25(iv)). This rotation predominantly occurred in the negative direction for Volunteer 1. In contrast, Volunteers 2 and 3 displayed an additional positive peak, indicating increased motion in the coronal plane.

Sagittal rotation (y angular velocity) in both directions was observed (Figure 25(v)) when firing Rifle C. This suggests that the head moves forward and backward during the firing process. The magnitude of the first trough was similar for all three volunteers (Figure 25(v)). However, Volunteer 1 demonstrated a higher second peak, indicating higher sagittal plane motion than Volunteers 2 and 3.

A relatively symmetrical motion can be observed in the axial plane (z angular velocity) for all three volunteers when firing Rifle C, characterized by a positive peak followed by a negative trough (Figure 25(vi)). This peak refers to the rotation of the head towards the shoulder impacted by the rifle's buttstock. Subsequently, the trough indicated the volunteer's head returning to its initial position. Higher magnitudes of angular velocity were observed for Volunteer 2 in this direction. Similar patterns were also observed when the volunteers fired Rifles A and B (Appendix Figure 57,Appendix Figure 58).

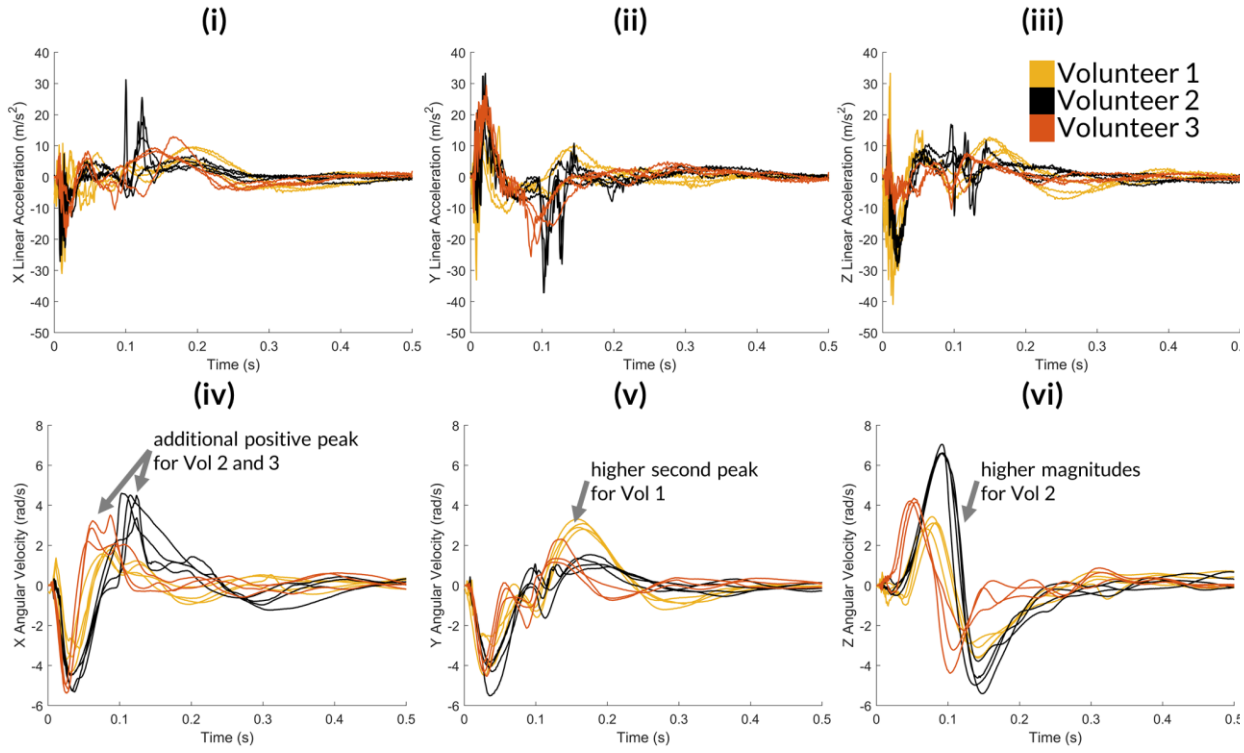


Figure 25: The head kinematics of Volunteers 1, 2, and 3 (from Dataset 1: May 2021) firing Rifle C, including (i) linear acceleration in X, (ii) linear acceleration in Y, (iii) linear acceleration in Z, (iv) angular velocity in X, (v) angular velocity in Y and (vi) angular velocity in Z.

4.1.2 Head Kinematic Results for Dataset 2: May 2022

4.1.2.1 Inter-Rifle Head Kinematic Comparison for Two Rifle Configurations

In Dataset 2, the head kinematics of the volunteers displayed similar characteristics between rifles, with peak accelerations consistently occurring within the initial 0.05 seconds. Firing Rifle E resulted in higher kinematics than Rifle D (Figure 26, Appendix Figure 59-Appendix Figure 61).

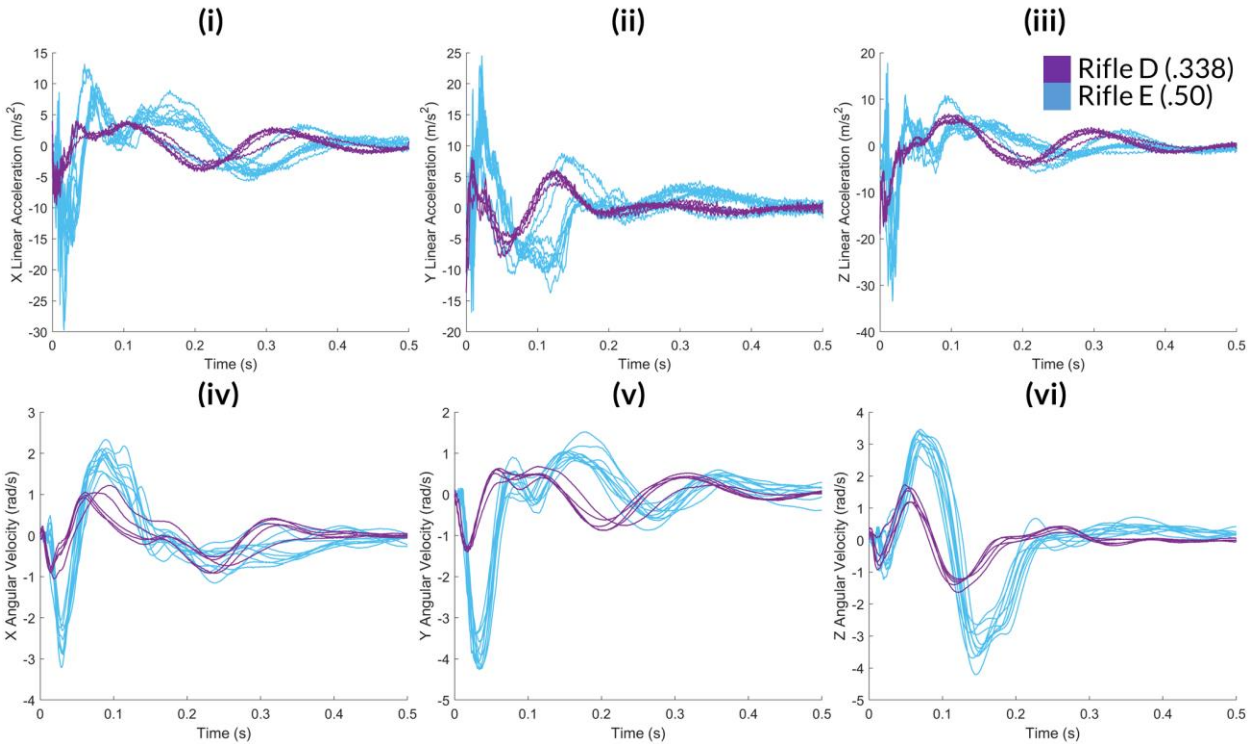


Figure 26: The head kinematics for Volunteer 8 (from Dataset 2: May 2022), including (i) linear acceleration in X, (ii) linear acceleration in Y, (iii) linear acceleration in Z, (iv) angular velocity in X, (v) angular velocity in Y and (vi) angular velocity in Z for all the shots fired using Rifles D and E. Note that the designation in brackets represents the features of each rifle; for example Rifle D (.338) indicates that Rifle D is a .338 caliber rifle.

4.1.2.2 Inter-Volunteer Head Kinematic Comparison for Five Volunteers

Minor variations were observed between volunteers firing the same rifle in Dataset 2. For example, pronounced peaks were observed in the linear acceleration signals of Volunteers 4, 5, and 6 exclusively when firing Rifle E (Figure 27 and Appendix Figure 59-Appendix Figure 61). These pronounced peaks had very high magnitudes and occurred over a very short time frame.

For instance, there was a rapid transition from -265 m/s² to +800 m/s² at 0.03 s, followed by a subsequent drop to -600 m/s² occurring within a timeframe of less than 0.006 s (Figure 27(i)). These high peaks in the signals may not represent gross kinematics and may produce values greater than the recoil loading condition investigated. These pronounced peaks were observed in 9 out of 11 shots for Volunteer 4, 5 out of 15 shots for Volunteer 5, and 1 out of 6 shots for Volunteer 6. They occurred in regions that deviated from the typical signal patterns observed in other shots by the same volunteers, as well as from Volunteers 7 and 8 in Dataset 2.

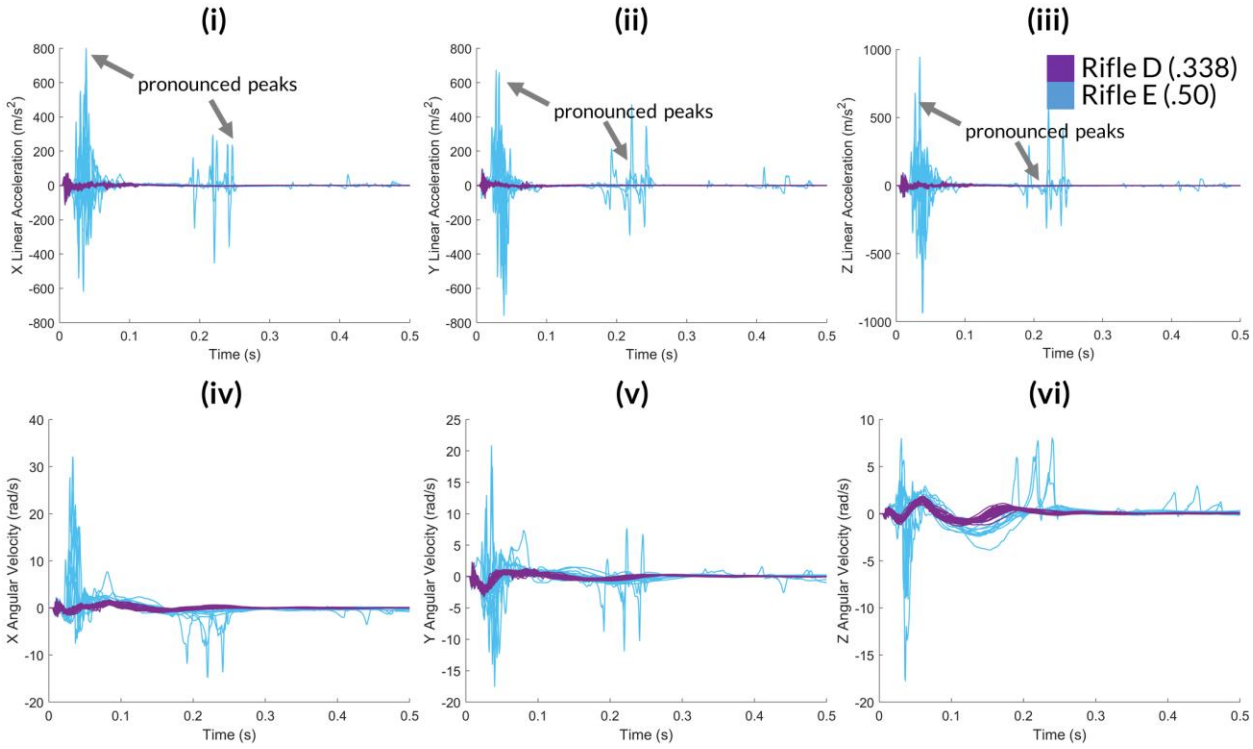


Figure 27: The head kinematics for Volunteer 4 (from Dataset 2: May 2022), including (i) linear acceleration in X, (ii) linear acceleration in Y, (iii) linear acceleration in Z, (iv) angular velocity in X, (v) angular velocity in Y and (vi) angular velocity in Z for all the shots fired using Rifles D and E. Note that the designation in brackets represents the features of each rifle; for example Rifle D (.338) indicates that Rifle D is .338 caliber rifle.

In Dataset 2, differences in angular motion between volunteers were more apparent when firing Rifle D compared to Rifle E (Figure 28). When firing Rifle D, Volunteers 7 and 8 displayed the lowest first trough in angular velocity along the x-axis (coronal plane) (Figure 28 (i)). Volunteer 6

exhibited the highest first trough as well as the highest peak following the first trough in angular velocity along the x-axis (coronal plane) (Figure 28 (i)). Volunteer 8 maintained the lowest first trough in angular velocity along the y-axis (sagittal plane) (Figure 28 (ii)). Additionally, Volunteer 6 maintained the highest peak after the first trough in angular velocity along the y-axis (sagittal plane) (Figure 28 (ii)). All volunteers displayed similar signal shapes and magnitudes in angular velocity along the z-axis (axial plane) (Figure 28 (iii)). While most volunteers exhibited similar shapes and magnitudes of signals in all three directions when firing Rifle E, Volunteer 5 stood out, showing slightly higher magnitudes in angular velocity along the x and y axes Figure 28 (iv-vi).

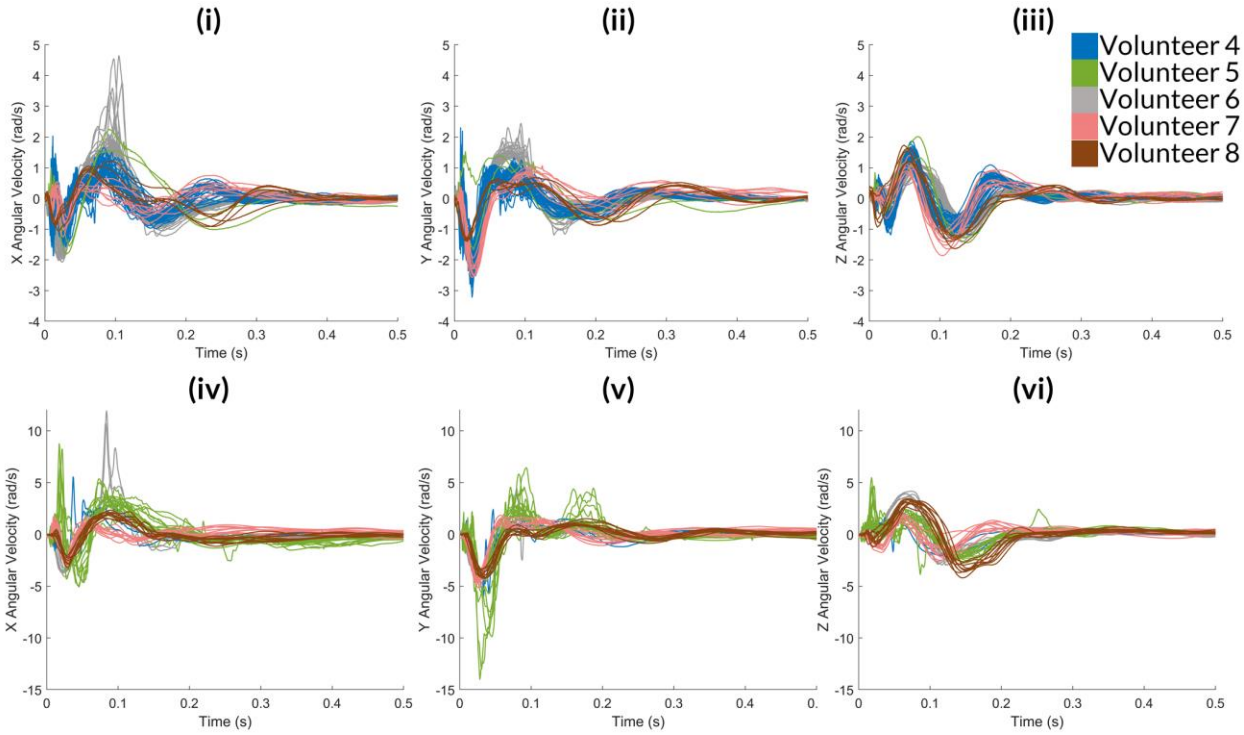


Figure 28: The (i) X, (ii) Y, (iii) Z angular velocity signals of all volunteers from Dataset 2 firing Rifle D. The (iv) X, (v) Y, (vi) Z angular velocity signals of all volunteers from Dataset 2 firing Rifle E.

4.1.3 Summary of Head Kinematic Results from Datasets 1 and 2

- The kinematic signals, when grouped by rifle, displayed consistent features such as the number and timing of peaks.
- Variations in magnitude across rifles were observed, with Rifle C consistently exhibiting higher magnitudes than Rifles A and B across all volunteers in Dataset 1 and Rifle E exhibiting higher magnitudes than Rifle D across all volunteers in Dataset 2.
- Peak linear accelerations were consistently observed within the first 0.05 seconds in Datasets 1 and 2.
- Volunteers 4, 5, and 6 from Dataset 2 displayed pronounced peaks in certain acceleration signals, with peaks reaching up to 800 m/s^2. These peaks may not be representative of head motion during firing.
- When grouping by volunteers, more apparent variations emerged, particularly in angular velocity signals.
- Volunteer 2 from Dataset 1 typically demonstrated the highest magnitudes in the angular velocity signals.
- Differences in angular motion between volunteers in Dataset 2 were more apparent when firing Rifle D compared to Rifle E, with Volunteers 5 and 6 typically exhibiting higher peaks when firing Rifles E and D, respectively.

4.2 Kinematic-based Metric Results

Two kinematic-based metrics, HIC_{15} and BrIC, were calculated for all shots in Datasets 1 and 2, and a comprehensive listing of these values is provided in Appendix B and C, respectively.

4.2.1 Comparison of HIC_{15} Between Different Rifles and Volunteers

The HIC_{15} values computed for all shots from every volunteer are provided in Appendix B. The mean HIC_{15} values of each rifle were calculated across all volunteers (Figure 29-Figure 32). The detailed methodology for calculating HIC_{15} is explained in Appendix B.

4.2.1.1 HIC_{15} Results for Dataset 1: May 2021

4.2.1.1.1 Inter-Rifle HIC_{15} Comparison for Three Rifle Configurations

Volunteer 1 exhibited higher mean HIC_{15} when firing Rifle C compared to A. Volunteers 2 and 3 displayed an opposite trend, with higher HIC_{15} values when firing Rifle A compared to C. Rifle B consistently showcased the lowest HIC_{15} values across all three volunteers (Figure 29). It can be observed that the standard deviation is substantially higher for Volunteer 2 when firing Rifle A (Figure 29(ii)), where only two shots were considered. As outlined in the methods section, only two of the four shots were included in this case, while the remaining two were excluded due to being identified as scope bites. The increased HIC_{15} value resulted from the prominent high-magnitude peaks at t=100 ms in the linear acceleration data (Appendix Figure 55 (i)-(iii)). Given that the calculation of HIC_{15} relies on determining the maximum area under the resultant linear acceleration-time curve, the higher standard deviation, in this case, is due to the short-duration high magnitude in the linear acceleration signals for one of the two shots fired by Volunteer 2 using Rifle A. This resulted in an uncharacteristic HIC_{15} value.

In addition to calculating the standard deviation, the coefficient of variation (CV) was also computed. This metric is valuable for comparing variability among datasets with differing means, as it standardizes dispersion relative to each dataset's mean. The CV for each rifle was determined for every volunteer in Dataset 1. The CV values followed a descending order when firing Rifles C, A, B for Volunteer 1; Rifles A, C, B for Volunteer 2; and Rifles B, A, C for Volunteer 3. Hence, no trend between rifles was observed regarding variability for HIC_{15}. Note that a low

CV value signifies low variability, while a high CV value indicates high variability within the dataset.

A one-way ANOVA analysis (detailed in Appendix B) was conducted at a significance level of α=0.05 to explore differences between rifles for each volunteer. Significant differences in HIC_{15} values between rifles were observed for Volunteers 1 and 3, with p-values of 4.00E-3 and 2.75E-2, respectively. However, no statistically significant difference was identified between the rifles for Volunteer 2, with a p-value of 1.39E-1. The Tukey-Kramer test (detailed in Appendix B) identified a statistical difference between Rifles B and C for Volunteer 1 and between Rifles A and B for Volunteer 3.

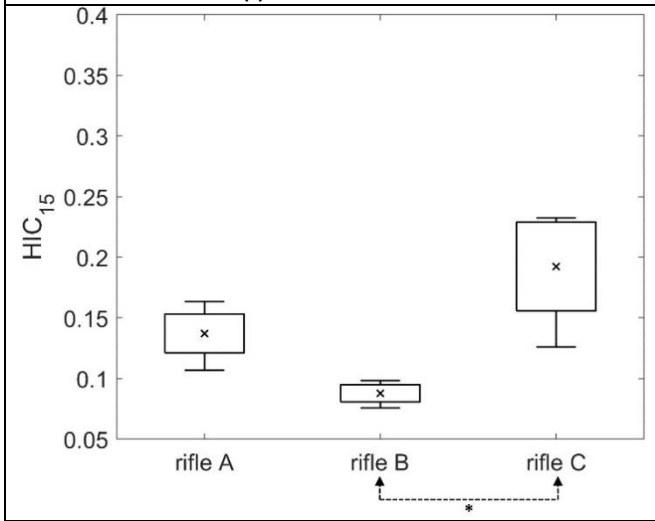
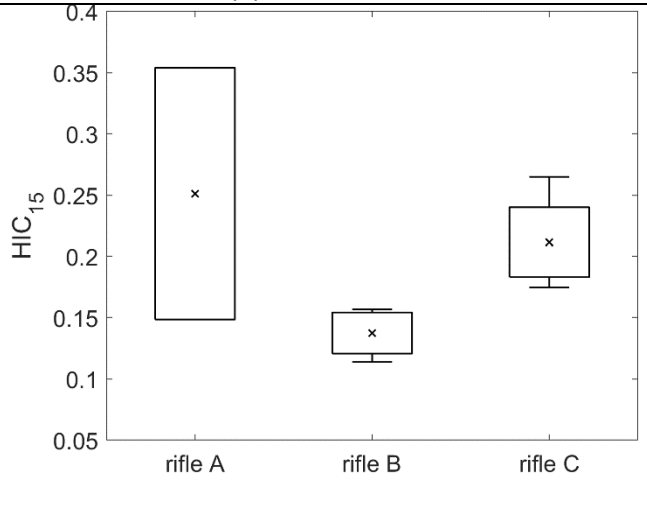
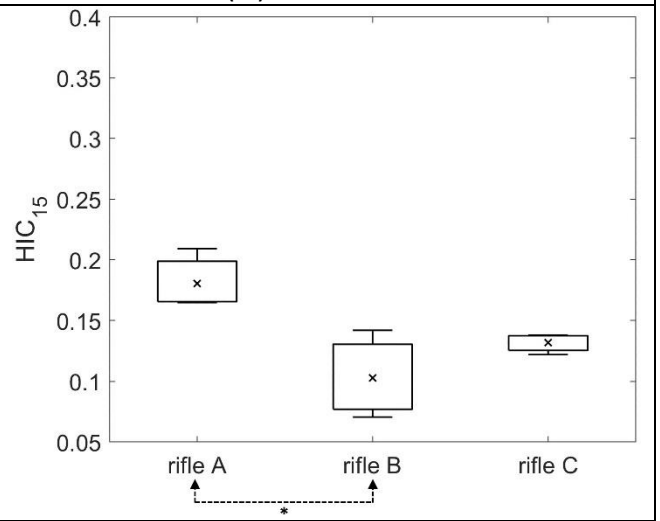
(i) Volunteer 1				(ii) Volunteer 2				(iii) Volunteer 3			
											
Mean	0.1372	0.0878	0.1923	Mean	0.2512	0.1374	0.2116	Mean	0.1807	0.1029	0.1320
Std. Dev.	0.0235	0.0095	0.0488	Std. Dev.	0.1452	0.0203	0.0392	Std. Dev.	0.0248	0.0362	0.0087
CV (%)	17.12	10.82	25.38	CV (%)	57.82	14.75	18.54	CV (%)	13.73	35.17	6.63

Figure 29: Mean HIC_{15} and variation of the three rifles for (i) Volunteer 1, (ii) Volunteer 2, and (iii) Volunteer 3 (Dataset 1: May 2021). * = statistically significant difference detected between rifles. CV = coefficient of variation. Number of shots for Volunteer 1 (Rifles A:4, B:4, C:4), Volunteer 2 (Rifles A:2, B:4, C:4) and Volunteer 3 (Rifles A:3, B:3, C:3).

4.2.1.1.2 Inter-Volunteer HIC_{15} Comparison for Three Volunteers

The mean HIC_{15} ranges for Rifles A, B, and C were 0.1371 to 0.2512, 0.0878 to 0.1374, and 0.1320 to 0.2116, respectively. Rifle A exhibited the widest range, followed by Rifle C and B (Figure 30). When firing Rifles A and B, the mean HIC_{15} values followed a descending order, with Volunteers 2, 3, and 1 showing progressively higher to lower values. Conversely, when firing Rifle C, this order shifted to Volunteers 2, 1, and 3. As a result, Volunteer 2 displayed the highest HIC_{15} values when firing all three rifles. In contrast, Volunteer 1 demonstrated the lowest HIC_{15} values when firing Rifles A and B, whereas Volunteer 3 exhibited the lowest HIC_{15} value when firing Rifle C. The CV range was between 13% to 58% for Rifle A, 10% to 35% for Rifle B, and 6% to 25% for Rifle C, with the widest range being for Rifle A, followed by B, then C.

A one-way ANOVA analysis (detailed in Appendix B) was conducted at a significance level of α=0.05 to explore differences between volunteers for each rifle. Significant differences in HIC_{15} values between volunteers were only observed for Rifle B, with p-values of 0.04. However, the Tukey-Kramer test (detailed in Appendix B) identified no statistical difference between volunteers for Rifle B. This may be a consequence of the small sample sizes in this dataset. No statistically significant difference was identified between the volunteers for Rifles A and C, with p-values of 0.195 and 0.0679, respectively.

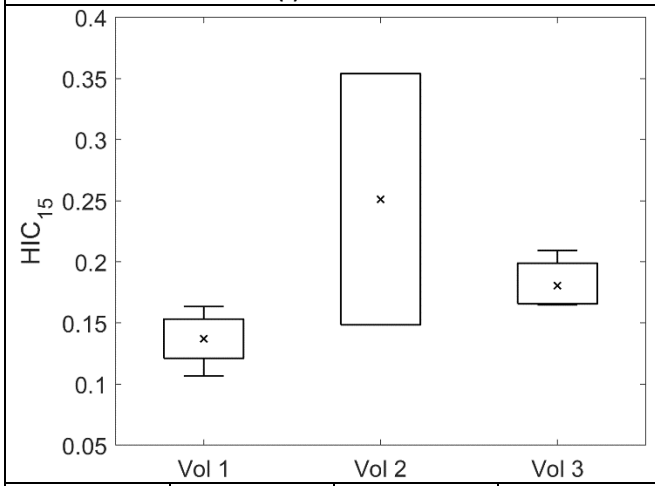
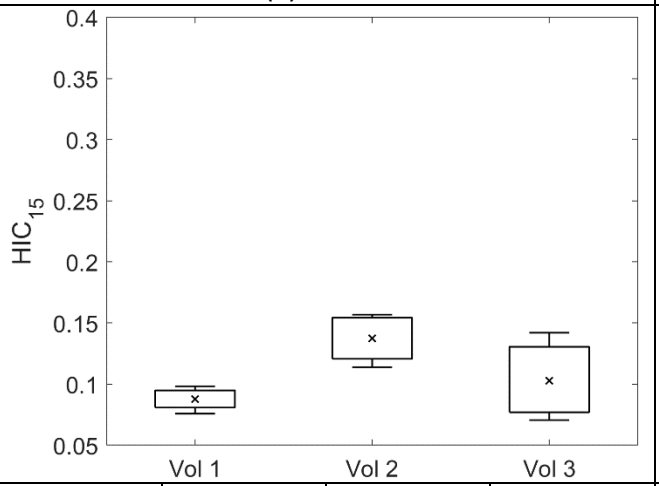
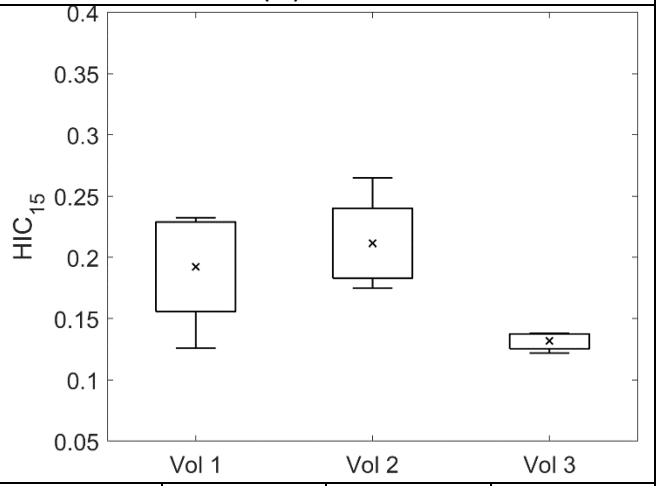
(i) Rifle A				(ii) Rifle B				(iii) Rifle C			
											
Mean	0.1372	0.2512	0.1807	Mean	0.0878	0.1374	0.1029	Mean	0.1923	0.2116	0.1320
Std. Dev.	0.0235	0.1452	0.0248	Std. Dev.	0.0095	0.0203	0.0362	Std. Dev.	0.0488	0.0392	0.0087
CV (%)	17.12	57.82	13.73	CV (%)	10.82	14.75	35.17	CV (%)	25.38	18.54	6.63

Figure 30: Mean HIC_{15} and variation of the three volunteers for (i) Rifle A, (ii) Rifle B, and (iii) Rifle C (Dataset 1: May 2021). CV = coefficient of variation. Number of shots for Volunteer 1 (Rifles A:4, B:4, C:4), Volunteer 2 (Rifles A:2, B:4, C:4) and Volunteer 3 (Rifles A:3, B:3, C:3).

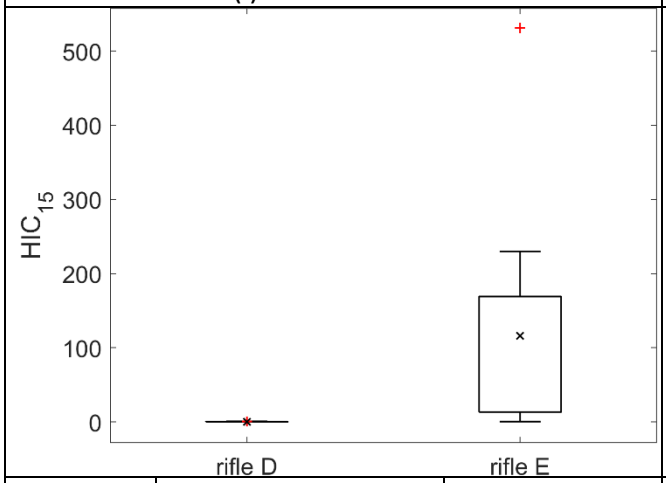
4.2.1.2 HIC_{15} Results for Dataset 2: May 2022

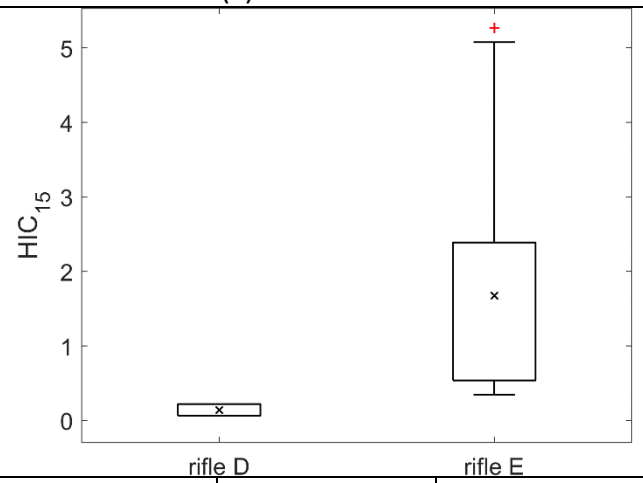
4.2.1.2.1 Inter-Rifle HIC_{15} Comparison for Two Rifle Configurations

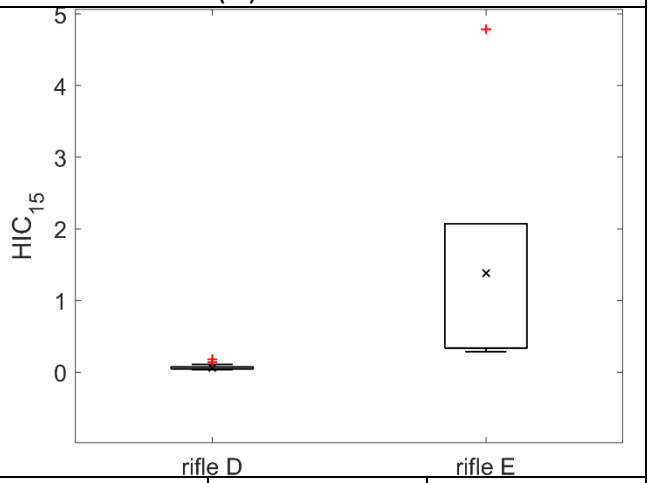
It can be noted that all volunteers in Dataset 2 had higher mean HIC_{15} values while firing Rifle E compared to Rifle D (Figure 31). Volunteer 4 notably exhibited substantially higher mean HIC_{15} values when firing both rifles, while Volunteers 5 and 6 demonstrated comparatively elevated values compared to Volunteers 7 and 8. These increased HIC_{15} values corresponded with high-magnitude peaks in the linear acceleration data within this dataset. Additionally, the standard deviation was consistently higher for Rifle E compared to D, indicating lower variability when firing Rifle D. It's important to note that high mean HIC_{15} values in certain signals may bias the standard deviation range of values.

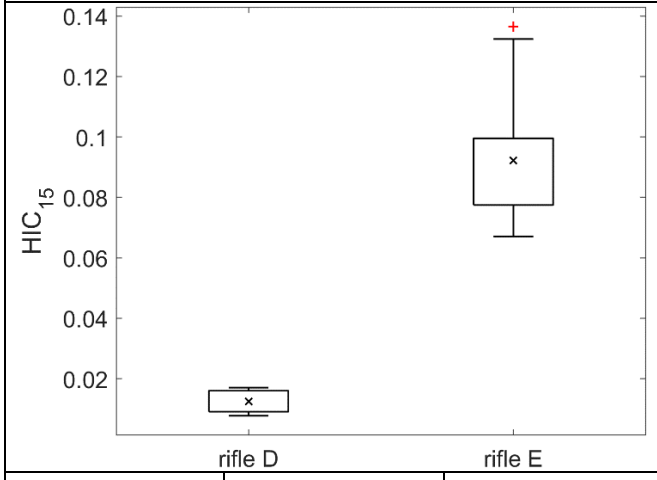
The mean HIC_{15} values for Volunteers 7 and 8, who did not exhibit uncharacteristically high magnitude peaks in their head kinematics when firing Rifle E, were in a similar range to HIC_{15} values of Rifles A and C from Dataset 1. Note that all three rifles are of the same caliber (.50 cal). Additionally, the CV values for these two volunteers in Dataset 2 mirrored those of Rifle C in Dataset 1, except for Volunteer 3, which had a CV value of 6.63 when firing Rifle C, signifying lower variability.

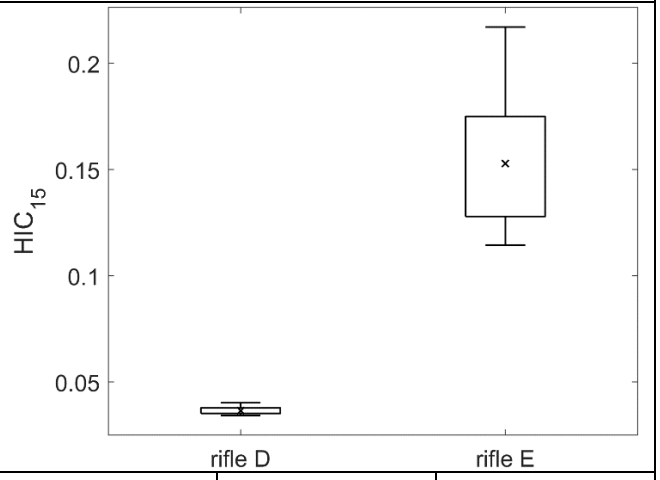
A t-test (detailed in Appendix B) was conducted at a significance level of α=0.05 to explore differences between rifles for each volunteer. Significant differences in HIC_{15} values between rifles were observed for Volunteers 4, 5, 7, and 8, with p-values of 1.72E-2, 1.28E-3, 1.73E-13, and 7.66E-06 respectively. However, no statistically significant difference was identified between the rifles for Volunteer 6, with a p-value of 6.68E-2.

(i) Volunteer 4*		
		
Mean	0.2992	116.1877
Std. Dev.	0.2042	156.9768
CV (%)	68.24	135.11

(ii) Volunteer 5*		
		
Mean	0.1428	1.6772
Std. Dev.	0.1115	1.6160
CV (%)	78.08	96.35

(iii) Volunteer 6		
		
Mean	0.0614	1.3802
Std. Dev.	0.0304	1.8055
CV (%)	49.50	130.81

(iv) Volunteer 7*		
		
Mean	0.0125	0.0922
Std. Dev.	0.0037	0.0195
CV (%)	29.74	21.18

(v) Volunteer 8*		
		
Mean	0.0366	0.1528
Std. Dev.	0.0023	0.0331
CV (%)	6.25	21.64

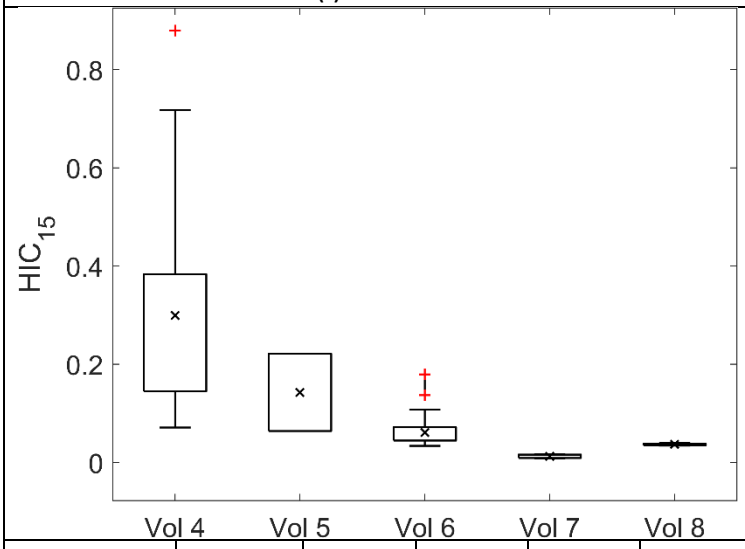
Note that data points greater than 1.5 times the interquartile range are indicated by the red "+" hereafter.

Figure 31: Mean HIC_{15} and variation of the two rifles for (i) Volunteer 4, (ii) Volunteer 5, (iii) Volunteer 6, (iv) Volunteer 7, (v) Volunteer 8 (Dataset 2: May 2022). *= statistically significant difference detected between rifles. CV = coefficient of variation. Number of shots for Volunteer 4 (Rifles D:36, E:11), Volunteer 5 (Rifles D:2, E:15), Volunteer 6 (Rifles D:33, E:6), Volunteer 7 (Rifles D:8, E:18) and Volunteer 8 (Rifles D:5, E:10).

4.2.1.2.2 Inter-Volunteer HIC_{15} Comparison for Five Volunteers

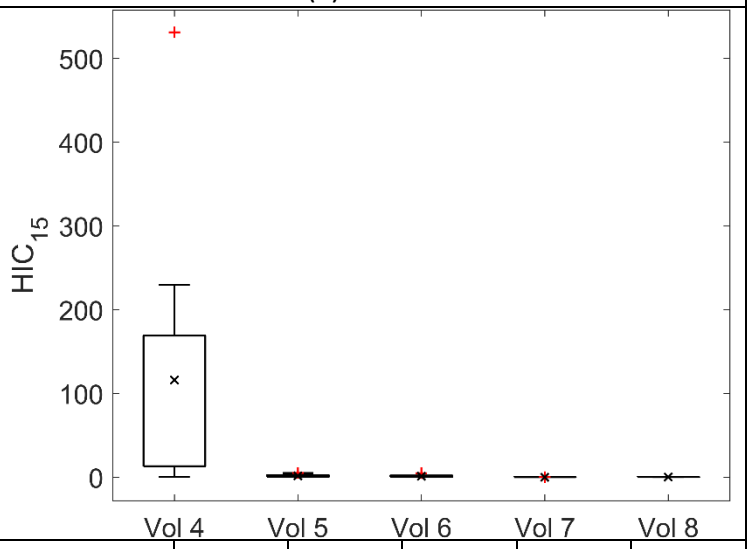
As mentioned above, volunteers in Dataset 2 generally had higher mean HIC_{15} values while firing Rifle E compared to Rifle D. The mean HIC_{15} ranges for Rifles D and E were 0.0125 to 0.2992 and 0.0922 to 116.19, respectively, with Rifle E exhibiting the widest range. Volunteers 4 and 5 clearly exhibited high HIC_{15} values when firing both Rifles D and E, biasing the overall trend between volunteers. When examining the CV, Volunteers 7 and 8 exhibited a lower CV, indicating low variability when firing both rifles. A one-way ANOVA was not conducted for this dataset as it would inherently detect a difference between volunteers given the substantially higher HIC_{15} values of Volunteers 4 and 5.

(i) Rifle D



Mean	0.2992	0.1428	0.0614	0.0125	0.0366
Std. Dev.	0.2042	0.1115	0.0304	0.0037	0.0023
CV (%)	68.24	78.08	49.50	29.74	6.25

(ii) Rifle E



Mean	116.19	1.6772	1.3802	0.0922	0.1528
Std. Dev.	156.98	1.6160	1.8055	0.0195	0.0331
CV (%)	135.11	96.35	130.81	21.18	21.64

Figure 32: Mean HIC_{15} and variation of the five volunteers for (i) Rifle D and (ii) Rifle E (Dataset 2: May 2022). Number of shots for Volunteer 1 (Rifles A:4, B:4, C:4), Volunteer 2 (Rifles A:2, B:4, C:4) and Volunteer 3 (Rifles A:3, B:3, C:3).

4.2.2 Summary of HIC_{15} Results from Datasets 1 and 2

Table 8: Summary of HIC_{15} results from Dataset 1

Dataset 1		
Comparisons		**Notes**
Rifle order for each volunteer based on mean HIC_{15}		• All volunteers exhibited the lowest HIC_{15} values with Rifle B • Volunteers exhibited the highest HIC_{15} values with either Rifle A or C
Vol 1	C > A > B	
Vol 2	A > C > B	
Vol 3	A > C > B	
Range of mean HIC_{15} values		
Rifle A	0.1371 to 0.2512	• Rifle A has the widest range of mean HIC_{15}, followed by Rifle C, then Rifle B
Rifle B	0.0878 to 0.1374	
Rifle C	0.1320 to 0.2116	
Order of CV between rifles for each volunteer		• No trend in CV between rifles, i.e., no common rifle where volunteers always exhibit higher or lower variability
Vol 1	C > A > B	
Vol 2	A > C > B	
Vol 3	B > A > C	
Volunteer order for each rifle based on mean HIC_{15}		• Volunteer 2 always exhibits the highest HIC_{15} • Either Volunteer 1 or 3 exhibits the lowest HIC_{15}
Rifle A	Vol 2 > 3 > 1	
Rifle B	Vol 2 > 3 > 1	
Rifle C	Vol 2 > 1 > 3	
Order of CV between volunteers for each rifle		• Volunteer 2 usually has a higher CV apart from Rifle B • Volunteer 3 usually has a lower CV apart from Rifle B
Rifle A	Vol 2 > 1 > 3	
Rifle B	Vol 3 > 2 > 1	
Rifle C	Vol 2 > 1 > 3	

Table 9: Summary of HIC_{15} results from Dataset 2

Dataset 2		
Comparisons		**Notes**
Rifle order for each volunteer based on mean HIC_{15}		• All volunteers had higher mean HIC_{15} with Rifle E compared to D
Vol 4	E > D	
Vol 5	E > D	
Vol 6	E > D	
Vol 7	E > D	
Vol 8	E > D	
Range of mean HIC_{15} values		
Rifle D	0.125 to 0.2992	• Rifle E has the widest range of mean HIC_{15} • Volunteers 4,5 and 6 exhibited uncharacteristically high mean HIC_{15} values
Rifle E	0.0922 to 116.19	
Order of CV between rifles for each volunteer		• Usually, volunteers exhibited higher CV, hence variability when firing Rifle E compared to Rifle D apart from Volunteer 6
Vol 4	E > D	
Vol 5	E > D	
Vol 6	E > D	
Vol 7	D > E	
Vol 8	E > D	
Volunteer order for each rifle based on mean HIC_{15}		• Volunteers 4 and 5 exhibited the highest mean HIC_{15} irrespective of rifle • Volunteer 7 exhibited the lowest mean HIC_{15} irrespective of the rifle
Rifle D	Vol4 > 5 > 6 > 8 > 7	
Rifle E	Vol4 > 5 > 8 > 6 > 7	
Order of CV between volunteers for each rifle		• Volunteers 7 and 8 exhibited a lower CV, indicating low variability when firing both rifles
Rifle D	Vol5 > 4 > 6 > 7 > 8	
Rifle E	Vol4 > 6 > 5 > 8 > 7	

4.2.3 Comparison of BrIC Between Different Rifles and Volunteers

The BrIC values computed for all shots from every volunteer are provided in Appendix C. The mean BrIC values were calculated for each rifle across all volunteers of datasets 1 and 2 (Figure 33-Figure 36)**.**

4.2.3.1 BrIC Results for Dataset 1: May 2021

4.2.3.1.1 Inter-Rifle BrIC Comparison for Three Rifle Configurations

Volunteers 1 and 2 exhibited higher mean BrIC when firing Rifle C in contrast to Rifle A. Conversely, Volunteer 3 exhibited higher mean BrIC when firing Rifle A compared to Rifle C. Volunteers 1 and 2 displayed the lowest BrIC value when using Rifle B, while Volunteer 3 maintained relatively consistent BrIC values across Rifles B and C. The CV followed a descending pattern for Volunteers 1 and 2, firing Rifles B, C, and A, whereas for Volunteer 3, the order was A, B, and C. This suggests that Volunteers 1 and 2 experienced increased variability when using Rifle B. In contrast, Volunteer 3 exhibited consistently low variability (0.5-3%) across all three rifles compared to Volunteers 1 and 2.

A one-way ANOVA analysis (detailed in Appendix C) was conducted at a significance level of α=0.05 to explore differences between rifles for each volunteer. Significant differences in BrIC values between rifles were observed for Volunteers 2 and 3, with p-values of 3.78E-2 and 2.24E-2, respectively. However, no statistically significant difference was identified between the rifles for Volunteer 1, with a p-value of 5.78E-2. The Tukey-Kramer test (detailed in Appendix C) identified a statistical difference between Rifles B and C for Volunteer 2, and between Rifles A and B as well as A and C for Volunteer 3.

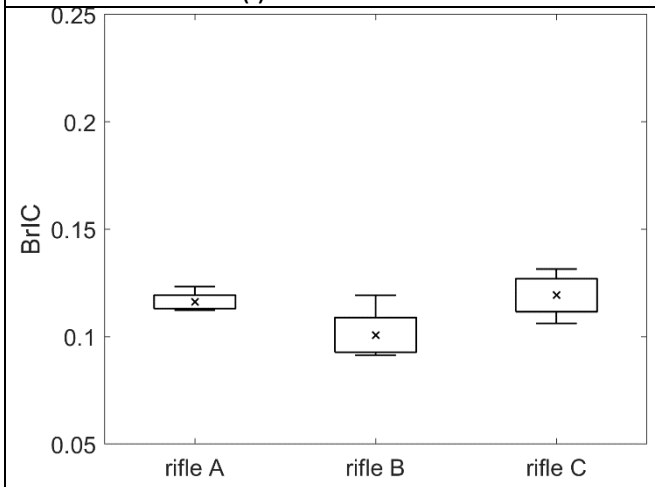
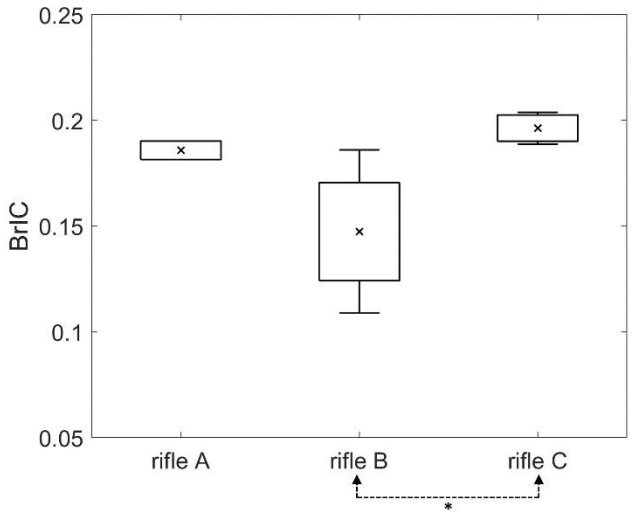
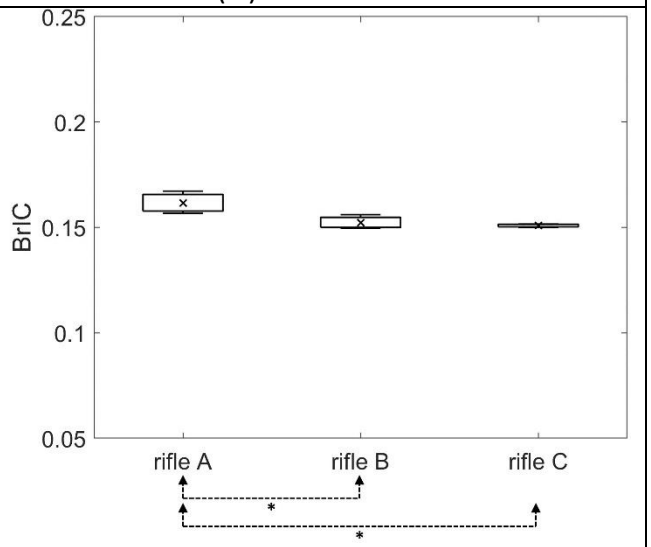
(i) Volunteer 1				(ii) Volunteer 2				(iii) Volunteer 3			
											
Mean	0.1162	0.1008	0.1193	Mean	0.1858	0.1474	0.1963	Mean	0.1616	0.1523	0.1509
Std. Dev.	0.0049	0.0126	0.0106	Std. Dev.	0.0062	0.0321	0.0073	Std. Dev.	0.0053	0.0034	0.0008
CV (%)	4.22	12.54	8.88	CV (%)	3.32	21.81	3.73	CV (%)	3.28	2.21	0.54

Figure 33: Mean BrIC and variation of the three rifles for (i) Volunteer 1, (ii) Volunteer 2, and (iii) Volunteer 3 (Dataset 1: May 2021). * = statistically significant difference detected between rifles. CV = coefficient of variation. Number of shots for Volunteer 1 (Rifle s A:4, B:4, C:4), Volunteer 2 (Rifles A:2, B:4, C:4) and Volunteer 3 (Rifles A:3, B:3, C:3).

4.2.3.1.2 Inter-Volunteer BrIC Comparison for Three Volunteers

The mean BrIC ranges for Rifles A, B, and C were 0.1162 to 0.1858, 0.1008 to 0.1523, and 0.1193 to 0.1963, respectively. Rifle C exhibited the widest range, followed by Rifles A and B. When firing Rifles A and C, the BrIC values followed a descending order, with Volunteers 2, 3, and 1 showing progressively higher to lower values. Conversely, when firing Rifle B, this order shifted to Volunteers 3, 2, and 1. As a result, Volunteer 1 consistently displayed the lowest BrIC values across all three rifles, while Volunteer 2 exhibited higher BrIC values when firing Rifles A and C but not B.

The CV range for firing Rifle A remained consistent across all volunteers, fluctuating between 3 and 4%, indicating uniform variability among them. However, the CV range widened for Rifle C, spanning from 0.5 to 9%. Volunteer 3 demonstrated minimal variability when firing Rifle C, followed by Volunteer 2 and then Volunteer 1. All volunteers showed an increase in CV when firing Rifle B, ranging from 2% to 12%. Volunteer 2 experienced the most significant increase in variability, transitioning from approximately 3% for Rifle s A and C to around 21% for Rifle B.

A one-way ANOVA analysis (detailed in Appendix C) was conducted at a significance level of α=0.05 to explore differences between volunteers for each rifle. Significant differences in BrIC values between volunteers were identified for all three rifles, with a p-value of 1.04E-05, 1.92E-02, and 2.55E-06 for Rifles A, B, and C, respectively. The Tukey-Kramer test (detailed in Appendix C) identified a statistical difference between all groups for Rifles A and C, and between Volunteers 1 and 2, as well as between Volunteers 1 and 3, for Rifle B.

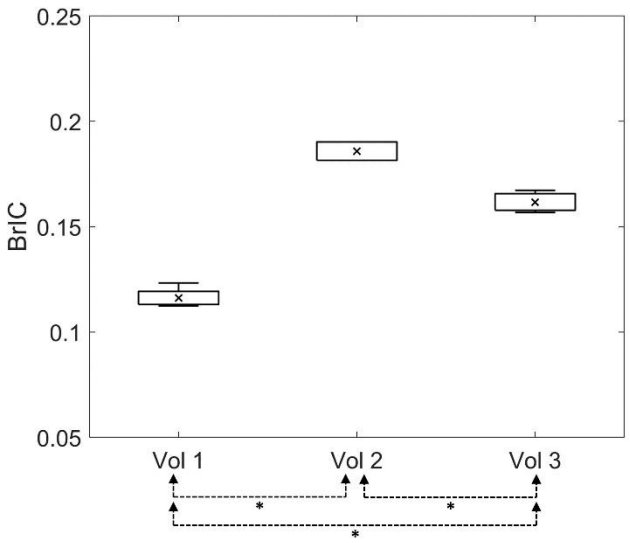
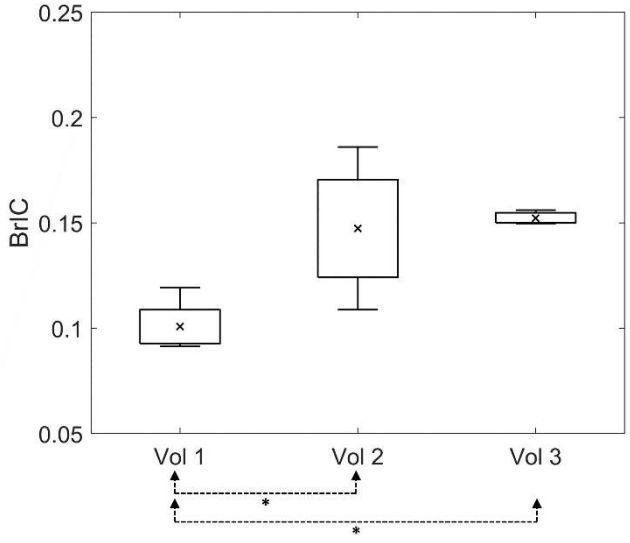
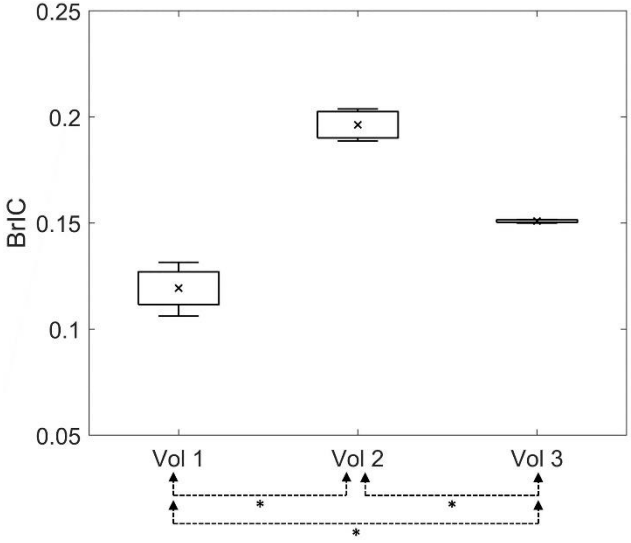
(i) Rifle A				(ii) Rifle B				(iii) Rifle C			
											
Mean	0.1162	0.1858	0.1616	Mean	0.1008	0.1474	0.1523	Mean	0.1193	0.1963	0.1509
Std. Dev.	0.0049	0.0062	0.0053	Std. Dev.	0.0126	0.0321	0.0034	Std. Dev.	0.0106	0.0073	0.0008
CV (%)	4.22	3.32	3.28	CV (%)	12.54	21.81	2.21	CV (%)	8.88	3.73	0.54

Figure 34: Mean BrIC and variation of the three volunteers for (i) Rifle A, (ii) Rifle B, and (iii) Rifle C (Dataset 1: May 2021). *= statistically significant difference detected between volunteers. CV=coefficient of variation. Number of shots for Volunteer 1 (Rifle s A:4, B:4, C:4), Volunteer 2 (Rifles A:2, B:4, C:4) and Volunteer 3 (Rifles A:3, B:3, C:3).

4.2.3.2 BrIC Results for Dataset 2: May 2022

4.2.3.2.1 Inter-Rifle BrIC Comparison for Two Rifle Configurations

In Dataset 2, all volunteers demonstrated higher mean BrIC values when firing Rifle E compared to Rifle D. Notably, Volunteers 4, 5, and 6 exhibited significantly elevated CV (ranging between 20-50%) when using Rifle E, suggesting high variability for these individuals with this rifle. Conversely, Volunteers 7 and 8 showed only slightly higher CV when firing Rifle D, with the difference in CV between Rifles D and E being minimal, less than a delta of 2. This indicates that Volunteers 7 and 8 maintained consistent variability regardless of the rifle used.

Furthermore, the mean BrIC values for Volunteers 5, 6, 7, and 8 when firing Rifle E in Dataset 2 fell within the range of BrIC values for Rifles A and C in Dataset 1. Note that all three rifles were of the same caliber (.50 cal). Although the mean values closely mirrored those of Dataset 1, Volunteers 4, 5, and 6 displayed higher CV values when using Rifle E. In contrast, Volunteers 7 and 8 CV values while using Rifle E were within the range of CV values exhibited by Volunteers 1, 2, and 3 from Dataset 1.

A t-test (detailed in Appendix C) was conducted at a significance level of $\alpha=0.05$ to explore differences between rifles for each volunteer. Significant differences in BrIC values between rifles were observed for all volunteers, with p-values of 1.34E-4, 5.92E-5, 5.21E-4, 4.78E-19, and 7.50E-12 for Volunteers 4, 5, 6, 7, and 8 respectively.

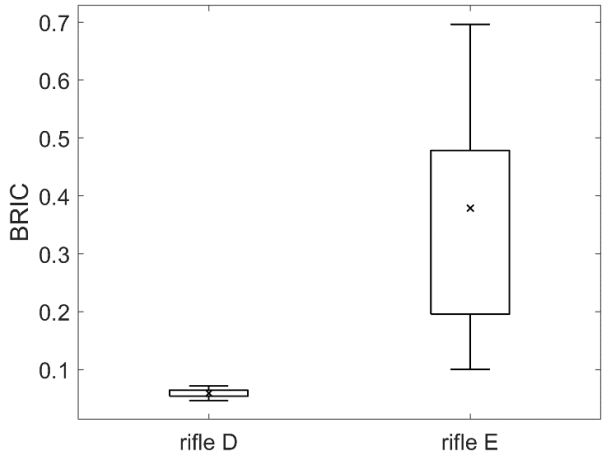
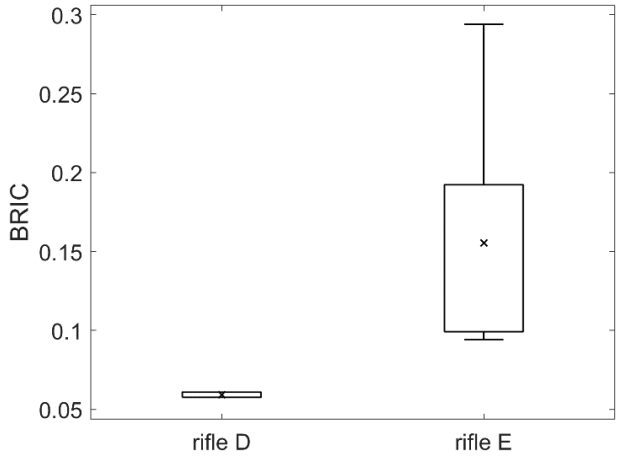
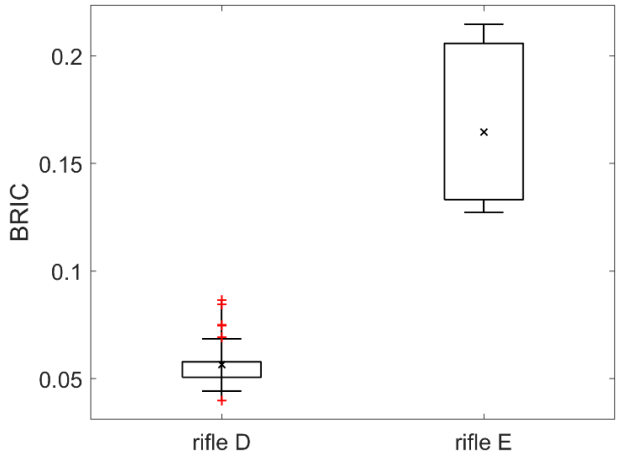
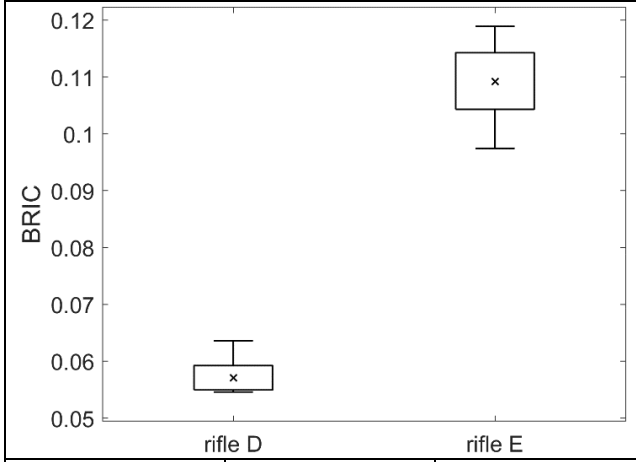
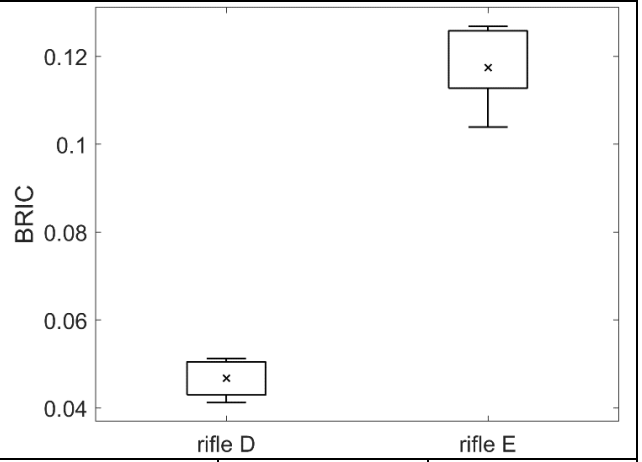
(i) Volunteer 4*			(ii) Volunteer 5*			(iii) Volunteer 6*		
								
Mean	0.0589	0.3788	Mean	0.0592	0.1555	Mean	0.0565	0.1646
Std. Dev.	0.0067	0.1935	Std. Dev.	0.0023	0.0705	Std. Dev.	0.0108	0.0386
CV (%)	11.43	51.08	CV (%)	3.88	45.32	CV (%)	19.16	23.46
(iv) Volunteer 7*			(v) Volunteer 8*					
								
Mean	0.0571	0.1092	Mean	0.0468	0.1174			
Std. Dev.	0.0034	0.0060	Std. Dev.	0.0043	0.0084			
CV (%)	5.97	5.46	CV (%)	9.20	7.16			

Figure 35: Mean BrIC and variation of the two rifles for (i) Volunteer 4, (ii) Volunteer 5, (iii) Volunteer 6, (iv) Volunteer 7, (v) Volunteer 8 (Dataset 2: May 2022). *= statistically significant difference detected between rifles. CV = coefficient of variation. Number of shots for Volunteer 4 (Rifles D:36, E:11), Volunteer 5 (Rifles D:2, E:15), Volunteer 6 (Rifles D:33, E:6), Volunteer 7 (Rifles D:8, E:18) and Volunteer 8(Rifles D:5, E:10).

4.2.3.2.2 Inter-Volunteer BrIC Comparison for Five Volunteers

The mean BrIC ranges for Rifles D and E were 0.0468 to 0.0592 and 0.1092 to 0.3788, respectively, with Rifle E exhibiting the widest range. When firing Rifle D, the BrIC values followed a descending order, with Volunteers 4,5,7,6, and 8 showing progressively higher to lower values. This order shifted to Volunteers 4,6,5,8, and 7 when firing Rifle E. The CV range for firing Rifle D was between 3% and 19%, with Volunteers 4 and 6 having the higher CV values. The CV range widened for Rifle E, spanning from 5% to 51%. Specifically, Volunteer 4 demonstrated a really high CV at 51% when firing Rifle E.

A one-way ANOVA analysis (detailed in Appendix C) was conducted at a significance level of α=0.05 to explore differences between volunteers for each rifle. No statistically significant difference was identified between the volunteers for Rifle D, with a p-value of 5.67E-2. A statistically significant difference was identified between the volunteers for Rifle E with a p-value of 2.7E-9. The Tukey-Kramer test (detailed in Appendix C) identified a statistical difference between the following groups for Rifle E: Volunteers 4 and 5, 4 and 6, 4 and 7 ,and 4 and 8.

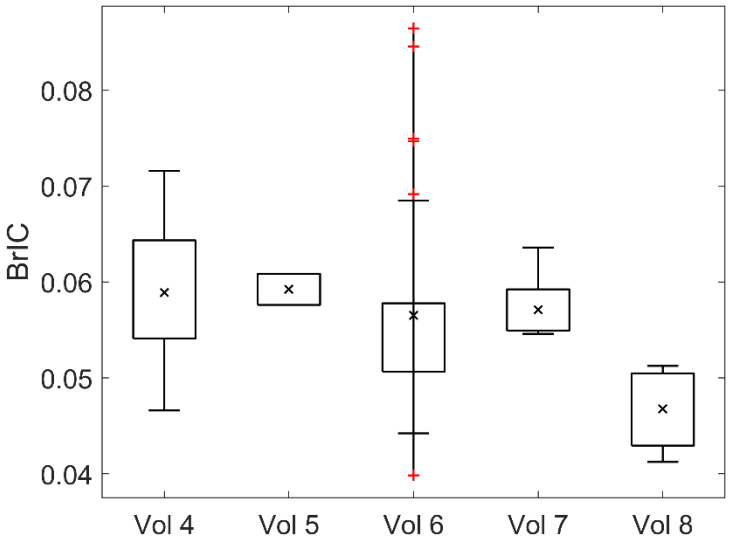
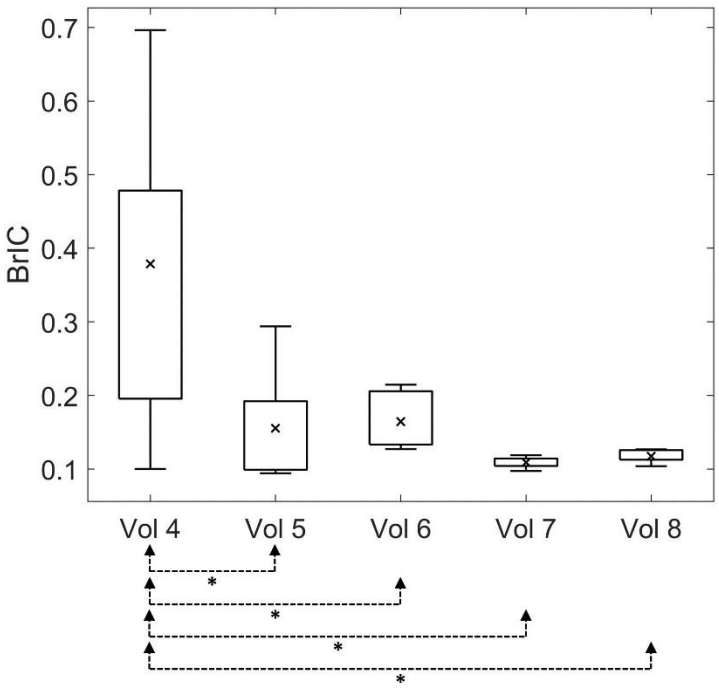
(i) Rifle D						(ii) Rifle E					
											
Mean	0.0589	0.0592	0.0565	0.0571	0.0468	Mean	0.3788	0.1555	0.1646	0.1092	0.1174
Std. Dev.	0.0067	0.0023	0.0108	0.0034	0.0043	Std. Dev.	0.1935	0.0705	0.0386	0.0060	0.0084
CV (%)	11.43	3.88	19.16	5.97	9.20	CV (%)	51.08	45.32	23.46	5.46	7.16

Figure 36: Mean BrIC and variation of the five volunteers for (i) Rifle D and (ii) Rifle E (Dataset 2: May 2022). *= statistically significant difference detected between rifles. CV = coefficient of variation. Number of shots for Volunteer 1 (Rifles A:4, B:4, C:4), Volunteer 2 (Rifles A:2, B:4, C:4) and Volunteer 3 (Rifles A:3, B:3, C:3).

4.2.4 Summary of BrIC Results from Datasets 1 and 2

Table 10: Summary of BrIC Results from Dataset 1

Dataset 1		
Comparisons		**Notes**
Rifle order for each volunteer based on mean BrIC		• Volunteers usually exhibited higher BrIC values when firing Rifle C apart from Vol 3 • Volunteers usually exhibited lower BrIC values when firing Rifle B apart from Vol 3
Vol 1	C > A > B	
Vol 2	C > A > B	
Vol 3	A > B > C	
Range of mean BrIC values		
Rifle A	0.1162 to 0.1858	• Rifle C exhibited the widest range, followed by Rifle A and then Rifle B
Rifle B	0.1008 to 0.1523	
Rifle C	0.1193 to 0.1963	
Order of CV between rifles for each volunteer		• Volunteers usually exhibited higher variability with Rifle B apart from Volunteer 3
Vol 1	B > C > A	
Vol 2	B > C > A	
Vol 3	A > B > C	
Volunteer order for each rifle based on mean BrIC		• Volunteer 2 usually exhibited the highest BrIC apart from Rifle B • Volunteer 1 exhibited the lowest BrIC irrespective of the rifle
Rifle A	Vol 2 > 3 > 1	
Rifle B	Vol 3 > 2 > 1	
Rifle C	Vol 2 > 3 > 1	
Order of CV between volunteers for each rifle		• Volunteer 1 usually exhibited higher variability apart from Rifle B • Volunteer 3 usually exhibited lower variability apart from Rifle B
Rifle A	Vol 1 > 2 > 3	
Rifle B	Vol 2 > 1 > 3	
Rifle C	Vol 1 > 2 > 3	

Table 11: Summary of BrIC Results from Dataset 2

Dataset 2		
Comparisons		**Notes**
Rifle order for each volunteer based on mean BrIC		• All volunteers had higher mean BrIC with Rifle E compared to D
Vol 4	E > D	
Vol 5	E > D	
Vol 6	E > D	
Vol 7	E > D	
Vol 8	E > D	
Range of mean BrIC values		
Rifle D	0.0468 to 0.0592	• Rifle E has the widest range of mean BrIC
Rifle E	0.1092 to 0.3788	
Order of CV between rifles for each volunteer		• Usually, volunteers exhibited higher CV, hence variability when firing Rifle E compared to Rifle D apart from Volunteers 7 and 8
Vol 4	E > D	
Vol 5	E > D	
Vol 6	E > D	
Vol 7	D > E	
Vol 8	D > E	
Volunteer order for each rifle based on mean BrIC		• The volunteers exhibiting the highest and lowest BrIC values differed for each rifle
Rifle D	Vol5 > 4 > 7 > 6 > 8	
Rifle E	Vol4 > 6 > 5 > 8 > 7	
Order of CV between volunteers for each rifle		• The order of CV between volunteers differed between rifles
Rifle D	Vol6 > 4 > 8 > 7 > 5	
Rifle E	Vol4 > 5 > 6 > 8 > 7	

4.3 Strain-based Metrics Results

Two strain-based metrics, MPS_{95} and CSV, were calculated using the finite element head model for all shots in Datasets 1 and 2, and a comprehensive listing of these values is provided in Appendix D, E, and F. Hereafter, when comparing the FE outcomes for Volunteers 1, 2, and 3, the reference is to the accelerative inputs measured for each individual shot, applied to the GHBMC FE model.

4.3.1 Comparison of MPS_{95} Between Different Rifles and Volunteers

Each shot in both datasets was individually simulated, with MPS_{95} values computed for the whole brain region of every shot from each volunteer, as outlined in Appendix D. Mean MPS_{95} values were then calculated for each rifle across all volunteers in Datasets 1 and 2 (Figure 37-Figure 40).

4.3.1.1 MPS_{95} Results for Dataset 1: May 2021

4.3.1.1.1 Inter-Rifle MPS_{95} Comparison for Three Rifle Configurations

Volunteers 1 and 2 exhibited higher mean MPS_{95} when firing Rifle C compared to Rifle A. Conversely, Volunteer 3 exhibited a higher mean MPS_{95} when firing Rifle A than Rifle C. Across all volunteers, the MPS_{95} values were consistently lowest when using Rifle B compared to Rifles A and C. The CV values exhibited a descending order when firing Rifles B, A, and C for Volunteer 1; Rifles B, C, and A for Volunteer 2; and Rifles A, C, and B for Volunteer 3. Consequently, no apparent trend in variability for MPS_{95} was observed between rifles. However, Volunteers 1 and 2 showed a significant increase in variability, nearly doubling, when firing Rifle B compared to the other two rifles. Volunteer 3 displayed the opposite trend, with a decrease in CV when firing Rifle B in contrast with the other two rifles.

A one-way ANOVA analysis (detailed in Appendix D) was conducted at a significance level of α=0.05 to explore differences between rifles for each volunteer. Significant differences in MPS_{95} values between rifles were observed for Volunteers 1 and 2, with p-values of 7.41E-3 and 1.91E-3, respectively. However, no statistically significant difference was identified between the rifles for Volunteer 3, with a p-value of 1.14E-1. The Tukey-Kramer test (detailed in Appendix D)

identified a statistical difference between Rifles B and C for Volunteer 1 and between Rifles A and B as well as B and C for Volunteer 2.

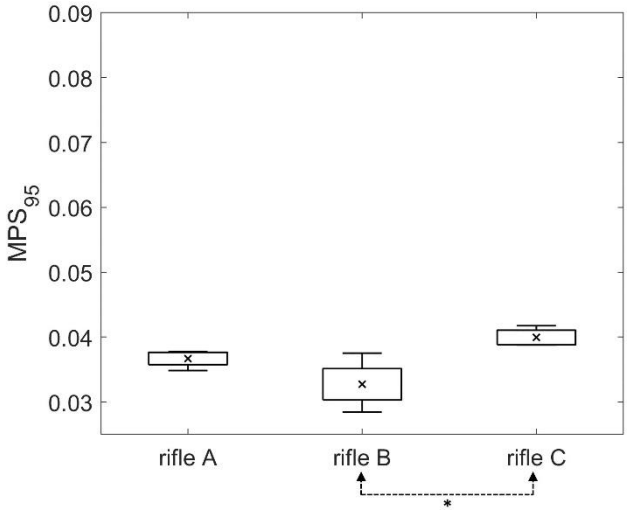
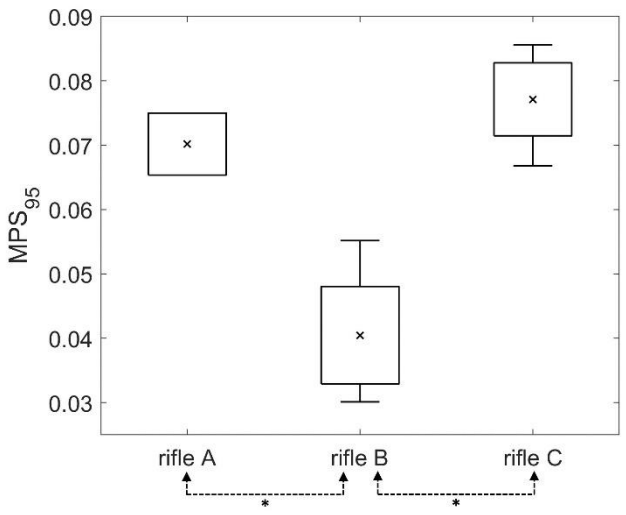
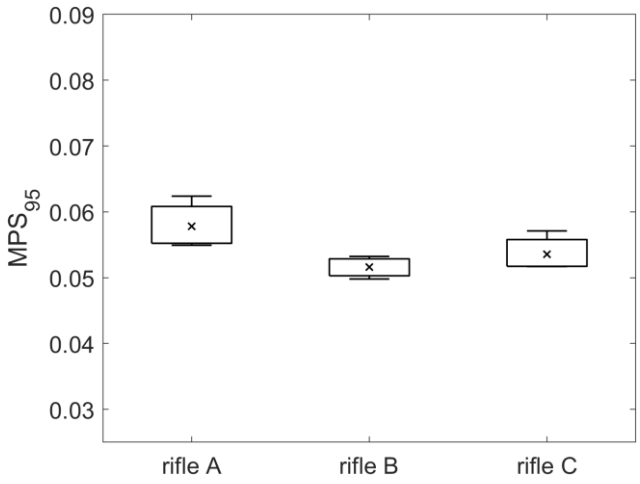
(i) Volunteer 1				(ii) Volunteer 2				(iii) Volunteer 3			
											
Mean	0.0367	0.0327	0.0399	Mean	0.0702	0.0405	0.0771	Mean	0.0578	0.0516	0.0535
Std. Dev.	0.0013	0.0037	0.0014	Std. Dev.	0.0068	0.0107	0.0079	Std. Dev.	0.0040	0.0017	0.0031
CV (%)	3.61	11.39	3.54	CV (%)	9.70	26.56	10.25	CV (%)	6.93	3.33	5.76

Figure 37: Mean MPS_{95} and variation of the three rifles for (i) Volunteer 1, (ii) Volunteer 2, and (iii) Volunteer 3 (Dataset 1: May 2021). * = statistically significant difference detected between rifles. CV = coefficient of variation. Number of shots for Volunteer 1 (Rifles A:4, B:4, C:4), Volunteer 2 (Rifles A:2, B:4, C:4) and Volunteer 3 (Rifles A:3, B:3, C:3).

4.3.1.1.2 Inter-Volunteer MPS_{95} Comparison for Three Volunteers

The mean MPS_{95} ranges for Rifles A, B, and C were 0.0367 to 0.0702, 0.0327 to 0.0516, and 0.0399 to 0.0771, respectively. Rifle C exhibited the widest range, followed by Rifles A and B. When firing Rifles A and C, the MPS_{95} values followed a descending order, with Volunteers 2, 3, and 1 showing progressively higher to lower values. Conversely, when firing Rifle B, this order shifted to Volunteers 3, 2, and 1. As a result, Volunteer 1 consistently displayed the lowest MPS_{95} values across all three rifles, while Volunteer 2 exhibited higher MPS_{95} values when firing Rifles A and C but not B.

The CV range for firing Rifle A and C were similar, ranging between 3% and 10%. However, the CV range widened for Rifle C, spanning from 3 to 26%. Volunteer 2 demonstrated the highest variability when firing Rifle B, with a CV of 26%.

A one-way ANOVA analysis (detailed in Appendix D) was conducted at a significance level of α=0.05 to explore differences between volunteers for each rifle. Significant differences in MPS_{95} values between volunteers were identified for all three rifles, with a p-value of 1.05E-4, 2.73E-2, and 2.415E-5 for Rifles A, B, and C, respectively. The Tukey-Kramer test (detailed in Appendix D) identified a statistical difference between Volunteers 1 and 2, as well as between 1 and 3 for Rifle A; between Volunteers 1 and 3 for Rifle B; and between all volunteers for Rifle C.

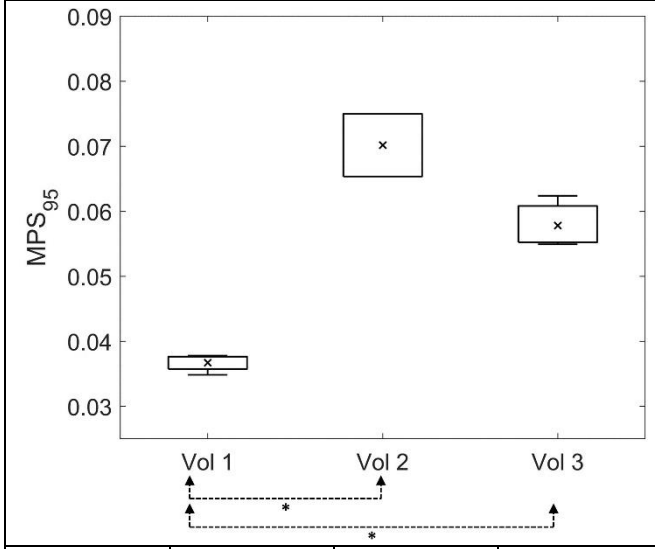
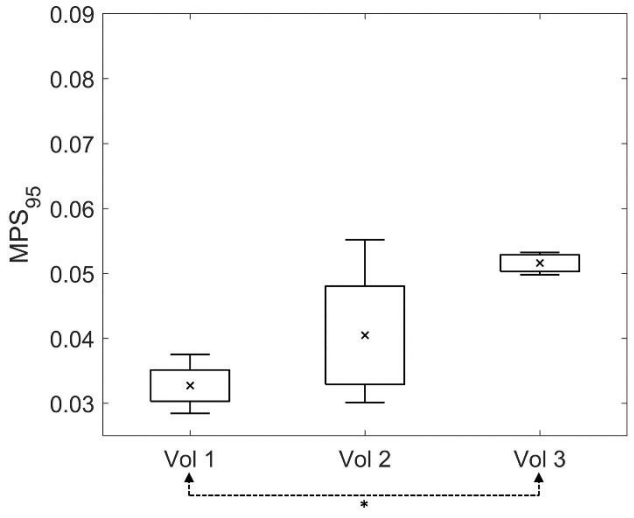
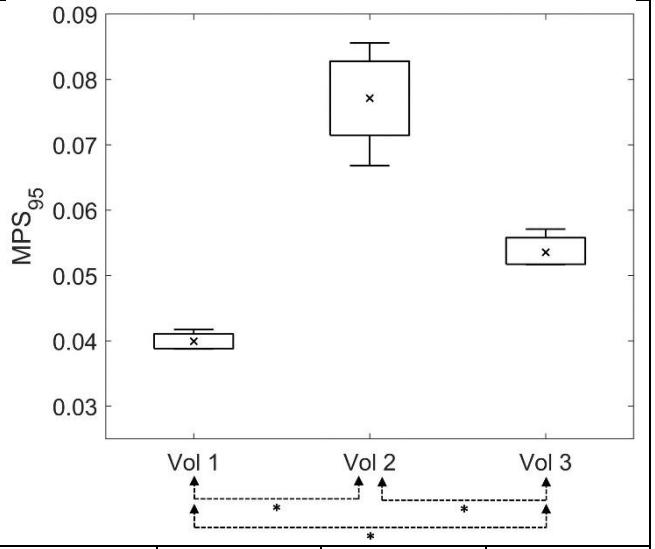
(i) Rifle A				(ii) Rifle B				(iii) Rifle C			
											
Mean	0.0367	0.0702	0.0578	Mean	0.0327	0.0405	0.0516	Mean	0.0399	0.0771	0.0535
Std. Dev.	0.0013	0.0068	0.0040	Std. Dev.	0.0037	0.0107	0.0017	Std. Dev.	0.0014	0.0079	0.0031
CV (%)	3.61	9.70	6.93	CV (%)	11.39	26.56	3.33	CV (%)	3.54	10.25	5.76

Figure 38: Mean MPS_{95} and variation of the three volunteers for (i) Rifle A, (ii) Rifle B, and (iii) Rifle C (Dataset 1: May 2021). * = statistically significant difference detected between volunteers. CV = coefficient of variation. Number of shots for Volunteer 1 (Rifles A:4, B:4, C:4), Volunteer 2 (Rifles A:2, B:4, C:4) and Volunteer 3 (Rifles A:3, B:3, C:3).

4.3.1.2 MPS_{95} Results for Dataset 2: May 2022

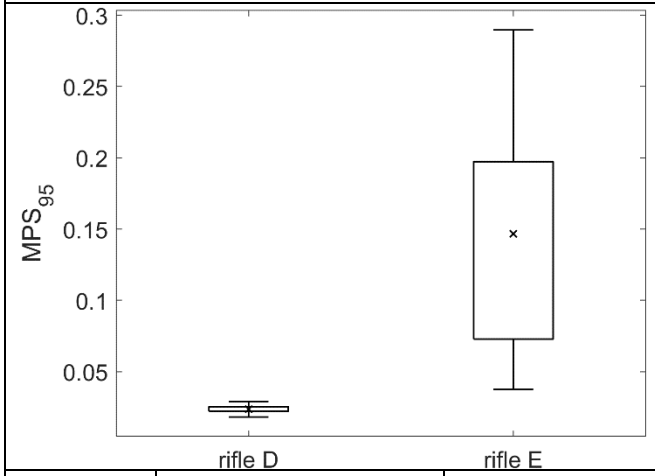
4.3.1.2.1 Inter-Rifle MPS_{95} Comparison for Two Rifle Configurations

In Dataset 2, all volunteers consistently showed higher mean MPS_{95} values when firing Rifle E compared to Rifle D. Echoing the trends observed with BrIC values, Volunteers 4, 5, and 6 exhibited significantly elevated CV (ranging between 30% and 50%) when using Rifle E, indicating considerable variability among these individuals with this rifle. Conversely, the difference in CV between Rifles D and E for Volunteers 7 and 8 was minimal, less than a delta of 2, suggesting low variability irrespective of the rifle used.

Similar to the findings with BrIC values, the mean MPS_{95} values for Volunteers 5, 6, 7, and 8 in Dataset 2 fell within the range of BrIC values for Rifles A and C in Dataset 1, with all three rifles being of the same caliber. While the mean values closely aligned with Dataset 1, Volunteers 4, 5, and 6 exhibited higher CV values when using Rifle E. In contrast, Volunteers 7 and 8 CV values while using Rifle E were within the range of CV values exhibited by Volunteers 1, 2, and 3 from Dataset 1.

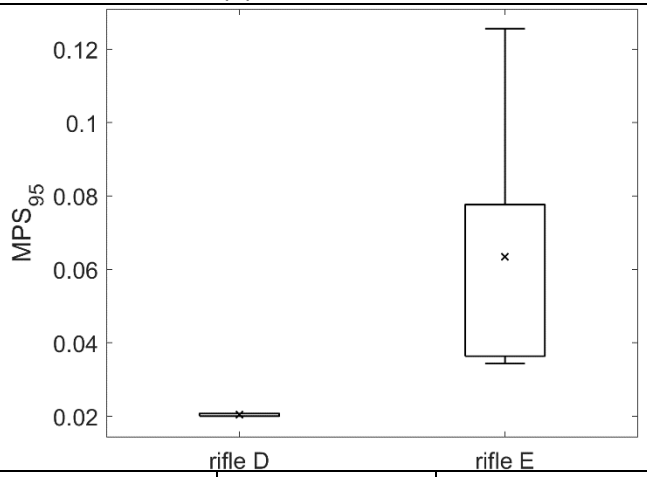
A t-test (detailed in Appendix D) was conducted at a significance level of $\alpha=0.05$ to explore differences between rifles for each volunteer. Significant differences in MPS_{95} values between rifles were observed for all volunteers, with p-values 4.92E-5, 2.59E-3, 2.26E-22, and 1.12E-9 for Volunteers 4,5, 6,7, and 8, respectively.

(i) Volunteer 4*



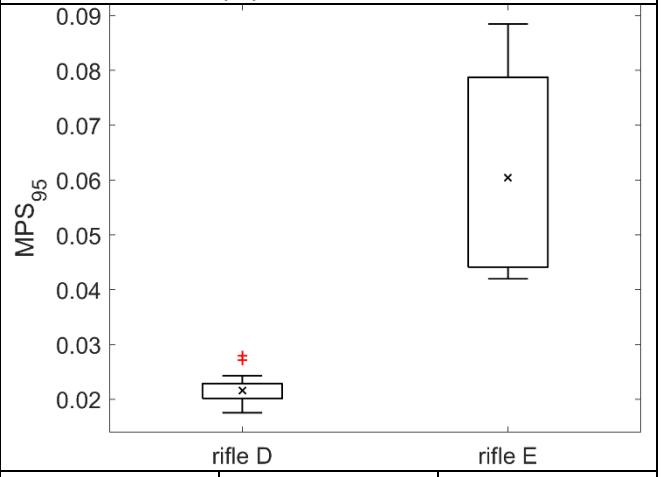
Mean	0.0238	0.1466
Std. Dev.	0.0025	0.0783
CV (%)	10.49	53.38

(ii) Volunteer 5*



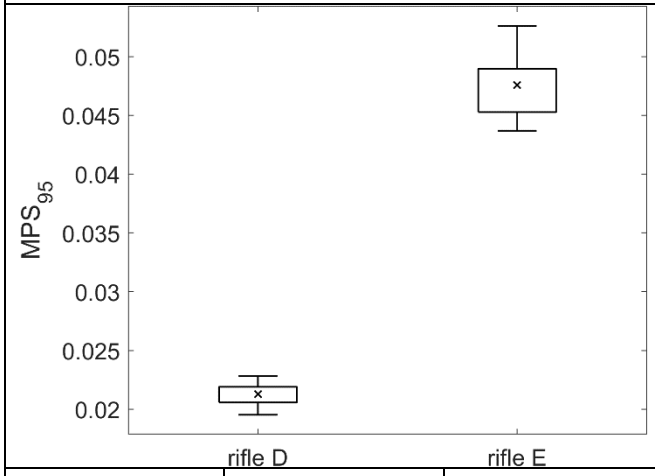
Mean	0.0204	0.0635
Std. Dev.	0.0005	0.0310
CV (%)	2.50	48.87

(iii) Volunteer 6*



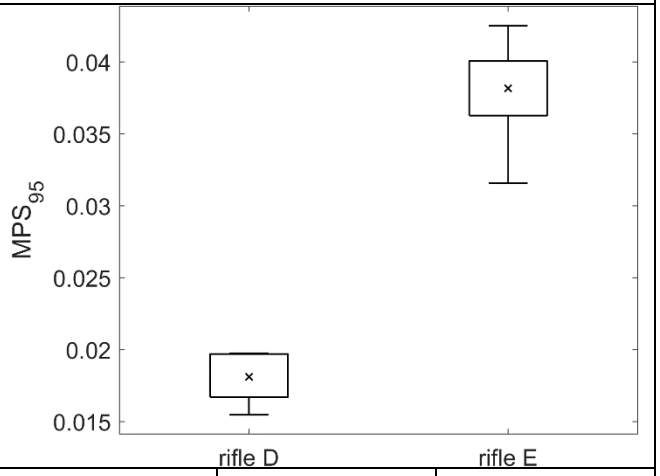
Mean	0.0216	0.0604
Std. Dev.	0.0023	0.0201
CV (%)	10.42	33.20

(iv) Volunteer 7*



Mean	0.0213	0.0476
Std. Dev.	0.0011	0.0027
CV (%)	5.21	5.74

(v) Volunteer 8*



Mean	0.0181	0.0382
Std. Dev.	0.0018	0.0031
CV (%)	10.04	8.15

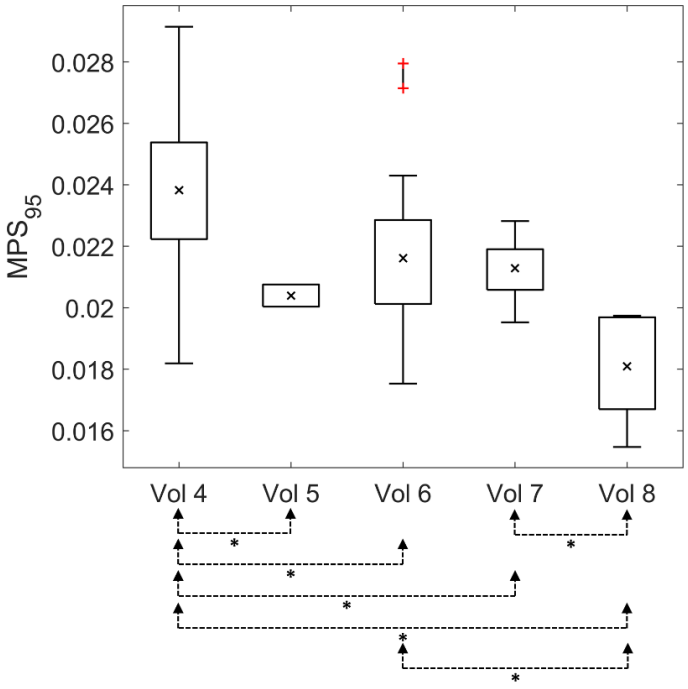
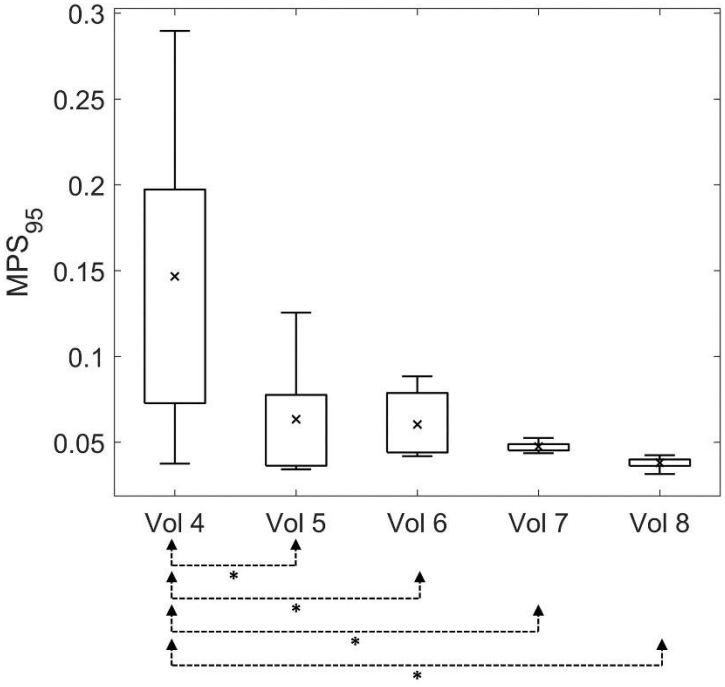
Figure 39: Mean MPS_{95} and variation of the two rifles for (i) Volunteer 4, (ii) Volunteer 5, (iii) Volunteer 6, (iv) Volunteer 7, (v) Volunteer 8 (Dataset 2: May 2022). *= statistically significant difference detected between rifles. CV=coefficient of variation. Number of shots for Volunteer 4 (Rifles D:36, E:11), Volunteer 5 (Rifles D:2, E:15), Volunteer 6 (Rifles D:33, E:6), Volunteer 7 (Rifles D:8, E:18) and Volunteer 8 (Rifles D:5, E:10).

4.3.1.2.2 Inter-Volunteer MPS_{95} Comparison for Five Volunteers

The mean MPS_{95} ranges for Rifles D and E were 0.0181 to 0.0238 and 0.0382 to 0.1466, respectively, with Rifle E exhibiting the widest range.

When firing Rifle D, the MPS_{95} values followed a descending order, with Volunteers 4,6,7,5 and 8 showing progressively higher to lower values. This order shifted to Volunteers 4,5,6,7 and 8 when firing Rifle E. The CV range for firing Rifle D was between 2% and 10%, with Volunteers 4 and 8 having the higher CV values. The CV range widened for Rifle E, spanning from 5% to 53%. Specifically, Volunteer 4 demonstrated a really high CV at 53% when firing Rifle E.

A one-way ANOVA analysis (detailed in Appendix D) was conducted at a significance level of α=0.05 to explore differences between volunteers for each rifle. A statistically significant difference was identified between the volunteers for both rifles, with a p-value of 1.44E-6 and 2.01E-8 for Rifles D and E, respectively. The Tukey-Kramer test (detailed in Appendix D) identified a statistical difference for Rifle D between the following volunteers: 4 and 5, 4 and 6, 4 and 7,4 and 8, 6 and 8, and 7 and 8. It also identified a statistical difference for Rifle E between Volunteers 4 and 5, 4 and 6, 4 and 7, and 4 and 8.

(i) Rifle D	(ii) Rifle E
	

Mean	0.0238	0.0204	0.0216	0.0213	0.0181	Mean	0.1466	0.0635	0.0604	0.0476	0.0382
Std. Dev.	0.0025	0.0005	0.0023	0.0011	0.0018	Std. Dev.	0.0783	0.0310	0.0201	0.0027	0.0031
CV (%)	10.49	2.50	10.42	5.21	10.04	CV (%)	53.38	48.87	33.20	5.74	8.15

Figure 40: Mean MPS_{95} and variation of the five volunteers for (i) Rifle D and (ii) Rifle E (Dataset 2: May 2022). *= statistically significant difference detected between rifles. CV=coefficient of variation. Number of shots for Volunteer 1 (Rifles A:4, B:4, C:4), Volunteer 2 (Rifles A:2, B:4, C:4) and Volunteer 3 (Rifles A:3, B:3, C:3).

4.3.2 Summary of MPS_{95} Results from Datasets 1 and 2

Table 12: Summary of MPS_{95} Results from Dataset 1

Comparisons		**Notes**
Dataset 1		
Rifle order for each volunteer based on mean MPS_{95}		• Volunteers usually exhibited higher MPS_{95} values when firing Rifle C apart from Vol 3 • All volunteers usually exhibited lower MPS_{95} values when firing Rifle B
Vol 1	C > A > B	
Vol 2	C > A > B	
Vol 3	A > C > B	
Range of mean MPS_{95} values		
Rifle A	0.0367 to 0.0702	• Rifle C exhibited the widest range, followed by Rifle A and then Rifle B
Rifle B	0.0327 to 0.0516	
Rifle C	0.0399 to 0.0771	
Order of CV between rifles for each volunteer		• No apparent trend in variability for MPS_{95} was observed between rifles • Volunteers 1 and 2 showed a significant increase in variability, nearly doubling • Volunteer 3 displayed the opposite trend, with a decrease in CV when firing Rifle B in contrast with the other two rifles.
Vol 1	B > A > C	
Vol 2	B > C > A	
Vol 3	A > C > B	
Volunteer order for each rifle based on mean MPS_{95}		• Volunteer 1 consistently displayed the lowest MPS_{95} values across all three rifles • Volunteer 2 exhibited higher MPS_{95} values when firing Rifles A and C but not B
Rifle A	Vol 2 > 3 > 1	
Rifle B	Vol 3 > 2 > 1	
Rifle C	Vol 2 > 3 > 1	
Order of CV between volunteers for each rifle		• Volunteer 2 exhibited the highest CV, i.e. variability across all three rifles
Rifle A	Vol 2 > 3 > 1	
Rifle B	Vol 2 > 1 > 3	
Rifle C	Vol 2 > 3 > 1	

Table 13: Summary of MPS_{95} Results from Dataset 2

Dataset 2		
Comparisons		**Notes**
Rifle order for each volunteer based on mean MPS_{95}		• All volunteers had higher mean MPS_{95} with Rifle E compared to D
Vol 4	E > D	
Vol 5	E > D	
Vol 6	E > D	
Vol 7	E > D	
Vol 8	E > D	
Range of mean HIC_{15} values		
Rifle D	0.0181 to 0.0238	• Rifle E has the widest range of mean MPS_{95}
Rifle E	0.0382 to 0.1466	
Order of CV between rifles for each volunteer		• All volunteers exhibited higher CV, i.e., variability when firing Rifle E compared to Rifle D
Vol 4	E > D	
Vol 5	E > D	
Vol 6	E > D	
Vol 7	E > D	
Vol 8	E > D	
Volunteer order for each rifle based on mean MPS_{95}		• Volunteer 4 always had the highest mean MPS_{95} value for both Rifles D and E • Volunteer 8 always had the lowest mean MPS_{95} value for both Rifles D and E
Rifle D	Vol4 > 6 > 7 > 5 > 8	
Rifle E	Vol4 > 5 > 6 > 7 > 8	
Order of CV between volunteers for each rifle		• Volunteer 4 exhibited the highest CV, i.e., variability irrespective of the rifle used
Rifle D	Vol4 > 6 > 8 > 7 > 5	
Rifle E	Vol4 > 5 > 6 > 8 > 7	

4.3.3 Comparison of CSV Curves of the Whole Brain Between Different Rifles and Volunteers

Mean A_{CSV} values were computed for all rifle configurations and each volunteer, with the complete list of A_{CSV} values computed outlined in Appendix E. The CSV curves for every shot from all volunteers were plotted individually (Figure 41-Figure 45).

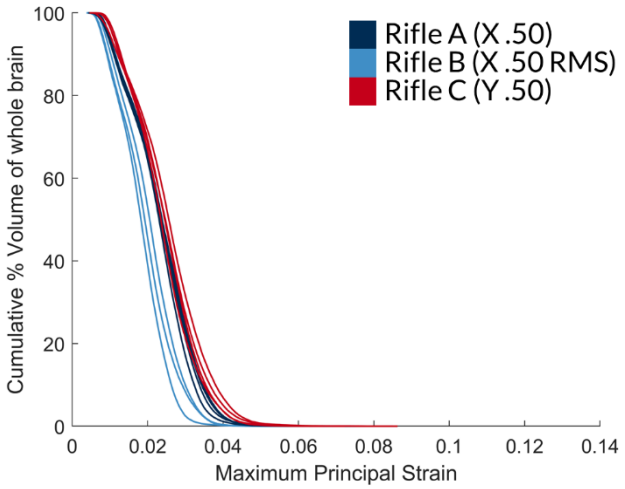
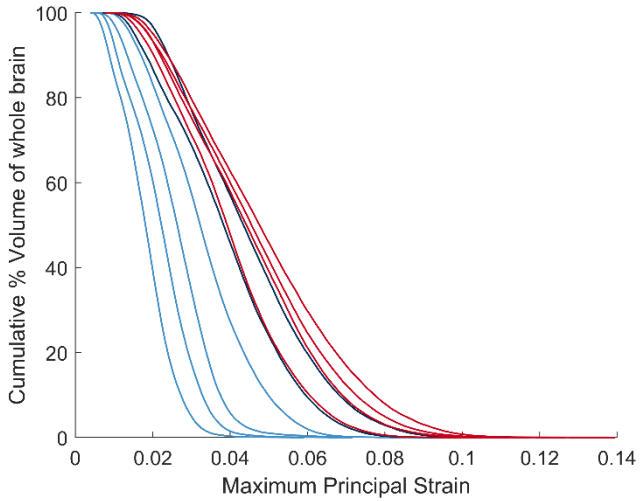
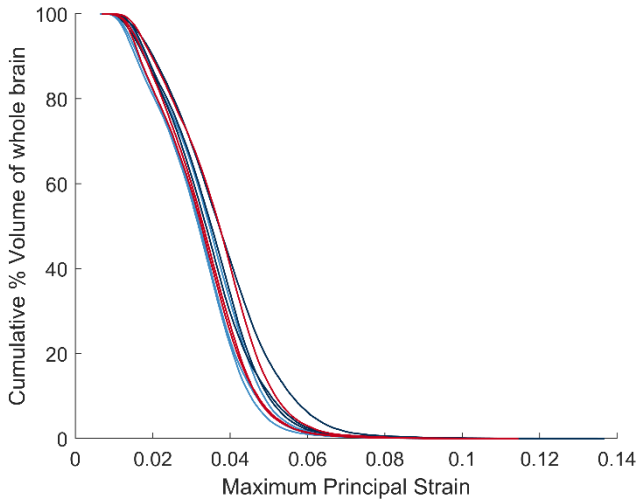
4.3.3.1 CSV Curves of the Whole Brain for Dataset 1: May 2021

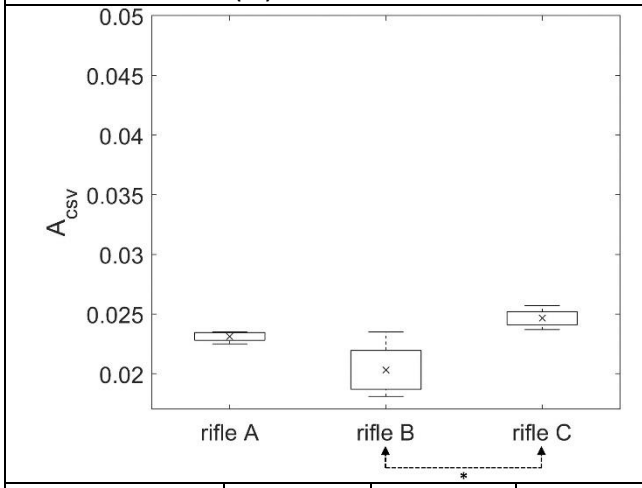
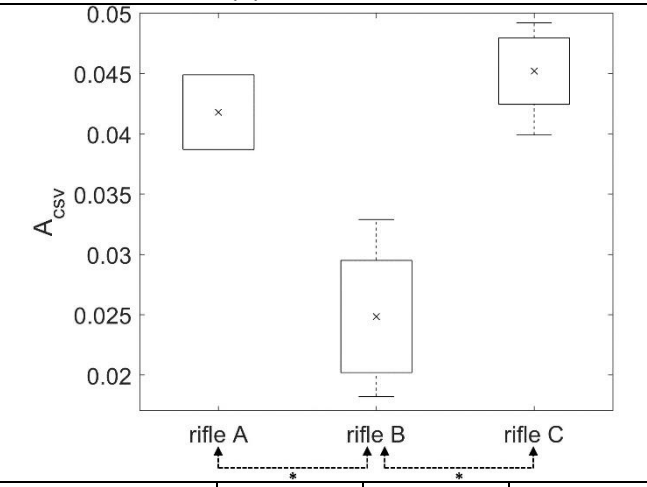
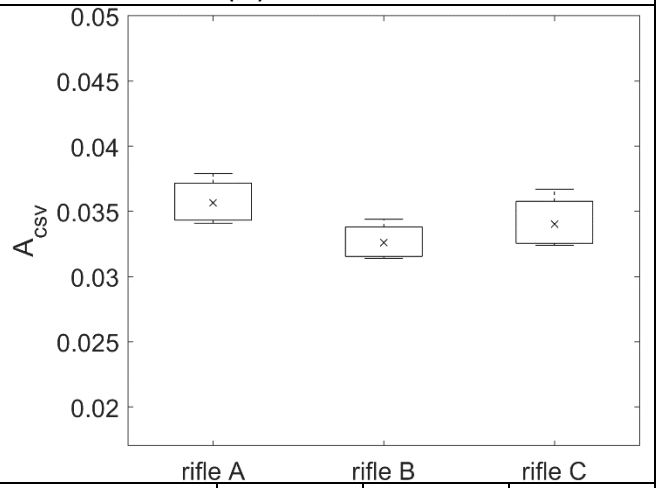
4.3.3.1.1 Inter-Rifle CSV Curve Comparison for Three Rifle Configurations

The CSV curves for Volunteers 1 and 2 visually revealed a decrease in MPS levels in the descending order of Rifles C, A, and B. Volunteer 3 exhibited small differences in CSV curves across all three rifles, with curves nearly overlapping. When examining the A_{CSV} box plots, Volunteers 1 and 2 exhibited higher mean A_{CSV} when firing Rifle C in contrast to Rifle A. The range of A_{CSV} for Volunteer 3 was between 0.0326 and 0.0357, indicating small differences between the rifles. Across all volunteers, the mean A_{CSV} values were consistently lowest when using Rifle B in comparison to Rifles A and C.

There was a difference in variability among rifles and volunteers. Volunteer 2 consistently displayed higher CV, i.e., variability, compared to Volunteers 1 and 3, irrespective of the rifle used. No consistent trend emerged among volunteers regarding CV when comparing different rifles; the descending order of CV values varied: Rifles B, C, A for Volunteer 1, Rifles B, A, C for Volunteer 2, and Rifles C, A, B for Volunteer 3. However, a notable increase in variability was observed for Volunteers 1 and 2 when using Rifle B compared to Rifles A and C. In contrast, Volunteer 3 maintained consistently low variability across all rifles.

A one-way ANOVA analysis (detailed in Appendix E) was conducted at a significance level of α=0.05 to explore differences between rifles for each volunteer. Significant differences in A_{CSV} values between rifles were observed for Volunteers 1 and 2, with p-values of 6.90E-03 and 2.04E-03, respectively. However, no statistically significant difference was identified between the rifles for Volunteer 3, with a p-value of 2.42E-01. The Tukey-Kramer test (detailed in Appendix E) identified a statistical difference between Rifles B and C for Volunteer 1, Rifles A and B, and Rifles B and C for Volunteer 2.

(i) Volunteer 1	(ii) Volunteer 2	(iii) Volunteer 3
		

(iv) Volunteer 1	(v) Volunteer 2	(vi) Volunteer 3
		

Mean	0.0231	0.0203	0.0246
Std. Dev.	0.0005	0.0023	0.0008
CV (%)	2.00	11.51	3.25

Mean	0.0418	0.0249	0.0452
Std. Dev.	0.0044	0.0063	0.0040
CV (%)	10.45	25.30	8.77

Mean	0.0357	0.0326	0.0341
Std. Dev.	0.0019	0.0016	0.0023
CV (%)	5.45	4.87	6.77

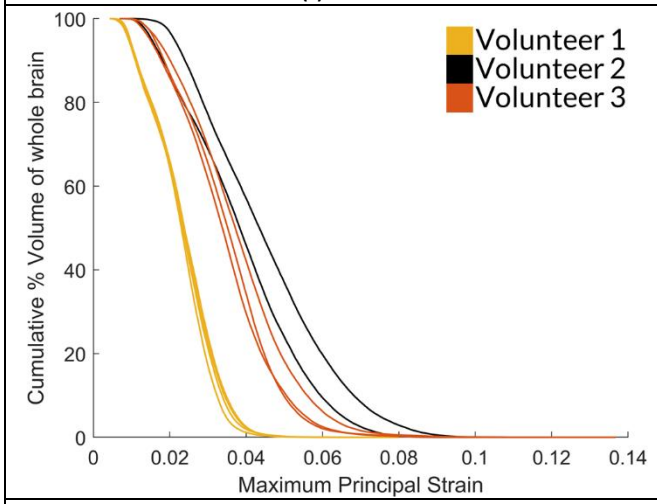
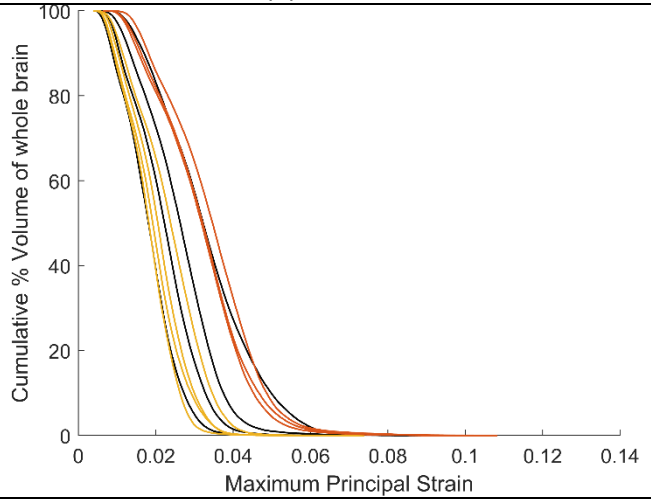
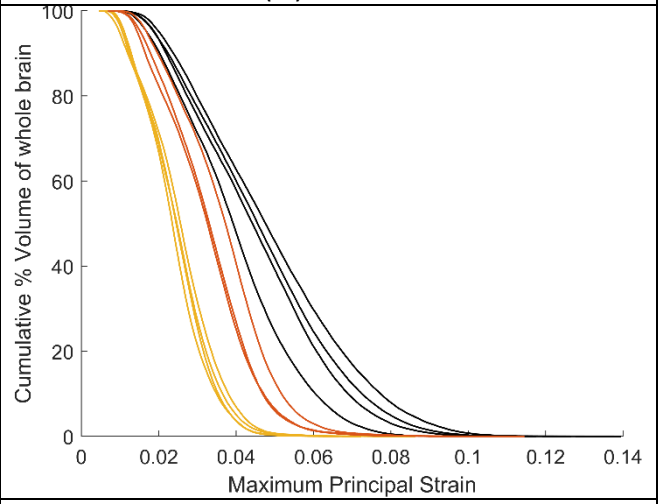
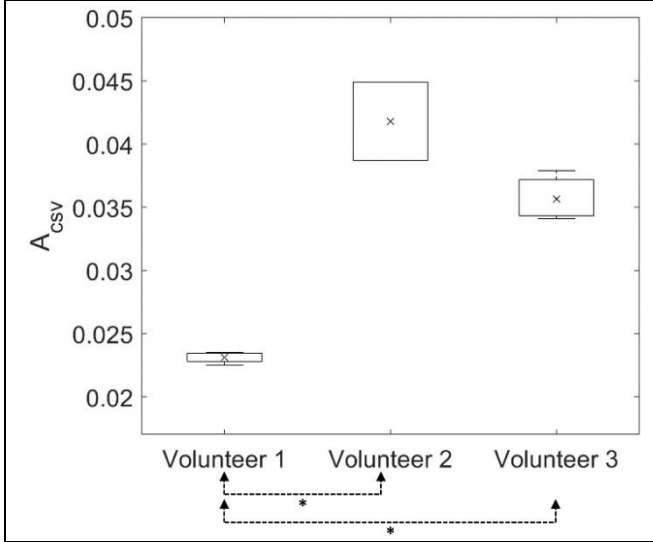
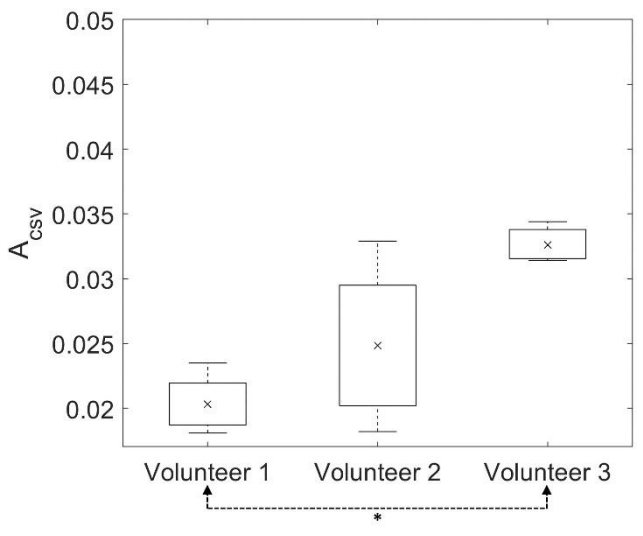
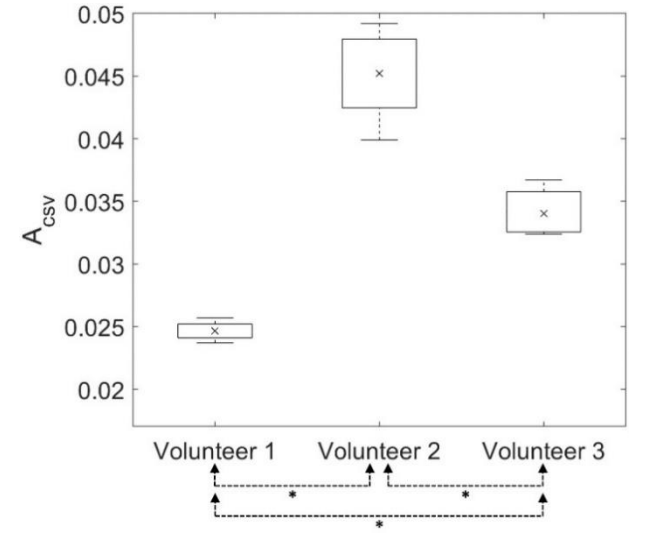
Figure 41: Cumulative strain-volume curves, mean A_{CSV} and variation of the three rifles for (i,iv) Volunteer 1, (ii,v) Volunteer 2, (iii,vi) Volunteer 3 (Dataset 1: May 2021). * = statistically significant difference detected between rifles. CV = coefficient of variation. Number of shots for Volunteer 1 (Rifles A:4, B:4, C:4), Volunteer 2 (Rifles A:2, B:4, C:4) and Volunteer 3 (Rifles A:3, B:3, C:3).

4.3.3.1.2 Inter-Volunteer CSV Curve Comparison for Three Volunteers

Volunteer 1 clearly displayed lower strains compared to Volunteers 2 and 3 across all rifles, which was evident upon visually inspecting the CSV plots (Figure 42). Conversely, Volunteer 2 exhibited higher strains when using Rifles A and C, while Volunteer 3 experienced the highest strain when firing Rifle B compared to the other volunteers. The mean A_{CSV} ranges for Rifles A, B, and C were 0.0418 to 0.0231, 0.0326 to 0.0203, and 0.0246 to 0.0452, respectively. Rifle C exhibited the widest range, followed by Rifle A and then Rifle B.

Besides experiencing lower strains, Volunteer 1 demonstrated the lowest CV when firing Rifles A and C, indicating minimal variability. However, Volunteer 1 witnessed an increase in variability when firing Rifle B, with the CV value rising from 2-3% for Rifles A and C to 11% when using Rifle B. Similarly, Volunteer 2 saw a significant increase in variability, escalating from 8-10% with rifles A and C to 25% when firing Rifle B. Volunteer 3 maintained low variability when firing Rifle B, even as the other volunteers saw an increase in CV. Volunteer 2 consistently had the highest CV and, thus, the highest variability, irrespective of the rifle being fired.

A one-way ANOVA analysis (detailed in Appendix E) was conducted at a significance level of α=0.05 to explore differences between volunteers for each rifle. Significant differences in A_{CSV} values between volunteers were identified for all three rifles, with p-values of 1.09E-04, 1.50E-02, and 1.88E-05 for Rifles A, B, and C, respectively. The Tukey-Kramer test (detailed in Appendix E) identified a statistical difference between Volunteers 1 and 2, as well as between Volunteers 1 and 3 for Rifle A; between Volunteers 1 and 3 for Rifle B, and between all volunteers for Rifle C.

(i) Rifle A	(ii) Rifle B	(iii) Rifle C
		
(iv) Rifle A	(v) Rifle B	(vi) Rifle C
		

Mean	0.0231	0.0418	0.0357	Mean	0.0203	0.0249	0.0326	Mean	0.0246	0.0452	0.0341
Std. Dev.	0.0005	0.0044	0.0019	Std. Dev.	0.0023	0.0063	0.0016	Std. Dev.	0.0008	0.004	0.0023
CV (%)	2.16	10.53	5.32	CV (%)	11.33	25.30	4.91	CV (%)	3.25	8.85	6.74

Figure 42: Cumulative strain-volume curves, mean A_{CSV} and variation for each shot across the three volunteers for (i,iv) Rifle A, (ii,v) Rifle B, (iii,vi) Rifle C (Dataset 1: May 2021). * = statistically significant difference detected between volunteers. CV = coefficient of variation. Number of shots for Volunteer 1 (Rifles A:4, B:4, C:4), Volunteer 2 (Rifles A:2, B:4, C:4) and Volunteer 3 (Rifles A:3, B:3, C:3).

4.3.3.2 CSV Curves of the Whole Brain for Dataset 2: May 2022

4.3.3.2.1 Inter-Rifle CSV Curve Comparison for Two Rifle Configurations

The CSV curves from Dataset 2 revealed a consistent trend across all volunteers with a rise in MPS levels when firing Rifle E compared to Rifle D. However, it is important to note that variability in responses differed among volunteers. Specifically, Volunteers 4, 5, and 6 exhibited significantly higher variability when using Rifle E compared to Rifle D. In contrast, the variability observed in Rifle D firing remained low (within 2-11%) across all volunteers. Volunteers 7 and 8 displayed low variability when using Rifle E, in contrast to the higher variability observed in Volunteers 4, 5, and 6.

As observed with previous metrics, the mean A_{CSV} values for Volunteers 5, 6, 7, and 8 when firing Rifle E fell within the range of A_{CSV} values for Rifles A and C in Dataset 1. Interestingly, when considering this metric, the difference between Volunteer 4's mean A_{CSV} was not significantly different from the range of mean A_{CSV} values from Dataset 1, unlike the notable disparities observed in other metrics. However, Volunteers 4, 5, and 6 still exhibited higher CV values when using Rifle E compared to Volunteers 7 and 8.

A t-test (detailed in Appendix E) was conducted at a significance level of $\alpha=0.05$ to explore differences between rifles for each volunteer. Significant differences in A_{CSV} values between rifles were observed for all volunteers, with p-values 1.27E-4, 5.53E-5, 3.29E-3, 1.63E-21, and 7.88E-11 for Volunteers 4,5, 6,7, and 8, respectively.

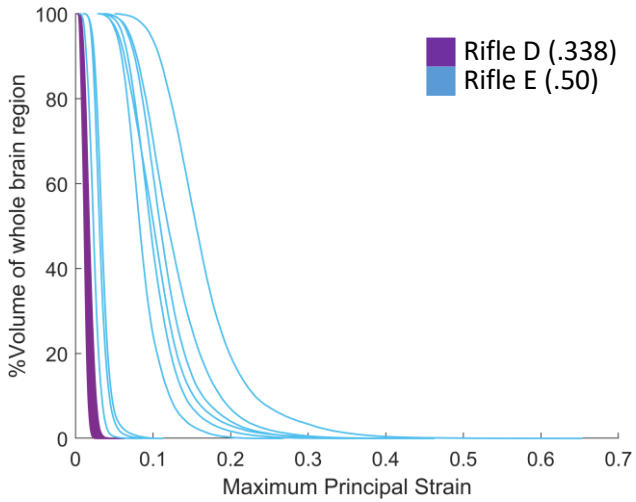
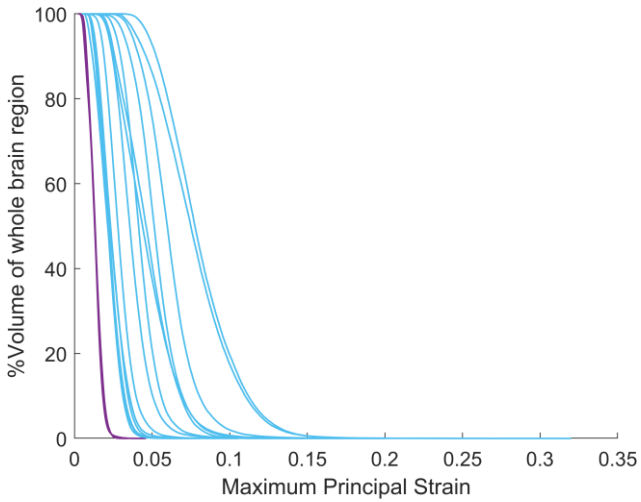
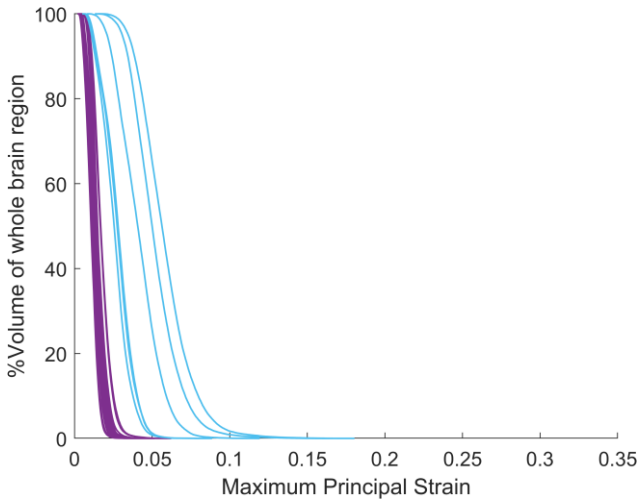
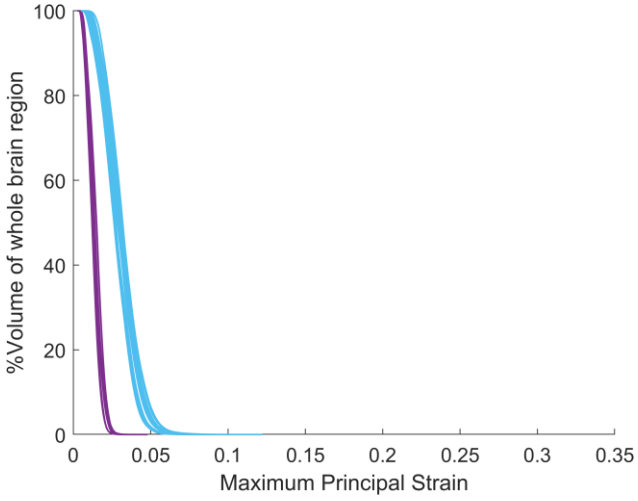
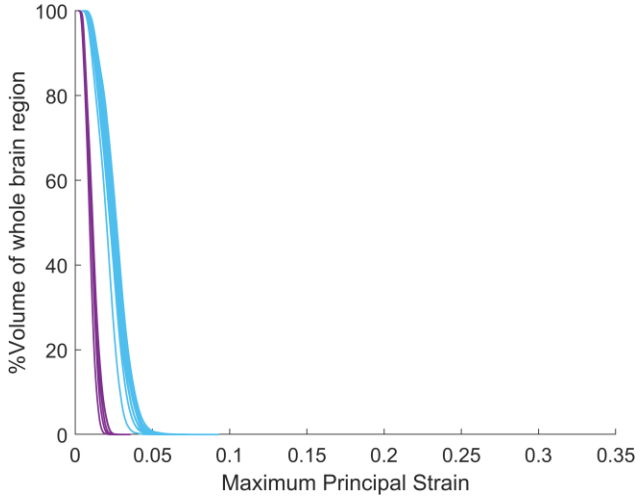
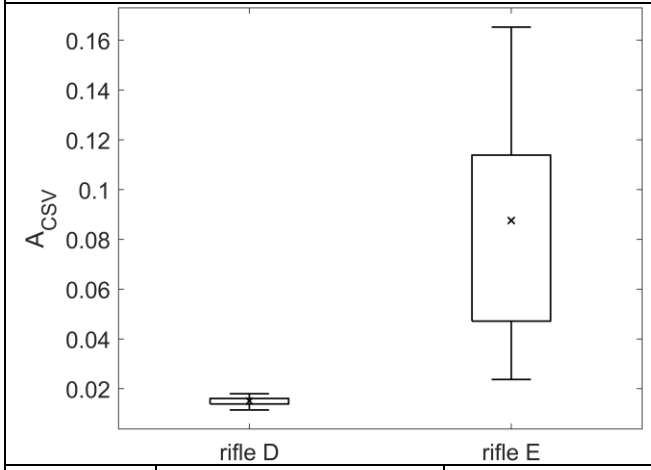
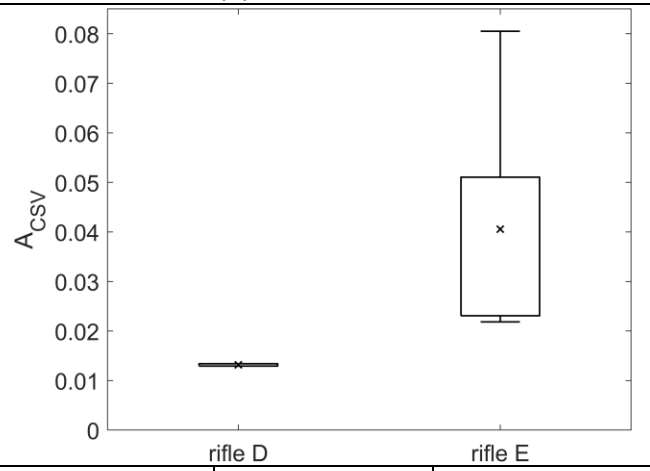
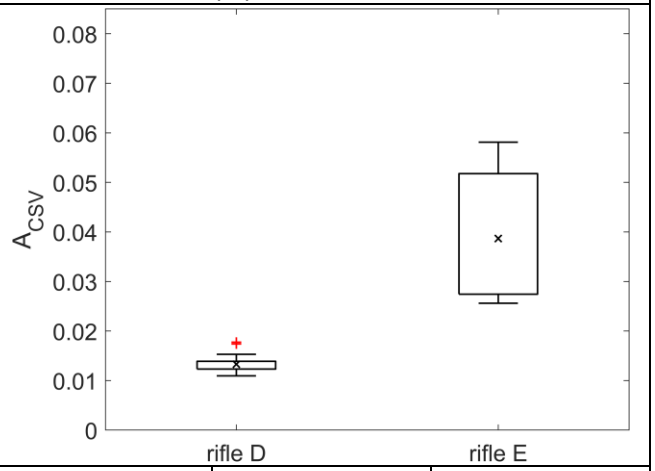
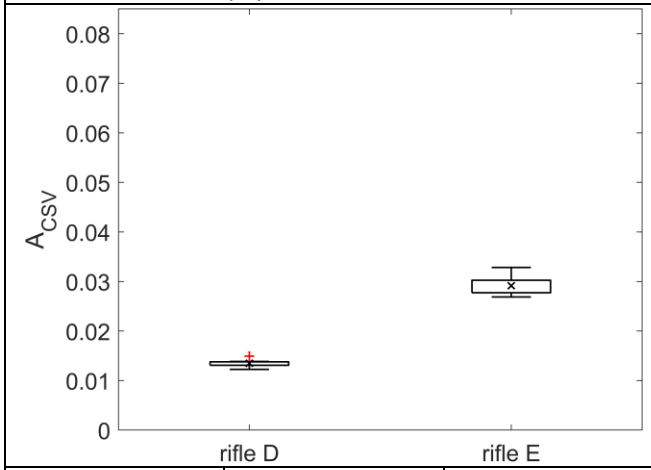
(i) Volunteer 4	(ii) Volunteer 5	(iii) Volunteer 6
		
(iv) Volunteer 7	(v) Volunteer 8	
		

Figure 43: Cumulative strain-volume curves for each shot across the two rifles for (i) Volunteer 4, (ii) Volunteer 5, (iii) Volunteer 6, (iv) Volunteer 7, (v) Volunteer 8 (Dataset 2: May 2022). *= statistically significant difference detected between rifles. CV=coefficient of variation. Number of shots for Volunteer 4 (Rifles D:36, E:11), Volunteer 5 (Rifles D:2, E:15), Volunteer 6 (Rifles D:33, E:6), Volunteer 7 (Rifles D:8, E:18) and Volunteer 8(Rifles D:5, E:10).

(i) Volunteer 4*		
		
Mean	0.0150	0.0875
Std. Dev.	0.0015	0.0435
CV (%)	10.25	49.72

(ii) Volunteer 5*		
		
Mean	0.0132	0.0406
Std. Dev.	0.0003	0.0200
CV (%)	2.54	49.24

(iii) Volunteer 6*		
		
Mean	0.0133	0.0387
Std. Dev.	0.0015	0.0139
CV (%)	11.57	35.94

(iv) Volunteer 7*		
		
Mean	0.0135	0.0292
Std. Dev.	0.0008	0.0017
CV (%)	5.77	5.87

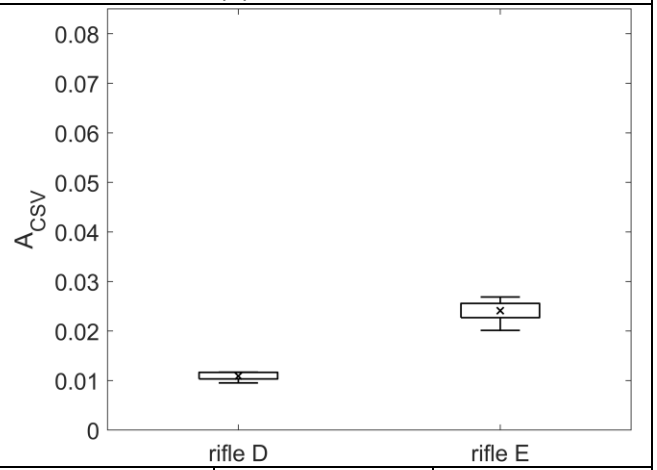
(v) Volunteer 8*		
		
Mean	0.0109	0.0241
Std. Dev.	0.0009	0.0020
CV (%)	8.20	8.15

Figure 44: Mean A_{CSV} and variation across the two rifles for (i) Volunteer 4, (ii) Volunteer 5, (iii) Volunteer 6, (iv) Volunteer 7, (v) Volunteer 8 (Dataset 2: May 2022). *= statistically significant difference detected between rifles. CV=coefficient of variation. Number of shots for Volunteer 4 (Rifles D:36, E:11), Volunteer 5 (Rifles D:2, E:15), Volunteer 6 (Rifles D:33, E:6), Volunteer 7 (Rifles D:8, E:18) and Volunteer 8(Rifles D:5, E:10).

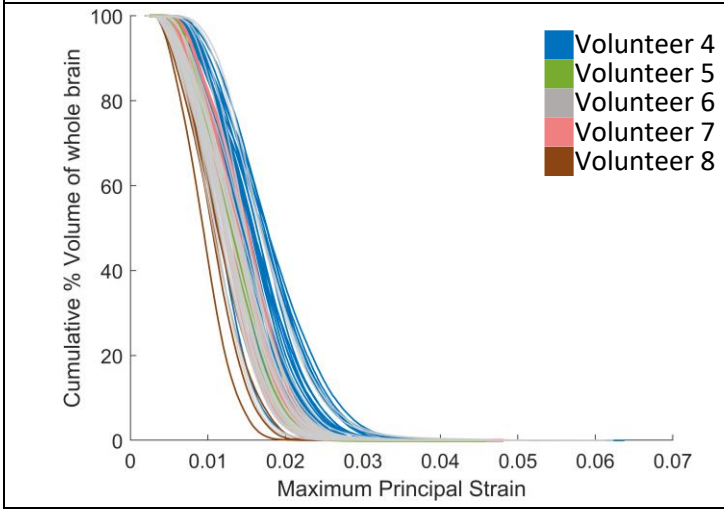
4.3.3.2.2 Inter-Volunteer CSV Curve Comparison for Five Volunteers

The volunteers in Dataset 2 exhibited slight differences in the magnitude of strains, with Volunteer 8 experiencing the lowest strain and Volunteer 4 experiencing the highest strain values for both Rifles D and E. The mean A_{CSV} for all volunteers ranged between 0.0109 and 0.0150 when firing Rifle D. While the mean A_{CSV} values were relatively close when firing Rifle D, variations in CV, i.e., variability, were evident. The descending order of CV was as follows: Volunteer 6, 4, 8, 7, and 5.

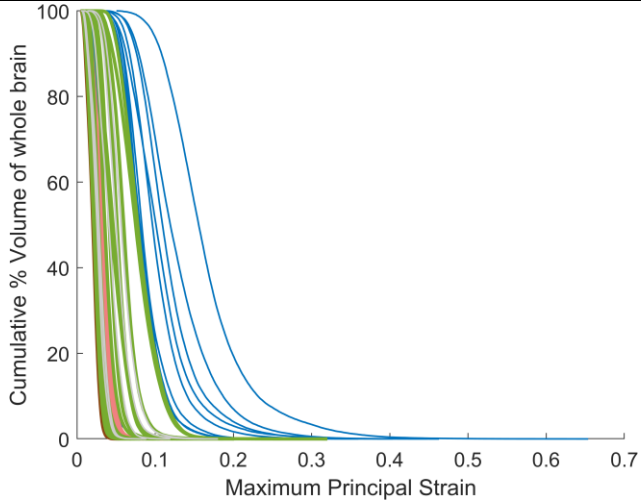
The range of A_{CSV} for the volunteers was higher for Rifle E compared to Rifle D. Notably, a higher CV was noted for Volunteers 4, 5, and 6 when firing Rifle E, in contrast to Volunteers 7 and 8, who maintained CV levels of 5% and 8% respectively. Furthermore, when comparing Rifle E to Rifles A and C from Dataset 1, considering they were all rifles of the same caliber, it was observed that all volunteers from Dataset 2, except Volunteer 4, fell within the range of mean A_{CSV} values from Dataset 1. This suggests some degree of consistency in mean A_{CSV} when firing the same caliber rifle.

A one-way ANOVA analysis (detailed in Appendix E) was conducted at a significance level of α=0.05 to explore differences between volunteers for each rifle. Significant differences in A_{CSV} values between volunteers were identified for both rifles, with p-values of 6.13E-08 and 1.36E-08 for Rifles D and E, respectively. The Tukey-Kramer test (detailed in Appendix E) identified a statistical difference for Rifle D between the following volunteers: 4 and 6, 4 and 7, 4 and 8, 5 and 8, 6 and 8, and 7 and 8. It also identified a statistical difference for Rifle E between Volunteers 4 and 5, 4 and 6, 4 and 7, and 4 and 8.

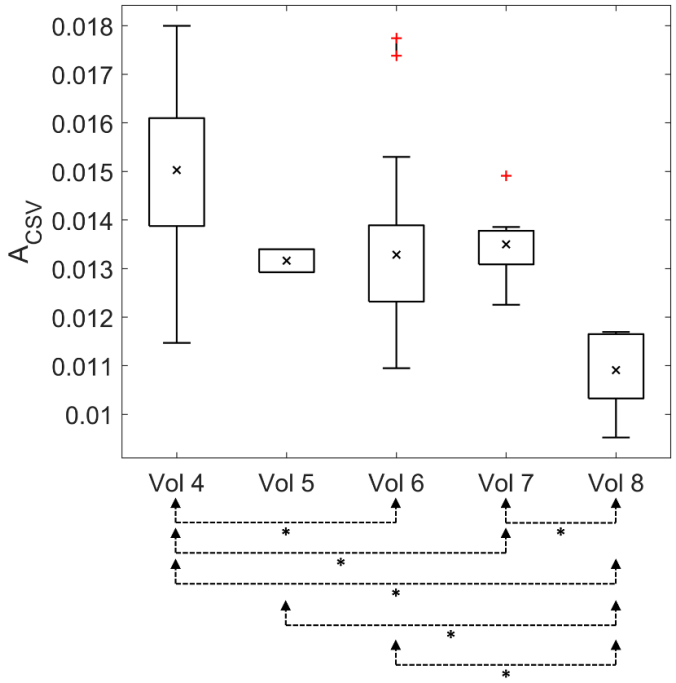
(i) Rifle D



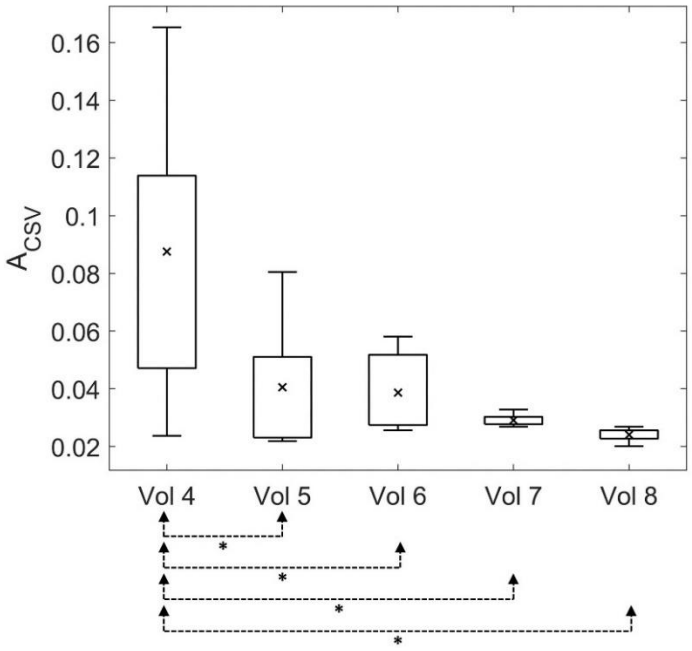
(ii) Rifle E



(iii) Rifle D



(iv) Rifle E



Mean	0.0150	0.0132	0.0133	0.0135	0.0109	Mean	0.0875	0.0406	0.0387	0.0292	0.0241
Std. Dev.	0.0015	0.0003	0.0015	0.0008	0.0009	Std. Dev.	0.0435	0.0200	0.0139	0.0017	0.0020
CV (%)	10.25	2.54	11.57	5.77	8.20	CV (%)	49.72	49.24	35.94	5.87	8.15

Figure 45: Cumulative strain-volume curves, mean A_{CSV} and variation for each shot across all volunteers for (i,iii) Rifle D and (ii,iv) Rifle E (Dataset 2: May 2022). *= statistically significant difference detected between rifles. CV=coefficient of variation. Number of shots for Volunteer 1 (Rifles A:4, B:4, C:4), Volunteer 2 (Rifles A:2, B:4, C:4) and Volunteer 3 (Rifles A:3, B:3, C:3).

4.3.4 Summary of CSV Results for the Whole Brain from Datasets 1 and 2

For Dataset 1:

When grouped by volunteers (Inter-rifle comparison)

- The CSV curves for Volunteers 1 and 2 visually revealed a decrease in MPS levels in the descending order of Rifles C, A, and B.
- Volunteer 3 exhibited small differences in CSV curves across all three rifles, with curves nearly overlapping.
- Volunteers 1 and 2 exhibited higher mean A_{CSV} when firing Rifle C in contrast to Rifle A, while Volunteer 3 exhibited minimal difference in A_{CSV} between rifles.
- For all volunteers, the mean A_{CSV} values were consistently lowest when using Rifle B compared to Rifles A and C.
- Volunteer 2 consistently displayed higher CV, i.e., variability, compared to Volunteers 1 and 3, irrespective of the rifle used.
- Volunteers 1 and 2 experienced an increase in variability when using Rifle B compared to Rifles A and C. In contrast, Volunteer 3 maintained consistently low variability across all rifles.
- There was a statistical difference in A_{CSV} values between rifles for Volunteers 1 and 2.

When grouped by rifles (Inter-volunteer comparison)

- Volunteer 1 clearly displayed lower strains than Volunteers 2 and 3 across all rifles.
- Volunteer 2 exhibited the highest strains when using Rifles A and C, while Volunteer 3 experienced the highest strain when firing Rifle B.
- Rifle C exhibited the widest range in A_{CSV}, followed by Rifle A and then Rifle B.
- There was a statistical difference in A_{CSV} between volunteers for all three rifles.

For Dataset 2:

When grouped by volunteers (Inter-rifle comparison)

- All volunteers experienced higher strains when using Rifle E compared to Rifle D.

- Volunteers 4, 5, and 6 exhibited significantly higher variability when using Rifle E compared to Rifle D.
- A statistical difference in A_{CSV} values between rifles was observed for all volunteers.

When grouped by rifles (Inter-volunteer comparison)

- Volunteer 8 experienced the lowest strain for both Rifles D and E.
- Volunteer 4 experienced the highest strain values for both Rifles D and E.
- There was a statistical difference in A_{CSV} between volunteers for both rifles.

4.3.5 Comparison of CSV Curves of Eight Brain Regions Between Different Rifles and Volunteers

The CSV curves for the shots fired by all volunteers in both datasets were plotted for the eight primary brain regions of the GHBMC M50 head model. The goal was to calculate and use the A_{CSV} to compare the magnitude of strain experienced by these different brain regions, aiming to identify any regions particularly prone to higher strains. All A_{CSV} values are tabulated in Appendix F.

4.3.5.1 CSV Curves of the Eight Brain Regions for Dataset 1: May 2021

4.3.5.1.1 Inter-Rifle CSV Curve Comparison for Three Rifle Configurations

The observation between rifles remains consistent with prior findings: Volunteers 1 and 2 consistently experience higher strains when firing Rifle C compared to A, while Volunteer 3 exhibits slightly reduced strains with Rifle C compared to A. All volunteers experienced the least strain when firing Rifle B. Across all volunteers, regardless of the rifle used, the cerebellum and brainstem consistently displayed the lowest strains (Figure 46). Conversely, the brainstem midbrain and corpus callosum consistently exhibited the highest strains for Volunteers 1 and 3, regardless of the rifle, and for Volunteer 2 when using Rifle B. When firing Rifles A and C, Volunteer 2 displayed higher strains in either the corpus callosum or the thalamus instead of the brainstem midbrain. Furthermore, the basal ganglia consistently ranked third in strain magnitude, irrespective of the rifle or volunteer. However, no consistent trend emerged for the

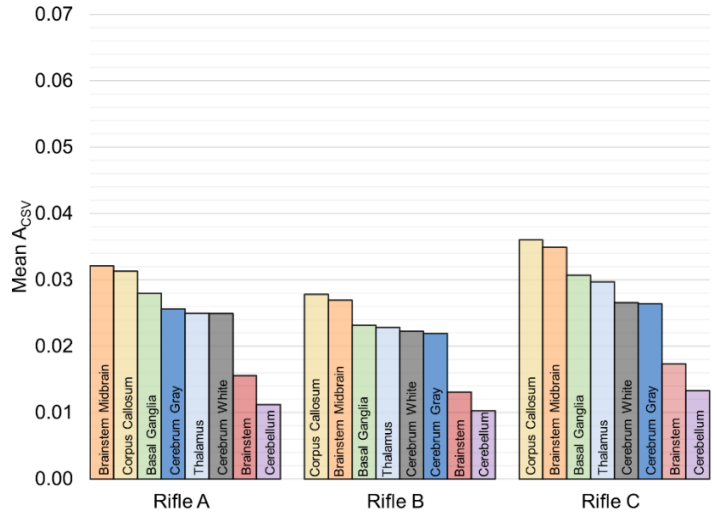
remaining three regions—the cerebrum gray, cerebrum white, and thalamus—as their rankings varied across volunteers and rifles when the A_{CSV} was ordered in descending order (Figure 46).

When calculating the percentage difference in A_{CSV} between Rifles A and C (both being the same caliber rifles but from different chassis manufacturers) and A and B (both being of the same caliber and chassis manufacturer but B has the RMS system mounted), the aim was to identify which brain regions experienced the most changes in strain levels (Table 14).

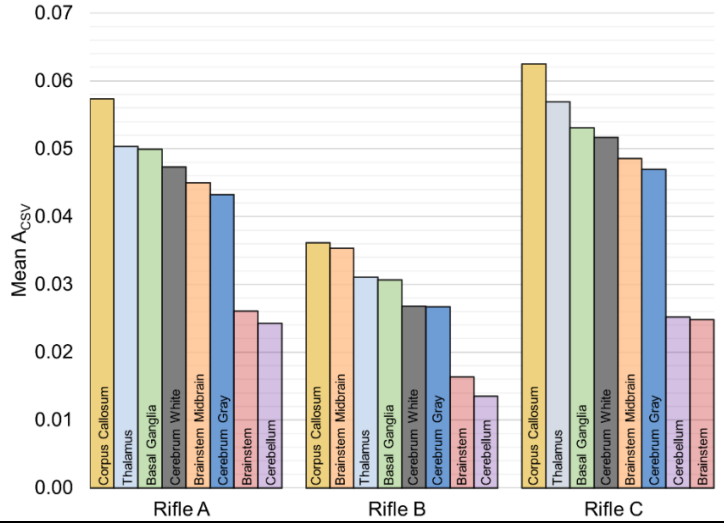
It is evident that all volunteers experienced a reduction in strain when comparing the percentage difference in A_{CSV} between Rifles A and B. However, the extent of this reduction varied among volunteers. For instance, the percentage difference ranged from 8 to 17% (a difference of 9%) for Volunteer 1, 21 to 44% (a difference of 23%) for Volunteer 2, and 5 to 20% (a difference of 15%) for Volunteer 3. Furthermore, the brain region with the most substantial decrease in strain differed for each volunteer: the basal ganglia for Volunteer 1, the cerebellum for Volunteer 2, and the brainstem for Volunteer 3. Note that none of these regions ranked highest when ordering the A_{CSV} of all regions in descending order for a particular rifle or volunteer.

Comparing Rifles A to C, Volunteers 1 and 2 exhibited clear increases in A_{CSV}, except for the brainstem of Volunteer 2 and all regions in Volunteer 3. When focusing solely on the CSVs for Volunteer 3, the curves overlapped. However, upon examining individual brain region strain, it becomes apparent that firing Rifle C results in lower strain compared to Rifle A for Volunteer 3. The brain region with the most substantial change in strain was the thalamus for Volunteers 1 and 2 and the brainstem for Volunteer 3. When comparing Rifles A to C, the range of percentage differences is narrower than when comparing A to B. Volunteer 1's percentage difference ranges from 3 to 18%, Volunteer 2's percentage difference ranges from 3 to 13%, and Volunteer 3's percentage difference ranges from 2 to 11% across all regions.

(i) Volunteer 1



(ii) Volunteer 2



(iii) Volunteer 3

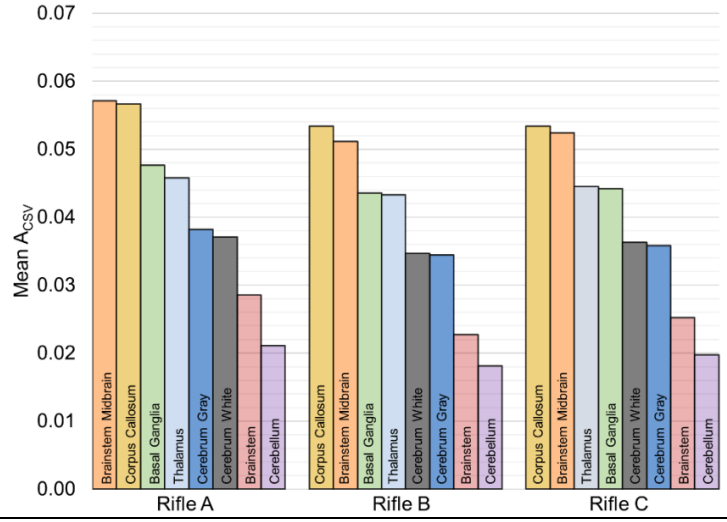


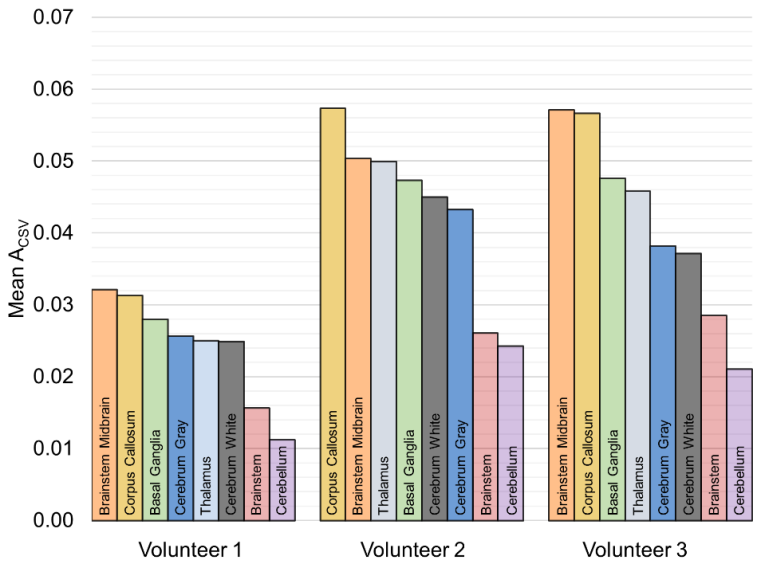
Figure 46: Mean A_{CSV} of the eight brain regions for (i) Volunteer 1, (ii) Volunteer 2, and (iii) Volunteer 3 (Dataset 1: May 2021), arranged in descending order of A_{CSV}

Table 14: Percentage difference between Rifles A and B and A and C for each brain region in descending order. A more detailed table can be found in Appendix F.			
	RMS effect		**chassis effect**
Brain Region	**% diff b/w A and B**	**Brain Region**	**% diff b/w A and C**
Volunteer 1			
Basal Ganglia	-17.4	Thalamus	18.8
Brainstem Midbrain	-16.2	Cerebellum	18.6
Brainstem	-16.0	Corpus Callosum	15.0
Cerebrum Gray	-14.5	Brainstem	11.1
Corpus Callosum	-11.2	Basal Ganglia	9.8
Cerebrum White	-10.6	Brainstem Midbrain	8.6
Thalamus	-8.5	Cerebrum White	6.5
Cerebellum	-8.3	Cerebrum Gray	3.0
Volunteer 2			
Cerebellum	-44.3	Thalamus	13.1
Cerebrum White	-43.4	Cerebrum White	9.2
Basal Ganglia	-38.6	Corpus Callosum	9.0
Thalamus	-38.3	Cerebrum Gray	8.6
Cerebrum Gray	-38.2	Brainstem Midbrain	7.9
Brainstem	-37.4	Basal Ganglia	6.3
Corpus Callosum	-37.0	Brainstem	-5.1
Brainstem Midbrain	-21.6	Cerebellum	3.7
Volunteer 3			
Brainstem	-20.4	Brainstem	-11.5
Cerebellum	-14.1	Brainstem Midbrain	-8.3
Brainstem Midbrain	-10.5	Basal Ganglia	-7.2
Cerebrum Gray	-10.0	Cerebellum	-6.3
Basal Ganglia	-8.5	Cerebrum Gray	-6.2
Cerebrum White	-6.7	Corpus Callosum	-5.7
Corpus Callosum	-5.7	Thalamus	-2.9
Thalamus	-5.6	Cerebrum White	-2.2

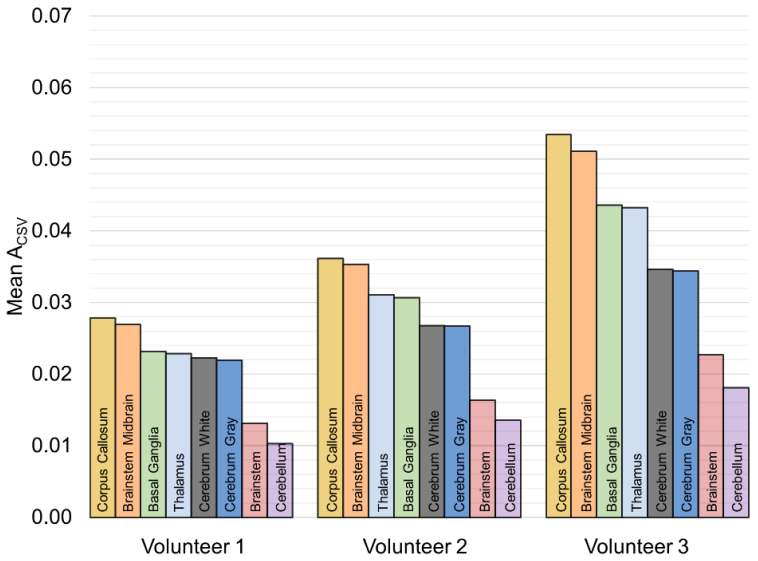
4.3.5.1.2 Inter-Volunteer CSV Curve Comparison for Three Volunteers

When plotting the mean A_{CSV} for all volunteers across each rifle, it is clear that each volunteer experiences a different range of strains with the same rifle (Figure 47).

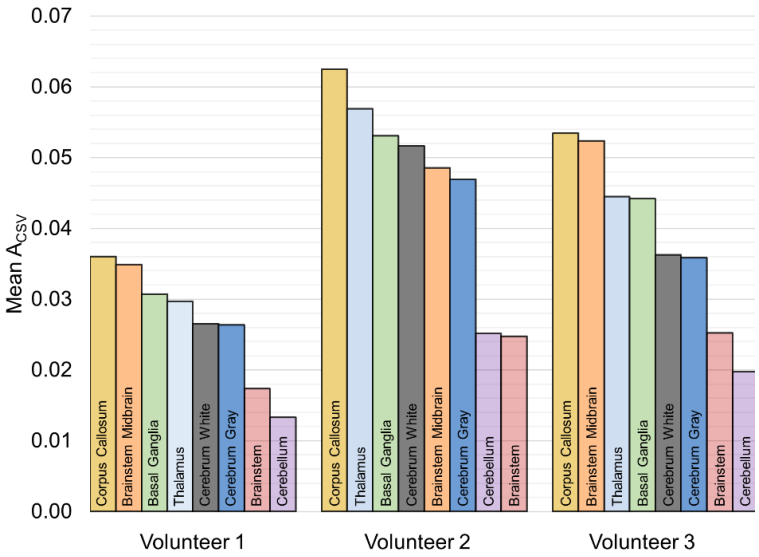
(i) Rifle A



(ii) Rifle B



(iii) Rifle C



Legend

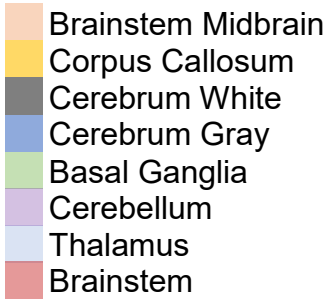


Figure 47: Mean A_{CSV} of the eight brain regions for (i) Rifle A, (ii) Rifle B, and (iii) Rifle C (Dataset 1: May 2021), arranged in descending order of A_{CSV}

The mean A_{CSV} values varied across rifles, with Rifle A ranging from 0.0112 to 0.0573 (a difference of 0.0461), Rifle B ranging from 0.0103 to 0.0534 (a difference of 0.0431), and Rifle C ranging from 0.0133 to 0.0625 (a difference of 0.0492). This indicates that Rifle C exhibited the widest range, while Rifle B showed the narrowest range when considering all volunteers. Breaking it down further, within Rifle A, A_{CSV} ranged from 0.0112 to 0.0321 (a difference of 0.0209) for Volunteer 1, from 0.0243 to 0.0573 (a difference of 0.0331) for Volunteer 2, and from 0.0211 to 0.0571 (a difference of 0.0361) for Volunteer 3. Within Rifle B, A_{CSV} ranged from 0.0103 to 0.0278 (a difference of 0.0175) for Volunteer 1, from 0.0135 to 0.0361 (a difference of 0.0226) for Volunteer 2, and from 0.0181 to 0.0534 (a difference of 0.0353) for Volunteer 3. Within Rifle C, A_{CSV} ranged from 0.0133 to 0.0360 (a difference of 0.0227) for Volunteer 1, from 0.0248 to 0.0625 (a difference of 0.0377) for Volunteer 2, and from 0.0197 to 0.0534 (a difference of 0.0337) for Volunteer 3 (See Appendix F for tabulated format). In summary, Volunteer 3 displayed the widest range for A_{CSV} between brain regions when firing Rifles A and B, while Volunteer 2 exhibited the widest range for A_{CSV} between brain regions when firing Rifle C.

When using Rifle A, Volunteer 1 consistently showed the lowest strain across all brain regions compared to Volunteers 2 and 3. The A_{CSV} of the brainstem midbrain and corpus callosum were interchangeably the highest for all volunteers when firing Rifle A. In contrast, the A_{CSV} of the brainstem and cerebellum were interchangeably the lowest for all volunteers with Rifle A. The basal ganglia maintained its ranking as third for all three volunteers, while the order of the remaining regions varied among volunteers. It was observed that volunteers with Rifle B had a more consistent trend in their brain regions. The order of A_{CSV}, from highest to lowest, was as follows: corpus callosum, brainstem, midbrain, basal ganglia, thalamus, cerebrum white, cerebrum gray, and cerebellum. However, there was an exception with Volunteer 2, who exhibited a switch in the position of the thalamus and basal ganglia. The observation for Rifle C was similar to Rifle A, where the order of regions varied more between volunteers. The corpus callosum had the highest $A_{CSV,}$ while the cerebellum and brainstem were interchangeably the lowest.

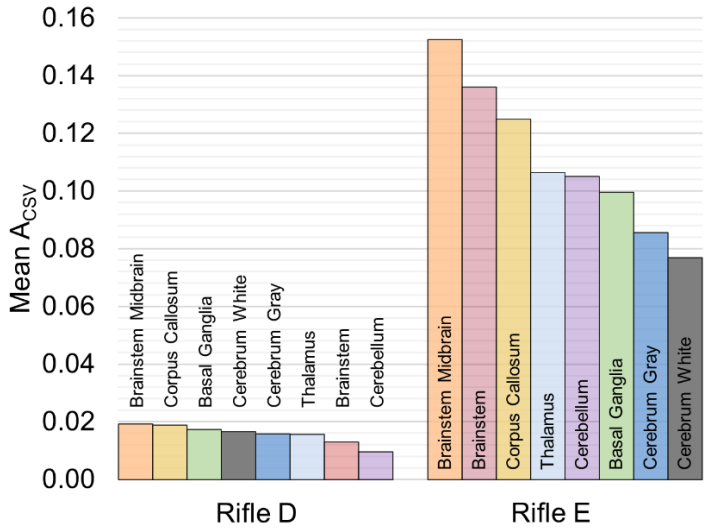
4.3.5.2 CSV Curves of the Eight Brain Regions for Dataset 2: May 2022

4.3.5.2.1 Inter-Rifle CSV Curve Comparison for Two Rifle Configurations

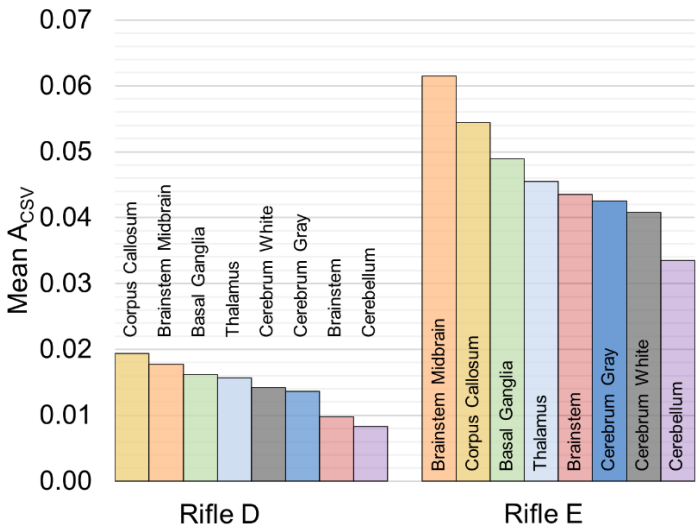
It is evident that across all volunteers, there was a consistent pattern of higher strains experienced in all brain regions when using Rifle E compared to Rifle D. Similar to Dataset 1, regardless of the rifle used, the cerebellum and brainstem consistently exhibited the lowest strains, while the brainstem midbrain and corpus callosum consistently showed the highest strains for all volunteers except Volunteer 4 with Rifle E. However, other regions varied across volunteers and rifles, indicating no consistent trend (Figure 48).

Analyzing the percentage difference in A_{CSV} between Rifles D and E (outlined in Appendix F), it is clear that all brain regions in all volunteers experienced a reduction in strain. Nonetheless, the extent of this reduction varied among volunteers. For instance, the percentage difference ranged from 365% to 1008% (a difference of 643%) for Volunteer 4, 180% to 343% (a difference of 163%) for Volunteer 5, 181% to 252% (a difference of 71%) for Volunteer 6, and 114% to 144% (a difference of 30%) for Volunteer 7, and 103% to 145% (a difference of 42%) for Volunteer 8. Moreover, the brain region experiencing the most substantial decrease in strain differed for each volunteer: the cerebellum for Volunteers 4 and 6, the brainstem for Volunteer 5, the corpus callosum for Volunteer 7, and the brainstem midbrain for Volunteer 8.

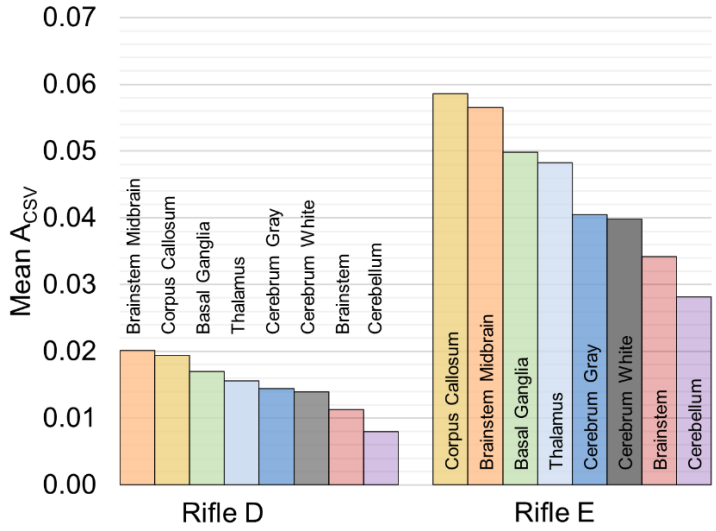
(i) Volunteer 4



(ii) Volunteer 5



(iii) Volunteer 6



Legend

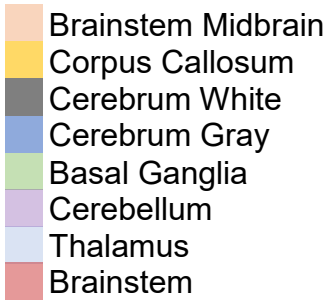


Figure 48: Mean A_{CSV} and variation across the two rifles for (i) Volunteer 4, (ii) Volunteer 5, (iii) Volunteer 6 (Dataset 2: May 2022). *= statistically significant difference detected between rifles. CV=coefficient of variation. Number of shots for Volunteer 4 (Rifles D:36, E:11), Volunteer 5 (Rifles D:2, E:15), Volunteer 6 (Rifles D:33, E:6), Volunteer 7 (Rifles D:8, E:18) and Volunteer 8(Rifles D:5, E:10).

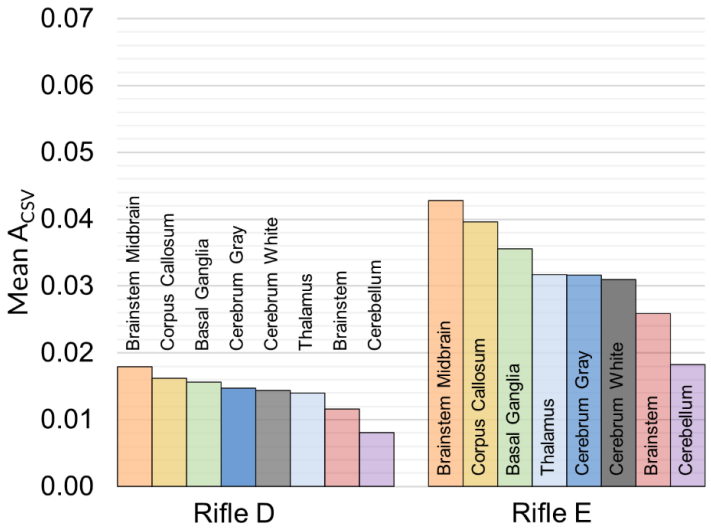
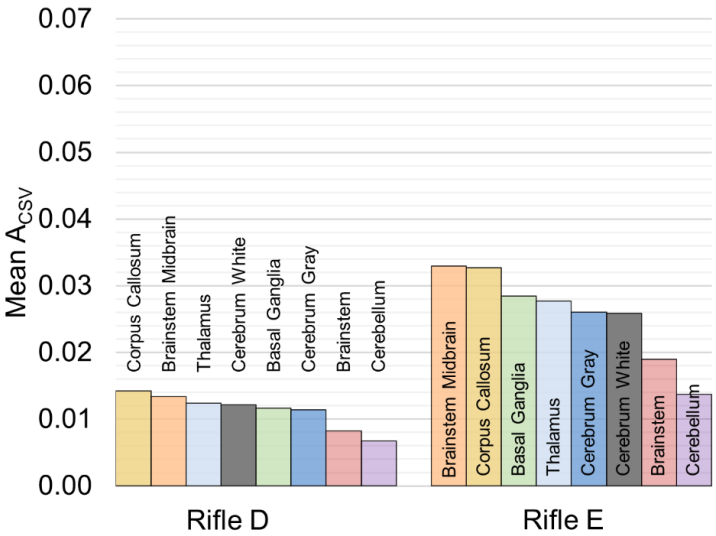
(i) Volunteer 7	(ii) Volunteer 8
	

Figure 49: Mean A_{CSV} of the eight brain regions for (i) Volunteer 7, (ii) Volunteer 8 (Dataset 2: May 2022), arranged in descending order of A_{CSV}

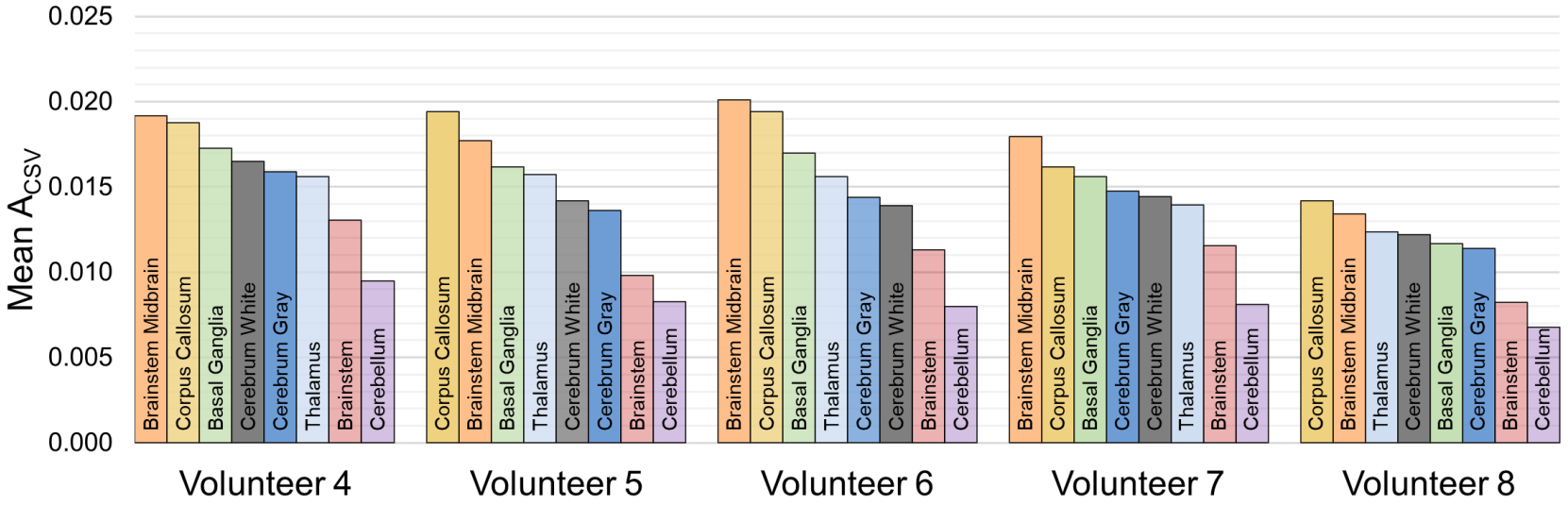
4.3.5.2.2 Inter-Volunteer CSV Curve Comparison for Five Volunteers

The mean A_{CSV} values were plotted across each rifle for all volunteers in Dataset 2 (Figure 50). It is evident that the mean A_{CSV} values varied for each rifle. For instance, the A_{CSV} ranged from 0.068 to 0.0201 for Rifle D, representing a difference of 0.0133, whereas Rifle E displayed a broader range, spanning from 0.0137 to 0.1526, indicating a higher difference of 0.1389. This observation highlights that Rifle E not only demonstrated the widest range but also higher A_{CSV} values overall. When excluding Volunteer 4, whose linear acceleration signals while firing Rifle E exhibited pronounced peaks, the A_{CSV} range for Rifle E narrowed to 0.0137 to 0.0615, with a difference of 0.0478. Despite this adjustment, Rifle E still had the widest range and higher A_{CSV} values among the rifles. A breakdown of A_{CSV} ranges for each volunteer is provided in Appendix F.

In summary, Volunteer 6 exhibited the widest range for A_{CSV} between brain regions when firing Rifle D, while Volunteer 4 displayed the widest range for ACSV between brain regions, followed by Volunteer 6 when firing Rifle E. Conversely, Volunteer 8 demonstrated the narrowest range of A_{CSV} for both Rifles D and E. Additionally, Volunteer 8 consistently showed the lowest A_{CSV} values across all brain regions for both rifles. When comparing the different brain regions, the A_{CSV} of the brainstem midbrain and corpus callosum consistently emerged as the highest among all volunteers when firing both Rifles D and E. In contrast, the A_{CSV} of the brainstem and cerebellum consistently ranked as the lowest across all volunteers and both rifles. An exception to this trend occurred with Volunteer 4 when firing Rifle D, where the brainstem midbrain and the brainstem exhibited the highest A_{CSV} values, while the Cerebrum gray and white displayed the lowest A_{CSV}.

When considering Rifle C from Dataset 1 across all volunteers, the A_{CSV} range was similar in terms of both range and magnitudes to that of Rifle E in Dataset 2 when excluding Volunteer 4. Note that Rifle C from Dataset 1 and Rifle E from Dataset 2 are both .50 caliber rifles. Specifically, for Rifle C, the A_{CSV} range spanned from 0.0133 to 0.0625, representing a difference of 0.0492, closely resembling the range of A_{CSV} for Rifle E, which was 0.0137 to 0.0615, with a difference of 0.0478, when Volunteer 4 was not taken into account.

(i) Rifle D



(ii) Rifle E

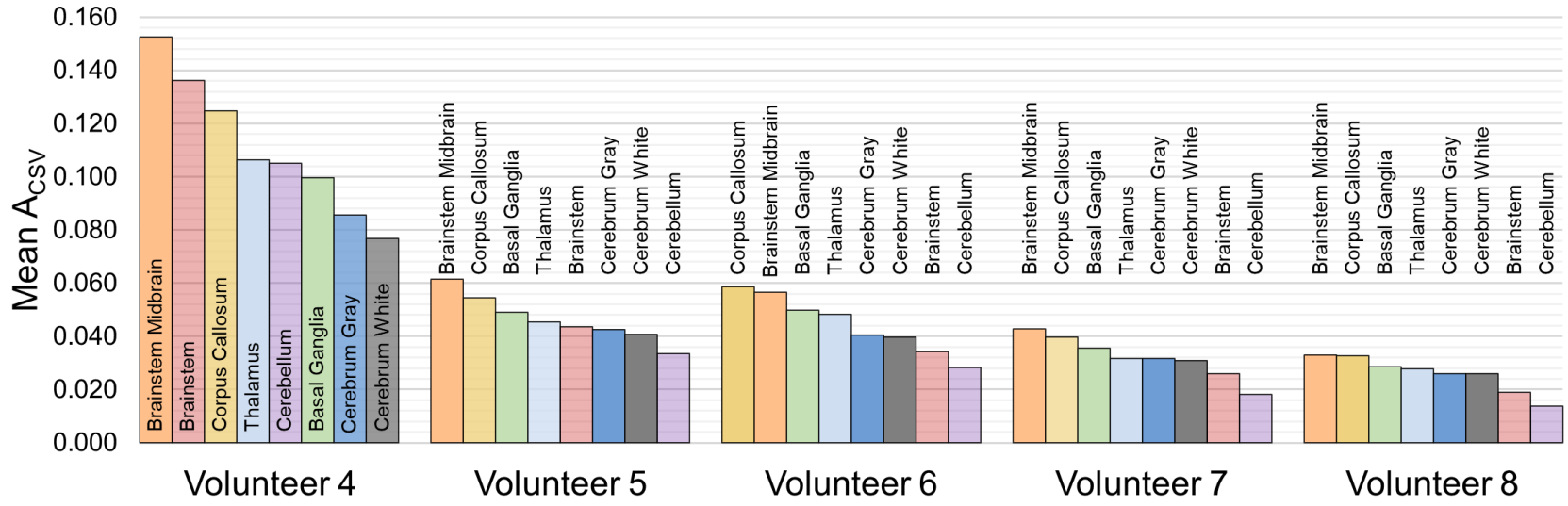


Figure 50: Mean A_{CSV} of the eight brain regions for (i) Rifle D and (ii) Rifle E, arranged in descending order of A_{CSV}

4.3.6 Summary of CSV Results for the Eight Brain Regions from Datasets 1 and 2

- The brainstem midbrain and corpus callosum commonly experienced the highest strains.
- The brainstem and cerebellum experienced the lowest strains.
- The order of the remaining regions varied across rifles and volunteers.
- When comparing different rifles, the regions experiencing the biggest change in strain differ for each volunteer.
    - For instance, when comparing rifles A to B, the basal ganglia experienced the most substantial decrease in strain for Volunteer 1, the cerebellum for Volunteer 2, and the brainstem for Volunteer 3.
    - Additionally, none of these regions ranked highest when ordering the A_{CSV} of all regions in descending order.
    - When comparing rifles A to C, Volunteers 1 and 2 exhibited clear increases in A_{CSV}, except for the brainstem of Volunteer 2 and all regions in Volunteer 3.
    - The brain region with the most substantial change in strain was the thalamus for Volunteers 1 and 2 and the brainstem for Volunteer 3.

4.4 Rotational vs Linear Head Motion Results

To investigate the importance of rotational kinematics within the context of CAF volunteers engaged in long-range rifle firing, the CSV and A_{CSV} were used to discern the relative contributions of linear acceleration and angular velocity on strain outputs. As outlined in the methods section, 6DOF head kinematics (comprising X, Y, Z linear acceleration, and X, Y, Z angular velocity) have been used as inputs to the GHBMC M50 head model to simulate the head motion during firing. The following investigation is divided into two parts: Study 1 and Study 2. In Study 1, angular velocities (x, y, z) and linear accelerations (x, y, z) were simulated separately and compared with cases where all 6 DOF curves were used as inputs. In Study 2, each axis was simulated individually to determine if any axis had a greater influence on strain outputs.

4.4.1 Study 1: Linear Acceleration vs Angular Velocity

Nine cases were simulated from Dataset 1, which includes one signal from Volunteers 1, 2, and 3 firing Rifles A, B, and C. Additionally, six cases were simulated from Dataset 2, involving one signal from Volunteers 4, 7, and 8 firing Rifles D and E. While both angular velocity and linear acceleration contribute to the area under the CSV curve (A_{CSV}), it was observed that angular velocity has a more pronounced effect compared to linear acceleration. This is demonstrated by the larger areas under the CSV curves when simulated separately. The "angular velocity only" curves almost entirely overlap with "all included" curves when visually comparing CSV curves. Additionally, when comparing the A_{CSV} for the "linear acceleration only" curves, it is consistently found to be only between 1-3% of the A_{CSV} of the "all included" cases. This trend persists across all volunteers used in this study, regardless of the rifle being fired.

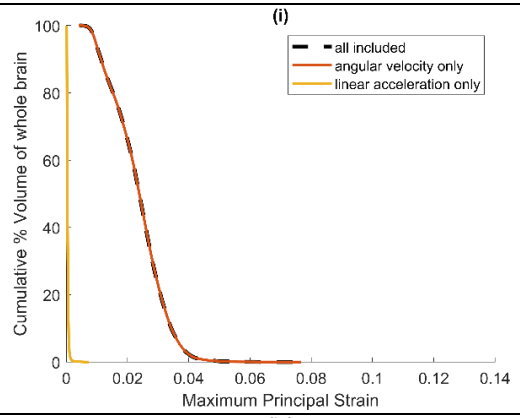
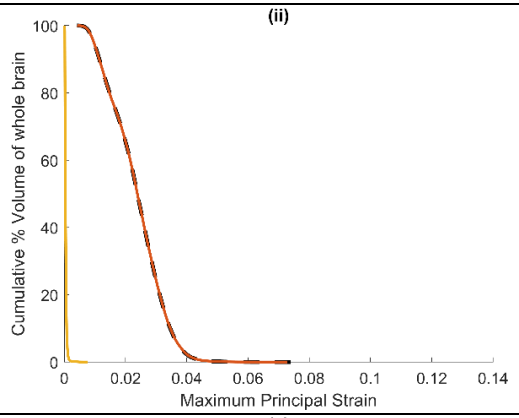
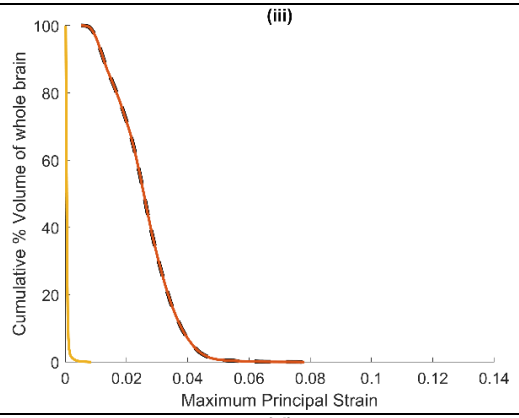
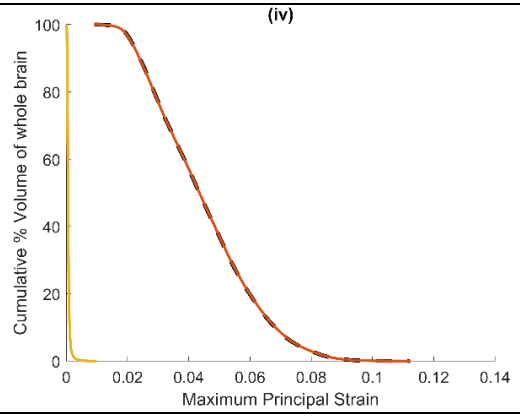
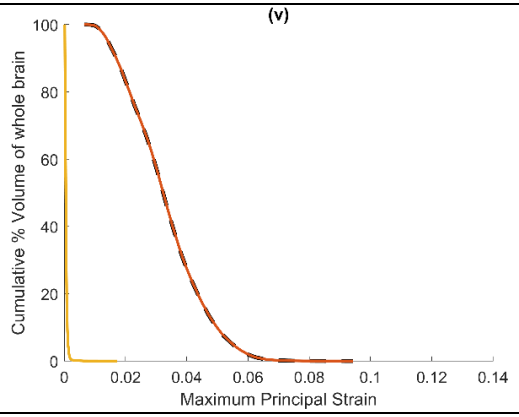
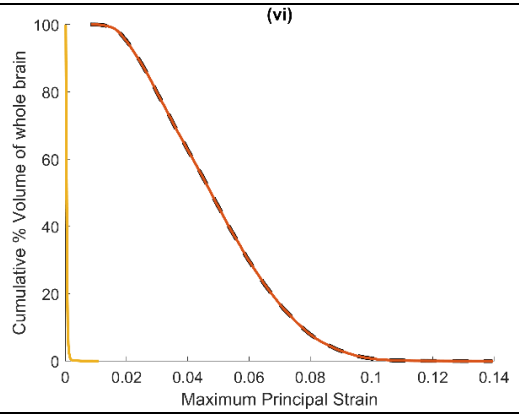
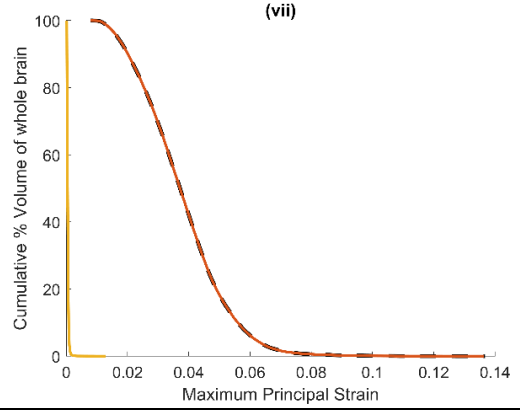
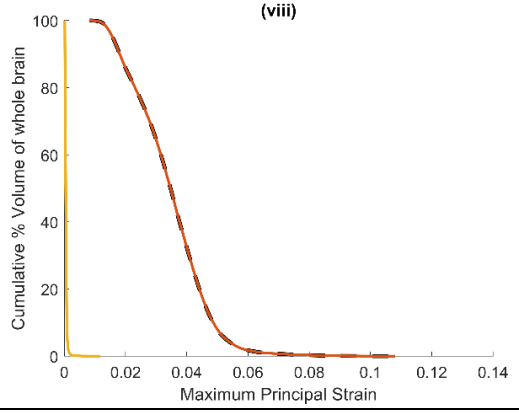
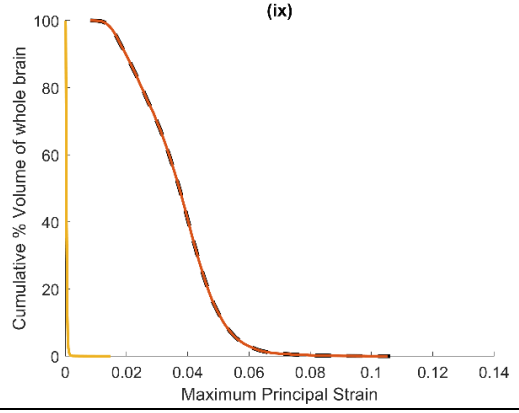
	Rifle A	Rifle B	Rifle C
Vol 1			
Vol 2			
Vol 3			

Figure 51: Cumulative strain-volume curves for one shot across the three rifles in Dataset 1 for (i,ii,iii) Volunteer 1, (iv,v,vi) Volunteer 2 and (vii,viii,ix) Volunteer 3 showing the difference between angular velocity only inputs, linear acceleration only inputs and 6 DOF inputs to the head model

Table 15: A_{CSV} values for linear acceleration only and angular velocity only curves

	All included	Angular Velocity only	Linear Acceleration only	$\left(\frac{linear\ accel}{all\ included} * 100\right)$
Dataset 1				
Rifle A				
Vol 1	0.0235	0.0235	0.000456	2
Vol 2	0.0449	0.0449	0.000689	2
Vol 3	0.0379	0.0379	0.000496	1
Rifle B				
Vol 1	0.0235	0.0236	0.000461	2
Vol 2	0.0329	0.0330	0.000595	2
Vol 3	0.0344	0.0344	0.000546	2
Rifle C				
Vol 1	0.0257	0.0257	0.000576	2
Vol 2	0.0492	0.0492	0.000524	1
Vol 3	0.0367	0.0367	0.000442	1
Dataset 2				
Rifle D				
Vol 4	0.0140	0.0140	0.000354	3
Vol 8	0.0116	0.0116	0.000258	2
Vol 7	0.0275	0.0251	0.000411	1
Rifle E				
Vol 4	0.0237	0.0237	0.000537	2
Vol 8	0.0251	0.0136	0.000182	1
Vol 7	0.0136	0.0275	0.000372	3

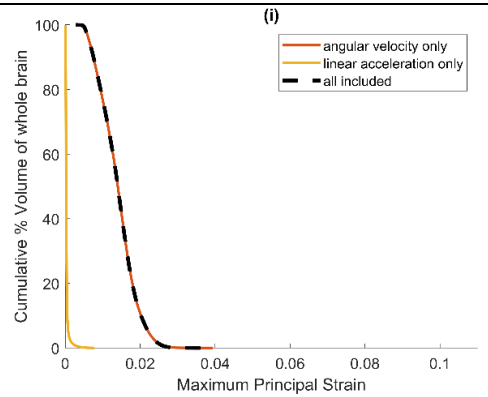
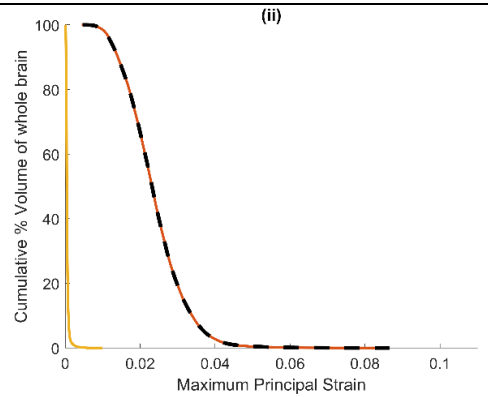
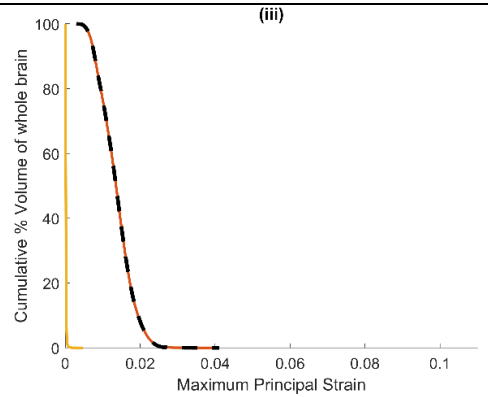
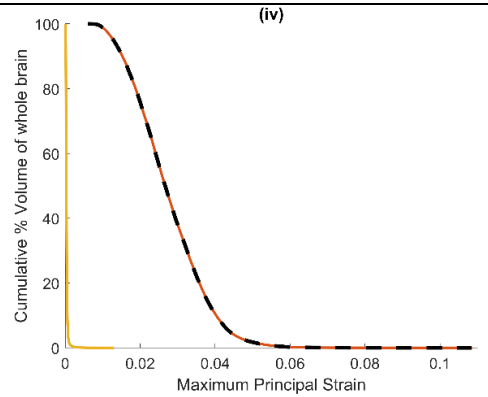
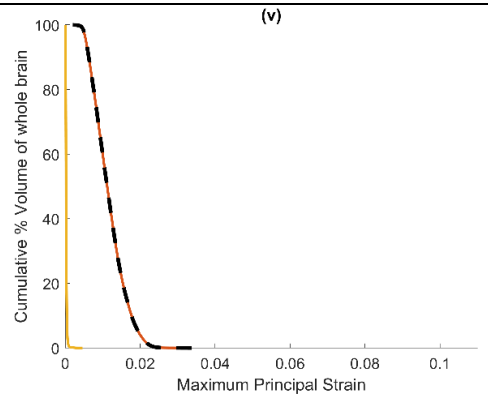
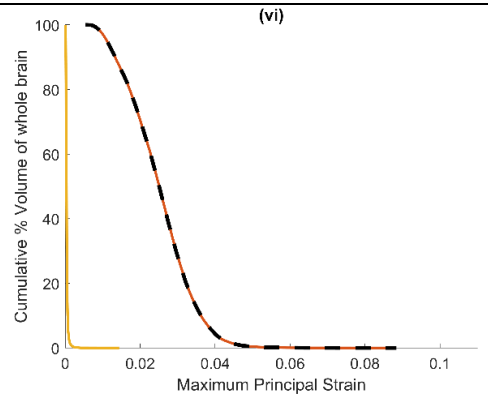
	Rifle D	Rifle E
Vol 4		
Vol 7		
Vol 8		

Figure 52: Cumulative strain-volume curves for one shot across the two rifles in Dataset 2 for (i,ii) Volunteer 4, (iii,iv) Volunteer 7 and (v,vi) Volunteer 8 showing the difference between angular velocity only inputs, linear acceleration only inputs and 6 DOF inputs to the head model

4.4.2 Study 2: Directional Dependence

In the second part of the study, each axis of the cases above was simulated separately to determine if any axis had a greater influence on strain outputs.

4.4.2.1 Dataset 1: May 2021

Angular velocity in Z had a greater influence on strain outputs in seven out of nine cases, with the highest A_{CSV}. However, in two cases (i and vii), angular velocity in Y exhibited the highest A_{CSV}. The percentage of area under AVZ curve relative to "all included" curve ranged from 50% to 80% for Rifle A, showcasing the widest variability, followed by Rifle C with a range of 73% to 90%, and Rifle B with a narrower range of 79% to 86%. Additionally, within each rifle, Volunteer 2 consistently exhibited the highest percentage of area under AVZ curve relative to "all included" curve. For instance, when using Rifle A, Volunteer 2 accounted for 80% of the AVZ area, while Volunteer 1 and Volunteer 3 represented 69% and 50%, respectively.

4.4.2.2 Dataset 2: May 2022

In Dataset 2, the angular velocity in Z and Y still had the greater influence on strain outputs. However, the difference between the two different directions was less compared to Dataset 1, especially when firing Rifle D. For instance, the difference between %AVY and % AVZ for Volunteers 4,7 and 8 was 1, 2 and 26 % respectively. The percentage of area under AVZ curve relative to "all included" curve ranged from 70% to 82% for Rifle D and 50% to 73% for Rifle E, exhibiting the widest range. Within each rifle, Volunteer 8 consistently exhibited the highest percentage of area under AVZ curve relative to "all included" curve. For instance, Volunteer 8 accounted for 82% when using Rifle D and 73% when using Rifle E.

Overall, these observations suggest that angular velocity has a more substantial influence on strain outputs.

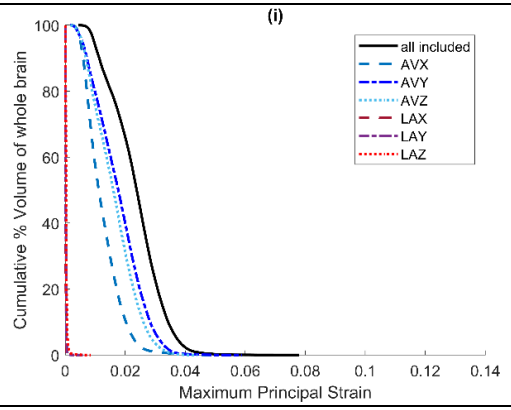
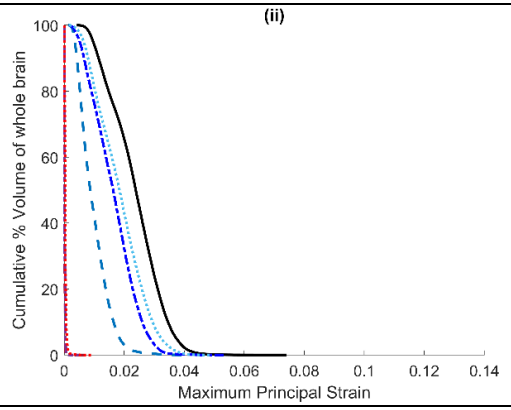
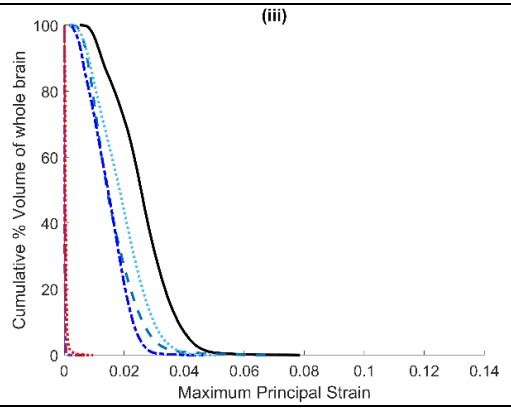
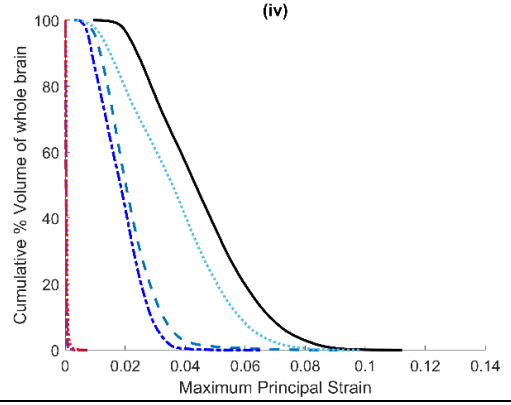
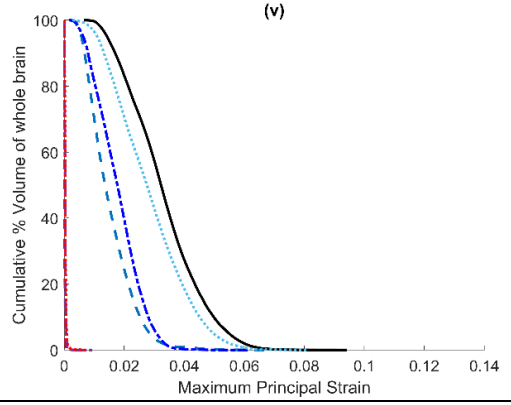
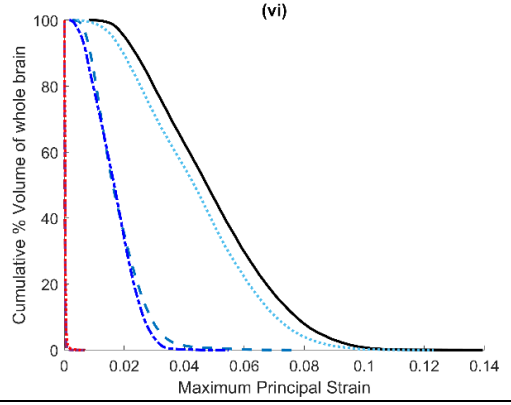
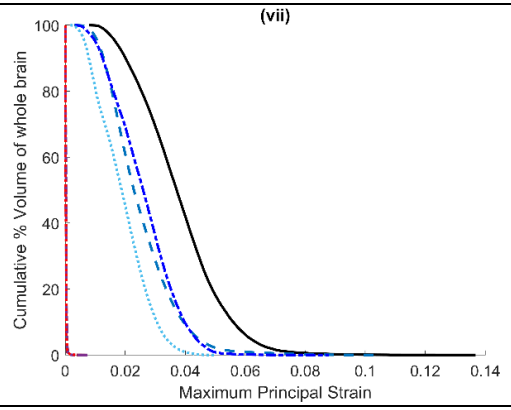
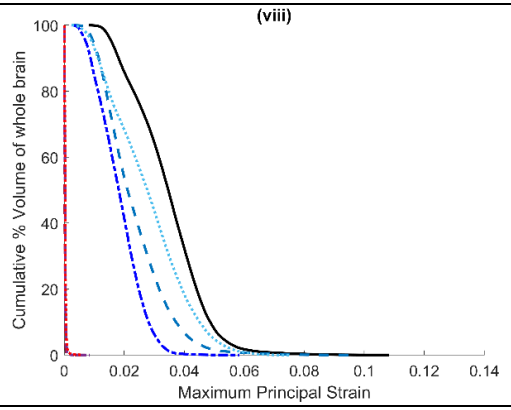
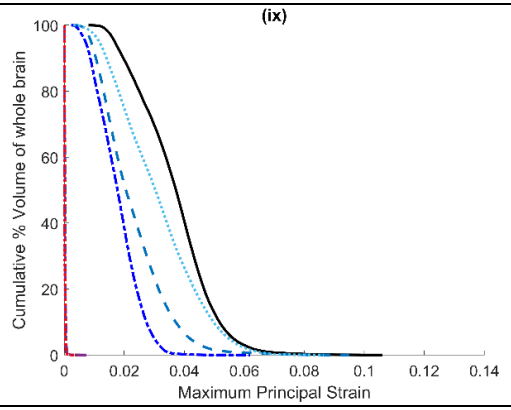
	Rifle A	Rifle B	Rifle C
Vol 1			
Vol 2			
Vol 3			

Figure 53: Cumulative strain-volume curves for one shot across the three rifles in Dataset 1 for (i,ii,iii) Volunteer 1, (iv,v,vi) Volunteer 2 and (vii,viii,ix) Volunteer 3 showing the difference between separate angular velocity and linear acceleration inputs to the head model

Table 16: A_{CSV} values for the separate angular velocity input signal

	All included	AVX only	AVY only	AVZ only	AVX only (%)	AVY only (%)	AVZ only (%)
DATASET 1							
Rifle A							
Vol 1	0.0235	0.0124	0.0178	0.0163	53	76	69
Vol 2	0.0449	0.0216	0.0187	0.0361	48	42	80
Vol 3	0.0379	0.0249	0.0261	0.0190	66	69	50
Rifle B							
Vol 1	0.0235	0.0097	0.0163	0.0185	41	69	79
Vol 2	0.0329	0.0151	0.0179	0.0284	46	54	86
Vol 3	0.0344	0.0232	0.0184	0.0279	67	53	81
Rifle C							
Vol 1	0.0257	0.0160	0.0146	0.0188	62	57	73
Vol 2	0.0492	0.0178	0.0168	0.0442	36	34	90
Vol 3	0.0367	0.0227	0.0179	0.0311	62	49	85
DATASET 2							
Rifle D							
Vol 4	0.0140	0.0052	0.0099	0.0098	37	71	70
Vol 7	0.0136	0.0053	0.0100	0.0104	39	73	76
Vol 8	0.0116	0.0045	0.0065	0.0095	38	56	82
Rifle E							
Vol 4	0.0237	0.0156	0.0165	0.0142	66	69	60
Vol 7	0.0275	0.0138	0.0231	0.0138	50	84	50
Vol 8	0.0251	0.0124	0.0192	0.0184	49	77	73

Where

AVX only $= \left(\frac{\boldsymbol{AVX}}{\boldsymbol{all\ included}} * \mathbf{100}\right)$

AVY only $= \left(\frac{\boldsymbol{AVY}}{\boldsymbol{all\ included}} * \mathbf{100}\right)$

AVZ only $= \left(\frac{\boldsymbol{AVZ}}{\boldsymbol{all\ included}} * \mathbf{100}\right)$

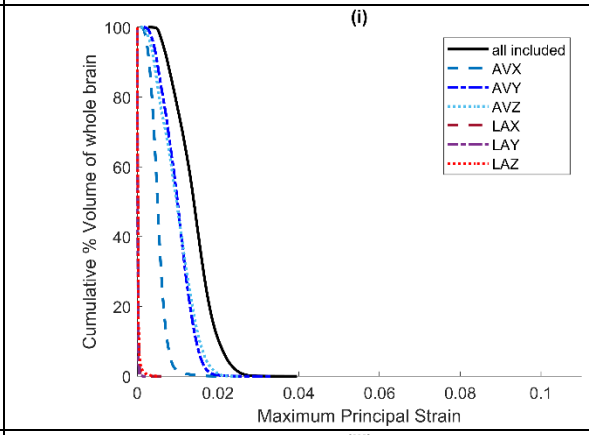
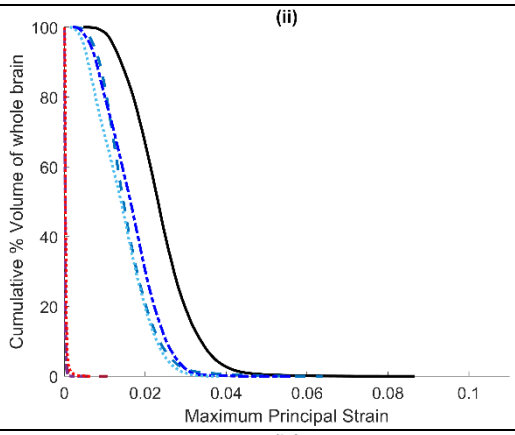
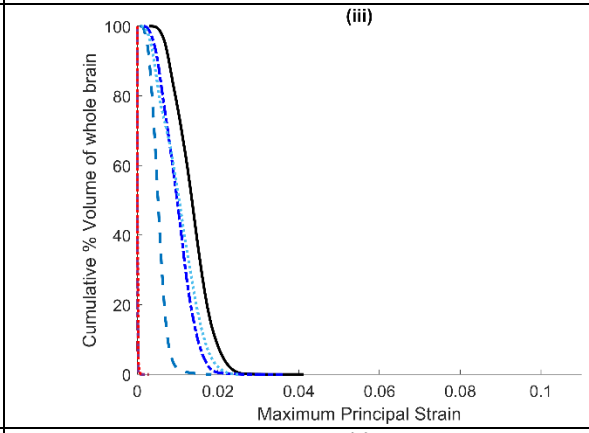
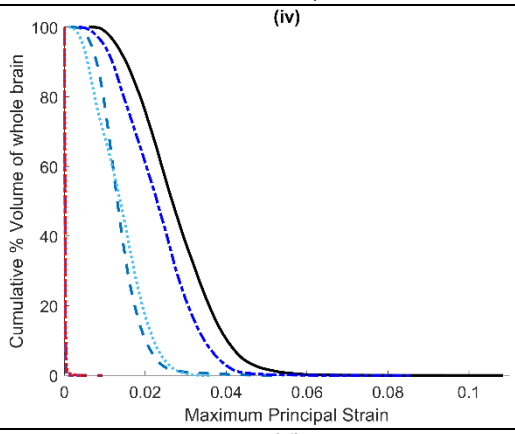
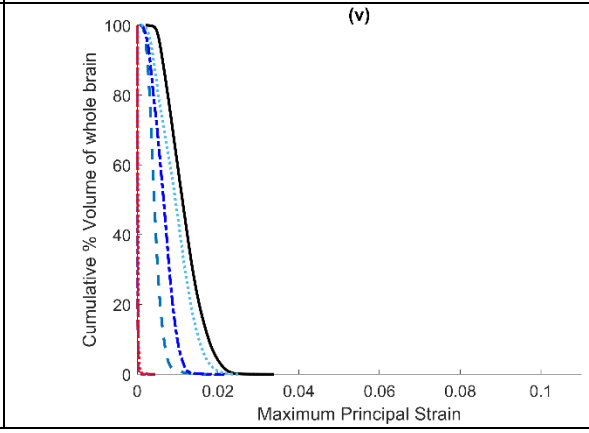
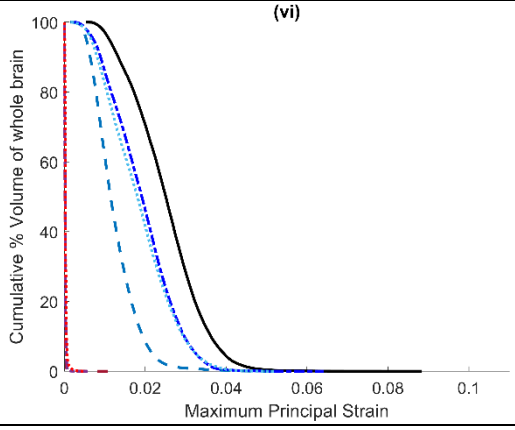
	Rifle D	Rifle E
Vol 4		
Vol 7		
Vol 8		

Figure 54: Cumulative strain-volume curves for one shot across the two rifles in Dataset 2 for (i,ii) Volunteer 4, (iii,iv) Volunteer 7 and (v,vi) Volunteer 8 showing the difference between separate angular velocity and linear acceleration inputs to the head model

5 Discussion

In this study, the head response and brain deformation of CAF volunteers subjected to recoil forces when firing long-range rifles were assessed and quantified. The head kinematics of volunteers exposed to recoil forces from various long-range rifles were recorded using mouthguards and subsequently analyzed using kinematics-based head response criteria, and a detailed finite element head model. The objectives of the research were to quantify head kinematics for volunteers, assess the head response using kinematic-based metrics, and assess brain response using a detailed finite element head model. Two data collections were analyzed in this study. Dataset 1 provided the opportunity to explore the effect of different rifle chassis and a recoil mitigation system. Dataset 2 allowed for comparing head kinematics resulting from discharging a .338 caliber rifle, and a .50 caliber rifle.

The experiments conducted in this study were unique in several aspects. Firstly, head kinematics were measured under controlled conditions, including the consistent use of the same ammunition, rifle type, and impact direction between shots and volunteers. Moreover, the study investigated head kinematics measured as a result of recoil forces. This differs from many previous studies, which have primarily examined the effects of blast waves generated by diverse sources, such as small explosive charges and large-caliber weapons, on brain injury. Instrumented mouthguards worn by the volunteers during firing recorded rotational and translational motion in all three axes. Previous research suggests that the combination of such kinematics may increase injury risk [59]. Additionally, instrumented mouthguards were used, known for their closer coupling with the skull compared to other wearable head or helmet devices [174]. Specifically, a custom version of the Prevent Biometrics mouthguards was used in this study, featuring modifications such as a low-g unit accelerometer, extended recording time, and an adjustable trigger threshold. These changes were necessary because the commercial version of the mouthguard was designed for impacts with higher accelerations and shorter durations, such as those experienced in sports settings like American football and rugby.

5.1 Head Kinematics Resulting from Rifle Discharge

Kinematics were evaluated by comparing processed linear acceleration and angular velocity signals obtained from the mouthguards. Previous studies in sports, where the bulk of research on mTBIs has been concentrated, have reported a spectrum of head acceleration values associated with concussions [69], [82], [196], [197], [198], [199], [200], [201], [202]. These values range from 73.6 to 151 g for the mean peak resultant linear acceleration observed among male athletes participating in sports without helmets (soccer, Australian football) and sports with helmets (hockey, American football). The reported thresholds are lower for female athletes, with Wilcox et al. documenting a mean peak linear acceleration of 43 g in concussed cases within ice hockey [128]. Among all athletes, the mean maximum resultant angular acceleration associated with concussions extends from 5022 to 7951 rad/s^2.

The head kinematics measured in the volunteers ranged from 3.4 to 4.5 g for peak resultant linear acceleration and 0.5 to 0.7 rad/s^2 for peak angular acceleration. When compared to the head kinematic ranges in sports-related studies, the measured head kinematics in this study are below reported injury thresholds. However, CAF members have reported multiple mTBI symptoms after either exposure to repeated blasts from explosive charges or repeated firing of long-range rifles [24]. These findings suggest that the effects of rifle recoil exposure may be cumulative, emphasizing the need to understand exposure limits and introduce measures to reduce long-term neurological damage from occupational exposures.

Some differences were observed among rifles when plotting the kinematic traces of all rifles for each volunteer in both datasets. For instance, in Dataset 1, Rifle C usually exhibited higher magnitudes for linear acceleration and angular velocity, followed by Rifles A and B. This suggests that each rifle induced different inputs to the shoulders of the volunteers, even though the same ammunition was used in all rifles of the same caliber. More specifically, in Dataset 1, Rifle B consistently demonstrated the lowest head kinematics, particularly noticeable among Volunteers 1 and 2. This observation suggests that the RMS mounted on the rifle may have effectively decreased the amount of kinematics experienced by the volunteers.

Additionally, Rifle C yielded higher kinematic measurements than Rifle A, specifically for Volunteers 1 and 2. Rifles A and C share the same caliber but have different chassis manufacturers. This suggests a potential correlation between the type of chassis and the amount of recoil experienced by the volunteers. Such a connection may stem from variations in chassis design elements such as weight and barrel length, all of which can impact the firing technique employed by the volunteers and subsequently influence the transmission of forces to their shoulders. For example, a heavier chassis will generally result in less felt recoil for the shooter compared to a lighter one because the mass of the chassis absorbs and dissipates some of the recoil energy generated [203], [204]. Osborne et al. reported that most U.S. military personnel favor conventional rifles over bullpup rifles, known for their shorter length and reduced weight compared to conventional rifles, for their capacity to decrease recoil because of the rifle's larger size and weight [205].

The barrel length may also affect recoil in a couple of ways. For instance, a longer barrel may result in slightly less felt recoil due to the added weight to the rifle. Additionally, when gunpowder ignites, it generates gases that propel the bullet forward. A longer barrel provides more space for these gases to expand and burn, allowing for more complete combustion of the gunpowder. As a result, the pressure buildup behind the bullet is more gradual. With a smoother, more gradual release of pressure, the recoil felt by the shooter is typically reduced.

Differences in head kinematics between rifles were smaller for certain volunteers. For instance, the differences between rifles were less evident when comparing the kinematic traces for Volunteer 3. This implies that the different rifle configurations, including the RMS, had a minimal impact on the resulting kinematics experienced by Volunteer 3. It is possible that Volunteer 3 employed a specific posture and firing technique that resulted in lower variations in head kinematics across different rifle configurations. The consistency in a volunteer's head kinematics may also reflect their experience level. It is hypothesized that with prolonged training, a volunteer might have ample time to develop and refine a firing technique that could be easily adapted to different rifles, even those with which they may not be familiar. Hence, in addition to adjusting rifle configurations (including chassis type, setup, and recoil mitigating systems) to

minimize head kinematics in volunteers firing long-range rifles potentially, it is also essential to consider the individualized firing techniques of each volunteer.

In Dataset 2, head kinematics were compared between volunteers firing Rifle D, a .338 caliber rifle, and Rifle E, a .50 caliber rifle. The .50 caliber Rifle E exhibited a mean peak resultant acceleration of 138 m/s², including all volunteers of Dataset 2, while the .338 caliber Rifle D had 51 m/s², indicating a 63% average decrease in acceleration. Regarding angular velocity, the mean peak resultant was 8 rad/s for the .50 caliber Rifle E and 3 rad/s for the .338 caliber Rifle D, indicating an average decrease of 62%. These findings may be related to the differences in kinetic energy of the projectile for each caliber.

5.2 Kinematic-Based Injury Metrics

In the background section, various kinematic-based metrics were outlined, all of which are mathematical expressions typically involving translational or rotational components of acceleration, velocity, or a combination thereof. These metrics typically focus on quantifying the severity of acute impacts rather than the cumulative burden of repetitive impacts.

HIC_{15} was included in this thesis due to its widespread use as a kinematic-based metric for evaluating head injury risk. It is also the primary metric for assessing occupant crash safety in motor vehicles under regulations like FMVSS 208. BrIC was included as the rotational kinematic-based metric due to its strong correlation with strain-based metrics in a study by Gabler et al. The study evaluated the effectiveness of fifteen kinematic-based metrics, such as maximum resultant angular velocity, linear acceleration, angular acceleration, GSI, HIC, GAMBIT, HIP, KLC, PCS, CP, PRHIC, BrIC, and RVCI, in predicting strain-based metrics like MPS and CSDM through linear regression and ordinary least squares [114]. Among these metrics, BrIC demonstrated the highest correlation. The analysis in this thesis aimed to identify trends between the different rifles in both Datasets 1 and 2 and variations between the volunteers.

In Datasets 1 and 2, two kinematic-based measures, HIC_{15} and BrIC, were calculated for all the shots. The HIC_{15} values in these datasets reached up to 5.3, lower than HIC_{15} values reported in

other sports-related studies, such as 12.5 in hockey, 22.5 in American football, and 48.5 in soccer [200].

The HIC_{15} threshold for head injury in automotive cases, as reported in the FMVSS 208, is 700 for a 50_{th} percentile male. Additionally, a study indicated that a HIC_{15} value of 240 corresponds to a 50% probability of sustaining an mTBI in American football [148].

Regarding BrIC, developed by Takhounts et al., a 50% probability of sustaining an AIS 1 and 4 injury correlates to BrIC values of 0.15 and 1.1, respectively [124]. The calculated BrIC values in this study were lower than those associated with AIS 1 injuries. Thus, the relatively low HIC_{15} and BrIC values obtained in this study suggest that the individual shots, irrespective of the rifle fired, were unlikely to cause injury. This implies that prolonged exposure to rifle recoil may result in symptoms associated with concussions, underscoring the critical importance of implementing measures to mitigate such occupational exposures [24].

All volunteers in Dataset 1 had the lowest HIC_{15} values when using Rifle B. This indicated that the RMS decreased head kinematics for all volunteers. This observation aligns with the comparison of linear acceleration and angular velocity signals between rifles. Volunteer 1 had the highest mean HIC_{15} value when using Rifle C, followed by Rifles A and B, consistent with the observed pattern in the measured head kinematic peaks. However, Volunteers 2 and 3 showed higher mean HIC_{15} values when using Rifle A compared to Rifle C. This finding contradicts the observed head kinematics for Volunteer 2. In Dataset 2, all volunteers had higher HIC_{15} values when using Rifle E than D, which aligns with the observed trend between rifles for measured head kinematics.

However, HIC_{15} may not be the appropriate measure for this study because it may be sensitive to high-frequency noise, as observed by Simms and Wood in 2009. Pronounced peaks were observed in specific linear acceleration signals, such as those of Volunteer 1 with Rifle A in Dataset 1 and Volunteers 4, 5, and 6 with Rifle E in Dataset 2. These peaks exhibited high magnitudes and occurred within a brief timeframe, suggesting that they may not accurately reflect the head motion induced by the rifle's recoil force. One potential explanation for these anomalous peaks could be that volunteers clenched onto the mouthguard while firing, or it could also be because the volunteer usually rested their cheek on the rifle's buttstock. Depending on

the pressure between their cheek and the buttstock, high-frequency acceleration could be introduced in the mouthguard signals. Since the calculation of HIC_{15} depends on identifying the maximum area under the resultant linear acceleration-time curve, the presence of these short-duration, high-magnitude peaks in the linear acceleration signals contributed to elevated HIC_{15} values, thus biasing the trends between rifles and the range of HIC_{15} values. These elevated values emphasize that HIC_{15} is sensitive to high signal peaks, which might not accurately reflect overall kinematics and could result in values exceeding the investigated loading condition. HIC_{15} exclusively uses linear acceleration, neglecting the effect of head rotation. Consequently, it may not be sufficient for independently assessing the risk of mTBI, which Holbourn identified as a shear strain injury predominantly resulting from rotational kinematics.

Regarding the trends observed, the order of BrIC values between rifles was consistent with the measured head kinematics trend for Volunteers 1 and 2, with Rifle B resulting in the lowest BrIC value and Rifle C yielding higher values than Rifle A. However, the trend in BrIC values for Volunteer 3 differed from that of the other two volunteers and contradicted their respective trends using HIC_{15}. Volunteer 3 had the lowest BrIC value with Rifle C, followed by Rifles B and A, suggesting that the RMS system may not have effectively mitigated the kinematic impact on Volunteer 3's head to a magnitude lower than that induced by Rifles A and C. In Dataset 2, all volunteers had higher BrIC values when using Rifle E than D, which aligns with the observed trend between rifles for measured head kinematics and HIC_{15}. Nevertheless, BrIC also has some limitations as it solely relies on angular velocity.

5.3 Strain-Based Metrics for Whole Brain Response

MPS_{95}, a commonly used strain-based metric used in studies with computational modeling for injury risk prediction [116], [123], [124], [140], [154], was also included in the analysis in this thesis. CSV curves, a more recent metric, were introduced, and their sensitivity and effectiveness were explored in this thesis.

The results indicated that Rifle B consistently had the lowest MPS_{95} values across all volunteers, aligning with the observed trends in measured head kinematics and HIC_{15}. Additionally, Rifle C yielded higher MPS_{95} values than Rifle A for Volunteers 1 and 2, consistent with the findings from

the measured head kinematics and HIC_{15} analyses. However, for Volunteer 3, the trend between Rifles A and B resembled BrIC rather than the observed head kinematics and HIC_{15}, with higher MPS_{95} values recorded with Rifle A than Rifle C. As for Dataset 2, similar to the findings using the previously mentioned metrics, all volunteers had higher MPS_{95} values using Rifle E (mean MPS_{95} = 0.0924) than D (mean MPS_{95} =0.02095), indicating that the volunteers experienced approximately four times higher MPS_{95} on average when firing the .50 caliber rifle compared to the .338 caliber rifle.

Various brain strain thresholds have been reported in sports-related studies. For example, Kimpara et al. proposed a strain threshold of 0.32 corresponding to a 50% probability of mild traumatic brain injury but did not specify a specific brain region associated with this threshold [122]. Takhounts et al. simulated impacts from collegiate American football and reported strains ranging from 0.08 to 0.96, with a mean of 0.58 [140]. Within the study, no concussive injuries were diagnosed [140]. However, the MPS_{95} values in this study, similar to HIC_{15} and BrIC, were at least an order of magnitude lower than the strain range typically considered injurious.

While MPS_{95} has been extensively used to evaluate brain response [154], it has some limitations. It is a single value typically extracted for the whole brain, which does not give insight into how brain deformation is distributed throughout different brain regions. CSV curves, on the other hand, provide a comprehensive representation of the strain distribution within each brain region. Currently, the CSV curve primarily functions as an indicator quantifying the amount of strain within specific brain regions. A key advantage of CSV is that it does not require a cut-off value (e.g., 95^{th} percentile) and clearly represents the percentage volume of the brain region experiencing a specific magnitude of maximum principal strain (MPS).

When comparing the CSV curves, Volunteer 1 had the highest magnitudes with Rifle C, followed by A and B (Figure 41 (i)). Additionally, their CSV curves with the same rifle showed minimal variation. Volunteer 2 also demonstrated a similar pattern across rifles, but there was a greater spread between CSV curves with each rifle, especially with Rifle B (Figure 41 (ii)). On the other hand, Volunteer 3 had overlapping CSV curves (Figure 41 (iii)), indicating a similar amount of strain observed regardless of the rifles being used. These results suggest that the strain

experienced by each volunteer depended not solely on the type of rifle but also on the individual volunteers themselves.

It was also observed that having consistent CSV curves (i.e., low variability in CSV curves) did not necessarily mean that the amount of strain was reduced. For example, in Dataset 1, after analyzing the CSV curves for each volunteer (Figure 41), it was observed that Volunteers 1, 2, and 3 experienced an MPS range of approximately 0.019 to 0.024, 0.019 to 0.044, and 0.03 to 0.038, respectively, at 50% volume of the brain. Even though Volunteer 3 had lower variability between CSV curves, they experienced a higher range of strains for all rifles. Therefore, the effectiveness of the RMS varied among volunteers. Additionally, using Rifle B, which shared the same chassis as Rifle A but had an additional RMS, increased the variability of CSV curves for all volunteers. The lack of familiarity with the RMS of the volunteers potentially affected the variability in CSV curves between each firing event.

Several potential reasons exist for the differences between volunteers when using a particular rifle. There may be anthropometric differences between volunteers. Numerous studies in sports have investigated how neck strength and muscle activation may help reduce the probability of sports-related concussion (SRC). According to [151], having a larger and stronger neck may decrease the impact of external forces on the head, which can lower the chances of getting a concussion. Additionally, a pilot study by Eckner et al. investigated the effects of targeted neck-strengthening exercises on young athletes, which resulted in an increase in neck strength and size [208]. The study found that this increased neck strength led to a decrease in head kinematics, indicating that resistance training exercises could possibly help decrease the risk of SRC among young athletes.

Another investigation by Tierney et al. explored the timing and muscle activation patterns during external force application among males and females [209]. It was found that pre-activating neck muscles, particularly in males, resulted in a 25% reduction in angular acceleration during known force application trials compared to unknown trials. These findings, along with the research conducted by Eckner et al., underscore the importance of neck strength and muscle activation in decreasing head acceleration during impacts, thus suggesting a potential approach for preventing

SRC. Further studies should investigate the efficacy of incorporating head-neck resistance training for the sniper population. This may involve strengthening muscles, increasing neck girth, and activating primary stabilizing muscles in preparation for recoil force. Such training could potentially enhance the ability of snipers to absorb external forces and utilize dynamic stabilizers, thus reducing the risk of head injuries.

5.4 Strain-Based Response of Individual Brain Regions

Typically, the brainstem midbrain and corpus callosum exhibited higher strains relative to other brain regions, whereas the brainstem and cerebellum tended to experience lower strains, as predicted by the head finite element model for all volunteer simulations. In the majority of cases, the corpus callosum exhibited the highest strain. A potential reason why the corpus callosum tends to experience the highest strains, as suggested by Hernandez et al. (2019) in a previous study, is that a large amount of rotation in the coronal plane might induce stress in the corpus callosum by initiating a wave falx cerebri. Since this region's central role is to facilitate information transmission between cerebral hemispheres, impairment in this area could disrupt communication, resulting in disorientation and impaired vision, aligning with common symptoms of mTBI.

Following the corpus callosum and brainstem midbrain, the basal ganglia and thalamus are additional regions with higher A_{CSV}. These findings align with earlier studies indicating that deeper brain regions are more likely correlated with concussions [53], [54], [55]. However, the ranking of remaining regions varies across different rifles and volunteers. Additionally, when comparing the effects of different rifles, the regions experiencing the most significant change in strain differ for each volunteer. For example, in comparing Rifles A (without RMS) and B (with RMS), Volunteer 1 experienced the most substantial decrease in A_{CSV} in the basal ganglia, Volunteer 2 in the cerebellum, and Volunteer 3 in the brainstem. Interestingly, none of these regions ranked highest when ordering the A_{CSV} of all regions in descending order, suggesting that the region experiencing the highest strain may not undergo the largest change in strain upon recoil mitigation measures, such as adding a recoil management system (RMS) to the rifle.

Understanding the primary brain region affected during mTBI is vital for several reasons. Different brain regions serve distinct functions like movement, language, and memory. For instance, damage to the temporal lobe may lead to memory problems, while damage to the occipital lobe could result in visual disturbances. Identifying the most affected region can aid in diagnosis and symptom management. Additionally, the severity and duration of symptoms vary depending on the affected brain area, influencing prognosis. This understanding also informs research efforts to develop better diagnostic tools, treatment strategies, and preventive measures by pinpointing the mechanisms underlying mTBI.

5.5 Linear Acceleration vs Angular Velocity Contribution to Brain Response

The linear acceleration and angular velocity curves were applied separately to the FE head model to assess the relative effect of angular velocity and linear acceleration on brain strain. The results showed that angular velocity contributed between 97 and 99% of the area under the CSV curve compared to linear acceleration across all volunteers and rifle types, highlighting the critical role of angular velocity in brain strain. These results have the potential to guide the improvement of protection systems.

Specifically, angular velocity in the Z direction was the primary contributor to cumulative strain. Note that Z direction refers to the “saying no” motion or motion towards and away from the rifle. Angular velocity in Z is the highest in this population because of the nature of the event. However, in two cases, angular velocity in Y exhibited the highest A_{CSV}. The Y direction refers to the forward and backward motion of the head. Additionally, the percentage of area under the angular velocity in the Z (AVZ) curve relative to the "all included" curve varied across different rifles and volunteers within Dataset 1, highlighting the importance of considering individual variations when assessing head injury risk. For instance, Volunteer 2 consistently exhibited a higher percentage of area under the AVZ curve relative to the "all included" curve compared to other volunteers, suggesting potential variations in firing technique leading to higher brain strains. In Dataset 2, similar trends were observed, with angular velocity in the Z and Y directions having the most significant influence on A_{CSV}. However, the difference between the two directions was less pronounced compared to Dataset 1, particularly when firing Rifle D.

The findings suggest that focusing on mitigating angular velocity-induced strains, particularly by designing protective devices or implementing training protocols to reduce angular velocity in Z, could potentially mitigate recoil effects.

5.6 Limitations

This study had several limitations. For instance, although the mouthguard effectively detected differences in kinematics when firing different rifles, the volunteer rested their cheek on the buttstock of the rifle, which potentially introduced high-frequency acceleration in the mouthguard signals due to direct coupling with the rifle. The origin of these short duration high magnitude peaks should be investigated further since they can influence certain head injury metrics such as HIC_{15}.

In this study, the assumption is made that the maxilla is rigidly attached to the skull, allowing the motion measured at the dentition by the mouthguard to be translated into the head center of gravity. It is important to note that the firing technique of all volunteers includes resting the cheek against the buttstock of the rifle. Consequently, the kinematics measured by the mouthguards represent not only head accelerations occurring from the shoulder to the neck and head but also loading due to the cheek resting on the buttstock. Although it is possible for loading to occur to the head directly via the buttstock, the motion of the rifle is parallel to the cheek and underlying hard tissues, which suggests that direct loading is not the prominent load path to generate gross head accelerations.

As mentioned in the methods section, the process involved in dealing with signals deemed as late captures (signals with no pre-trigger data) was to infer the stationary head position based on the average head position from signals considered “good captures” of the same volunteer. This step assumes that every volunteer returns to the same head orientation after firing each shot, which limits the methodology.

While this particular population offered a controlled environment for data collection, it is worth considering that their threshold for injury may potentially be elevated compared to the general population, owing to the rigorous intensity of their training regimen. The individual concussion

histories and cognitive tests of this study cohort was not performed to assess the cumulative effects. Consequently, the investigation only provides insights into head kinematics for a single recoil impulse.

The FE model used in this study, despite being validated using cadaveric data, did not consider anatomical and physiological variations between specific volunteers. Additionally, different types of head models have been used to estimate injury thresholds, and it is important to note that the predicted strain for the same kinematic input may vary among different FE models [160].

Despite each group under comparison consisting of only 4 data points (shots), ANOVA analysis and t-tests were conducted under the assumption of normal distribution. Given the small sample size, other non-parametric tests were not explored in this study. It should be emphasized that small dataset sizes are an inherent limitation in studies of this nature. This limitation is driven by the primary study objective, which aims to gain a comprehensive understanding of the injury mechanisms to ultimately minimize exposure risk. Striking this balance between comprehending injury mechanisms and minimizing risk naturally leads to the presence of relatively small datasets, thereby challenging the conduct of statistical analysis. However, the analysis did provide valuable insights into the observed trends.

6 Conclusion

The head motion of CAF volunteers was monitored using instrumented mouthguards as they fired different long-range rifles, including those from different chassis manufacturers and with different calibers. The data collected was then used as direct inputs to the CoG of a 50th percentile male GHBMC head model to analyze the brain deformations from re-creations of the recoil forces transmitted to the shoulder, neck, head, and mouthguard, causing head accelerations. The goal of this study was to quantify the magnitude of head kinematics and brain response experienced by members of the CAF, a population that has previously reported symptoms of mTBI.

The measured kinematic and strain quantities in the population under study were significantly lower than those typically reported in sports injury studies. Four metrics based on head kinematics and brain deformation were investigated. It was found that the CSV curves were more sensitive and offered a better representation of the strain distribution in the brain than MPS_{95}, BrIC, and HIC_{15}. The CSV curves account not only for the degree of tissue deformation in the brain but also for the degree to which the entire brain is loaded. The other metrics had certain limitations. For instance, HIC_{15} only considered linear acceleration, while BrIC only used angular velocity. As for MPS_{95}, it is a single value that is usually extracted for the entire brain, and it requires a cut-off value (i.e., 95th percentile for MPS_{95}) without any clear explanation of why the cut-off is 95th percentile in literature.

During the study, several differences were noted between the rifles and volunteers. For instance, Rifle C produced higher kinematic measurements than Rifle A, especially among Volunteers 1 and 2 of Dataset 1. This implies that there might be a correlation between the type of chassis and the amount of recoil experienced by volunteers. This connection could be due to variations in chassis design elements like weight and barrel length, which can affect the firing technique used by volunteers and, consequently, influence the transmission of forces to their shoulders.

The results also revealed individual variability among the volunteers. When comparing the CSV curves, Volunteer 1 showed a clear difference between rifles with the highest magnitudes with Rifle C, followed by A and B. Moreover, their shots with the same rifle showed minimal variation. Volunteer 2 also demonstrated a similar pattern across rifles, but there was a greater spread

between shots fired with each rifle, especially with Rifle B. On the other hand, Volunteer 3 had overlapping CSV curves, indicating a similar amount of strain observed regardless of the rifles used. When comparing the volunteers for specific rifle configurations, Volunteer 1 clearly displayed lower strains compared to Volunteers 2 and 3 across all rifles. Conversely, Volunteer 2 exhibited the highest strains when using Rifles A and C, while Volunteer 3 experienced the highest strain when firing rifle B compared to the other volunteers. These results suggest that the amount and variability of strain experienced by each volunteer depended not solely on the type of rifle but also on the individual volunteers.

Therefore, while all volunteers experienced a decrease in strains when firing Rifle B with the RMS system, indicating that the RMS system effectively reduced the recoil force to the shoulder, the extent to which the RMS reduced head response depended on the volunteer. Additionally, specific volunteers consistently experienced lower strains. For example, Volunteer 1 from Dataset 1 always experienced lower strains regardless of the rifle used. This indicates that while protective equipment can help reduce recoil, training to hone specific firing techniques could also be helpful.

The comparative analysis in Dataset 2 between different caliber rifles revealed an interesting finding. The .50 caliber rifle showed a mean peak resultant linear acceleration of 138 m/s^2, while the .338 caliber rifle showed only 51 m/s^2. This indicates a 63% decrease in resultant linear acceleration. Similarly, angular velocity showed a similar percentage decrease between the two calibers, with the .50 caliber rifle showing 8 rad/s for mean peak resultant angular velocity and the .338 caliber rifle showing only 3 rad/s.

Comparing the CSV curves between the eight brain regions revealed that the corpus callosum consistently emerged as the primary site of higher strains, followed by the brainstem midbrain, basal ganglia, and thalamus. This observation suggested that specific regions may serve as more reliable indicators of mTBI. However, it is important to note that the ranking of strain distribution across remaining regions varied among different rifles and volunteers. Understanding the primary brain region affected during mTBI is vital to inform research looking at advancing diagnostic tools, treatment modalities, and preventive measures.

Investigating the relative contributions of angular velocity and linear acceleration to the strain experienced by the volunteers using long-range rifles demonstrated that angular velocity was the primary contributor to brain strain. Furthermore, angular velocity-induced strains were typically highest, resulting from rotation in the Z direction. Such information could inform the design of protective devices and tailoring training regimens to mitigate these effects effectively.

Overall, the findings from this study mark an initial stride towards research aimed at informing training procedures and establishing exposure limits for CAF members to mitigate any potential long-term effects stemming from occupational exposures to recoil forces.

The recommendations for future work are as follows:

1. **Individualistic Differences Tracking**: It is recommended to conduct more comprehensive tracking of individual differences among volunteers, including factors such as posture, cheek-buttstock positioning, and years of experience. Consistent monitoring of time taken by volunteers from given the “go-ahead” signal to making the shot could be implemented to help understand individual firing rituals. This could provide insights into how these variables influence head kinematics and could inform personalized training regimens.
2. **Measurement of Shoulder Force**: Measurements of shoulder force could be taken to better understand the translation of force to the head during recoil. This could provide insights into volunteer bracing behaviors, help optimize equipment design, and update training regimens for mitigating head accelerations.
3. **Evaluation of Adjustable Buttstock**: The volunteers usually rest their cheeks against the cheek rest on the rifle's buttstock. Investigating the effects of adjustable cheek rest positions on mouthguard measurements could help assess whether high magnitude, short duration pikes in kinematic signals are linked to the cheek-rest position.
4. **Mouth Guard Sensor Placement Optimization**: The sensor placement could be optimized in mouthguards to minimize the influence of non-representative head motion peaks. Positioning sensors on the opposite side of the cheek from the buttstock contact point may allow for more accurate measurement of recoil-induced head motion.

5. **Orientation of Volunteer**: When processing mouthguard data, the methodology assumed that all volunteers returned to the same head orientation when positioning themselves for the next shot. Hence, additional sensors could be added to the mouthguard to help track head orientation.
6. **Increase Pre-Trigger Data**: Currently, the amount of pre-trigger data is only 7.5 ms. The duration of pre-trigger data acquisition could be extended to avoid data augmentation from signals deemed as “good captures.”
7. **Integration of "Engaged/Disengaged" Mode**: Mouthguards could be upgraded to include an "engaged/disengaged" mode controlled by an accompanying app. This feature would allow the volunteers to position themselves without triggering sensor data collection during setup (before taking the shot).

Future research efforts should focus on implementing these recommendations for measuring more accurate head kinematics during rifle firing. This will contribute to a better understanding of volunteers' head motion and aid in developing more effective training procedures and occupational safety measures for military personnel.

Letters of Copyright Permission



This is a License Agreement between Tanvi Seeburrun/ University of Waterloo ("User") and Copyright Clearance Center, Inc. ("CCC") on behalf of the Rightsholder identified in the order details below. The license consists of the order details, the Marketplace Permissions General Terms and Conditions below, and any Rightsholder Terms and Conditions which are included below.

All payments must be made in full to CCC in accordance with the Marketplace Permissions General Terms and Conditions below.

Order Date	04-Jun-2024	**Type of Use**	Republish in a thesis/dissertation
Order License ID	1491273-1		
ISBN-13	9783030116583	**Publisher**	Springer International Publishing
		Portion	Chart/graph/table/figure

LICENSED CONTENT

Publication Title	Trauma Biomechanics : An Introduction to Injury Biomechanics	**Country**	Switzerland
		Rightsholder	Springer Nature BV
Author / Editor	Schmitt, Kai-Uwe, Niederer, Peter F., Cronin, Duane S., Morrison III, Barclay, Muser, Markus H., Walz, Felix	**Publication Type**	Book
Date	03/15/2019		
Language	English		

REQUEST DETAILS

Portion Type	Chart/graph/table/figure	**Distribution**	Worldwide
Number of Charts / Graphs / Tables / Figures Requested	1	**Translation**	Original language of publication
		Copies for the Disabled?	No
Format (select all that apply)	Electronic	**Minor Editing Privileges?**	No
Who Will Republish the Content?	Academic institution	**Incidental Promotional Use?**	No
Duration of Use	Life of current edition	**Currency**	CAD
Lifetime Unit Quantity	Up to 999		
Rights Requested	Main product		

NEW WORK DETAILS

Title	Investigation of Brain Response in Canadian Armed Forces Volunteers Subjected to Recoil Force from Firing Long-Range Rifles Using Instrumented Mouthguards and Finite Element Head Model	**Institution Name**	University of Waterloo
		Expected Presentation Date	2024-06-25
Instructor Name	Professor Duane Cronin		

ADDITIONAL DETAILS

The Requesting Person / Organization to Appear on the License	Tanvi Seeburrun/ University of Waterloo

REQUESTED CONTENT DETAILS

Title, Description or Numeric Reference of the Portion(s)	Table 4.1	**Title of the Article / Chapter the Portion Is From**	Head Injuries
Editor of Portion(s)	Schmitt, Kai-Uwe; Niederer, Peter F.; Cronin, Duane S.; Morrison III, Barclay; Muser, Markus H.; Walz, Felix	**Author of Portion(s)**	Schmitt, Kai-Uwe; Niederer, Peter F.; Cronin, Duane S.; Morrison III, Barclay; Muser, Markus H.; Walz, Felix
Volume / Edition	5th ed. 2019	**Publication Date of Portion**	2019-03-15
Page or Page Range of Portion	90		

Marketplace Permissions General Terms and Conditions

The following terms and conditions ("General Terms"), together with any applicable Publisher Terms and Conditions, govern User's use of Works pursuant to the Licenses granted by Copyright Clearance Center, Inc. ("CCC") on behalf of the applicable Rightsholders of such Works through CCC's applicable Marketplace transactional licensing services (each, a "Service").

1) **Definitions.** For purposes of these General Terms, the following definitions apply:

"License" is the licensed use the User obtains via the Marketplace platform in a particular licensing transaction, as set forth in the Order Confirmation.

"Order Confirmation" is the confirmation CCC provides to the User at the conclusion of each Marketplace transaction. "Order Confirmation Terms" are additional terms set forth on specific Order Confirmations not set forth in the General Terms that can include terms applicable to a particular CCC transactional licensing service and/or any Rightsholder-specific terms.

"Rightsholder(s)" are the holders of copyright rights in the Works for which a User obtains licenses via the Marketplace platform, which are displayed on specific Order Confirmations.

"Terms" means the terms and conditions set forth in these General Terms and any additional Order Confirmation Terms collectively.

"User" or "you" is the person or entity making the use granted under the relevant License. Where the person accepting the Terms on behalf of a User is a freelancer or other third party who the User authorized to accept the General Terms on the User's behalf, such person shall be deemed jointly a User for purposes of such Terms.

"Work(s)" are the copyright protected works described in relevant Order Confirmations.

2) **Description of Service.** CCC's Marketplace enables Users to obtain Licenses to use one or more Works in accordance with all relevant Terms. CCC grants Licenses as an agent on behalf of the copyright rightsholder identified in the relevant Order Confirmation.

3) **Applicability of Terms.** The Terms govern User's use of Works in connection with the relevant License. In the event of any conflict between General Terms and Order Confirmation Terms, the latter shall govern. User acknowledges that Rightsholders have complete discretion whether to grant any permission, and whether to place any limitations on any grant, and that CCC has no right to supersede or to modify any such discretionary act by a Rightsholder.

4) **Representations; Acceptance.** By using the Service, User represents and warrants that User has been duly authorized by the User to accept, and hereby does accept, all Terms.

5) **Scope of License; Limitations and Obligations.** All Works and all rights therein, including copyright rights, remain the sole and exclusive property of the Rightsholder. The License provides only those rights expressly set forth in the terms and conveys no other rights in any Works

6) **General Payment Terms.** User may pay at time of checkout by credit card or choose to be invoiced. If the User chooses to be invoiced, the User shall: (i) remit payments in the manner identified on specific invoices, (ii) unless otherwise specifically stated in an Order Confirmation or separate written agreement, Users shall remit payments upon receipt of the relevant invoice from CCC, either by delivery or notification of availability of the invoice via the Marketplace platform, and (iii) if the User does not pay the invoice within 30 days of receipt, the User may incur a service charge of 1.5% per month or the maximum rate allowed by applicable law, whichever is less. While User may exercise the rights in the License immediately upon receiving the Order Confirmation, the License is automatically revoked and is null and void, as if it had never been issued, if CCC does not receive complete payment on a timely basis.

7) **General Limits on Use.** Unless otherwise provided in the Order Confirmation, any grant of rights to User (i) involves only the rights set forth in the Terms and does not include subsequent or additional uses, (ii) is non-exclusive and non-transferable, and (iii) is subject to any and all limitations and restrictions (such as, but not limited to, limitations on duration of use or circulation) included in the Terms. Upon completion of the licensed use as set forth in the Order Confirmation, User shall either secure a new permission for further use of the Work(s) or immediately cease any new use of the Work(s) and shall render inaccessible (such as by deleting or by removing or severing links or other locators) any further copies of the Work. User may only make alterations to the Work if and as expressly set forth in the Order Confirmation. No Work may be used in any way that is unlawful, including without limitation if such use would violate applicable sanctions laws or regulations, would be defamatory, violate the rights of third parties (including such third parties' rights of copyright, privacy, publicity, or other tangible or intangible property), or is otherwise illegal, sexually explicit, or obscene. In addition, User may not conjoin a Work with any other material that may result in damage to the reputation of the Rightsholder. Any unlawful use will render any licenses hereunder null and void. User agrees to inform CCC if it becomes aware of any infringement of any rights in a Work and to cooperate with any reasonable request of CCC or the Rightsholder in connection therewith.

8) **Third Party Materials.** In the event that the material for which a License is sought includes third party materials (such as photographs, illustrations, graphs, inserts and similar materials) that are identified in such material as having been used by permission (or a similar indicator), User is responsible for identifying, and seeking separate licenses (under this Service, if available, or otherwise) for any of such third party materials; without a separate license, User may not use such third party materials via the License.

9) **Copyright Notice.** Use of proper copyright notice for a Work is required as a condition of any License granted under the Service. Unless otherwise provided in the Order Confirmation, a proper copyright notice will read substantially as follows: "Used with permission of [Rightsholder's name], from [Work's title, author, volume, edition number and year of copyright]; permission conveyed through Copyright Clearance Center, Inc." Such notice must be provided in a reasonably legible font size and must be placed either on a cover page or in another location that any person, upon gaining access to the material which is the subject of a permission, shall see, or in the case of republication Licenses, immediately adjacent to the Work as used (for example, as part of a by-line or footnote) or in the place where substantially all other credits or notices for the new work containing the republished Work are located. Failure to include the required notice results in loss to the Rightsholder and CCC, and the User shall be liable to pay liquidated damages for each such failure equal to twice the use fee specified in the Order Confirmation, in addition to the use fee itself and any other fees and charges specified.

10) **Indemnity.** User hereby indemnifies and agrees to defend the Rightsholder and CCC, and their respective employees and directors, against all claims, liability, damages, costs, and expenses, including legal fees and expenses, arising out of any use of a Work beyond the scope of the rights granted herein and in the Order Confirmation, or any use of a Work which has been altered in any unauthorized way by User, including claims of defamation or infringement of rights of copyright, publicity, privacy, or other tangible or intangible property.

11) **Limitation of Liability.** UNDER NO CIRCUMSTANCES WILL CCC OR THE RIGHTSHOLDER BE LIABLE FOR ANY DIRECT, INDIRECT, CONSEQUENTIAL, OR INCIDENTAL DAMAGES (INCLUDING WITHOUT LIMITATION DAMAGES FOR LOSS OF BUSINESS PROFITS OR INFORMATION, OR FOR BUSINESS INTERRUPTION) ARISING OUT OF THE USE OR INABILITY TO USE A WORK, EVEN IF ONE OR BOTH OF THEM HAS BEEN ADVISED OF THE POSSIBILITY OF SUCH DAMAGES. In any event, the total liability of the Rightsholder and CCC (including their respective employees and directors) shall not exceed the total amount actually paid by User for the relevant License. User assumes full liability for the actions and omissions of its principals, employees, agents, affiliates, successors, and assigns.

12) **Limited Warranties.** THE WORK(S) AND RIGHT(S) ARE PROVIDED "AS IS." CCC HAS THE RIGHT TO GRANT TO USER THE RIGHTS GRANTED IN THE ORDER CONFIRMATION DOCUMENT. CCC AND THE RIGHTSHOLDER DISCLAIM ALL OTHER WARRANTIES RELATING TO THE WORK(S) AND RIGHT(S), EITHER EXPRESS OR IMPLIED, INCLUDING WITHOUT LIMITATION IMPLIED WARRANTIES OF MERCHANTABILITY OR FITNESS FOR A PARTICULAR PURPOSE. ADDITIONAL RIGHTS MAY BE REQUIRED TO USE ILLUSTRATIONS, GRAPHS, PHOTOGRAPHS, ABSTRACTS, INSERTS, OR OTHER PORTIONS OF THE WORK (AS OPPOSED TO THE ENTIRE WORK) IN A MANNER CONTEMPLATED BY USER; USER UNDERSTANDS AND AGREES THAT NEITHER CCC NOR THE RIGHTSHOLDER MAY HAVE SUCH ADDITIONAL RIGHTS TO GRANT.

13) **Effect of Breach.** Any failure by User to pay any amount when due, or any use by User of a Work beyond the scope of the License set forth in the Order Confirmation and/or the Terms, shall be a material breach of such License. Any breach not cured within 10 days of written notice thereof shall result in immediate termination of such License without further notice. Any unauthorized (but licensable) use of a Work that is terminated immediately upon notice thereof may be liquidated by payment of the Rightsholder's ordinary license price therefor; any unauthorized (and unlicensable) use that is not terminated immediately for any reason (including, for example, because materials containing the Work cannot reasonably be recalled) will be subject to all remedies available at law or in equity, but in no event to a payment of less than three times the Rightsholder's ordinary license price for the most closely analogous licensable use plus Rightsholder's and/or CCC's costs and expenses incurred in collecting such payment.

14) **Additional Terms for Specific Products and Services.** If a User is making one of the uses described in this Section 14, the additional terms and conditions apply:

a) ***Print Uses of Academic Course Content and Materials (photocopies for academic coursepacks or classroom handouts).*** For photocopies for academic coursepacks or classroom handouts the following additional terms apply:

i) The copies and anthologies created under this License may be made and assembled by faculty members individually or at their request by on-campus bookstores or copy centers, or by off-campus copy shops and other similar entities.

ii) No License granted shall in any way: (i) include any right by User to create a substantively non-identical copy of the Work or to edit or in any other way modify the Work (except by means of deleting material immediately preceding or following the entire portion of the Work copied) (ii) permit "publishing ventures" where any particular anthology would be systematically marketed at multiple institutions.

iii) Subject to any Publisher Terms (and notwithstanding any apparent contradiction in the Order Confirmation arising from data provided by User), any use authorized under the academic pay-per-use service is limited as follows:

A) any License granted shall apply to only one class (bearing a unique identifier as assigned by the institution, and thereby including all sections or other subparts of the class) at one institution;

B) use is limited to not more than 25% of the text of a book or of the items in a published collection of essays, poems or articles;

C) use is limited to no more than the greater of (a) 25% of the text of an issue of a journal or other periodical or (b) two articles from such an issue;

D) no User may sell or distribute any particular anthology, whether photocopied or electronic, at more than one institution of learning;

E) in the case of a photocopy permission, no materials may be entered into electronic memory by User except in order to produce an identical copy of a Work before or during the academic term (or analogous period) as to which any particular permission is granted. In the event that User shall choose to retain materials that are the subject of a photocopy permission in electronic memory for purposes of producing identical copies more than one day after such retention (but still within the scope of any permission granted), User must notify CCC of such fact in the applicable permission request and such retention shall constitute one copy actually sold for purposes of calculating permission fees due; and

F) any permission granted shall expire at the end of the class. No permission granted shall in any way include any right by User to create a substantively non-identical copy of the Work or to edit or in any other way modify the Work (except by means of deleting material immediately preceding or following the entire portion of the Work copied).

iv) Books and Records; Right to Audit. As to each permission granted under the academic pay-per-use Service, User shall maintain for at least four full calendar years books and records sufficient for CCC to determine the numbers of copies made by User under such permission. CCC and any representatives it may designate shall have the right to audit such books and records at any time during User's ordinary business hours, upon two days' prior notice. If any such audit shall determine that User shall have underpaid for, or underreported, any photocopies sold or by three percent (3%) or more, then User shall bear all the costs of any such audit; otherwise, CCC shall bear the costs of any such audit. Any amount determined by such audit to have been underpaid by User shall immediately be paid to CCC by User, together with interest thereon at the rate of 10% per annum from the date such amount was originally due. The provisions of this paragraph shall survive the termination of this License for any reason.

b) ***Digital Pay-Per-Uses of Academic Course Content and Materials (e-coursepacks, electronic reserves, learning management systems, academic institution intranets).*** For uses in e-coursepacks, posts in electronic reserves, posts in learning management systems, or posts on academic institution intranets, the following additional terms apply:

i) The pay-per-uses subject to this Section 14(b) include:

A) **Posting e-reserves, course management systems, e-coursepacks for text-based content,** which grants authorizations to import requested material in electronic format, and allows electronic access to this material to members of a designated college or university class, under the direction of an instructor designated by the college or university, accessible only under appropriate electronic controls (e.g., password);

B) **Posting e-reserves, course management systems, e-coursepacks for material consisting of photographs or other still images not embedded in text,** which grants not only the authorizations described in Section 14(b)(i)(A) above, but also the following authorization: to include the requested material in course materials for use consistent with Section 14(b)(i)(A) above, including any necessary resizing, reformatting or modification of the resolution of such requested material (provided that such modification does not alter the underlying editorial content or meaning of the requested material, and provided that the resulting modified content is used solely within the scope of, and in a manner consistent with, the particular authorization described in the Order Confirmation and the Terms), but not including any other form of manipulation, alteration or editing of the requested material;

C) **Posting e-reserves, course management systems, e-coursepacks or other academic distribution for audiovisual content,** which grants not only the authorizations described in Section 14(b)(i)(A) above, but also the following authorizations: (i) to include the requested material in course materials for use consistent with Section 14(b)(i)(A) above; (ii) to display and perform the requested material to such members of such class in the physical classroom or remotely by means of streaming media or other video formats; and (iii) to "clip" or reformat the requested material for purposes of time or content management or ease of delivery, provided that such "clipping" or reformatting does not alter the underlying editorial content or meaning of the requested material and that the resulting material is used solely within the scope of, and in a manner consistent with, the particular authorization described in the Order Confirmation and the Terms. Unless expressly set forth in the relevant Order Conformation, the License does not authorize any other form of manipulation, alteration or editing of the requested material.

ii) Unless expressly set forth in the relevant Order Confirmation, no License granted shall in any way: (i) include any right by User to create a substantively non-identical copy of the Work or to edit or in any other way modify the Work (except by means of deleting material immediately preceding or following the entire portion of the Work copied or, in the case of Works subject to Sections 14(b)(1)(B) or (C) above, as described in such Sections) (ii) permit "publishing ventures" where any particular course materials would be systematically marketed at multiple institutions.

iii) Subject to any further limitations determined in the Rightsholder Terms (and notwithstanding any apparent contradiction in the Order Confirmation arising from data provided by User), any use authorized under the electronic course content pay-per-use service is limited as follows:

A) any License granted shall apply to only one class (bearing a unique identifier as assigned by the institution, and thereby including all sections or other subparts of the class) at one institution;

B) use is limited to not more than 25% of the text of a book or of the items in a published collection of essays, poems or articles;

C) use is limited to not more than the greater of (a) 25% of the text of an issue of a journal or other periodical or (b) two articles from such an issue;

D) no User may sell or distribute any particular materials, whether photocopied or electronic, at more than one institution of learning;

E) electronic access to material which is the subject of an electronic-use permission must be limited by means of electronic password, student identification or other control permitting access solely to students and instructors in the class;

F) User must ensure (through use of an electronic cover page or other appropriate means) that any person, upon gaining electronic access to the material, which is the subject of a permission, shall see:

- a proper copyright notice, identifying the Rightsholder in whose name CCC has granted permission,
- a statement to the effect that such copy was made pursuant to permission,
- a statement identifying the class to which the material applies and notifying the reader that the material has been made available electronically solely for use in the class, and
- a statement to the effect that the material may not be further distributed to any person outside the class, whether by copying or by transmission and whether electronically or in paper form, and User must also ensure that such cover page or other means will print out in the event that the person accessing the material chooses to print out the material or any part thereof.

G) any permission granted shall expire at the end of the class and, absent some other form of authorization, User is thereupon required to delete the applicable material from any electronic storage or to block electronic access to the applicable material.

iv) Uses of separate portions of a Work, even if they are to be included in the same course material or the same university or college class, require separate permissions under the electronic course content pay-per-use Service. Unless otherwise provided in the Order Confirmation, any grant of rights to User is limited to use completed no later than the end of the academic term (or analogous period) as to which any particular permission is granted.

v) Books and Records; Right to Audit. As to each permission granted under the electronic course content Service, User shall maintain for at least four full calendar years books and records sufficient for CCC to determine the numbers of copies made by User under such permission. CCC and any representatives it may designate shall have the right to audit such books and records at any time during User's ordinary business hours, upon two days' prior notice. If any such audit shall determine that User shall have underpaid for, or underreported, any electronic copies used by three percent (3%) or more, then User shall bear all the costs of any such audit; otherwise, CCC shall bear the costs of any such audit. Any amount determined by such audit to have been underpaid by User shall immediately be paid to CCC by User, together with interest thereon at the rate of 10% per annum from the date such amount was originally due. The provisions of this paragraph shall survive the termination of this license for any reason.

c) ***Pay-Per-Use Permissions for Certain Reproductions (Academic photocopies for library reserves and interlibrary loan reporting) (Non-academic internal/external business uses and commercial document delivery).*** The License expressly excludes the uses listed in Section (c)(i)-(v) below (which must be subject to separate license from the applicable Rightsholder) for: academic photocopies for library reserves and interlibrary loan reporting; and non-academic internal/external business uses and commercial document delivery.

i) electronic storage of any reproduction (whether in plain-text, PDF, or any other format) other than on a transitory basis;

ii) the input of Works or reproductions thereof into any computerized database;

iii) reproduction of an entire Work (cover-to-cover copying) except where the Work is a single article;

iv) reproduction for resale to anyone other than a specific customer of User;

v) republication in any different form. Please obtain authorizations for these uses through other CCC services or directly from the rightsholder.

Any license granted is further limited as set forth in any restrictions included in the Order Confirmation and/or in these Terms.

d) ***Electronic Reproductions in Online Environments (Non-Academic-email, intranet, internet and extranet).*** For "electronic reproductions", which generally includes e-mail use (including instant messaging or other electronic transmission to a defined group of recipients) or posting on an intranet, extranet or Intranet site (including any display or performance incidental thereto), the following additional terms apply:

i) Unless otherwise set forth in the Order Confirmation, the License is limited to use completed within 30 days for any use on the Internet, 60 days for any use on an intranet or extranet and one year for any other use, all as measured from the "republication date" as identified in the Order Confirmation, if any, and otherwise from the date of the Order Confirmation.

ii) User may not make or permit any alterations to the Work, unless expressly set forth in the Order Confirmation (after request by User and approval by Rightsholder); provided, however, that a Work consisting of photographs or other still images not embedded in text may, if necessary, be resized, reformatted or have its resolution modified without additional express permission, and a Work consisting of audiovisual content may, if necessary, be "clipped" or reformatted for purposes of time or content management or ease of delivery (provided that any such resizing, reformatting, resolution modification or "clipping" does not alter the underlying editorial content or meaning of the Work used, and that the resulting material is used solely within the scope of, and in a manner consistent with, the particular License described in the Order Confirmation and the Terms.

15) **Miscellaneous.**

a) User acknowledges that CCC may, from time to time, make changes or additions to the Service or to the Terms, and that Rightsholder may make changes or additions to the Rightsholder Terms. Such updated Terms will replace the prior terms and conditions in the order workflow and shall be effective as to any subsequent Licenses but shall not apply to Licenses already granted and paid for under a prior set of terms.

b) Use of User-related information collected through the Service is governed by CCC's privacy policy, available online at www.copyright.com/about/privacy-policy/.

c) The License is personal to User. Therefore, User may not assign or transfer to any other person (whether a natural person or an organization of any kind) the License or any rights granted thereunder; provided, however, that, where applicable, User may assign such License in its entirety on written notice to CCC in the event of a transfer of all or substantially all of User's rights in any new material which includes the Work(s) licensed under this Service.

d) No amendment or waiver of any Terms is binding unless set forth in writing and signed by the appropriate parties, including, where applicable, the Rightsholder. The Rightsholder and CCC hereby object to any terms contained in any writing prepared by or on behalf of the User or its principals, employees, agents or affiliates and purporting to govern or otherwise relate to the License described in the Order Confirmation, which terms are in any way inconsistent with any Terms set forth in the Order Confirmation, and/or in CCC's standard operating procedures, whether such writing is prepared prior to, simultaneously with or subsequent to the Order Confirmation, and whether such writing appears on a copy of the Order Confirmation or in a separate instrument.

e) The License described in the Order Confirmation shall be governed by and construed under the law of the State of New York, USA, without regard to the principles thereof of conflicts of law. Any case, controversy, suit, action, or proceeding arising out of, in connection with, or related to such License shall be brought, at CCC's sole discretion, in any federal or state court located in the County of New York, State of New York, USA, or in any federal or state court whose geographical jurisdiction covers the location of the Rightsholder set forth in the Order Confirmation. The parties expressly submit to the personal jurisdiction and venue of each such federal or state court.

Last updated October 2022

Marketplace

This is a License Agreement between Tanvi Seeburrun/ University of Waterloo ("User") and Copyright Clearance Center, Inc. ("CCC") on behalf of the Rightsholder identified in the order details below. The license consists of the order details, the Marketplace Permissions General Terms and Conditions below, and any Rightsholder Terms and Conditions which are included below.

All payments must be made in full to CCC in accordance with the Marketplace Permissions General Terms and Conditions below.

Order Date	13-Jun-2024	**Type of Use**	Republish in a thesis/dissertation
Order License ID	1494368-1		
ISBN-13	9783030116583	**Publisher**	Springer International Publishing
		Portion	Chart/graph/table/figure

LICENSED CONTENT

Publication Title	Trauma Biomechanics : An Introduction to Injury Biomechanics	**Country**	Switzerland
		Rightsholder	Springer Nature BV
Author / Editor	Schmitt, Kai-Uwe, Niederer, Peter F., Cronin, Duane S., Morrison III, Barclay, Muser, Markus H., Walz, Felix	**Publication Type**	Book
Date	03/15/2019		
Language	English		

REQUEST DETAILS

Portion Type	Chart/graph/table/figure	**Distribution**	Worldwide
Number of Charts / Graphs / Tables / Figures Requested	2	**Translation**	Original language of publication
		Copies for the Disabled?	No
Format (select all that apply)	Electronic	**Minor Editing Privileges?**	Yes
Who Will Republish the Content?	Academic institution	**Incidental Promotional Use?**	No
Duration of Use	Life of current and all future editions	**Currency**	CAD
Lifetime Unit Quantity	Up to 999		
Rights Requested	Main product		

NEW WORK DETAILS

Title	Investigation of Brain Response in Canadian Armed Forces Volunteers Subjected to Recoil Force from Firing Long-Range Rifles Using Instrumented Mouthguards and Finite Element Head Model	**Institution Name**	University of Waterloo
		Expected Presentation Date	2024-06-22
Instructor Name	Professor Duane Cronin		

ADDITIONAL DETAILS

The Requesting Person / Organization to Appear on the License	Tanvi Seeburrun/ University of Waterloo

REQUESTED CONTENT DETAILS

Title, Description or Numeric Reference of the Portion(s)	Figure 4.1,4.2	**Title of the Article / Chapter the Portion Is From**	Head Injuries
Editor of Portion(s)	Schmitt, Kai-Uwe; Niederer, Peter F.; Cronin, Duane S.; Morrison III, Barclay; Muser, Markus H.; Walz, Felix	**Author of Portion(s)**	Schmitt, Kai-Uwe; Niederer, Peter F.; Cronin, Duane S.; Morrison III, Barclay; Muser, Markus H.; Walz, Felix
Volume / Edition	5th ed. 2019	**Publication Date of Portion**	2019-03-15
Page or Page Range of Portion	88-89		

Marketplace Permissions General Terms and Conditions

The following terms and conditions ("General Terms"), together with any applicable Publisher Terms and Conditions, govern User's use of Works pursuant to the Licenses granted by Copyright Clearance Center, Inc. ("CCC") on behalf of the applicable Rightsholders of such Works through CCC's applicable Marketplace transactional licensing services (each, a "Service").

1) **Definitions.** For purposes of these General Terms, the following definitions apply:

"License" is the licensed use the User obtains via the Marketplace platform in a particular licensing transaction, as set forth in the Order Confirmation.

"Order Confirmation" is the confirmation CCC provides to the User at the conclusion of each Marketplace transaction. "Order Confirmation Terms" are additional terms set forth on specific Order Confirmations not set forth in the General Terms that can include terms applicable to a particular CCC transactional licensing service and/or any Rightsholder-specific terms.

"Rightsholder(s)" are the holders of copyright rights in the Works for which a User obtains licenses via the Marketplace platform, which are displayed on specific Order Confirmations.

"Terms" means the terms and conditions set forth in these General Terms and any additional Order Confirmation Terms collectively.

"User" or "you" is the person or entity making the use granted under the relevant License. Where the person accepting the Terms on behalf of a User is a freelancer or other third party who the User authorized to accept the General Terms on the User's behalf, such person shall be deemed jointly a User for purposes of such Terms.

"Work(s)" are the copyright protected works described in relevant Order Confirmations.

2) **Description of Service.** CCC's Marketplace enables Users to obtain Licenses to use one or more Works in accordance with all relevant Terms. CCC grants Licenses as an agent on behalf of the copyright rightsholder identified in the relevant Order Confirmation.

3) **Applicability of Terms.** The Terms govern User's use of Works in connection with the relevant License. In the event of any conflict between General Terms and Order Confirmation Terms, the latter shall govern. User acknowledges that Rightsholders have complete discretion whether to grant any permission, and whether to place any limitations on any grant, and that CCC has no right to supersede or to modify any such discretionary act by a Rightsholder.

4) **Representations; Acceptance.** By using the Service, User represents and warrants that User has been duly authorized by the User to accept, and hereby does accept, all Terms.

5) **Scope of License; Limitations and Obligations.** All Works and all rights therein, including copyright rights, remain the sole and exclusive property of the Rightsholder. The License provides only those rights expressly set forth in the terms and conveys no other rights in any Works

6) **General Payment Terms.** User may pay at time of checkout by credit card or choose to be invoiced. If the User chooses to be invoiced, the User shall: (i) remit payments in the manner identified on specific invoices, (ii) unless otherwise specifically stated in an Order Confirmation or separate written agreement, Users shall remit payments upon receipt of the relevant invoice from CCC, either by delivery or notification of availability of the invoice via the Marketplace platform, and (iii) if the User does not pay the invoice within 30 days of receipt, the User may incur a service charge of 1.5% per month or the maximum rate allowed by applicable law, whichever is less. While User may exercise the rights in the License immediately upon receiving the Order Confirmation, the License is automatically revoked and is null and void, as if it had never been issued, if CCC does not receive complete payment on a timely basis.

7) **General Limits on Use.** Unless otherwise provided in the Order Confirmation, any grant of rights to User (i) involves only the rights set forth in the Terms and does not include subsequent or additional uses, (ii) is non-exclusive and non-transferable, and (iii) is subject to any and all limitations and restrictions (such as, but not limited to, limitations on duration of use or circulation) included in the Terms. Upon completion of the licensed use as set forth in the Order Confirmation, User shall either secure a new permission for further use of the Work(s) or immediately cease any new use of the Work(s) and shall render inaccessible (such as by deleting or by removing or severing links or other locators) any further copies of the Work. User may only make alterations to the Work if and as expressly set forth in the Order Confirmation. No Work may be used in any way that is unlawful, including without limitation if such use would violate applicable sanctions laws or regulations, would be defamatory, violate the rights of third parties (including such third parties' rights of copyright, privacy, publicity, or other tangible or intangible property), or is otherwise illegal, sexually explicit, or obscene. In addition, User may not conjoin a Work with any other material that may result in damage to the reputation of the Rightsholder. Any unlawful use will render any licenses hereunder null and void. User agrees to inform CCC if it becomes aware of any infringement of any rights in a Work and to cooperate with any reasonable request of CCC or the Rightsholder in connection therewith.

8) **Third Party Materials.** In the event that the material for which a License is sought includes third party materials (such as photographs, illustrations, graphs, inserts and similar materials) that are identified in such material as having been used by permission (or a similar indicator), User is responsible for identifying, and seeking separate licenses (under this Service, if available, or otherwise) for any of such third party materials; without a separate license, User may not use such third party materials via the License.

9) **Copyright Notice.** Use of proper copyright notice for a Work is required as a condition of any License granted under the Service. Unless otherwise provided in the Order Confirmation, a proper copyright notice will read substantially as follows: "Used with permission of [Rightsholder's name], from [Work's title, author, volume, edition number and year of copyright]; permission conveyed through Copyright Clearance Center, Inc." Such notice must be provided in a reasonably legible font size and must be placed either on a cover page or in another location that any person, upon gaining access to the material which is the subject of a permission, shall see, or in the case of republication Licenses, immediately adjacent to the Work as used (for example, as part of a by-line or footnote) or in the place where substantially all other credits or notices for the new work containing the republished Work are located. Failure to include the required notice results in loss to the Rightsholder and CCC, and the User shall be liable to pay liquidated damages for each such failure equal to twice the use fee specified in the Order Confirmation, in addition to the use fee itself and any other fees and charges specified.

10) **Indemnity.** User hereby indemnifies and agrees to defend the Rightsholder and CCC, and their respective employees and directors, against all claims, liability, damages, costs, and expenses, including legal fees and expenses, arising out of any use of a Work beyond the scope of the rights granted herein and in the Order Confirmation, or any use of a Work which has been altered in any unauthorized way by User, including claims of defamation or infringement of rights of copyright, publicity, privacy, or other tangible or intangible property.

11) **Limitation of Liability.** UNDER NO CIRCUMSTANCES WILL CCC OR THE RIGHTSHOLDER BE LIABLE FOR ANY DIRECT, INDIRECT, CONSEQUENTIAL, OR INCIDENTAL DAMAGES (INCLUDING WITHOUT LIMITATION DAMAGES FOR LOSS OF BUSINESS PROFITS OR INFORMATION, OR FOR BUSINESS INTERRUPTION) ARISING OUT OF THE USE OR INABILITY TO USE A WORK, EVEN IF ONE OR BOTH OF THEM HAS BEEN ADVISED OF THE POSSIBILITY OF SUCH DAMAGES. In any event, the total liability of the Rightsholder and CCC (including their respective employees and directors) shall not exceed the total amount actually paid by User for the relevant License. User assumes full liability for the actions and omissions of its principals, employees, agents, affiliates, successors, and assigns.

12) **Limited Warranties.** THE WORK(S) AND RIGHT(S) ARE PROVIDED "AS IS." CCC HAS THE RIGHT TO GRANT TO USER THE RIGHTS GRANTED IN THE ORDER CONFIRMATION DOCUMENT. CCC AND THE RIGHTSHOLDER DISCLAIM ALL OTHER WARRANTIES RELATING TO THE WORK(S) AND RIGHT(S), EITHER EXPRESS OR IMPLIED, INCLUDING WITHOUT LIMITATION IMPLIED WARRANTIES OF MERCHANTABILITY OR FITNESS FOR A PARTICULAR PURPOSE. ADDITIONAL RIGHTS MAY BE REQUIRED TO USE ILLUSTRATIONS, GRAPHS, PHOTOGRAPHS, ABSTRACTS, INSERTS, OR OTHER PORTIONS OF THE WORK (AS OPPOSED TO THE ENTIRE WORK) IN A MANNER CONTEMPLATED BY USER; USER UNDERSTANDS AND AGREES THAT NEITHER CCC NOR THE RIGHTSHOLDER MAY HAVE SUCH ADDITIONAL RIGHTS TO GRANT.

13) **Effect of Breach.** Any failure by User to pay any amount when due, or any use by User of a Work beyond the scope of the License set forth in the Order Confirmation and/or the Terms, shall be a material breach of such License. Any breach not cured within 10 days of written notice thereof shall result in immediate termination of such License without further notice. Any unauthorized (but licensable) use of a Work that is terminated immediately upon notice thereof may be liquidated by payment of the Rightsholder's ordinary license price therefor; any unauthorized (and unlicensable) use that is not terminated immediately for any reason (including, for example, because materials containing the Work cannot reasonably be recalled) will be subject to all remedies available at law or in equity, but in no event to a payment of less than three times the Rightsholder's ordinary license price for the most closely analogous licensable use plus Rightsholder's and/or CCC's costs and expenses incurred in collecting such payment.

14) **Additional Terms for Specific Products and Services.** If a User is making one of the uses described in this Section 14, the additional terms and conditions apply:

a) ***Print Uses of Academic Course Content and Materials (photocopies for academic coursepacks or classroom handouts).*** For photocopies for academic coursepacks or classroom handouts the following additional terms apply:

i) The copies and anthologies created under this License may be made and assembled by faculty members individually or at their request by on-campus bookstores or copy centers, or by off-campus copy shops and other similar entities.

ii) No License granted shall in any way: (i) include any right by User to create a substantively non-identical copy of the Work or to edit or in any other way modify the Work (except by means of deleting material immediately preceding or following the entire portion of the Work copied) (ii) permit "publishing ventures" where any particular anthology would be systematically marketed at multiple institutions.

iii) Subject to any Publisher Terms (and notwithstanding any apparent contradiction in the Order Confirmation arising from data provided by User), any use authorized under the academic pay-per-use service is limited as follows:

A) any License granted shall apply to only one class (bearing a unique identifier as assigned by the institution, and thereby including all sections or other subparts of the class) at one institution;

B) use is limited to not more than 25% of the text of a book or of the items in a published collection of essays, poems or articles;

C) use is limited to no more than the greater of (a) 25% of the text of an issue of a journal or other periodical or (b) two articles from such an issue;

D) no User may sell or distribute any particular anthology, whether photocopied or electronic, at more than one institution of learning;

E) in the case of a photocopy permission, no materials may be entered into electronic memory by User except in order to produce an identical copy of a Work before or during the academic term (or analogous period) as to which any particular permission is granted. In the event that User shall choose to retain materials that are the subject of a photocopy permission in electronic memory for purposes of producing identical copies more than one day after such retention (but still within the scope of any permission granted), User must notify CCC of such fact in the applicable permission request and such retention shall constitute one copy actually sold for purposes of calculating permission fees due; and

F) any permission granted shall expire at the end of the class. No permission granted shall in any way include any right by User to create a substantively non-identical copy of the Work or to edit or in any other way modify the Work (except by means of deleting material immediately preceding or following the entire portion of the Work copied).

iv) Books and Records; Right to Audit. As to each permission granted under the academic pay-per-use Service, User shall maintain for at least four full calendar years books and records sufficient for CCC to determine the numbers of copies made by User under such permission. CCC and any representatives it may designate shall have the right to audit such books and records at any time during User's ordinary business hours, upon two days' prior notice. If any such audit shall determine that User shall have underpaid for, or underreported, any photocopies sold or by three percent (3%) or more, then User shall bear all the costs of any such audit; otherwise, CCC shall bear the costs of any such audit. Any amount determined by such audit to have been underpaid by User shall immediately be paid to CCC by User, together with interest thereon at the rate of 10% per annum from the date such amount was originally due. The provisions of this paragraph shall survive the termination of this License for any reason.

b) ***Digital Pay-Per-Uses of Academic Course Content and Materials (e-coursepacks, electronic reserves, learning management systems, academic institution intranets).*** For uses in e-coursepacks, posts in electronic reserves, posts in learning management systems, or posts on academic institution intranets, the following additional terms apply:

i) The pay-per-uses subject to this Section 14(b) include:

A) **Posting e-reserves, course management systems, e-coursepacks for text-based content,** which grants authorizations to import requested material in electronic format, and allows electronic access to this material to members of a designated college or university class, under the direction of an instructor designated by the college or university, accessible only under appropriate electronic controls (e.g., password);

B) **Posting e-reserves, course management systems, e-coursepacks for material consisting of photographs or other still images not embedded in text,** which grants not only the authorizations described in Section 14(b)(i)(A) above, but also the following authorization: to include the requested material in course materials for use consistent with Section 14(b)(i)(A) above, including any necessary resizing, reformatting or modification of the resolution of such requested material (provided that such modification does not alter the underlying editorial content or meaning of the requested material, and provided that the resulting modified content is used solely within the scope of, and in a manner consistent with, the particular authorization described in the Order Confirmation and the Terms), but not including any other form of manipulation, alteration or editing of the requested material;

C) **Posting e-reserves, course management systems, e-coursepacks or other academic distribution for audiovisual content,** which grants not only the authorizations described in Section 14(b)(i)(A) above, but also the following authorizations: (i) to include the requested material in course materials for use consistent with Section 14(b)(i)(A) above; (ii) to display and perform the requested material to such members of such class in the physical classroom or remotely by means of streaming media or other video formats; and (iii) to "clip" or reformat the requested material for purposes of time or content management or ease of delivery, provided that such "clipping" or reformatting does not alter the underlying editorial content or meaning of the requested material and that the resulting material is used solely within the scope of, and in a manner consistent with, the particular authorization described in the Order Confirmation and the Terms. Unless expressly set forth in the relevant Order Conformation, the License does not authorize any other form of manipulation, alteration or editing of the requested material.

ii) Unless expressly set forth in the relevant Order Confirmation, no License granted shall in any way: (i) include any right by User to create a substantively non-identical copy of the Work or to edit or in any other way modify the Work (except by means of deleting material immediately preceding or following the entire portion of the Work copied or, in the case of Works subject to Sections 14(b)(1)(B) or (C) above, as described in such Sections) (ii) permit "publishing ventures" where any particular course materials would be systematically marketed at multiple institutions.

iii) Subject to any further limitations determined in the Rightsholder Terms (and notwithstanding any apparent contradiction in the Order Confirmation arising from data provided by User), any use authorized under the electronic course content pay-per-use service is limited as follows:

A) any License granted shall apply to only one class (bearing a unique identifier as assigned by the institution, and thereby including all sections or other subparts of the class) at one institution;

B) use is limited to not more than 25% of the text of a book or of the items in a published collection of essays, poems or articles;

C) use is limited to not more than the greater of (a) 25% of the text of an issue of a journal or other periodical or (b) two articles from such an issue;

D) no User may sell or distribute any particular materials, whether photocopied or electronic, at more than one institution of learning;

E) electronic access to material which is the subject of an electronic-use permission must be limited by means of electronic password, student identification or other control permitting access solely to students and instructors in the class;

F) User must ensure (through use of an electronic cover page or other appropriate means) that any person, upon gaining electronic access to the material, which is the subject of a permission, shall see:

- a proper copyright notice, identifying the Rightsholder in whose name CCC has granted permission,
- a statement to the effect that such copy was made pursuant to permission,
- a statement identifying the class to which the material applies and notifying the reader that the material has been made available electronically solely for use in the class, and
- a statement to the effect that the material may not be further distributed to any person outside the class, whether by copying or by transmission and whether electronically or in paper form, and User must also ensure that such cover page or other means will print out in the event that the person accessing the material chooses to print out the material or any part thereof.

G) any permission granted shall expire at the end of the class and, absent some other form of authorization, User is thereupon required to delete the applicable material from any electronic storage or to block electronic access to the applicable material.

iv) Uses of separate portions of a Work, even if they are to be included in the same course material or the same university or college class, require separate permissions under the electronic course content pay-per-use Service. Unless otherwise provided in the Order Confirmation, any grant of rights to User is limited to use completed no later than the end of the academic term (or analogous period) as to which any particular permission is granted.

v) Books and Records; Right to Audit. As to each permission granted under the electronic course content Service, User shall maintain for at least four full calendar years books and records sufficient for CCC to determine the numbers of copies made by User under such permission. CCC and any representatives it may designate shall have the right to audit such books and records at any time during User's ordinary business hours, upon two days' prior notice. If any such audit shall determine that User shall have underpaid for, or underreported, any electronic copies used by three percent (3%) or more, then User shall bear all the costs of any such audit; otherwise, CCC shall bear the costs of any such audit. Any amount determined by such audit to have been underpaid by User shall immediately be paid to CCC by User, together with interest thereon at the rate of 10% per annum from the date such amount was originally due. The provisions of this paragraph shall survive the termination of this license for any reason.

c) ***Pay-Per-Use Permissions for Certain Reproductions (Academic photocopies for library reserves and interlibrary loan reporting) (Non-academic internal/external business uses and commercial document delivery).*** The License expressly excludes the uses listed in Section (c)(i)-(v) below (which must be subject to separate license from the applicable Rightsholder) for: academic photocopies for library reserves and interlibrary loan reporting; and non-academic internal/external business uses and commercial document delivery.

i) electronic storage of any reproduction (whether in plain-text, PDF, or any other format) other than on a transitory basis;

ii) the input of Works or reproductions thereof into any computerized database;

iii) reproduction of an entire Work (cover-to-cover copying) except where the Work is a single article;

iv) reproduction for resale to anyone other than a specific customer of User;

v) republication in any different form. Please obtain authorizations for these uses through other CCC services or directly from the rightsholder.

Any license granted is further limited as set forth in any restrictions included in the Order Confirmation and/or in these Terms.

d) ***Electronic Reproductions in Online Environments (Non-Academic-email, intranet, internet and extranet).*** For "electronic reproductions", which generally includes e-mail use (including instant messaging or other electronic transmission to a defined group of recipients) or posting on an intranet, extranet or Intranet site (including any display or performance incidental thereto), the following additional terms apply:

i) Unless otherwise set forth in the Order Confirmation, the License is limited to use completed within 30 days for any use on the Internet, 60 days for any use on an intranet or extranet and one year for any other use, all as measured from the "republication date" as identified in the Order Confirmation, if any, and otherwise from the date of the Order Confirmation.

ii) User may not make or permit any alterations to the Work, unless expressly set forth in the Order Confirmation (after request by User and approval by Rightsholder); provided, however, that a Work consisting of photographs or other still images not embedded in text may, if necessary, be resized, reformatted or have its resolution modified without additional express permission, and a Work consisting of audiovisual content may, if necessary, be "clipped" or reformatted for purposes of time or content management or ease of delivery (provided that any such resizing, reformatting, resolution modification or "clipping" does not alter the underlying editorial content or meaning of the Work used, and that the resulting material is used solely within the scope of, and in a manner consistent with, the particular License described in the Order Confirmation and the Terms.

15) **Miscellaneous.**

a) User acknowledges that CCC may, from time to time, make changes or additions to the Service or to the Terms, and that Rightsholder may make changes or additions to the Rightsholder Terms. Such updated Terms will replace the prior terms and conditions in the order workflow and shall be effective as to any subsequent Licenses but shall not apply to Licenses already granted and paid for under a prior set of terms.

b) Use of User-related information collected through the Service is governed by CCC's privacy policy, available online at www.copyright.com/about/privacy-policy/.

c) The License is personal to User. Therefore, User may not assign or transfer to any other person (whether a natural person or an organization of any kind) the License or any rights granted thereunder; provided, however, that, where applicable, User may assign such License in its entirety on written notice to CCC in the event of a transfer of all or substantially all of User's rights in any new material which includes the Work(s) licensed under this Service.

d) No amendment or waiver of any Terms is binding unless set forth in writing and signed by the appropriate parties, including, where applicable, the Rightsholder. The Rightsholder and CCC hereby object to any terms contained in any writing prepared by or on behalf of the User or its principals, employees, agents or affiliates and purporting to govern or otherwise relate to the License described in the Order Confirmation, which terms are in any way inconsistent with any Terms set forth in the Order Confirmation, and/or in CCC's standard operating procedures, whether such writing is prepared prior to, simultaneously with or subsequent to the Order Confirmation, and whether such writing appears on a copy of the Order Confirmation or in a separate instrument.

e) The License described in the Order Confirmation shall be governed by and construed under the law of the State of New York, USA, without regard to the principles thereof of conflicts of law. Any case, controversy, suit, action, or proceeding arising out of, in connection with, or related to such License shall be brought, at CCC's sole discretion, in any federal or state court located in the County of New York, State of New York, USA, or in any federal or state court whose geographical jurisdiction covers the location of the Rightsholder set forth in the Order Confirmation. The parties expressly submit to the personal jurisdiction and venue of each such federal or state court.

Last updated October 2022

Marketplace

This is a License Agreement between Tanvi Seeburrun/University of Waterloo ("User") and Copyright Clearance Center, Inc. ("CCC") on behalf of the Rightsholder identified in the order details below. The license consists of the order details, the Marketplace Permissions General Terms and Conditions below, and any Rightsholder Terms and Conditions which are included below.

All payments must be made in full to CCC in accordance with the Marketplace Permissions General Terms and Conditions below.

Order Date	04-Jun-2024	**Type of Use**	Republish in a thesis/dissertation
Order License ID	1491270-1		
ISBN-13	9780128098318	**Publisher**	Elsevier Science
		Portion	Chart/graph/table/figure

LICENSED CONTENT

Publication Title	Basic Finite Element Method as Applied to Injury Biomechanics	**Country**	United States of America
		Rightsholder	Elsevier Science & Technology Journals
Author / Editor	Yang, King-Hay	**Publication Type**	Book
Date	09/20/2017		
Language	English		

REQUEST DETAILS

Portion Type	Chart/graph/table/figure	**Distribution**	Worldwide
Number of Charts / Graphs / Tables / Figures Requested	2	**Translation**	Original language of publication
		Copies for the Disabled?	No
Format (select all that apply)	Electronic	**Minor Editing Privileges?**	No
Who Will Republish the Content?	Academic institution	**Incidental Promotional Use?**	No
Duration of Use	Life of current edition	**Currency**	CAD
Lifetime Unit Quantity	Up to 999		
Rights Requested	Main product		

NEW WORK DETAILS

Title	Investigation of Brain Response in Canadian Armed Forces Volunteers Subjected to Recoil Force from Firing Long-Range Rifles Using Instrumented Mouthguards and Finite Element Head Model	**Institution Name**	University of Waterloo
		Expected Presentation Date	2024-06-22
Instructor Name	Professor Duane Cronin		

ADDITIONAL DETAILS

Order Reference Number	N/A	**The Requesting Person / Organization to Appear on the License**	Tanvi Seeburrun/University of Waterloo

REQUESTED CONTENT DETAILS

Title, Description or Numeric Reference of the Portion(s)	Figure 12.6, 12.13	**Title of the Article / Chapter the Portion Is From**	Modeling the Head for Impact Scenarios
Editor of Portion(s)	Yang, King-Hay	**Author of Portion(s)**	Haojie Mao
Volume / Edition	1	**Issue, if Republishing an Article From a Serial**	N/A
Page or Page Range of Portion	475-480	**Publication Date of Portion**	2017-09-20

RIGHTSHOLDER TERMS AND CONDITIONS

Elsevier publishes Open Access articles in both its Open Access journals and via its Open Access articles option in subscription journals, for which an author selects a user license permitting certain types of reuse without permission. Before proceeding please check if the article is Open Access on http://www.sciencedirect.com and refer to the user license for the individual article. Any reuse not included in the user license terms will require permission. You must always fully and appropriately credit the author and source. If any part of the material to be used (for example, figures) has appeared in the Elsevier publication for which you are seeking permission, with credit or acknowledgement to another source it is the responsibility of the user to ensure their reuse complies with the terms and conditions determined by the rights holder. Please contact permissions@elsevier.com with any queries.

Marketplace Permissions General Terms and Conditions

The following terms and conditions ("General Terms"), together with any applicable Publisher Terms and Conditions, govern User's use of Works pursuant to the Licenses granted by Copyright Clearance Center, Inc. ("CCC") on behalf of the applicable Rightsholders of such Works through CCC's applicable Marketplace transactional licensing services (each, a "Service").

1) **Definitions.** For purposes of these General Terms, the following definitions apply:

"License" is the licensed use the User obtains via the Marketplace platform in a particular licensing transaction, as set forth in the Order Confirmation.

"Order Confirmation" is the confirmation CCC provides to the User at the conclusion of each Marketplace transaction. "Order Confirmation Terms" are additional terms set forth on specific Order Confirmations not set forth in the General Terms that can include terms applicable to a particular CCC transactional licensing service and/or any Rightsholder-specific terms.

"Rightsholder(s)" are the holders of copyright rights in the Works for which a User obtains licenses via the Marketplace platform, which are displayed on specific Order Confirmations.

"Terms" means the terms and conditions set forth in these General Terms and any additional Order Confirmation Terms collectively.

"User" or "you" is the person or entity making the use granted under the relevant License. Where the person accepting the Terms on behalf of a User is a freelancer or other third party who the User authorized to accept the General Terms on the User's behalf, such person shall be deemed jointly a User for purposes of such Terms.

"Work(s)" are the copyright protected works described in relevant Order Confirmations.

2) **Description of Service.** CCC's Marketplace enables Users to obtain Licenses to use one or more Works in accordance with all relevant Terms. CCC grants Licenses as an agent on behalf of the copyright rightsholder identified in the relevant Order Confirmation.

3) **Applicability of Terms.** The Terms govern User's use of Works in connection with the relevant License. In the event of any conflict between General Terms and Order Confirmation Terms, the latter shall govern. User acknowledges that Rightsholders have complete discretion whether to grant any permission, and whether to place any limitations on any grant, and that CCC has no right to supersede or to modify any such discretionary act by a Rightsholder.

4) **Representations; Acceptance.** By using the Service, User represents and warrants that User has been duly authorized by the User to accept, and hereby does accept, all Terms.

5) **Scope of License; Limitations and Obligations.** All Works and all rights therein, including copyright rights, remain the sole and exclusive property of the Rightsholder. The License provides only those rights expressly set forth in the terms and conveys no other rights in any Works

6) **General Payment Terms.** User may pay at time of checkout by credit card or choose to be invoiced. If the User chooses to be invoiced, the User shall: (i) remit payments in the manner identified on specific invoices, (ii) unless otherwise specifically stated in an Order Confirmation or separate written agreement, Users shall remit payments upon receipt of the relevant invoice from CCC, either by delivery or notification of availability of the invoice via the Marketplace platform, and (iii) if the User does not pay the invoice within 30 days of receipt, the User may incur a service charge of 1.5% per month or the maximum rate allowed by applicable law, whichever is less. While User may exercise the rights in the License immediately upon receiving the Order Confirmation, the License is automatically revoked and is null and void, as if it had never been issued, if CCC does not receive complete payment on a timely basis.

7) **General Limits on Use.** Unless otherwise provided in the Order Confirmation, any grant of rights to User (i) involves only the rights set forth in the Terms and does not include subsequent or additional uses, (ii) is non-exclusive and non-transferable, and (iii) is subject to any and all limitations and restrictions (such as, but not limited to, limitations on duration of use or circulation) included in the Terms. Upon completion of the licensed use as set forth in the Order Confirmation, User shall either secure a new permission for further use of the Work(s) or immediately cease any new use of the Work(s) and shall render inaccessible (such as by deleting or by removing or severing links or other locators) any further copies of the Work. User may only make alterations to the Work if and as expressly set forth in the Order Confirmation. No Work may be used in any way that is unlawful, including without limitation if such use would violate applicable sanctions laws or regulations, would be defamatory, violate the rights of third parties (including such third parties' rights of copyright, privacy, publicity, or other tangible or intangible property), or is otherwise illegal, sexually explicit, or obscene. In addition, User may not conjoin a Work with any other material that may result in damage to the reputation of the Rightsholder. Any unlawful use will render any licenses hereunder null and void. User agrees to inform CCC if it becomes aware of any infringement of any rights in a Work and to cooperate with any reasonable request of CCC or the Rightsholder in connection therewith.

8) **Third Party Materials.** In the event that the material for which a License is sought includes third party materials (such as photographs, illustrations, graphs, inserts and similar materials) that are identified in such material as having been used by permission (or a similar indicator), User is responsible for identifying, and seeking separate licenses (under this Service, if available, or otherwise) for any of such third party materials; without a separate license, User may not use such third party materials via the License.

9) **Copyright Notice.** Use of proper copyright notice for a Work is required as a condition of any License granted under the Service. Unless otherwise provided in the Order Confirmation, a proper copyright notice will read substantially as follows: "Used with permission of [Rightsholder's name], from [Work's title, author, volume, edition number and year of copyright]; permission conveyed through Copyright Clearance Center, Inc." Such notice must be provided in a reasonably legible font size and must be placed either on a cover page or in another location that any person, upon gaining access to the material which is the subject of a permission, shall see, or in the case of republication Licenses, immediately adjacent to the Work as used (for example, as part of a by-line or footnote) or in the place where substantially all other credits or notices for the new work containing the republished Work are located. Failure to include the required notice results in loss to the Rightsholder and CCC, and the User shall be liable to pay liquidated damages for each such failure equal to twice the use fee specified in the Order Confirmation, in addition to the use fee itself and any other fees and charges specified.

10) **Indemnity.** User hereby indemnifies and agrees to defend the Rightsholder and CCC, and their respective employees and directors, against all claims, liability, damages, costs, and expenses, including legal fees and expenses, arising out of any use of a Work beyond the scope of the rights granted herein and in the Order Confirmation, or any use of a Work which has been altered in any unauthorized way by User, including claims of defamation or infringement of rights of copyright, publicity, privacy, or other tangible or intangible property.

11) **Limitation of Liability.** UNDER NO CIRCUMSTANCES WILL CCC OR THE RIGHTSHOLDER BE LIABLE FOR ANY DIRECT, INDIRECT, CONSEQUENTIAL, OR INCIDENTAL DAMAGES (INCLUDING WITHOUT LIMITATION DAMAGES FOR LOSS OF BUSINESS PROFITS OR INFORMATION, OR FOR BUSINESS INTERRUPTION) ARISING OUT OF THE USE OR INABILITY TO USE A WORK, EVEN IF ONE OR BOTH OF THEM HAS BEEN ADVISED OF THE POSSIBILITY OF SUCH DAMAGES. In any event, the total liability of the Rightsholder and CCC (including their respective employees and directors) shall not exceed the total amount actually paid by User for the relevant License. User assumes full liability for the actions and omissions of its principals, employees, agents, affiliates, successors, and assigns.

12) **Limited Warranties.** THE WORK(S) AND RIGHT(S) ARE PROVIDED "AS IS." CCC HAS THE RIGHT TO GRANT TO USER THE RIGHTS GRANTED IN THE ORDER CONFIRMATION DOCUMENT. CCC AND THE RIGHTSHOLDER DISCLAIM ALL OTHER WARRANTIES RELATING TO THE WORK(S) AND RIGHT(S), EITHER EXPRESS OR IMPLIED, INCLUDING WITHOUT LIMITATION IMPLIED WARRANTIES OF MERCHANTABILITY OR FITNESS FOR A PARTICULAR PURPOSE. ADDITIONAL RIGHTS MAY BE REQUIRED TO USE ILLUSTRATIONS, GRAPHS, PHOTOGRAPHS, ABSTRACTS, INSERTS, OR OTHER PORTIONS OF THE WORK (AS OPPOSED TO THE ENTIRE WORK) IN A MANNER CONTEMPLATED BY USER; USER UNDERSTANDS AND AGREES THAT NEITHER CCC NOR THE RIGHTSHOLDER MAY HAVE SUCH ADDITIONAL RIGHTS TO GRANT.

13) **Effect of Breach.** Any failure by User to pay any amount when due, or any use by User of a Work beyond the scope of the License set forth in the Order Confirmation and/or the Terms, shall be a material breach of such License. Any breach not cured within 10 days of written notice thereof shall result in immediate termination of such License without further notice. Any unauthorized (but licensable) use of a Work that is terminated immediately upon notice thereof may be liquidated by payment of the Rightsholder's ordinary license price therefor; any unauthorized (and unlicensable) use that is not terminated immediately for any reason (including, for example, because materials containing the Work cannot reasonably be recalled) will be subject to all remedies available at law or in equity, but in no event to a payment of less than three times the Rightsholder's ordinary license price for the most closely analogous licensable use plus Rightsholder's and/or CCC's costs and expenses incurred in collecting such payment.

14) **Additional Terms for Specific Products and Services.** If a User is making one of the uses described in this Section 14, the additional terms and conditions apply:

a) ***Print Uses of Academic Course Content and Materials (photocopies for academic coursepacks or classroom handouts).*** For photocopies for academic coursepacks or classroom handouts the following additional terms apply:

i) The copies and anthologies created under this License may be made and assembled by faculty members individually or at their request by on-campus bookstores or copy centers, or by off-campus copy shops and other similar entities.

ii) No License granted shall in any way: (i) include any right by User to create a substantively non-identical copy of the Work or to edit or in any other way modify the Work (except by means of deleting material immediately preceding or following the entire portion of the Work copied) (ii) permit "publishing ventures" where any particular anthology would be systematically marketed at multiple institutions.

iii) Subject to any Publisher Terms (and notwithstanding any apparent contradiction in the Order Confirmation arising from data provided by User), any use authorized under the academic pay-per-use service is limited as follows:

A) any License granted shall apply to only one class (bearing a unique identifier as assigned by the institution, and thereby including all sections or other subparts of the class) at one institution;

B) use is limited to not more than 25% of the text of a book or of the items in a published collection of essays, poems or articles;

C) use is limited to no more than the greater of (a) 25% of the text of an issue of a journal or other periodical or (b) two articles from such an issue;

D) no User may sell or distribute any particular anthology, whether photocopied or electronic, at more than one institution of learning;

E) in the case of a photocopy permission, no materials may be entered into electronic memory by User except in order to produce an identical copy of a Work before or during the academic term (or analogous period) as to which any particular permission is granted. In the event that User shall choose to retain materials that are the subject of a photocopy permission in electronic memory for purposes of producing identical copies more

than one day after such retention (but still within the scope of any permission granted), User must notify CCC of such fact in the applicable permission request and such retention shall constitute one copy actually sold for purposes of calculating permission fees due; and

F) any permission granted shall expire at the end of the class. No permission granted shall in any way include any right by User to create a substantively non-identical copy of the Work or to edit or in any other way modify the Work (except by means of deleting material immediately preceding or following the entire portion of the Work copied).

iv) Books and Records; Right to Audit. As to each permission granted under the academic pay-per-use Service, User shall maintain for at least four full calendar years books and records sufficient for CCC to determine the numbers of copies made by User under such permission. CCC and any representatives it may designate shall have the right to audit such books and records at any time during User's ordinary business hours, upon two days' prior notice. If any such audit shall determine that User shall have underpaid for, or underreported, any photocopies sold or by three percent (3%) or more, then User shall bear all the costs of any such audit; otherwise, CCC shall bear the costs of any such audit. Any amount determined by such audit to have been underpaid by User shall immediately be paid to CCC by User, together with interest thereon at the rate of 10% per annum from the date such amount was originally due. The provisions of this paragraph shall survive the termination of this License for any reason.

b) ***Digital Pay-Per-Uses of Academic Course Content and Materials (e-coursepacks, electronic reserves, learning management systems, academic institution intranets).*** For uses in e-coursepacks, posts in electronic reserves, posts in learning management systems, or posts on academic institution intranets, the following additional terms apply:

i) The pay-per-uses subject to this Section 14(b) include:

A) **Posting e-reserves, course management systems, e-coursepacks for text-based content,** which grants authorizations to import requested material in electronic format, and allows electronic access to this material to members of a designated college or university class, under the direction of an instructor designated by the college or university, accessible only under appropriate electronic controls (e.g., password);

B) **Posting e-reserves, course management systems, e-coursepacks for material consisting of photographs or other still images not embedded in text,** which grants not only the authorizations described in Section 14(b)(i)(A) above, but also the following authorization: to include the requested material in course materials for use consistent with Section 14(b)(i)(A) above, including any necessary resizing, reformatting or modification of the resolution of such requested material (provided that such modification does not alter the underlying editorial content or meaning of the requested material, and provided that the resulting modified content is used solely within the scope of, and in a manner consistent with, the particular authorization described in the Order Confirmation and the Terms), but not including any other form of manipulation, alteration or editing of the requested material;

C) **Posting e-reserves, course management systems, e-coursepacks or other academic distribution for audiovisual content,** which grants not only the authorizations described in Section 14(b)(i)(A) above, but also the following authorizations: (i) to include the requested material in course materials for use consistent with Section 14(b)(i)(A) above; (ii) to display and perform the requested material to such members of such class in the physical classroom or remotely by means of streaming media or other video formats; and (iii) to "clip" or reformat the requested material for purposes of time or content management or ease of delivery, provided that such "clipping" or reformatting does not alter the underlying editorial content or meaning of the requested material and that the resulting material is used solely within the scope of, and in a manner consistent with, the particular authorization described in the Order Confirmation and the Terms. Unless expressly set forth in the relevant Order Conformation, the License does not authorize any other form of manipulation, alteration or editing of the requested material.

ii) Unless expressly set forth in the relevant Order Confirmation, no License granted shall in any way: (i) include any right by User to create a substantively non-identical copy of the Work or to edit or in any other way modify the Work (except by means of deleting material immediately preceding or following the entire portion of the Work copied or, in the case of Works subject to Sections 14(b)(1)(B) or (C) above, as described in such Sections) (ii) permit "publishing ventures" where any particular course materials would be systematically marketed at multiple institutions.

iii) Subject to any further limitations determined in the Rightsholder Terms (and notwithstanding any apparent contradiction in the Order Confirmation arising from data provided by User), any use authorized under the electronic course content pay-per-use service is limited as follows:

A) any License granted shall apply to only one class (bearing a unique identifier as assigned by the institution, and thereby including all sections or other subparts of the class) at one institution;

B) use is limited to not more than 25% of the text of a book or of the items in a published collection of essays, poems or articles;

C) use is limited to not more than the greater of (a) 25% of the text of an issue of a journal or other periodical or (b) two articles from such an issue;

D) no User may sell or distribute any particular materials, whether photocopied or electronic, at more than one institution of learning;

E) electronic access to material which is the subject of an electronic-use permission must be limited by means of electronic password, student identification or other control permitting access solely to students and instructors in the class;

F) User must ensure (through use of an electronic cover page or other appropriate means) that any person, upon gaining electronic access to the material, which is the subject of a permission, shall see:

- a proper copyright notice, identifying the Rightsholder in whose name CCC has granted permission,
- a statement to the effect that such copy was made pursuant to permission,
- a statement identifying the class to which the material applies and notifying the reader that the material has been made available electronically solely for use in the class, and
- a statement to the effect that the material may not be further distributed to any person outside the class, whether by copying or by transmission and whether electronically or in paper form, and User must also ensure that such cover page or other means will print out in the event that the person accessing the material chooses to print out the material or any part thereof.

G) any permission granted shall expire at the end of the class and, absent some other form of authorization, User is thereupon required to delete the applicable material from any electronic storage or to block electronic access to the applicable material.

iv) Uses of separate portions of a Work, even if they are to be included in the same course material or the same university or college class, require separate permissions under the electronic course content pay-per-use Service. Unless otherwise provided in the Order Confirmation, any grant of rights to User is limited to use completed no later than the end of the academic term (or analogous period) as to which any particular permission is granted.

v) Books and Records; Right to Audit. As to each permission granted under the electronic course content Service, User shall maintain for at least four full calendar years books and records sufficient for CCC to determine the numbers of copies made by User under such permission. CCC and any representatives it may designate shall have the right to audit such books and records at any time during User's ordinary business hours, upon two days' prior notice. If any such audit shall determine that User shall have underpaid for, or underreported, any electronic copies used by three percent (3%) or more, then User shall bear all the costs of any such audit; otherwise, CCC shall bear the costs of any such audit. Any amount determined by such audit to have been underpaid by User shall immediately be paid to CCC by User, together with interest thereon at the rate of 10% per annum from the date such amount was originally due. The provisions of this paragraph shall survive the termination of this license for any reason.

c) ***Pay-Per-Use Permissions for Certain Reproductions (Academic photocopies for library reserves and interlibrary loan reporting) (Non-academic internal/external business uses and commercial document delivery).*** The License expressly excludes the uses listed in Section (c)(i)-(v) below (which must be subject to separate license from the applicable Rightsholder) for: academic photocopies for library reserves and interlibrary loan reporting; and non-academic internal/external business uses and commercial document delivery.

i) electronic storage of any reproduction (whether in plain-text, PDF, or any other format) other than on a transitory basis;

ii) the input of Works or reproductions thereof into any computerized database;

iii) reproduction of an entire Work (cover-to-cover copying) except where the Work is a single article;

iv) reproduction for resale to anyone other than a specific customer of User;

v) republication in any different form. Please obtain authorizations for these uses through other CCC services or directly from the rightsholder.

Any license granted is further limited as set forth in any restrictions included in the Order Confirmation and/or in these Terms.

d) ***Electronic Reproductions in Online Environments (Non-Academic-email, intranet, internet and extranet).*** For "electronic reproductions", which generally includes e-mail use (including instant messaging or other electronic transmission to a defined group of recipients) or posting on an intranet, extranet or Intranet site (including any display or performance incidental thereto), the following additional terms apply:

i) Unless otherwise set forth in the Order Confirmation, the License is limited to use completed within 30 days for any use on the Internet, 60 days for any use on an intranet or extranet and one year for any other use, all as measured from the "republication date" as identified in the Order Confirmation, if any, and otherwise from the date of the Order Confirmation.

ii) User may not make or permit any alterations to the Work, unless expressly set forth in the Order Confirmation (after request by User and approval by Rightsholder); provided, however, that a Work consisting of photographs or other still images not embedded in text may, if necessary, be resized, reformatted or have its resolution modified without additional express permission, and a Work consisting of audiovisual content may, if necessary, be "clipped" or reformatted for purposes of time or content management or ease of delivery (provided that any such resizing, reformatting, resolution modification or "clipping" does not alter the underlying editorial content or meaning of the Work used, and that the resulting material is used solely within the scope of, and in a manner consistent with, the particular License described in the Order Confirmation and the Terms.

15) **Miscellaneous.**

a) User acknowledges that CCC may, from time to time, make changes or additions to the Service or to the Terms, and that Rightsholder may make changes or additions to the Rightsholder Terms. Such updated Terms will replace the prior terms and conditions in the order workflow and shall be effective as to any subsequent Licenses but shall not apply to Licenses already granted and paid for under a prior set of terms.

b) Use of User-related information collected through the Service is governed by CCC's privacy policy, available online at www.copyright.com/about/privacy-policy/.

c) The License is personal to User. Therefore, User may not assign or transfer to any other person (whether a natural person or an organization of any kind) the License or any rights granted thereunder; provided, however, that, where applicable, User may assign such License in its entirety on written notice to CCC in the event of a transfer of all or substantially all of User's rights in any new material which includes the Work(s) licensed under this Service.

d) No amendment or waiver of any Terms is binding unless set forth in writing and signed by the appropriate parties, including, where applicable, the Rightsholder. The Rightsholder and CCC hereby object to any terms contained in any writing prepared by or on behalf of the User or its principals, employees, agents or affiliates and purporting to govern or otherwise relate to the License described in the Order Confirmation, which terms are in any way inconsistent with any Terms set forth in the Order Confirmation, and/or in CCC's standard operating procedures, whether such writing is prepared prior to, simultaneously with or subsequent to the Order Confirmation, and whether such writing appears on a copy of the Order Confirmation or in a separate instrument.

e) The License described in the Order Confirmation shall be governed by and construed under the law of the State of New York, USA, without regard to the principles thereof of conflicts of law. Any case, controversy, suit, action, or proceeding arising out of, in connection with, or related to such License shall be brought, at CCC's sole discretion, in any federal or state court located in the County of New York, State of New York, USA, or in any federal or state court

whose geographical jurisdiction covers the location of the Rightsholder set forth in the Order Confirmation. The parties expressly submit to the personal jurisdiction and venue of each such federal or state court.

Last updated October 2022

Marketplace

This is a License Agreement between Tanvi Seeburrun/University of Waterloo ("User") and Copyright Clearance Center, Inc. ("CCC") on behalf of the Rightsholder identified in the order details below. The license consists of the order details, the Marketplace Permissions General Terms and Conditions below, and any Rightsholder Terms and Conditions which are included below.

All payments must be made in full to CCC in accordance with the Marketplace Permissions General Terms and Conditions below.

Order Date	07-Jun-2024	Type of Use	Republish in a thesis/dissertation
Order License ID	1492555-1		
ISSN	0090-6964	Publisher	SPRINGER NEW YORK LLC
		Portion	Chart/graph/table/figure

LICENSED CONTENT

Publication Title	Annals of biomedical engineering	Rightsholder	Springer Nature BV
Article Title	Validation and Comparison of Instrumented Mouthguards for Measuring Head Kinematics and Assessing Brain Deformation in Football Impacts.	Publication Type	Journal
		Start Page	2580
		End Page	2598
		Issue	11
		Volume	48
Author / Editor	BIOMEDICAL ENGINEERING SOCIETY.		
Date	01/01/1972		
Language	English		
Country	United States of America		

REQUEST DETAILS

Portion Type	Chart/graph/table/figure	Distribution	Worldwide
Number of Charts / Graphs / Tables / Figures Requested	1	Translation	Original language of publication
		Copies for the Disabled?	No
Format (select all that apply)	Electronic	Minor Editing Privileges?	Yes
Who Will Republish the Content?	Academic institution	Incidental Promotional Use?	No
Duration of Use	Life of current and all future editions	Currency	CAD
Lifetime Unit Quantity	Up to 499		
Rights Requested	Main product and any product related to main product		

NEW WORK DETAILS

Title	Investigation of Brain Response in Canadian Armed Forces Volunteers Subjected to Recoil Force from Firing Long-Range Rifles Using Instrumented Mouthguards and Finite Element Head Model	**Institution Name**	University of Waterloo
		Expected Presentation Date	2024-06-07
Instructor Name	Professor Duane Cronin		

ADDITIONAL DETAILS

The Requesting Person / Organization to Appear on the License	Tanvi Seeburrun/University of Waterloo

REQUESTED CONTENT DETAILS

Title, Description or Numeric Reference of the Portion(s)	Figure 2	**Title of the Article / Chapter the Portion Is From**	Validation and Comparison of Instrumented Mouthguards for Measuring Head Kinematics and Assessing Brain Deformation in Football Impacts.
Editor of Portion(s)	Liu, Yuzhe; Domel, August G.; Yousefsani, Seyed Abdolmajid; Kondic, Jovana; Grant, Gerald; Zeineh, Michael; Camarillo, David B.	**Author of Portion(s)**	Liu, Yuzhe; Domel, August G.; Yousefsani, Seyed Abdolmajid; Kondic, Jovana; Grant, Gerald; Zeineh, Michael; Camarillo, David B.
Volume / Edition	48		
Page or Page Range of Portion	2580-2598	**Publication Date of Portion**	2020-11-01

Marketplace Permissions General Terms and Conditions

The following terms and conditions ("General Terms"), together with any applicable Publisher Terms and Conditions, govern User's use of Works pursuant to the Licenses granted by Copyright Clearance Center, Inc. ("CCC") on behalf of the applicable Rightsholders of such Works through CCC's applicable Marketplace transactional licensing services (each, a "Service").

1) **Definitions.** For purposes of these General Terms, the following definitions apply:

"License" is the licensed use the User obtains via the Marketplace platform in a particular licensing transaction, as set forth in the Order Confirmation.

"Order Confirmation" is the confirmation CCC provides to the User at the conclusion of each Marketplace transaction. "Order Confirmation Terms" are additional terms set forth on specific Order Confirmations not set forth in the General Terms that can include terms applicable to a particular CCC transactional licensing service and/or any Rightsholder-specific terms.

"Rightsholder(s)" are the holders of copyright rights in the Works for which a User obtains licenses via the Marketplace platform, which are displayed on specific Order Confirmations.

"Terms" means the terms and conditions set forth in these General Terms and any additional Order Confirmation Terms collectively.

"User" or "you" is the person or entity making the use granted under the relevant License. Where the person accepting the Terms on behalf of a User is a freelancer or other third party who the User authorized to accept the General Terms on the User's behalf, such person shall be deemed jointly a User for purposes of such Terms.

"Work(s)" are the copyright protected works described in relevant Order Confirmations.

2) **Description of Service.** CCC's Marketplace enables Users to obtain Licenses to use one or more Works in accordance with all relevant Terms. CCC grants Licenses as an agent on behalf of the copyright rightsholder identified in the relevant Order Confirmation.

3) **Applicability of Terms.** The Terms govern User's use of Works in connection with the relevant License. In the event of any conflict between General Terms and Order Confirmation Terms, the latter shall govern. User acknowledges that Rightsholders have complete discretion whether to grant any permission, and whether to place any limitations on any grant, and that CCC has no right to supersede or to modify any such discretionary act by a Rightsholder.

4) **Representations; Acceptance.** By using the Service, User represents and warrants that User has been duly authorized by the User to accept, and hereby does accept, all Terms.

5) **Scope of License; Limitations and Obligations.** All Works and all rights therein, including copyright rights, remain the sole and exclusive property of the Rightsholder. The License provides only those rights expressly set forth in the terms and conveys no other rights in any Works

6) **General Payment Terms.** User may pay at time of checkout by credit card or choose to be invoiced. If the User chooses to be invoiced, the User shall: (i) remit payments in the manner identified on specific invoices, (ii) unless otherwise specifically stated in an Order Confirmation or separate written agreement, Users shall remit payments upon receipt of the relevant invoice from CCC, either by delivery or notification of availability of the invoice via the Marketplace platform, and (iii) if the User does not pay the invoice within 30 days of receipt, the User may incur a service charge of 1.5% per month or the maximum rate allowed by applicable law, whichever is less. While User may exercise the rights in the License immediately upon receiving the Order Confirmation, the License is automatically revoked and is null and void, as if it had never been issued, if CCC does not receive complete payment on a timely basis.

7) **General Limits on Use.** Unless otherwise provided in the Order Confirmation, any grant of rights to User (i) involves only the rights set forth in the Terms and does not include subsequent or additional uses, (ii) is non-exclusive and non-transferable, and (iii) is subject to any and all limitations and restrictions (such as, but not limited to, limitations on duration of use or circulation) included in the Terms. Upon completion of the licensed use as set forth in the Order Confirmation, User shall either secure a new permission for further use of the Work(s) or immediately cease any new use of the Work(s) and shall render inaccessible (such as by deleting or by removing or severing links or other locators) any further copies of the Work. User may only make alterations to the Work if and as expressly set forth in the Order Confirmation. No Work may be used in any way that is unlawful, including without limitation if such use would violate applicable sanctions laws or regulations, would be defamatory, violate the rights of third parties (including such third parties' rights of copyright, privacy, publicity, or other tangible or intangible property), or is otherwise illegal, sexually explicit, or obscene. In addition, User may not conjoin a Work with any other material that may result in damage to the reputation of the Rightsholder. Any unlawful use will render any licenses hereunder null and void. User agrees to inform CCC if it becomes aware of any infringement of any rights in a Work and to cooperate with any reasonable request of CCC or the Rightsholder in connection therewith.

8) **Third Party Materials.** In the event that the material for which a License is sought includes third party materials (such as photographs, illustrations, graphs, inserts and similar materials) that are identified in such material as having been used by permission (or a similar indicator), User is responsible for identifying, and seeking separate licenses (under this Service, if available, or otherwise) for any of such third party materials; without a separate license, User may not use such third party materials via the License.

9) **Copyright Notice.** Use of proper copyright notice for a Work is required as a condition of any License granted under the Service. Unless otherwise provided in the Order Confirmation, a proper copyright notice will read substantially as follows: "Used with permission of [Rightsholder's name], from [Work's title, author, volume, edition number and year of copyright]; permission conveyed through Copyright Clearance Center, Inc." Such notice must be provided in a reasonably legible font size and must be placed either on a cover page or in another location that any person, upon gaining access to the material which is the subject of a permission, shall see, or in the case of republication Licenses, immediately adjacent to the Work as used (for example, as part of a by-line or footnote) or in the place where substantially all other credits or notices for the new work containing the republished Work are located. Failure to include the required notice results in

loss to the Rightsholder and CCC, and the User shall be liable to pay liquidated damages for each such failure equal to twice the use fee specified in the Order Confirmation, in addition to the use fee itself and any other fees and charges specified.

10) **Indemnity.** User hereby indemnifies and agrees to defend the Rightsholder and CCC, and their respective employees and directors, against all claims, liability, damages, costs, and expenses, including legal fees and expenses, arising out of any use of a Work beyond the scope of the rights granted herein and in the Order Confirmation, or any use of a Work which has been altered in any unauthorized way by User, including claims of defamation or infringement of rights of copyright, publicity, privacy, or other tangible or intangible property.

11) **Limitation of Liability.** UNDER NO CIRCUMSTANCES WILL CCC OR THE RIGHTSHOLDER BE LIABLE FOR ANY DIRECT, INDIRECT, CONSEQUENTIAL, OR INCIDENTAL DAMAGES (INCLUDING WITHOUT LIMITATION DAMAGES FOR LOSS OF BUSINESS PROFITS OR INFORMATION, OR FOR BUSINESS INTERRUPTION) ARISING OUT OF THE USE OR INABILITY TO USE A WORK, EVEN IF ONE OR BOTH OF THEM HAS BEEN ADVISED OF THE POSSIBILITY OF SUCH DAMAGES. In any event, the total liability of the Rightsholder and CCC (including their respective employees and directors) shall not exceed the total amount actually paid by User for the relevant License. User assumes full liability for the actions and omissions of its principals, employees, agents, affiliates, successors, and assigns.

12) **Limited Warranties.** THE WORK(S) AND RIGHT(S) ARE PROVIDED "AS IS." CCC HAS THE RIGHT TO GRANT TO USER THE RIGHTS GRANTED IN THE ORDER CONFIRMATION DOCUMENT. CCC AND THE RIGHTSHOLDER DISCLAIM ALL OTHER WARRANTIES RELATING TO THE WORK(S) AND RIGHT(S), EITHER EXPRESS OR IMPLIED, INCLUDING WITHOUT LIMITATION IMPLIED WARRANTIES OF MERCHANTABILITY OR FITNESS FOR A PARTICULAR PURPOSE. ADDITIONAL RIGHTS MAY BE REQUIRED TO USE ILLUSTRATIONS, GRAPHS, PHOTOGRAPHS, ABSTRACTS, INSERTS, OR OTHER PORTIONS OF THE WORK (AS OPPOSED TO THE ENTIRE WORK) IN A MANNER CONTEMPLATED BY USER; USER UNDERSTANDS AND AGREES THAT NEITHER CCC NOR THE RIGHTSHOLDER MAY HAVE SUCH ADDITIONAL RIGHTS TO GRANT.

13) **Effect of Breach.** Any failure by User to pay any amount when due, or any use by User of a Work beyond the scope of the License set forth in the Order Confirmation and/or the Terms, shall be a material breach of such License. Any breach not cured within 10 days of written notice thereof shall result in immediate termination of such License without further notice. Any unauthorized (but licensable) use of a Work that is terminated immediately upon notice thereof may be liquidated by payment of the Rightsholder's ordinary license price therefor; any unauthorized (and unlicensable) use that is not terminated immediately for any reason (including, for example, because materials containing the Work cannot reasonably be recalled) will be subject to all remedies available at law or in equity, but in no event to a payment of less than three times the Rightsholder's ordinary license price for the most closely analogous licensable use plus Rightsholder's and/or CCC's costs and expenses incurred in collecting such payment.

14) **Additional Terms for Specific Products and Services.** If a User is making one of the uses described in this Section 14, the additional terms and conditions apply:

a) ***Print Uses of Academic Course Content and Materials (photocopies for academic coursepacks or classroom handouts).*** For photocopies for academic coursepacks or classroom handouts the following additional terms apply:

i) The copies and anthologies created under this License may be made and assembled by faculty members individually or at their request by on-campus bookstores or copy centers, or by off-campus copy shops and other similar entities.

ii) No License granted shall in any way: (i) include any right by User to create a substantively non-identical copy of the Work or to edit or in any other way modify the Work (except by means of deleting material immediately preceding or following the entire portion of the Work copied) (ii) permit "publishing ventures" where any particular anthology would be systematically marketed at multiple institutions.

iii) Subject to any Publisher Terms (and notwithstanding any apparent contradiction in the Order Confirmation arising from data provided by User), any use authorized under the academic pay-per-use service is limited as follows:

A) any License granted shall apply to only one class (bearing a unique identifier as assigned by the institution, and thereby including all sections or other subparts of the class) at one institution;

B) use is limited to not more than 25% of the text of a book or of the items in a published collection of essays, poems or articles;

C) use is limited to no more than the greater of (a) 25% of the text of an issue of a journal or other periodical or (b) two articles from such an issue;

D) no User may sell or distribute any particular anthology, whether photocopied or electronic, at more than one institution of learning;

E) in the case of a photocopy permission, no materials may be entered into electronic memory by User except in order to produce an identical copy of a Work before or during the academic term (or analogous period) as to which any particular permission is granted. In the event that User shall choose to retain materials that are the subject of a photocopy permission in electronic memory for purposes of producing identical copies more than one day after such retention (but still within the scope of any permission granted), User must notify CCC of such fact in the applicable permission request and such retention shall constitute one copy actually sold for purposes of calculating permission fees due; and

F) any permission granted shall expire at the end of the class. No permission granted shall in any way include any right by User to create a substantively non-identical copy of the Work or to edit or in any other way modify the Work (except by means of deleting material immediately preceding or following the entire portion of the Work copied).

iv) Books and Records; Right to Audit. As to each permission granted under the academic pay-per-use Service, User shall maintain for at least four full calendar years books and records sufficient for CCC to determine the numbers of copies made by User under such permission. CCC and any representatives it may designate shall have the right to audit such books and records at any time during User's ordinary business hours, upon two days' prior notice. If any such audit shall determine that User shall have underpaid for, or underreported, any photocopies sold or by three percent (3%) or more, then User shall bear all the costs of any such audit; otherwise, CCC shall bear the costs of any such audit. Any amount determined by such audit to have been underpaid by User shall immediately be paid to CCC by User, together with interest thereon at the rate of 10% per annum from the date such amount was originally due. The provisions of this paragraph shall survive the termination of this License for any reason.

b) ***Digital Pay-Per-Uses of Academic Course Content and Materials (e-coursepacks, electronic reserves, learning management systems, academic institution intranets).*** For uses in e-coursepacks, posts in electronic reserves, posts in learning management systems, or posts on academic institution intranets, the following additional terms apply:

i) The pay-per-uses subject to this Section 14(b) include:

A) **Posting e-reserves, course management systems, e-coursepacks for text-based content,** which grants authorizations to import requested material in electronic format, and allows electronic access to this material to members of a designated college or university class, under the direction of an instructor designated by the college or university, accessible only under appropriate electronic controls (e.g., password);

B) **Posting e-reserves, course management systems, e-coursepacks for material consisting of photographs or other still images not embedded in text,** which grants not only the authorizations described in Section 14(b)(i)(A) above, but also the following authorization: to include the requested material in course materials for use consistent with Section 14(b)(i)(A) above, including any necessary resizing, reformatting or modification of the resolution of such requested material (provided that such modification does not alter the underlying editorial content or meaning of the requested material, and provided that the resulting modified content is used solely within the scope of, and in a manner consistent with, the particular authorization described in the Order Confirmation and the Terms), but not including any other form of manipulation, alteration or editing of the requested material;

C) **Posting e-reserves, course management systems, e-coursepacks or other academic distribution for audiovisual content,** which grants not only the authorizations described in Section 14(b)(i)(A) above, but also the following authorizations: (i) to include the requested material in course materials for use consistent with Section 14(b)(i)(A) above; (ii) to display and perform the requested material to such members of such class in the physical classroom or remotely by means of streaming media or other video formats; and (iii) to "clip" or reformat the requested material for purposes of time or content management or ease of delivery, provided that such "clipping" or reformatting does not alter the underlying editorial content or meaning of the requested material and that the resulting material is used solely within the scope of, and in a manner consistent with, the particular authorization described in the Order Confirmation and the Terms. Unless

expressly set forth in the relevant Order Conformation, the License does not authorize any other form of manipulation, alteration or editing of the requested material.

ii) Unless expressly set forth in the relevant Order Confirmation, no License granted shall in any way: (i) include any right by User to create a substantively non-identical copy of the Work or to edit or in any other way modify the Work (except by means of deleting material immediately preceding or following the entire portion of the Work copied or, in the case of Works subject to Sections 14(b)(1)(B) or (C) above, as described in such Sections) (ii) permit "publishing ventures" where any particular course materials would be systematically marketed at multiple institutions.

iii) Subject to any further limitations determined in the Rightsholder Terms (and notwithstanding any apparent contradiction in the Order Confirmation arising from data provided by User), any use authorized under the electronic course content pay-per-use service is limited as follows:

A) any License granted shall apply to only one class (bearing a unique identifier as assigned by the institution, and thereby including all sections or other subparts of the class) at one institution;

B) use is limited to not more than 25% of the text of a book or of the items in a published collection of essays, poems or articles;

C) use is limited to not more than the greater of (a) 25% of the text of an issue of a journal or other periodical or (b) two articles from such an issue;

D) no User may sell or distribute any particular materials, whether photocopied or electronic, at more than one institution of learning;

E) electronic access to material which is the subject of an electronic-use permission must be limited by means of electronic password, student identification or other control permitting access solely to students and instructors in the class;

F) User must ensure (through use of an electronic cover page or other appropriate means) that any person, upon gaining electronic access to the material, which is the subject of a permission, shall see:

- a proper copyright notice, identifying the Rightsholder in whose name CCC has granted permission,
- a statement to the effect that such copy was made pursuant to permission,
- a statement identifying the class to which the material applies and notifying the reader that the material has been made available electronically solely for use in the class, and
- a statement to the effect that the material may not be further distributed to any person outside the class, whether by copying or by transmission and whether electronically or in paper form, and User must also ensure that such cover page or other means will print out in the event that the person accessing the material chooses to print out the material or any part thereof.

G) any permission granted shall expire at the end of the class and, absent some other form of authorization, User is thereupon required to delete the applicable material from any electronic storage or to block electronic access to the applicable material.

iv) Uses of separate portions of a Work, even if they are to be included in the same course material or the same university or college class, require separate permissions under the electronic course content pay-per-use Service. Unless otherwise provided in the Order Confirmation, any grant of rights to User is limited to use completed no later than the end of the academic term (or analogous period) as to which any particular permission is granted.

v) Books and Records; Right to Audit. As to each permission granted under the electronic course content Service, User shall maintain for at least four full calendar years books and records sufficient for CCC to determine the numbers of copies made by User under such permission. CCC and any representatives it may designate shall have the right to audit such books and records at any time during User's ordinary business hours, upon two days' prior notice. If any such audit shall determine that User shall have underpaid for, or underreported, any electronic copies used by three percent (3%) or more, then User shall bear all the costs of any such audit; otherwise, CCC shall bear the costs of any such audit. Any amount determined by such audit to have been underpaid by User

shall immediately be paid to CCC by User, together with interest thereon at the rate of 10% per annum from the date such amount was originally due. The provisions of this paragraph shall survive the termination of this license for any reason.

c) ***Pay-Per-Use Permissions for Certain Reproductions (Academic photocopies for library reserves and interlibrary loan reporting) (Non-academic internal/external business uses and commercial document delivery).*** The License expressly excludes the uses listed in Section (c)(i)-(v) below (which must be subject to separate license from the applicable Rightsholder) for: academic photocopies for library reserves and interlibrary loan reporting; and non-academic internal/external business uses and commercial document delivery.

i) electronic storage of any reproduction (whether in plain-text, PDF, or any other format) other than on a transitory basis;

ii) the input of Works or reproductions thereof into any computerized database;

iii) reproduction of an entire Work (cover-to-cover copying) except where the Work is a single article;

iv) reproduction for resale to anyone other than a specific customer of User;

v) republication in any different form. Please obtain authorizations for these uses through other CCC services or directly from the rightsholder.

Any license granted is further limited as set forth in any restrictions included in the Order Confirmation and/or in these Terms.

d) ***Electronic Reproductions in Online Environments (Non-Academic-email, intranet, internet and extranet).*** For "electronic reproductions", which generally includes e-mail use (including instant messaging or other electronic transmission to a defined group of recipients) or posting on an intranet, extranet or Intranet site (including any display or performance incidental thereto), the following additional terms apply:

i) Unless otherwise set forth in the Order Confirmation, the License is limited to use completed within 30 days for any use on the Internet, 60 days for any use on an intranet or extranet and one year for any other use, all as measured from the "republication date" as identified in the Order Confirmation, if any, and otherwise from the date of the Order Confirmation.

ii) User may not make or permit any alterations to the Work, unless expressly set forth in the Order Confirmation (after request by User and approval by Rightsholder); provided, however, that a Work consisting of photographs or other still images not embedded in text may, if necessary, be resized, reformatted or have its resolution modified without additional express permission, and a Work consisting of audiovisual content may, if necessary, be "clipped" or reformatted for purposes of time or content management or ease of delivery (provided that any such resizing, reformatting, resolution modification or "clipping" does not alter the underlying editorial content or meaning of the Work used, and that the resulting material is used solely within the scope of, and in a manner consistent with, the particular License described in the Order Confirmation and the Terms.

15) **Miscellaneous.**

a) User acknowledges that CCC may, from time to time, make changes or additions to the Service or to the Terms, and that Rightsholder may make changes or additions to the Rightsholder Terms. Such updated Terms will replace the prior terms and conditions in the order workflow and shall be effective as to any subsequent Licenses but shall not apply to Licenses already granted and paid for under a prior set of terms.

b) Use of User-related information collected through the Service is governed by CCC's privacy policy, available online at www.copyright.com/about/privacy-policy/.

c) The License is personal to User. Therefore, User may not assign or transfer to any other person (whether a natural person or an organization of any kind) the License or any rights granted thereunder; provided, however, that, where applicable, User may assign such License in its entirety on written notice to CCC in the event of a transfer of all or substantially all of User's rights in any new material which includes the Work(s) licensed under this Service.

d) No amendment or waiver of any Terms is binding unless set forth in writing and signed by the appropriate parties, including, where applicable, the Rightsholder. The Rightsholder and CCC hereby object to any terms contained in any writing prepared by or on behalf of the User or its principals, employees, agents or affiliates and purporting to govern

or otherwise relate to the License described in the Order Confirmation, which terms are in any way inconsistent with any Terms set forth in the Order Confirmation, and/or in CCC's standard operating procedures, whether such writing is prepared prior to, simultaneously with or subsequent to the Order Confirmation, and whether such writing appears on a copy of the Order Confirmation or in a separate instrument.

e) The License described in the Order Confirmation shall be governed by and construed under the law of the State of New York, USA, without regard to the principles thereof of conflicts of law. Any case, controversy, suit, action, or proceeding arising out of, in connection with, or related to such License shall be brought, at CCC's sole discretion, in any federal or state court located in the County of New York, State of New York, USA, or in any federal or state court whose geographical jurisdiction covers the location of the Rightsholder set forth in the Order Confirmation. The parties expressly submit to the personal jurisdiction and venue of each such federal or state court.

Last updated October 2022

References

[1] CDC, “Facts About TBI,” Traumatic Brain Injury & Concussion, May 07, 2024. https://www.cdc.gov/traumatic-brain-injury/data-research/facts-stats/?CDC_AAref_Val=https://www.cdc.gov/traumaticbraininjury/get_the_facts.html

[2] National Institute of Neurological Disorders and Stroke, “Traumatic brain injury (TBI),” *www.ninds.nih.gov*, 2023. https://www.ninds.nih.gov/health-information/disorders/traumatic-brain-injury-tbi

[3] Johns Hopkins Medicine, “Traumatic Brain Injury,” *John Hopkins Medicine*, 2019. https://www.hopkinsmedicine.org/health/conditions-and-diseases/traumatic-brain-injury

[4] Y. Naumenko, I. Yuryshinetz, Y. Zabenko, and T. Pivneva, “Mild traumatic brain injury as a pathological process,” *Heliyon*, vol. 9, no. 7, p. e18342, Jul. 2023, doi: 10.1016/j.heliyon.2023.e18342.

[5] L. Langer, C. Levy, and M. Bayley, “Increasing Incidence of Concussion: True Epidemic or Better Recognition?,” *Journal of Head Trauma Rehabilitation*, vol. 35, no. 1, pp. E60–E66, Jan. 2020, doi: 10.1097/HTR.0000000000000503.

[6] N. D. Silverberg, G. L. Iverson; ACRM Brain Injury Special Interest Group Mild TBI Task Force members:; A. Cogan, K. Dams-O-Connor, R. Delmonico, M. J. P. Graf, M.A. Laccarino, M. Kajankova, J. Kamins, K. L. McCulloch, G. McKinney, D. Nagele, W. J. Panenka, A.R. Rabinowitz, N. Reed, J. V. Wethe, V. Whitehair; ACRM Mild TBI Diagnostic Criteria Expert Consensus Group:; V. Anderson, D. B. Arciniegas, M. T. Bayley, J. J. Bazarian, K. R. Bell, S. P. Broglio, D. Cifu, G. A. Davis, J. Dvorak, R. J. Echemendia, G. A. Gioia, C. C. Giza, S. R. Hinds 2nd, D. I. Katz, B. G. Kurowski, J. J. Leddy, N. L. Sage, A. Lumba-Brown, A.I. Maas, G.T. Manley, M. McCrea, D. K. Menon, J. Ponsford, M. Putukian, S. J. Suskauer, J. van der Naalt, W. C. Walker, K. O. Yeates, R. Zafonte, N. D. Zasler, and R. Zemek, “The American Congress of Rehabilitation Medicine Diagnostic Criteria for Mild Traumatic Brain Injury,” *Archives of Physical Medicine and Rehabilitation*, vol. 104, no. 8, pp. 1343–1355, Aug. 2023, doi: 10.1016/j.apmr.2023.03.036.

[7] G. Teasdale and B. Jennett, “Assessment of coma and impaired consciousness,” *The Lancet*, vol. 304, no. 7872, pp. 81–84, Jul. 1974, doi: 10.1016/S0140-6736(74)91639-0.

[8] P. Dixit and G. R. Liu, “A Review on Recent Development of Finite Element Models for Head Injury Simulations,” *Archives of Computational Methods in Engineering*, vol. 24, no. 4, pp. 979–1031, Nov. 2017, doi: 10.1007/s11831-016-9196-x.

[9] W. R. Russell and A. Smith, “Post-Traumatic Amnesia in Closed Head Injury,” *Archives of Neurology*, vol. 5, no. 1, pp. 4–17, Jul. 1961, doi: 10.1001/archneur.1961.00450130006002.

[10] R. J. Echemendia, W. Meeuwisse, P. McCrory,G. A. Davis, M. Putukian, J. Leddy, M. Makdissi, S. J. Sullivan, S. P. Broglio, M. Raftery, K. Schneider, J. Kissick, M. McCrea, J. Dvořák, A. K. Sills, M. Aubry, L. Engebretsen, M. Loosemore, G. Fuller, J. Kutcher, R. Ellenbogen, K. Guskiewicz, J. Patricios, and S. Herring, “The Sport Concussion Assessment Tool 5th Edition (SCAT5),” *British*

Journal of Sports Medicine, vol. 51, no. 11, p. bjsports-2017-097506, Apr. 2017, doi: https://doi.org/10.1136/bjsports-2017-097506.

[11] H. S. Levin and H. M. Eisenberg, "Neurobehavioral Outcome," *Neurosurgery Clinics of North America*, vol. 2, no. 2, pp. 457–472, Apr. 1991, doi: 10.1016/S1042-3680(18)30747-2.

[12] A. Lundin, C. de Boussard, G. Edman, and J. Borg, "Symptoms and disability until 3 months after mild TBI," *Brain Injury* vol. 20, no. 8, pp. 799–806, Jan. 2006, doi: 10.1080/02699050600744327.

[13] S. Kleiven, "Predictors for Traumatic Brain Injuries Evaluated through Accident Reconstructions," *SAE Technical Paper Series*, Oct. 2007, doi: 10.4271/2007-22-0003.

[14] T. W. McAllister, J. C. Ford, S. Ji, J. G. Beckwith, L. A. Flashman, K. Paulsen, and R. M. Greenwald, "Maximum Principal Strain and Strain Rate Associated with Concussion Diagnosis Correlates with Changes in Corpus Callosum White Matter Indices," *Annals of Biomedical Engineering*, vol. 40, no. 1, pp. 127–140, Jan. 2012, doi: 10.1007/s10439-011-0402-6.

[15] T. A. Smith, P. D. Halstead, E. McCalley, S. A. Kebschull, S. Halstead, and J. Killeffer, "Angular head motion with and without head contact: implications for brain injury," *Sports Engineering*, vol. 18, no. 3, pp. 165–175, Sep. 2015, doi: 10.1007/s12283-015-0175-5.

[16] B. Rowson and S. M. Duma, "A Review of Head Injury Metrics Used in Automotive Safety and Sports Protective Equipment," *Journal of Biomechanical Engineering*, vol. 144, no. 11, Nov. 2022, doi: 10.1115/1.4054379.

[17] D. H. Daneshvar, D. O. Riley, C. J. Nowinski, A. C. McKee, R. A. Stern, and R. C. Cantu, "Long-Term Consequences: Effects on Normal Development Profile After Concussion," *Physical Medicine and Rehabilitation Clinics of North America*, vol. 22, no. 4, pp. 683–700, Nov. 2011, doi: 10.1016/j.pmr.2011.08.009.

[18] K. G. Harmon, J. Drezner, M. Gammons, K. Guskiewicz, M. Halstead, S. Herring, J. Kutcher, A. Pana, M. Putukian, W. Roberts, and American Medical Society for Sports Medicine, "American Medical Society for Sports Medicine Position Statement," *Clinical Journal of Sport Medicine*, vol. 23, no. 1, pp. 1–18, Jan. 2013, doi: 10.1097/JSM.0b013e31827f5f93.

[19] A. C. McKee, R. A. Stern, C. J. Nowinski, T. D. Stein, V. E. Alvarez, D. H. Daneshvar, H. S. Lee, S. M. Wojtowicz, G. Hall, C. M. Baugh, D. O. Riley, C. A. Kubilus, K. A. Cormier, M. A. Jacobs, B. R. Martin, C. R. Abraham, T. Ikezu, R. R. Reichard, B. L. Wolozin, A. E. Budson, L. E. Goldstein, N. W. Kowall, and R. C. Cantu, "The spectrum of disease in chronic traumatic encephalopathy," *Brain*, vol. 136, no. 1, pp. 43–64, Jan. 2013, doi: 10.1093/brain/aws307.

[20] Y. Naumenko, I. Yuryshinetz, Y. Zabenko, and T. Pivneva, "Mild traumatic brain injury as a pathological process," *Heliyon*, vol. 9, no. 7, p. e18342, Jul. 2023, doi: 10.1016/j.heliyon.2023.e18342.

[21] A. M. Boutté, B. Thangavelu, C. R. LaValle, J. Nemes, J. Gilsdorf, D. A. Shear, and G. H. Kamimori, "Brain-related proteins as serum biomarkers of acute, subconcussive blast overpressure exposure: A cohort study of military personnel," *PLOS ONE*, vol. 14, no. 8, p. e0221036, Aug. 2019, doi: 10.1371/journal.pone.0221036.

[22] W. Carr, E. Polejaeva, A. Grome, B. Crandall, C. LaValle, S. E. Eonta, and L. A. Young, “Relation of Repeated Low-Level Blast Exposure with Symptomology Similar to Concussion,” *Journal of Head Trauma Rehabilitation*, vol. 30, no. 1, pp. 47–55, Jan. 2015, doi:10.1097/HTR.0000000000000064.

[23] C. M. Tate, K. K. Wang, S. Eonta, Y. Zhang, W. Carr, F. C. Tortella, R. L. Hayes, and G. H. Kamimori, “Serum Brain Biomarker Level, Neurocognitive Performance, and Self-Reported Symptom Changes in Soldiers Repeatedly Exposed to Low-Level Blast: A Breacher Pilot Study,” *Journal of Neurotrauma*, vol. 30, no. 19, pp. 1620–1630, Oct. 2013, doi: 10.1089/neu.2012.2683.

[24] D. Cardinal, I. Courchesne, R. Riddell, and I. Vallee, “Initial findings of the clinical screening of Special Operation Forces soldiers for mild traumatic brain injury,” *The 9th Annual Military and Veteran Health Research Forum, CIMVHR, Regina, Saskatchewan, Canada*, 2018.

[25] S. Ouellet and G. St-Onge, “Measurement of head kinematics of snipers firing a 0.50 caliber Rifle,” in *International Research Council on the Biomechanics of Injury*, Sep. 2021, pp. 211–212.

[26] H. Mao, L. Zhang, B. Jiang, V. V. Genthikatti, X. Jin, F. Zhu, R. Makwana, A. Gill, G. Jandir, A. Singh, and K. H. Yang, “Development of a Finite Element Human Head Model Partially Validated With Thirty Five Experimental Cases,” *Journal of Biomechanical Engineering*, vol. 135, no. 11, Nov. 2013, doi: 10.1115/1.4025101.

[27] D. A. Patton, A. S. McIntosh, and S. Kleiven, “The Biomechanical Determinants of Concussion: Finite Element Simulations to Investigate Tissue-Level Predictors of Injury During Sporting Impacts to the Unprotected Head,” *Journal of Applied Biomechanics*, vol. 31, no. 4, pp. 264–268, Aug. 2015, doi: 10.1123/jab.2014-0223.

[28] D. F. Meaney, B. Morrison, and C. Dale Bass, “The Mechanics of Traumatic Brain Injury: A Review of What We Know and What We Need to Know for Reducing Its Societal Burden,” *Journal of Biomechanical Engineering*, vol. 136, no. 2, Feb. 2014, doi: 10.1115/1.4026364.

[29] K.-U. Schmitt, P. F. Niederer, D. S. Cronin, B. Morrison III, M. H. Muser, and F. Walz, *Trauma Biomechanics - An Introduction to Injury Biomechanics, Fifth Edition*. Cham: Springer International Publishing, 2019. doi: 10.1007/978-3-030-11659-0.

[30] J. J. Bazarian, J. Mcclung, M. N. Shah, Y. Ting Cheng, W. Flesher, and J. Kraus, “Mild traumatic brain injury in the United States, 1998–2000,” *Brain Injury*, vol. 19, no. 2, pp. 85–91, Feb. 2005, doi: 10.1080/02699050410001720158.

[31] J. A. Langlois, W. Rutland-Brown, and M. M. Wald, “The Epidemiology and Impact of Traumatic Brain Injury,” *Journal of Head Trauma Rehabilitation*, vol. 21, no. 5, pp. 375–378, Sep. 2006, doi: 10.1097/00001199-200609000-00001.

[32] D. F. Meaney and D. H. Smith, “Biomechanics of Concussion,” *Clinics in Sports Medicine*, vol. 30, no. 1, pp. 19–31, Jan. 2011, doi: 10.1016/j.csm.2010.08.009.

[33] C. Eibner, T. L. Schell, and L. H. Jaycox, “Care of war veterans with mild traumatic brain injury.,” *The New England Journal of Medicine*, vol. 361, no. 5, pp. 537, Jul. 2009.

[34] S. J. Preiss-Farzanegan, B. Chapman, T. M. Wong, J. Wu, and J. J. Bazarian, “The Relationship Between Gender and Postconcussion Symptoms After Sport-Related Mild Traumatic Brain Injury,” *PM&R*, vol. 1, no. 3, pp. 245–253, Mar. 2009, doi: 10.1016/j.pmrj.2009.01.011.

[35] M. S. Xydakis, A. S. Robbins, and G. A. Grant, “Mild Traumatic Brain Injury in U.S. Soldiers Returning from Iraq,” *New England Journal of Medicine*, vol. 358, no. 20, pp. 2177–2179, May 2008, doi: 10.1056/NEJMc086083.

[36] S. Standring, *Gray’s Anatomy E-Book : The Anatomical Basis of Clinical Practice*. Elsevier, 2008.

[37] Y. King-Hay, *Basic finite element method as applied to injury biomechanics*. London Academic Press, 2018.

[38] J. W. Melvin, J. W. Lighthall, and K. Ueno, “Brain Injury Biomechanics,” *Accidental Injury*, pp. 268–291, 1993, doi: https://doi.org/10.1007/978-1-4757-2264-2_12.

[39] C. P. Carroll, J. A. Cochran, J. P. Price, C. E. Guse, and M. C. Wang, “The AIS-2005 Revision in Severe Traumatic Brain Injury: Mission Accomplished or Problems for Future Research?,” *Annals of advances in automotive medicine. Association for the Advancement of Automotive Medicine. Annual Scientific Conference*, vol. 54, pp. 233–8, 2010.

[40] American Congress of Rehabilitation Medicine, “Definition of mild traumatic brain injury,” *J Head Trauma Rehabil*, vol. 8, no. 3, pp. 86–87, Sep. 1993.

[41] L. J. Carroll, J. D. Cassidy, P. M. Peloso, J. Borg, H. von Holst, L. Holm, C. Paniak, M. Pépin, and WHO Collaborating Centre Task Force on Mild Traumatic Brain Injury, “Prognosis for mild traumatic brain injury: results of the who collaborating centre task force on mild traumatic brain injury,” *Journal of Rehabilitation Medicine*, vol. 36, no. 0, pp. 84–105, Feb. 2004, doi: https://doi.org/10.1080/16501960410023859.

[42] National Center for Injury Prevention and Control., “Report to Congress on mild traumatic brain injury in the United States: Steps to prevent a serious public health problem.,” Atlanta, GA, 2003.

[43] E. S. Gurdjian, H. R. Lissner, F. R. Latimer, B. F. Haddad, and J. E. Webster, “Quantitative Determination of Acceleration and Intracranial Pressure in Experimental Head Injury,” *Neurology*, vol. 3, no. 6, pp. 417–417, Jun. 1953, doi: 10.1212/WNL.3.6.417.

[44] E. S. Gurdjian, V. L. Roberts, and L. M. Thomas, “Tolerance Curves of Acceleration and Intracranial Pressure and Protective Index in Experimental Head Injury,” *The Journal of Trauma: Injury, Infection, and Critical Care*, vol. 6, no. 5, pp. 600–604, Sep. 1966, doi: 10.1097/00005373-196609000-00005.

[45] H. R. Lissner, M. Lebow, and F. G. Evans, “Experimental studies on the relation between acceleration and intracranial pressure changes in man.,” *PubMed*, vol. 111, pp. 329–38, Sep. 1960.

[46] A. H. S. Holbourn, “Mechanics of Head Injuries,” *The Lancet*, vol. 242, no. 6267, pp. 438–441, Oct. 1943, doi: 10.1016/S0140-6736(00)87453-X.

[47] T. A. Gennarelli, L. E. Thibault, J. H. Adams, D. I. Graham, C. J. Thompson, and R. P. Marcincin, "Diffuse axonal injury and traumatic coma in the primate," *Annals of Neurology*, vol. 12, no. 6, pp. 564–574, Dec. 1982, doi: 10.1002/ana.410120611.

[48] A. K. Ommaya and T. A. Gennarelli, "Cerebral Concussion and Traumatic Unconsciousness," *Brain*, vol. 97, no. 1, pp. 633–654, 1974, doi: 10.1093/brain/97.1.633.

[49] T. A. Gennarelli, "The Centripetal Theory of Concussion (CTC) revisited after 40 years and a proposed new Symptomcentric Concept of the Concussions," in *IRCOBI Conference*, Lyon, France, 2015, pp. 1131–1138.

[50] J. R. Stone, D. O. Okonkwo, A.O. Dialo, D. G. Rubin, L. K. Mutlu, J. T. Povlishock, and G. A. Helm, "Impaired axonal transport and altered axolemmal permeability occur in distinct populations of damaged axons following traumatic brain injury," *Experimental Neurology*, vol. 190, no. 1, pp. 59–69, Nov. 2004, doi: 10.1016/j.expneurol.2004.05.022.

[51] E. Khong, N. Odenwald, E. Hashim, and M. D. Cusimano, "Diffusion Tensor Imaging Findings in Post-Concussion Syndrome Patients after Mild Traumatic Brain Injury: A Systematic Review," *Frontiers in Neurology*, vol. 7, Sep. 2016, doi: 10.3389/fneur.2016.00156.

[52] C. Giordano and Svein Kleiven, "Evaluation of Axonal Strain as a Predictor for Mild Traumatic Brain Injuries Using Finite Element Modeling," *SAE technical paper series*, Nov. 2014, doi: 10.4271/2014-22-0002.

[53] D. A. Patton, A. S. McIntosh, and S. Kleiven, "The Biomechanical Determinants of Concussion: Finite Element Simulations to Investigate Brain Tissue Deformations During Sporting Impacts to the Unprotected Head," *Journal of Applied Biomechanics*, vol. 29, no. 6, pp. 721–730, Dec. 2013, doi: 10.1123/jab.29.6.721.

[54] D. A. Patton, A. S. McIntosh, and S. Kleiven, "The Biomechanical Determinants of Concussion: Finite Element Simulations to Investigate Tissue-Level Predictors of Injury During Sporting Impacts to the Unprotected Head," *Journal of Applied Biomechanics*, vol. 31, no. 4, pp. 264–268, Aug. 2015, doi: 10.1123/jab.2014-0223.

[55] D. C. Viano, I. R. Casson, E. J. Pellman, L. Zhang, A. I. King, and K. H. Yang, "Concussion in Professional Football: Brain Responses by Finite Element Analysis: Part 9," *Neurosurgery*, vol. 57, no. 5, pp. 891–916, Nov. 2005, doi: 10.1227/01.NEU.0000186950.54075.3B.

[56] S. Kleiven, "Why Most Traumatic Brain Injuries are Not Caused by Linear Acceleration but Skull Fractures are," *Frontiers in Bioengineering and Biotechnology*, vol. 1, 2013, doi: 10.3389/fbioe.2013.00015.

[57] J. Ho, Z. Zhou, X. Li, and S. Kleiven, "The peculiar properties of the falx and tentorium in brain injury biomechanics," *Journal of Biomechanics*, vol. 60, pp. 243–247, Jul. 2017, doi: 10.1016/j.jbiomech.2017.06.023.

[58] T. A. Gennarelli, L. E. Thibault, G. Tomei, R. Wiser, D. Graham, and J. Adams, "Directional Dependence of Axonal Brain Injury due to Centroidal and Non-Centroidal Acceleration," *SAE technical paper series,* Nov. 1987. doi: 10.4271/872197.

[59] F. Hernandez, L. C. Wu, M. C. Yip, K. Laksari, A. R. Hoffman, J. R. Lopez, G. A. Grant, S. Kleiven and D. B. Camarillo, “Six Degree-of-Freedom Measurements of Human Mild Traumatic Brain Injury,” *Annals of Biomedical Engineering*, vol. 43, no. 8, pp. 1918–1934, Aug. 2015, doi: 10.1007/s10439-014-1212-4.

[60] D. J. Lessley, R. W. Kent, J. R. Funk, C. P. Sherwood, J. M. Cormier, J. R. Crandall, K. B. Arbogast, and B. S. Myers, “Video Analysis of Reported Concussion Events in the National Football League During the 2015-2016 and 2016-2017 Seasons,” *The American Journal of Sports Medicine*, vol. 46, no. 14, pp. 3502–3510, Dec. 2018, doi: 10.1177/0363546518804498.

[61] D. R. S. Bradshaw and C. L. Morfey, “Pressure and shear response in brain injury models,” in *Proceedings of the 17th international technical conference on the enhanced safety of vehicles*, Amsterdam, The Netherlands, 2001.

[62] W. N. Hardy, M. J. Mason, C. D. Foster, C. S. Shah, J. M. Kopacz, K. H. Yang, A. I. King, J. Bishop, M. Bey, W. Anderst, and S. Tashman, “A Study of the Response of the Human Cadaver Head to Impact,” *SAE Technical Paper Series,* Oct. 2007. doi: 10.4271/2007-22-0002.

[63] W. N. Hardy, C. D. Foster, M. J. Mason, K. H. Yang, A. I. King, and S. Tashman, “Investigation of Head Injury Mechanisms Using Neutral Density Technology and High-Speed Biplanar X-ray,” *Stapp Car Crash Journal*, vol. 45, pp. 337–368, Nov. 2001, doi: https://doi.org/10.4271/2001-22-0016.

[64] A. Alshareef, J. S. Giudice, J. Forman, R. S. Salzar, and M. B. Panzer, “A Novel Method for Quantifying Human *In Situ* Whole Brain Deformation under Rotational Loading Using Sonomicrometry,” *Journal of Neurotrauma*, vol. 35, no. 5, pp. 780–789, Mar. 2018, doi: 10.1089/neu.2017.5362.

[65] A. Alshareef, J. S. Giudice, J. Forman, D. F. Shedd, K. A. Reynier, T. Wu, S. Sochor, R. S. Salzar, and M. B. Panzer, “Biomechanics of the Human Brain during Dynamic Rotation of the Head *Journal of Neurotrauma*, vol. 37, no. 13, pp. 1546–1555, Jul. 2020, doi: 10.1089/neu.2019.6847.

[66] B. Rowson and S. M. Duma, “A Review of Head Injury Metrics Used in Automotive Safety and Sports Protective Equipment,” *Journal of Biomechanical Engineering*, vol. 144, no. 11, Nov. 2022, doi: 10.1115/1.4054379.

[67] D. A. Patton, C. M. Huber, D. Jain, R. K. Myers, C. C. McDonald, S. S. Marguiles, C. L. Master, and K. B. Arbogast, “Head Impact Sensor Studies In Sports: A Systematic Review Of Exposure Confirmation Methods,” *Annals of Biomedical Engineering*, vol. 48, no. 11, pp. 2497–2507, Nov. 2020, doi: 10.1007/s10439-020-02642-6.

[68] E. J. Pellman, D. C. Viano, A. M. Tucker, I. R. Casson, and J. F. Waeckerle, “Concussion in Professional Football: Reconstruction of Game Impacts and Injuries,” *Neurosurgery*, vol. 53, no. 4, pp. 799–814, Oct. 2003, doi: 10.1227/01.NEU.0000083559.68424.3F.

[69] J. Newman, M. Beusenberg, E. Fournier, N. Shewchenko, C. Withnall, A. King, K. Yang, L. Zhang, J. McElhaney, L. Thibault, and G. McGinnis, “ A new biomechanical assessment of mild traumatic brain injury, part 1: methodology,” in *Proceedings of International Research Conference on the Biomechanics of Impacts*, Barcelona, Spain, 1999, pp. 17–36.

[70] J. Newman, C. Barr, M. Beusenberg, E. Fournier, N. Shewchenko, E. Welbourne, and C. Withnall, "A new biomechanical assessment of mild traumatic brain injury, part 2: results and conclusions," in *Proceedings of International Research Conference on the Biomechanics of Impacts*, Montpellier, France, 2000, pp. 223–230.

[71] J. A. Newman and N. Shewchenko, "A Proposed New Biomechanical Head Injury Assessment Function - the Maximum Power Index," *SAE technical paper series*, Nov. 2000. doi: 10.4271/2000-01-SC16.

[72] C. Withnall, "Biomechanical investigation of head impacts in football," *British Journal of Sports Medicine*, vol. 39, no. Supplement 1, pp. i49–i57, Aug. 2005, doi: 10.1136/bjsm.2005.019182.

[73] K. Laksari, M. Kurt, and L. C. Wu, "Concussion Mechanism: Biomechanical Perspectives," in *Tackling the Concussion Epidemic*, Cham: Springer International Publishing, 2022, pp. 1–24. doi: 10.1007/978-3-030-93813-0_1.

[74] A. M. Tyson, S. M. Duma, and S. Rowson, "Laboratory Evaluation of Low-Cost Wearable Sensors for Measuring Head Impacts in Sports," *Journal of Applied Biomechanics*, vol. 34, no. 4, pp. 320–326, Aug. 2018, doi: 10.1123/jab.2017-0256.

[75] S. Rowson, S. M. Duma, J. G. Beckwith, J. J. Chu, R. M. Greenwald, J. J. Crisco, P. G. Brolinson, A. Duhaime, T. W. McAllister, and A. C. Maerlender, "Rotational Head Kinematics in Football Impacts: An Injury Risk Function for Concussion," *Annals of Biomedical Engineering*, vol. 40, no. 1, pp. 1–13, Jan. 2012, doi: 10.1007/s10439-011-0392-4.

[76] J. R. Funk, S. Rowson, R. W. Daniel, and S. M. Duma, "Validation of Concussion Risk Curves for Collegiate Football Players Derived from HITS Data," *Annals of Biomedical Engineering*, vol. 40, no. 1, pp. 79–89, Jan. 2012, doi: 10.1007/s10439-011-0400-8.

[77] S. Rowson and S. M. Duma, "Development of the STAR Evaluation System for Football Helmets: Integrating Player Head Impact Exposure and Risk of Concussion," *Annals of Biomedical Engineering*, vol. 39, no. 8, pp. 2130–2140, Aug. 2011, doi: 10.1007/s10439-011-0322-5.

[78] Alexander C, "UNC's Guskiewicz talks about concussions, football." Accessed: Feb. 29, 2024. Available: http://www.newsobserver.com/sports/college/acc/unc/article30327246.html

[79] G. P. Siegmund, K. M. Guskiewicz, S. W. Marshall, A. L. DeMarco, and S. J. Bonin, "Laboratory Validation of Two Wearable Sensor Systems for Measuring Head Impact Severity in Football Players," *Annals of Biomedical Engineering*, vol. 44, no. 4, pp. 1257–1274, Apr. 2016, doi: 10.1007/s10439-015-1420-6.

[80] R. Jadischke, D. C. Viano, N. Dau, A. I. King, and J. McCarthy, "On the accuracy of the Head Impact Telemetry (HIT) System used in football helmets," *Journal of Biomechanics*, vol. 46, no. 13, pp. 2310–2315, Sep. 2013, doi: 10.1016/j.jbiomech.2013.05.030.

[81] M. A. Allison, Y. S. Kang, M. R. Maltese, J. H. Bolte, and K. B. Arbogast, "Measurement of Hybrid III Head Impact Kinematics Using an Accelerometer and Gyroscope System in Ice Hockey Helmets," *Annals of Biomedical Engineering*, vol. 43, no. 8, pp. 1896–1906, Aug. 2015, doi: 10.1007/s10439-014-1197-z.

[82] S. M. Duma, S. J. Manoogian, W. R. Bussone, P. G. Brolinson, M. w. Goforth, J. J. Donnenwerth, R. M. Greenwald, J. J. Chu, and J. J. Crisco, "Analysis of Real-time Head Accelerations in Collegiate Football Players," *Clinical Journal of Sport Medicine*, vol. 15, no. 1, pp. 3–8, Jan. 2005, doi: https://doi.org/10.1097/00042752-200501000-00002.

[83] S. Rowson, J. G. Beckwith, J. J. Chu, D. S. Leonard, R. M. Greenwald, and S. M. Duma, "A Six Degree of Freedom Head Acceleration Measurement Device for Use in Football," *Journal of Applied Biomechanics*, vol. 27, no. 1, pp. 8–14, Feb. 2011, doi: 10.1123/jab.27.1.8.

[84] C. M. Huber, D. A. Patton, K. L. Wofford, S. S. Margulies, D. K. Cullen, and K. B. Arbogast, "Laboratory Assessment of a Headband-Mounted Sensor for Measurement of Head Impact Rotational Kinematics," *Journal of biomechanical engineering*, vol. 143, no. 2, Feb. 2021, doi: 10.1115/1.4048574.

[85] E. E. Swartz, J. L. Myers, S. B. Cook, K. M. Guskiewicz, M. S. Ferrara, R. C. Cantu, H. Chang, and S. P. Brogolio, "A helmetless-tackling intervention in American football for decreasing head impact exposure: A randomized controlled trial," *Journal of Science and Medicine in Sport*, vol. 22, no. 10, pp. 1102–1107, Oct. 2019, doi: 10.1016/j.jsams.2019.05.018.

[86] L. C. Lamond, J. B. Caccese, T. A. Buckley, J. Glutting, and T. W. Kaminski, "Linear Acceleration in Direct Head Contact Across Impact Type, Player Position, and Playing Scenario in Collegiate Women's Soccer Players," *Journal of Athletic Training*, vol. 53, no. 2, pp. 115–121, Feb. 2018, doi: 10.4085/1062-6050-90-17.

[87] A. S. McIntosh, C. Wilmott, D. A. Patton, B. Mitra, J. P. Brennan, B. Dimech-Betancourt, T. Howard, J. V. Rosenfeld, "An assessment of the utility and functionality of wearable head impact sensors in Australian Football," *J Sci Med Sport*, vol. 22, no. 7, pp. 784–789, Jul. 2019, doi: 10.1016/j.jsams.2019.02.004.

[88] L. C. Wu, V. Nangia, K. Bui, B. Hammoor, M. Kurt, F. Hernandez, C. Kuo, and D. B. Camarillo, "In Vivo Evaluation of Wearable Head Impact Sensors," *Annals of Biomedical Engineering*, vol. 44, no. 4, pp. 1234–1245, Apr. 2016, doi: 10.1007/s10439-015-1423-3.

[89] M. B. Panzer, C. R. Bass, R. S. Salzar, J. Pellettiere, and B. Myers, "Evaluation of Ear-Mounted Sensors For Determining Impact Head Acceleration," in *IRCOBI Conference*, York, UK, 2009, pp. 319–322.

[90] R. S. Salzar, C. R. 'Dale' Bass, and J. A. Pellettiere, "Improving Earpiece Accelerometer Coupling to the Head," *SAE International Journal of Passenger Cars - Mechanical Systems*, vol. 1, no. 1, pp. 2008-01–2978, Dec. 2008, doi: 10.4271/2008-01-2978.

[91] L. F. Gabler, N. Z. Dau, G. Park, A. Miles, K. B. Arbogast, and J. R. Crandall, "Development of a Low-Power Instrumented Mouthpiece for Directly Measuring Head Acceleration in American Football," *Annals of Biomedical Engineering*, vol. 49, no. 10, pp. 2760–2776, Oct. 2021, doi: 10.1007/s10439-021-02826-8.

[92] D. B. Camarillo, P. B. Shull, J. Mattson, R. Shultz, and D. Garza, "An Instrumented Mouthguard for Measuring Linear and Angular Head Impact Kinematics in American Football," *Annals of*

Biomedical Engineering, vol. 41, no. 9, pp. 1939–1949, Sep. 2013, doi: 10.1007/s10439-013-0801-y.

[93] Y. Liu, A. G. Domel, S. A. Yousefsani, J. Kondic, G. Grant, M. Zeineh, and D. B. Camarillo , "Validation and Comparison of Instrumented Mouthguards for Measuring Head Kinematics and Assessing Brain Deformation in Football Impacts," *Annals of Biomedical Engineering*, vol. 48, no. 11, pp. 2580–2598, Nov. 2020, doi: 10.1007/s10439-020-02629-3.

[94] A. J. Bartsch, M. M. M cCrea, D. S. Hedin, P. L. Gibson, V. J. Miele, E. C. Benzel, J. L. Alberts, S. Samorezov, A. Shah, and B. S. Stemper , "Laboratory and On-field Data Collected by a Head Impact Monitoring Mouthguard," in *2019 41st Annual International Conference of the IEEE Engineering in Medicine and Biology Society (EMBC)*, IEEE, Jul. 2019, pp. 2068–2072. doi: 10.1109/EMBC.2019.8856907.

[95] K. R. Campbell, M. J. Warnica, I. C. Levine, J. S. Brooks, A. C. Laing, T. A. Burkhart, and J. P. Dickey, "Laboratory Evaluation of the gForce Tracker™, a Head Impact Kinematic Measuring Device for Use in Football Helmets," *Annals of Biomedical Engineering*, vol. 44, no. 4, pp. 1246–1256, Jul. 2015, doi: 10.1007/s10439-015-1391-7.

[96] M. Morrison and J. N. Daigle, "A Biosensing Approach for Detecting and Managing Head Injuries in American Football," *Journal of Biosensors & Bioelectronics*, vol. 06, no. 04, 2015, doi: 10.4172/2155-6210.1000189.

[97] Z. Y. Kerr, A. C. Littleton, L. M. Cox, J. D. DeFreese, E. Varangis, R. C. Lynall, J. D. Schmidt, S. W. Marshall, and K. M. Guskiewicz, "Estimating Contact Exposure in Football Using the Head Impact Exposure Estimate," *Journal of Neurotrauma*, vol. 32, no. 14, pp. 1083–1089, Jul. 2015, doi: 10.1089/neu.2014.3666.

[98] E. E. Swartz, S. P. Broglio, S. B. Cook, R. C. Cantu, M. S. Ferrara, K. M. Guskiewicz, and J. L. Myers , "Early Results of a Helmetless-Tackling Intervention to Decrease Head Impacts in Football Players," *Journal of Athletic Training*, vol. 50, no. 12, pp. 1219–1222, Dec. 2015, doi: 10.4085/1062-6050-51.1.06.

[99] D. O. Svaldi, E. C. McCuen, C. Joshi, M. E. Robinson, Y. Nho, R. E. Hannemann, E. A. Nauman, L. J. Leverenz, and T. M. Talavage, "Cerebrovascular reactivity changes in asymptomatic female athletes attributable to high school soccer participation," *Brain Imaging and Behavior*, vol. 11, no. 1, pp. 98–112, Feb. 2017, doi: 10.1007/s11682-016-9509-6.

[100] E. McCuen, D. Svaldi, K. Breedlove, N. Kraz, B. Cummiskey, E. L. Breedlove, J. Traver, K. F. Desmond, R. E. Hannemann, E. Zanath, A. Guerra, L. Leverenz, T. M. Talavage, E. A. Nauman , "Collegiate women's soccer players suffer greater cumulative head impacts than their high school counterparts," *Journal of Biomechanics*, vol. 48, no. 13, pp. 3720–3723, Oct. 2015, doi: 10.1016/j.jbiomech.2015.08.003.

[101] D. A. King, P. A. Hume, C. Gissane, and T. N. Clark, "Similar head impact acceleration measured using instrumented ear patches in a junior rugby union team during matches in comparison with other sports," *Journal of Neurosurgery: Pediatrics*, vol. 18, no. 1, pp. 65–72, Jul. 2016, doi: 10.3171/2015.12.PEDS15605.

[102] S. B. Sandmo, A. S. McIntosh, T. E. Andersen, I. K. Koerte, and R. Bahr, “Evaluation of an In-Ear Sensor for Quantifying Head Impacts in Youth Soccer,” *The American Journal of Sports Medicine*, vol. 47, no. 4, pp. 974–981, Mar. 2019, doi: 10.1177/0363546519826953.

[103] E. E. Kieffer, M. T. Begonia, A. M. Tyson, and S. Rowson, “A Two-Phased Approach to Quantifying Head Impact Sensor Accuracy: In-Laboratory and On-Field Assessments,” *Annals of Biomedical Engineering*, vol. 48, no. 11, pp. 2613–2625, Nov. 2020, doi: 10.1007/s10439-020-02647-1.

[104] R. C. Cantu and F. O. Mueller, “Brain Injury-related Fatalities in American Football, 1945–1999,” *Neurosurgery*, vol. 52, no. 4, pp. 846–853, Apr. 2003, doi:10.1227/01.NEU.0000053210.76063.E4.

[105] C. J. Kahane, “Lives Saved by Vehicle Safety Technologies and Associated Federal Motor Vehicle Safety Standards, 1960 to 2012—Passenger Cars and LTVs—With Reviews of 26 FMVSS and the Effectiveness of Their Associated Safety Technologies in Reducing Fatalities, Injuries, and Crashes,” Washington, DC, 2015. doi: Report No. DOT HS 812 069.

[106] C. J. Kahane, “Evaluation of the 1999-2003 Head Impact Upgrade of FMVSS No. 201–Upper-Interior Components: Effectiveness of Energy-Absorbing Materials Without Head-Protection Air Bags,” Washington, DC, 2011. doi: Report No. DOT HS 811 538.

[107] J. A. Newman, “On the Use of the Head Injury Criterion (HIC) in Protective Headgear Evaluation,” Feb. 1975. doi: 10.4271/751162.

[108] C. W. Gadd, “Use of a Weighted-Impulse Criterion for Estimating Injury Hazard,” Feb. 1966. doi: 10.4271/660793.

[109] J. Versace, “A Review of the Severity Index,” Feb. 1971. doi: 10.4271/710881.

[110] M. R. Bambach, R. J. Mitchell, R. H. Grzebieta, and J. Olivier, “The effectiveness of helmets in bicycle collisions with motor vehicles: A case–control study,” *Accident Analysis & Prevention*, vol. 53, pp. 78–88, Apr. 2013, doi: 10.1016/j.aap.2013.01.005.

[111] A. J. Padgaonkar, K. W. Krieger, and A. I. King, “Measurement of Angular Acceleration of a Rigid Body Using Linear Accelerometers,” *Journal of Applied Mechanics*, vol. 42, no. 3, pp. 552–556, Sep. 1975, doi: 10.1115/1.3423640.

[112] S. S. Margulies and L. E. Thibault, “A proposed tolerance criterion for diffuse axonal injury in man,” *Journal of Biomechanics*, vol. 25, no. 8, pp. 917–923, Aug. 1992, doi: 10.1016/0021-9290(92)90231-O.

[113] James A. Newman, “A generalized acceleration model for brain injury threshold (GAMBIT),” 1986.

[114] L. F. Gabler, J. R. Crandall, and M. B. Panzer, “Assessment of Kinematic Brain Injury Metrics for Predicting Strain Responses in Diverse Automotive Impact Conditions,” *Annals of Biomedical Engineering*, vol. 44, no. 12, pp. 3705–3718, Dec. 2016, doi: 10.1007/s10439-016-1697-0.

[115] F. Kramer and H. Appel, “Evaluation of Protection Criteria on the Basis of Statistical Biomechanics,” in *International Conference on the Biomechanics of Impacts (IRCOBI)*, Bron, France, 1990, pp. 45–47.

[116] S. Kleiven, “Predictors for Traumatic Brain Injuries Evaluated through Accident Reconstructions,” Oct. 2007. doi: 10.4271/2007-22-0003.

[117] R. M. Greenwald, J. T. Gwin, J. J. Chu, and J. J. Crisco, “Head Impact Severity Measures for Evaluating Mild Traumatic Brain Injury Risk Exposure,” *Neurosurgery*, vol. 62, no. 4, pp. 789–798, Apr. 2008, doi: 10.1227/01.neu.0000318162.67472.ad.

[118] S. Rowson and S. M. Duma, “Brain Injury Prediction: Assessing the Combined Probability of Concussion Using Linear and Rotational Head Acceleration,” *Annals of Biomedical Engineering*, vol. 41, no. 5, pp. 873–882, May 2013, doi: 10.1007/s10439-012-0731-0.

[119] M. Begonia, A. Tyson, B. Rowson, and S. Rowson, “Hockey STAR Methodology,” Blacksburg, VA, 2020. Accessed: Mar. 01, 2024. Available: https://vtechworks.lib.vt.edu/handle/10919/101013.2

[120] A. M. Tyson and S. Rowson, “Varsity Football STAR Methodology,” Blacksburg, VA, 2020. Accessed: Mar. 01, 2024. Available: https://vtechworks.lib.vt.edu/handle/10919/82953.2

[121] A. M. Tyson, J. Press, and S. Rowson, “Soccer Headgear STAR Protocol,” Blacksburg, VA, 2018. Accessed: Mar. 01, 2024.. Available: https://vtechworks.lib.vt.edu/handle/10919/82952

[122] H. Kimpara, Y. Nakahira, M. Iwamoto, S. Rowson, and S. Duma, “Head Injury Prediction Methods Based on 6 Degree of Freedom Head Acceleration Measurements during Impact,” *International Journal of Automotive Engineering*, vol. 2, no. 2, p. 20114490, 2011, doi: 10.20485/jsaeijae.2.2_13.

[123] E. G. Takhounts, V. Hasija, S. A. Ridella, S. Rowson, and S. M. Duma, “Kinematic rotational brain injury criterion (BRIC),” in *Proceedings of the 22nd Enhanced Safety of Vehicles Conference*, 2011.

[124] E. G. Takhounts, M. J. Craig, K. Moorhouse, J. McFadden, and V. Hasija, “Development of Brain Injury Criteria (BrIC),” Nov. 2013. doi: 10.4271/2013-22-0010.

[125] L. F. Gabler, H. Joodaki, J. R. Crandall, and M. B. Panzer, “Development of a Single-Degree-of-Freedom Mechanical Model for Predicting Strain-Based Brain Injury Responses,” *J Biomech Eng*, vol. 140, no. 3, Mar. 2018, doi: 10.1115/1.4038357.

[126] L. F. Gabler, J. R. Crandall, and M. B. Panzer, “Development of a Second-Order System for Rapid Estimation of Maximum Brain Strain,” *Annals of Biomedical Engineering*, vol. 47, no. 9, pp. 1971–1981, Sep. 2019, doi: 10.1007/s10439-018-02179-9.

[127] L. F. Gabler, J. R. Crandall, and M. B. Panzer, “Development of a Metric for Predicting Brain Strain Responses Using Head Kinematics,” *Annals of Biomedical Engineering*, vol. 46, no. 7, pp. 972–985, Jul. 2018, doi: 10.1007/s10439-018-2015-9.

[128] B. J. Wilcox, J. G. Beckwith, R. M. Greenwald, N. P. Raukar, J. J. Chu, T. W. McAllister, L. a. Flasman, A. C. Maerlender, A. Duhaime, and J. J. Crisco , “Biomechanics of head impacts associated with diagnosed concussion in female collegiate ice hockey players,” *Journal of Biomechanics*, vol. 48, no. 10, pp. 2201–2204, Jul. 2015, doi: 10.1016/j.jbiomech.2015.04.005.

[129] J. G. Beckwith, R. M. Greenwald, J. J. Chu, J. J. Crisco, S. Rowson, S. M. Duma, S. P. Broglio, T. W. McAllister, K. M. Guskiewicz, J. P. Mihalik, S. Anderson, B. Schnebel, P. G. Brolinson, and M. W.

Collis, “Head Impact Exposure Sustained by Football Players on Days of Diagnosed Concussion,” *Medicine & Science in Sports & Exercise*, vol. 45, no. 4, pp. 737–746, Apr. 2013, doi: 10.1249/MSS.0b013e3182792ed7.

[130] J. R. Funk, S. M. Duma, S. J. Manoogian, and S. Rowson, “Biomechanical risk estimates for mild traumatic brain injury.,” *Annu Proc Assoc Adv Automot Med*, vol. 51, pp. 343–61, 2007.

[131] S. Kleiven and H. von Holst, “Consequences of head size following trauma to the human head,” *Journal of Biomechanics*, vol. 35, no. 2, pp. 153–160, Feb. 2002, doi: 10.1016/S0021-9290(01)00202-0.

[132] S. Kleiven and W. N. Hardy, “Correlation of an FE Model of the Human Head with Local Brain Motion-Consequences for Injury Prediction,” Nov. 2002. doi: 10.4271/2002-22-0007.

[133] K. H. Yang and H. Mao, “Modelling of the Brain for Injury Simulation and Prevention,” 2019, pp. 97–133. doi: 10.1007/978-3-030-04996-6_5.

[134] C. Giordano, S. Zappalà, and S. Kleiven, “Anisotropic finite element models for brain injury prediction: the sensitivity of axonal strain to white matter tract inter-subject variability,” *Biomechanics and Modeling in Mechanobiology*, vol. 16, no. 4, pp. 1269–1293, Aug. 2017, doi: 10.1007/s10237-017-0887-5.

[135] C. Giordano and S. Kleiven, “Development of an Unbiased Validation Protocol to Assess the Biofidelity of Finite Element Head Models used in Prediction of Traumatic Brain Injury,” Nov. 2016. doi: 10.4271/2016-22-0013.

[136] A. M. Nahum, R. Smith, and C. C. Ward, “Intracranial Pressure Dynamics During Head Impact,” Feb. 1977. doi: 10.4271/770922.

[137] X. Trosseille, C. Tarriére, F. Lavaste, F. Guillon, and A. Domont, “Development of a F.E.M. of the Human Head According to a Specific Test Protocol,” Nov. 1992. doi: 10.4271/922527.

[138] Z. Y. Cui, N. Famaey, B. Depreitere, J. Ivens, S. Kleiven, and J. Vander Sloten, “On the assessment of bridging vein rupture associated acute subdural hematoma through finite element analysis,” *Computer Methods in Biomechanics and Biomedical Engineering*, vol. 20, no. 5, pp. 530–539, Apr. 2017, doi: 10.1080/10255842.2016.1255942.

[139] E. G. Takhounts, R. H. Eppinger, J. Q. Campbell, R. E. Tannous, E. D. Power, and L. S. Shook, “On the Development of the SIMon Finite Element Head Model,” Oct. 2003. doi: 10.4271/2003-22-0007.

[140] E. G. Takhounts, S. A. Ridella, V. Hasija, R. E. Tannous, J. Q. Campbell, D. Malone, K. A. Danelson, J. D. Stitzel, S. Rowson, and S. M. Duma, “Investigation of Traumatic Brain Injuries Using the Next Generation of Simulated Injury Monitor (SIMon) Finite Element Head Model,” *SAE technical paper series*, Nov. 2008. doi: 10.4271/2008-22-0001.

[141] Iwamoto M, Y. Kisanuki, I. Watanabe, K. Furusu, K. Miki, and J. Hasegawa, “Development of a finite element model of the total human model for safety (THUMS) and application to injury reconstruction,” in *Proceedings of the international research council on the biomechanics of injury conference*, 2002, pp. 1–12.

[142] H. Kimpara, Y. Nakahira, M. Iwamoto, K. Miki, K. Ichihara, S. Kawano, T. Taguchi, “Investigation of Anteroposterior Head-Neck Responses during Severe Frontal Impacts Using a Brain-Spinal Cord Complex FE Model,” *SAE technical paper series*, Nov. 2006. doi: 10.4271/2006-22-0019.

[143] M. J. Ackerman, “The Visible Human Project: a resource for anatomical visualization.,” *Stud Health Technol Inform*, vol. 52 Pt 2, pp. 1030–2, 1998.

[144] J. Hallquist, “LS-DYNA Theory Manual,” Livermore, California, 2006.

[145] J. A. Galbraith, L. E. Thibault, and D. R. Matteson, “Mechanical and Electrical Responses of the Squid Giant Axon to Simple Elongation,” *Journal of Biomechanical Engineering*, vol. 115, no. 1, pp. 13–22, Feb. 1993, doi: 10.1115/1.2895464.

[146] D. H. Smith, J. A. Wolf, T. A. Lusardi, V. M.-Y. Lee, and D. F. Meaney, “High Tolerance and Delayed Elastic Response of Cultured Axons to Dynamic Stretch Injury,” *The Journal of Neuroscience*, vol. 19, no. 11, pp. 4263–4269, Jun. 1999, doi: 10.1523/JNEUROSCI.19-11-04263.1999.

[147] W. Zhao, Y. Cai, Z. Li, and S. Ji, “Injury prediction and vulnerability assessment using strain and susceptibility measures of the deep white matter,” *Biomechanics and Modeling in Mechanobiology*, vol. 16, no. 5, pp. 1709–1727, Oct. 2017, doi: 10.1007/s10237-017-0915-5.

[148] L. Zhang, K. H. Yang, and A. I. King, “A Proposed Injury Threshold for Mild Traumatic Brain Injury,” *J Biomech Eng*, vol. 126, no. 2, pp. 226–236, Apr. 2004, doi: 10.1115/1.1691446.

[149] J. G. Beckwith, W. Zhao, S. Ji, A. G. Ajamil, R. P. Bolander, J. J. Chu, T. W. McAllister, J. J. Crisco, S. M. Duma, S. Rowson, S. P. Broglio, K. M. Guskiewicz, J. P. Mihalik, S. Anderson, B. Schnebel, P. Gunnar Brolinson, M. W. Collins, and R. M. Greenwald, “Estimated Brain Tissue Response Following Impacts Associated With and Without Diagnosed Concussion,” *Annals of Biomedical Engineering*, vol. 46, no. 6, pp. 819–830, Jun. 2018, doi: 10.1007/s10439-018-1999-5.

[150] A. Post, A. Oeur, B. Hoshizaki, and M. D. Gilchrist, “An examination of American football helmets using brain deformation metrics associated with concussion,” *Materials & Design*, vol. 45, pp. 653–662, Mar. 2013, doi: 10.1016/j.matdes.2012.09.017.

[151] X. Jin, Z. Feng, V. Mika, H. Li, D. C. Viano, and K. H. Yang, “The Role of Neck Muscle Activities on the Risk of Mild Traumatic Brain Injury in American Football,” *Journal of Biomechanical Engineering*, vol. 139, no. 10, Oct. 2017, doi: 10.1115/1.4037399.

[152] A. Post, T. Blaine Hoshizaki, M. D. Gilchrist, and M. D. Cusimano, “Peak linear and rotational acceleration magnitude and duration effects on maximum principal strain in the corpus callosum for sport impacts,” *Journal of Biomechanics*, vol. 61, pp. 183–192, Aug. 2017, doi: 10.1016/j.jbiomech.2017.07.013.

[153] T. W. McAllister, j. c. Ford, S. Ji. J. G. Beckwith, L. A. Flashman, K. Paulsen, and R. M. Greenwald, “Maximum Principal Strain and Strain Rate Associated with Concussion Diagnosis Correlates with Changes in Corpus Callosum White Matter Indices,” *Annals of Biomedical Engineering*, vol. 40, no. 1, pp. 127–140, Jan. 2012, doi: 10.1007/s10439-011-0402-6.

[154] L. F. Gabler, J. R. Crandall, and M. B. Panzer, “Investigating Brain Injury Tolerance in the Sagittal Plane Using a Finite Element Model of the Human Head,” *International Journal of Automotive Engineering*, vol. 7, no. 1, p. 20164082, 2016, doi: 10.20485/jsaeijae.7.1_37.

[155] B. S. Elkin, L. F. Gabler, M. B. Panzer, and G. P. Siegmund, “Brain tissue strains vary with head impact location: A possible explanation for increased concussion risk in struck versus striking football players,” *Clinical Biomechanics*, vol. 64, pp. 49–57, Apr. 2019, doi: 10.1016/j.clinbiomech.2018.03.021.

[156] D. A. Bruneau and D. S. Cronin, “Brain response of a computational head model for prescribed skull kinematics and simulated football helmet impact boundary conditions,” *Journal of the Mechanical Behavior of Biomedical Materials*, vol. 115, p. 104299, Mar. 2021, doi: 10.1016/j.jmbbm.2020.104299.

[157] W. Zhao and S. Ji, “Mesh Convergence Behavior and the Effect of Element Integration of a Human Head Injury Model,” *Annals of Biomedical Engineering*, vol. 47, no. 2, pp. 475–486, Feb. 2019, doi: 10.1007/s10439-018-02159-z.

[158] R. W. G. Anderson, “A study on the biomechanics of axonal injury,” Ph.D., University of Adelaide, 2000.

[159] A. Rycman, S. D. McLachlin, and D. S. Cronin, “Spinal Cord Boundary Conditions Affect Brain Tissue Strains in Impact Simulations,” *Annals of Biomedical Engineering*, vol. 51, no. 4, pp. 783–793, Apr. 2023, doi: 10.1007/s10439-022-03089-7.

[160] S. Ji, H. Ghandyani, R. P. Bolander, J. G. Beckwith, J. C. Ford, T. W. McAllister, L. A. Flashman, K. D. Paulsen, K. Ernstrom, S. Jain, R. Raman, L. Zhang, R. M. Greenwald, “Parametric Comparisons of Intracranial Mechanical Responses from Three Validated Finite Element Models of the Human Head,” *Annals of Biomedical Engineering*, vol. 42, no. 1, pp. 11–24, Jan. 2014, doi: 10.1007/s10439-013-0907-2.

[161] P. M. Arenth, K. C. Russell, J. M. Scanlon, L. J. Kessler, and J. H. Ricker, “Corpus Callosum Integrity and Neuropsychological Performance After Traumatic Brain Injury,” *Journal of Head Trauma Rehabilitation*, vol. 29, no. 2, pp. E1–E10, Mar. 2014, doi: 10.1097/HTR.0b013e318289ede5.

[162] T. Nishimoto and S. Murakami, “Relation Between Diffuse Axonal Injury and Internal Head Structures on Blunt Impact,” *Journal of Biomechanical Engineering*, vol. 120, no. 1, pp. 140–147, Feb. 1998, doi: 10.1115/1.2834294.

[163] P. V. Bayly, T. S. Cohen, E. P. Leister, D. Ajo, E. C. Leuthardt, and G. M. Genin, “Deformation of the Human Brain Induced by Mild Acceleration,” *Journal of Neurotrauma*, vol. 22, no. 8, pp. 845–856, Aug. 2005, doi: 10.1089/neu.2005.22.845.

[164] A. A. Sabet, E. Christoforou, B. Zatlin, G. M. Genin, and P. V. Bayly, “Deformation of the human brain induced by mild angular head acceleration,” *Journal of Biomechanics*, vol. 41, no. 2, pp. 307–315, 2008, doi: 10.1016/j.jbiomech.2007.09.016.

[165] Y. Feng, T. M. Abney, R. J. Okamoto, R. B. Pless, G. M. Genin, and P. V. Bayly, “Relative brain displacement and deformation during constrained mild frontal head impact,” *Journal of The Royal Society Interface*, vol. 7, no. 53, pp. 1677–1688, Dec. 2010, doi: 10.1098/rsif.2010.0210.

[166] F. Hernandez, C. Giordano, M. Goubran, S. N. Parivash, G. A. Grant, M. Zeineh, D. B. Camarillo, “Lateral impacts correlate with falx cerebri displacement and corpus callosum trauma in sports-related concussions,” *Biomechanics and Modeling in Mechanobiology*, vol. 18, no. 3, pp. 631–649, Jun. 2019, doi: 10.1007/s10237-018-01106-0.

[167] L. Zhang, K. H. Yang, and A. I. King, “Comparison of Brain Responses Between Frontal and Lateral Impacts by Finite Element Modeling,” *Journal of Neurotrauma*, vol. 18, no. 1, pp. 21–30, Jan. 2001, doi: 10.1089/089771501750055749.

[168] A. S. McINTOSH, P. McCRORY, and and J. COMERFORD, “The dynamics of concussive head impacts in rugby and Australian rules football,” *Medicine and Science in Sports and Exercise*, vol. 32, no. 12, pp. 1980–1984, Dec. 2000, doi: https://doi.org/10.1097/00005768-200012000-00002.

[169] A. S. McIntosh, D. A. Patton, B. Fréchède, P.-A. Pierré, E. Ferry, and T. Barthels, “The biomechanics of concussion in unhelmeted football players in Australia: a case–control study,” *BMJ Open*, vol. 4, no. 5, p. e005078, May 2014, doi: 10.1136/bmjopen-2014-005078.

[170] D. Bruneau, “Investigation of Head and Brain Response in Football Helmet Impacts using a Finite Element Model of the Head and Neck with Active Muscle,” Master of Applied Science, University of Waterloo, Waterloo, ON, 2019.

[171] J. J. Crisco, R. Fiore, J. G. Beckwith, J. J. Chu, P. Brolinson, S. Duma, T. W. McAllister, A. Duhaime, R. M. Greenwald, “Frequency and Location of Head Impact Exposures in Individual Collegiate Football Players,” *Journal of Athletic Training*, vol. 45, no. 6, pp. 549–559, Nov. 2010, doi: 10.4085/1062-6050-45.6.549.

[172] R. A. Stern, D. O. Riley, D. H. Daneshvar, C. J. Nowinski, R. C. Cantu, and A. C. McKee, “Long-term Consequences of Repetitive Brain Trauma: Chronic Traumatic Encephalopathy,” *PM&R*, vol. 3, pp. S460–S467, Oct. 2011, doi: 10.1016/j.pmrj.2011.08.008.

[173] J. E. Bailes, A. L. Petraglia, B. I. Omalu, E. Nauman, and T. Talavage, “Role of subconcussion in repetitive mild traumatic brain injury,” *Journal of Neurosurgery*, vol. 119, no. 5, pp. 1235–1245, Nov. 2013, doi: 10.3171/2013.7.JNS121822.

[174] G. Tierney, “Concussion biomechanics, head acceleration exposure and brain injury criteria in sport: a review,” *Sports Biomechanics*, pp. 1–29, Dec. 2021, doi: 10.1080/14763141.2021.2016929.

[175] T. M. Talavage, E. A. Nauman, E. L. Breedlove, U. Yoruk, A. E. Dye, K. E. Morigaki, H. Feuer, L. J. Leverenz, “Functionally-Detected Cognitive Impairment in High School Football Players without Clinically-Diagnosed Concussion,” *Journal of Neurotrauma*, vol. 31, no. 4, pp. 327–338, Feb. 2014, doi: 10.1089/neu.2010.1512.

[176] J. J. Bazarian, T. Zhu, B. Blyth, A. Borrino, and J. Zhong, “Subject-specific changes in brain white matter on diffusion tensor imaging after sports-related concussion,” *Magnetic Resonance Imaging*, vol. 30, no. 2, pp. 171–180, Feb. 2012, doi: 10.1016/j.mri.2011.10.001.

[177] B. I. Omalu, S. T. DeKosky, R. L. Minster, M. I. Kamboh, R. L. Hamilton, and C. H. Wecht, “Chronic Traumatic Encephalopathy in a National Football League Player,” *Neurosurgery*, vol. 57, no. 1, pp. 128–134, Jul. 2005, doi: 10.1227/01.NEU.0000163407.92769.ED.

[178] B. Omalu, J. L. Hammers, J. Bailes, R. L. Hamilton, M. I. Kamboh, G. Webster, R. P. Fitzsimmons, “Chronic traumatic encephalopathy in an Iraqi war veteran with posttraumatic stress disorder who committed suicide,” *Neurosurgical Focus*, vol. 31, no. 5, p. E3, Nov. 2011, doi: 10.3171/2011.9.FOCUS11178.

[179] A. C. McKee, R. C. Cantu, C. J. Nowinski, E. T. Hedley-Whyte, B. E. Gavett, A. E. Budson, V. E. Santini, H. Lee, C. A. Kublius, R. A. Stern, “Chronic Traumatic Encephalopathy in Athletes: Progressive Tauopathy After Repetitive Head Injury,” *Journal of Neuropathology & Experimental Neurology*, vol. 68, no. 7, pp. 709–735, Jul. 2009, doi: 10.1097/NEN.0b013e3181a9d503.

[180] E. J. Lehman, M. J. Hein, S. L. Baron, and C. M. Gersic, “Neurodegenerative causes of death among retired National Football League players,” *Neurology*, vol. 79, no. 19, pp. 1970–1974, Nov. 2012, doi: 10.1212/WNL.0b013e31826daf50.

[181] B. I. Omalu, J. Bailes, J. L. Hammers, and R. P. Fitzsimmons, “Chronic Traumatic Encephalopathy, Suicides and Parasuicides in Professional American Athletes,” *American Journal of Forensic Medicine & Pathology*, vol. 31, no. 2, pp. 130–132, Jun. 2010, doi: 10.1097/PAF.0b013e3181ca7f35.

[182] A. C. McKee, R. A. Stern, C. J. Nowinski, T. D. Stein, V. E. Alvarez, D. H. Daneshvar, H. S. Lee, S. M. Wojtowicz, G. Hall, C. M. Baugh, D. O. Riley, C. A. Kubilus, K. A. Cormier,M. A. Jacobs, B. R. Martin, C. R. Abraham, T. Ikezu, R. R. Reichard, B. L. Wolozin, A. E. Budson, L. E. Goldstein, N. W. Kowall, R. C. Cantu, “The spectrum of disease in chronic traumatic encephalopathy,” *Brain*, vol. 136, no. 1, pp. 43–64, Jan. 2013, doi: 10.1093/brain/aws307.

[183] J. D. Kocsis and A. Tessler, “Pathology of blast-related brain injury,” *The Journal of Rehabilitation Research and Development*, vol. 46, no. 6, p. 667, 2009, doi: 10.1682/JRRD.2008.08.0100.

[184] H. Terrio, L. A. Brenner, B. J. Ivins, J. M. Cho, K. Helmick, K. Schwab, K. Scally, R. Bretthauer, and D. Warden, “Traumatic Brain Injury Screening,” *Journal of Head Trauma Rehabilitation*, vol. 24, no. 1, pp. 14–23, Jan. 2009, doi: 10.1097/HTR.0b013e31819581d8.

[185] C. L. Mac Donald, A. M. Johnson, D. Cooper, E. C. Nelson, N. J. Werner, J. S. Shimony, A. Z. Snyder, M. E. Raichle, J. R. Witherow, R. Fang, S. F. Flaherty, and D. L. Brody, “Detection of Blast-Related Traumatic Brain Injury in U.S. Military Personnel,” *New England Journal of Medicine*, vol. 364, no. 22, pp. 2091–2100, Jun. 2011, doi: 10.1056/NEJMoa1008069.

[186] A. M. Boutté, B. Thangavelu, C. R. LaValle, J. Nemes, J. Gilsdorf, D. A. Shear, and G. H. Kamimori, “Brain-related proteins as serum biomarkers of acute, subconcussive blast overpressure exposure: A cohort study of military personnel,” *PLOS One*, vol. 14, no. 8, p. e0221036, Aug. 2019, doi: 10.1371/journal.pone.0221036.

[187] G. H. Kamimori, L. A. Reilly, C. R. LaValle, and U. B. Olaghere Da Silva, “Occupational overpressure exposure of breachers and military personnel,” *Shock Waves*, vol. 27, no. 6, pp. 837–847, Nov. 2017, doi: 10.1007/s00193-017-0738-4.

[188] F. G. Hirsch, “EFFECTS OF OVERPRESSURE ON THE EAR-A REVIEW*,” *Annals of the New York Academy of Sciences*, vol. 152, no. 1, pp. 147–162, Oct. 1968, doi: 10.1111/j.1749-6632.1968.tb11972.x.

[189] B. Thangavelu, C. R. LaValle, M. J. Egnoto, J. Nemes, A. M. Boutté, and G. H. Kamimori, “Overpressure Exposure From .50-Caliber Rifle Training Is Associated With Increased Amyloid Beta Peptides in Serum,” *Frontiers in Neurology*, vol. 11, Jul. 2020, doi: 10.3389/fneur.2020.00620.

[190] M. Lang, G. H. Kamimori, A. Misistia, C. R. LaValle, A. N. Ramos, M. Y. Ghebremedhin, and M. J. Egnoto, “Shooter-Experienced Blast Overpressure in .50-Caliber Rifle s,” *Journal of Special Operations Medicine*, vol. 18, no. 4, p. 87, 2018, doi: 10.55460/9YOK-PEQH.

[191] D. Meinke, D. S. Finan, G. A. Flamme, W. J. Murphy, M. Stewart, J. E. Lankford, and S. Tasko, “Prevention of Noise-Induced Hearing Loss from Recreational Firearms,” *Seminars in Hearing*, vol. 38, no. 04, pp. 267–281, Nov. 2017, doi: 10.1055/s-0037-1606323.

[192] S. Ouellet and G. St-Onge, “Measurement of head kinematics of snipers firing a 0.50 caliber Rifle ,” in *IRCOBI Conference*, 2021, pp. 211–212.

[193] Sharon Adams, “The toll on a sniper’s brain,” *Legion, Canada’s Military History Magazine*, Mar. 21, 2019.

[194] R. Gellner, M. Begonia, S. Gagliardi, G. Tierney, and S. Rowson, “Optimal Cutoff Frequencies for Filtering Linear Acceleration and Angular Velocity Signals Associated with Laboratory Head Impacts Measured with Externally Mounted Sensors,” in *2023 IRCOBI Conference Proceedings*, 2023, pp. 332–342.

[195] E. J. Sanchez, L. F. Gabler, A. B. Good, J. R. Funk, J. R. Crandall, and M. B. Panzer, “A reanalysis of football impact reconstructions for head kinematics and finite element modeling,” *Clinical Biomechanics*, vol. 64, pp. 82–89, Apr. 2019, doi: 10.1016/j.clinbiomech.2018.02.019.

[196] S. P. Broglio, J. J. Sosnoff, S. Shin, X. He, C. Alcaraz, and J. Zimmerman, “Head Impacts During High School Football: A Biomechanical Assessment,” *Journal of Athletic Training*, vol. 44, no. 4, pp. 342–349, Jul. 2009, doi: 10.4085/1062-6050-44.4.342.

[197] S. P. Broglio, B. Schnebel, J. J. Sosnoff, S. Shin, X. Feng, X. He, J. Zimmerman, “Biomechanical Properties of Concussions in High School Football,” *Medicine & Science in Sports & Exercise*, vol. 42, no. 11, pp. 2064–2071, Nov. 2010, doi: 10.1249/MSS.0b013e3181dd9156.

[198] P. G. Brolinson, S. Manoogian, D. McNeely, M. Goforth, R. Greenwald, and S. Duma, “Analysis of Linear Head Accelerations from Collegiate Football Impacts,” *Current Sports Medicine Reports*, vol. 5, no. 1, pp. 23–28, Feb. 2006, doi: 10.1097/01.CSMR.0000306515.87053.fa.

[199] K. M. Guskiewicz, J. P. Mihalik, V. Shankar, S. W. Marshall, D. H. Crowell, S. M. Oliaro, M. F. Ciocca, and D. N. Hooker, “Measurement of head impacts in collegiate football players:

relationship between head impact biomechanics and acute clinical outcome after concussion," *Neurosurgery*, vol. 61, no. 6, pp. 1244–1253, Dec. 2007, doi: 10.1227/01.neu.0000306103.68635.1a.

[200] R. S. Naunheim, J. Standeven, C. Richter, and L. M. Lewis, "Comparison of Impact Data in Hockey, Football, and Soccer," *Journal of Trauma: Injury, Infection, and Critical Care*, vol. 48, no. 5, 2000.

[201] J. A. Newman, M. C. Beusenberg, N. Shewchenko, C. Withnall, and E. Fournier, "Verification of biomechanical methods employed in a comprehensive study of mild traumatic brain injury and the effectiveness of American football helmets," *Journal of Biomechanics*, vol. 38, no. 7, pp. 1469–1481, Jul. 2005, doi: 10.1016/j.jbiomech.2004.06.025.

[202] B. Schnebel, J. T. Gwin, S. Anderson, and R. Gatlin, "In vivo study of head impacts in football: a comparison of National Collegiate Athletic Association Division I versus high school impacts," *Neurosurgery*, vol. 60, no. 3, pp. 490–496, Mar. 2007, doi: 10.1227/01.NEU.0000249286.92255.7F.

[203] R. T. Stone, B. F. Moeller, R. R. Mayer, B. Rosenquist, D. Van Ryswyk, and D. Eichorn, "Biomechanical and Performance Implications of Weapon Design," *Human Factors: The Journal of the Human Factors and Ergonomics Society*, vol. 56, no. 4, pp. 684–695, Jun. 2014, doi: 10.1177/0018720813509107.

[204] C. P. Kemnitz, R. F. Johnson, D. J. Merullo, and V. J. Rice, "Relation of Rifle Stock Length and Weight to Military Rifle Marksmanship Performance by Men and Women," *Perceptual and Motor Skills*, vol. 93, no. 2, pp. 479–485, Oct. 2001, doi: 10.2466/pms.2001.93.2.479.

[205] A. D. Osborne and S. Smith, "Analysis of M16A2 Rifle characteristics and recommended improvements.," Fort Benning, GA: Litton Mellonic System Development Division, 1986.

[206] K. M. Guskiewicz and J. P. Mihalik, "Biomechanics of Sport Concussion," *Exercise and Sport Sciences Reviews*, vol. 39, no. 1, pp. 4–11, Jan. 2011, doi: 10.1097/JES.0b013e318201f53e.

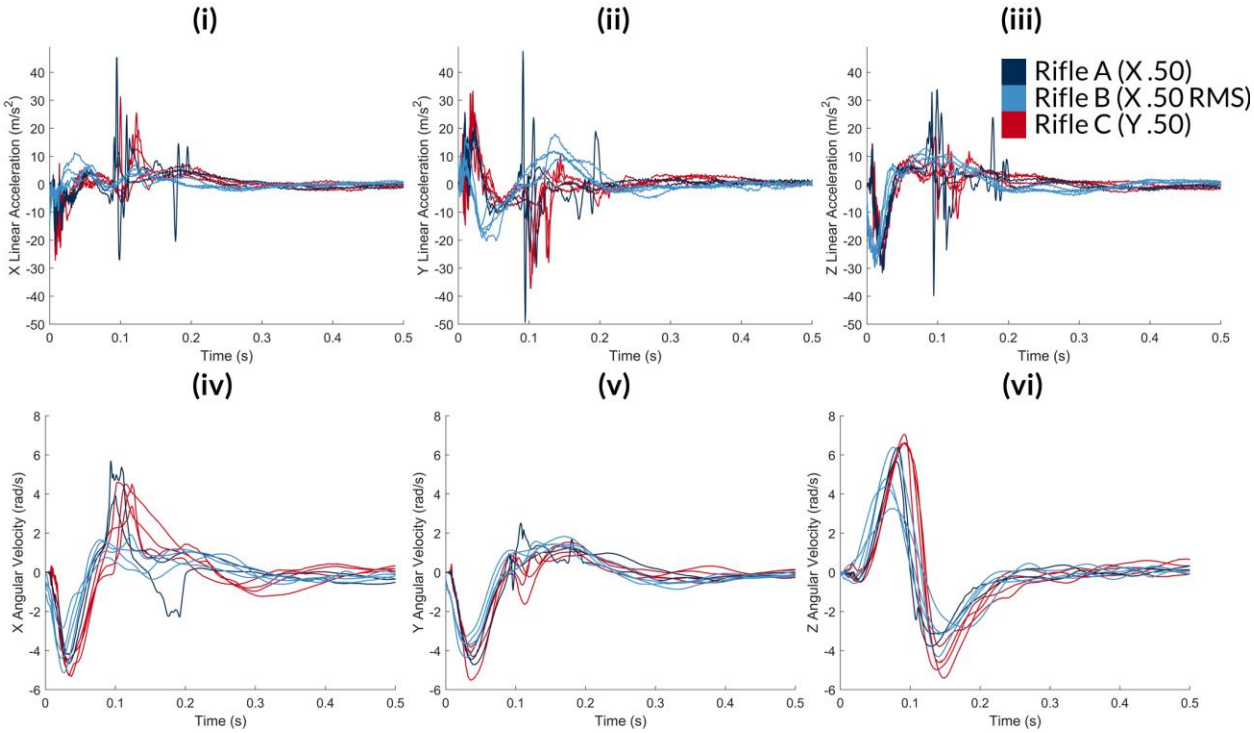
[207] B. S. Elkin, L. F. Gabler, M. B. Panzer, and G. P. Siegmund, "Brain tissue strains vary with head impact location: A possible explanation for increased concussion risk in struck versus striking football players," *Clinical Biomechanics*, vol. 64, pp. 49–57, Apr. 2019, doi: 10.1016/j.clinbiomech.2018.03.021.

[208] J. T. Eckner, A. Goshtasbi, K. Curtis, A. Kapshai, E. Myyra, L. M. Franco, M. Favre, J. A. Jacobson, J. A. Ashton-Miller, "Feasibility and Effect of Cervical Resistance Training on Head Kinematics in Youth Athletes," *American Journal of Physical Medicine & Rehabilitation*, vol. 97, no. 4, pp. 292–297, Apr. 2018, doi: 10.1097/PHM.0000000000000843.

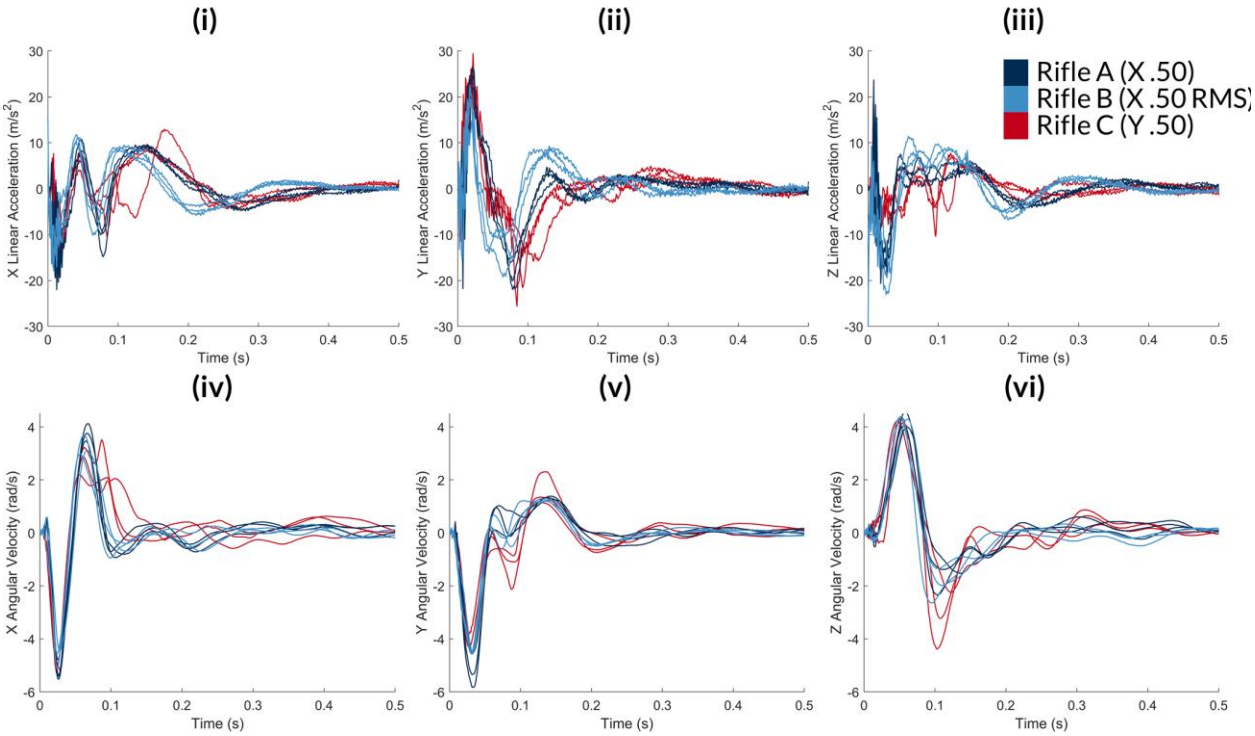
[209] R. T. Tierney, M. R. Sitler, C. B. Swanik, K. A. Swanik, M. Higgins, and J. Torg, "Gender Differences in Head-Neck Segment Dynamic Stabilization during Head Acceleration," *Medicine & Science in Sports & Exercise*, vol. 37, no. 2, pp. 272–279, Feb. 2005, doi: 10.1249/01.MSS.0000152734.47516.AA

Appendix

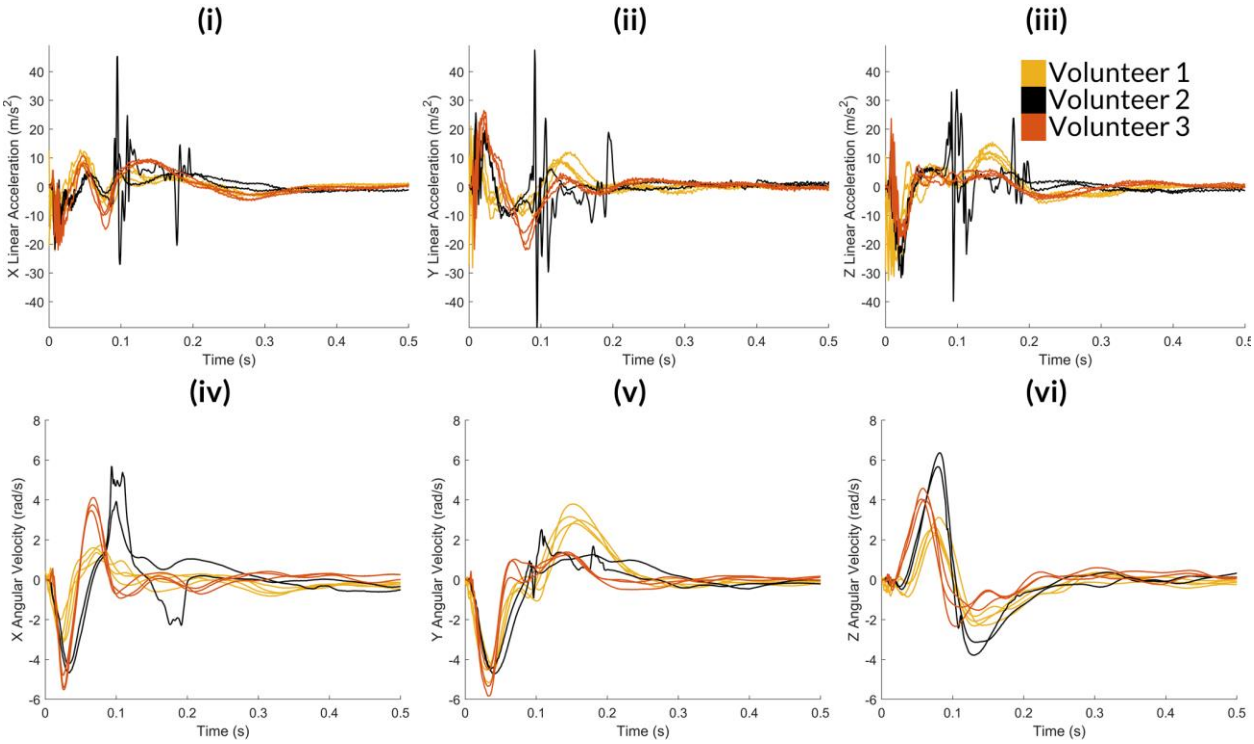
Appendix A: Head Kinematics



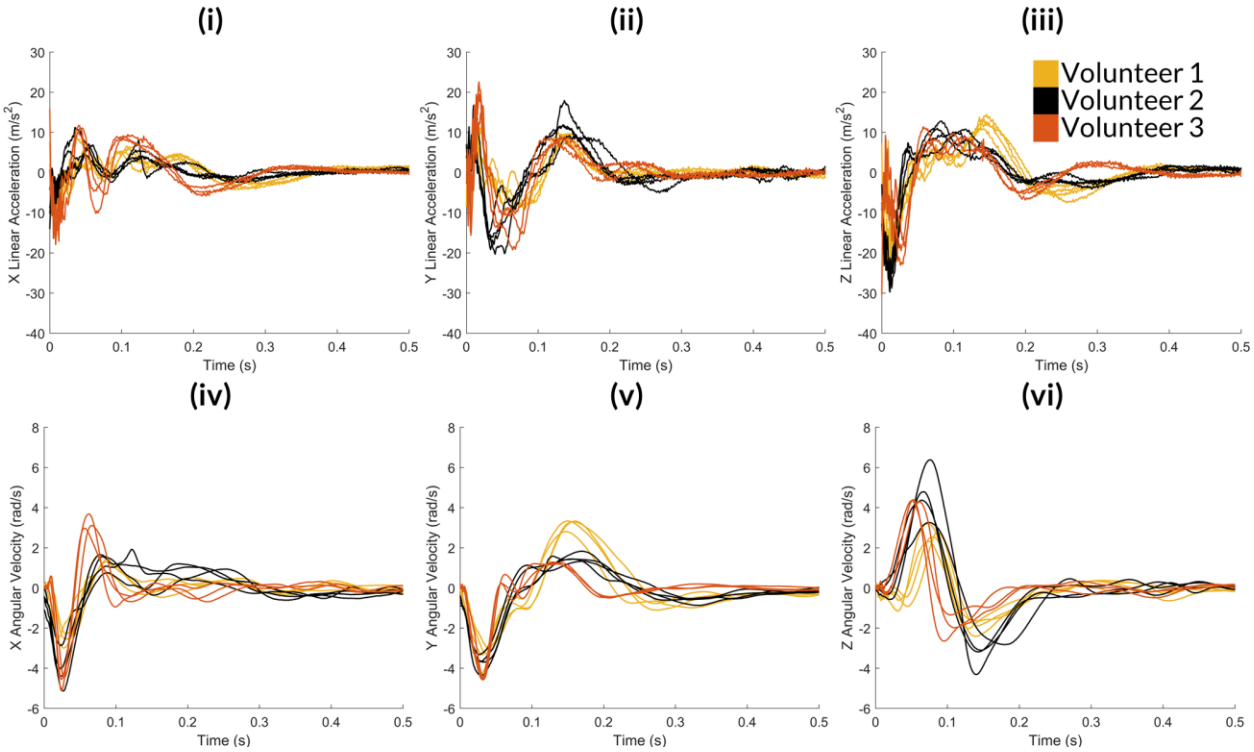
Appendix Figure 55: The head kinematics for Volunteer 2 (from Dataset 1: May 2021), including (i) linear acceleration in X, (ii) linear acceleration in Y, (iii) linear acceleration in Z, (iv) angular velocity in X, (v) angular velocity in Y and (vi) angular velocity in Z for all the shots fired using Rifles A, B and C. Note that the designation in brackets represents the features of each Rifle; for example, Rifle A (X .50) indicates that Rifle A has Chassis X and is a 50 caliber rifle.



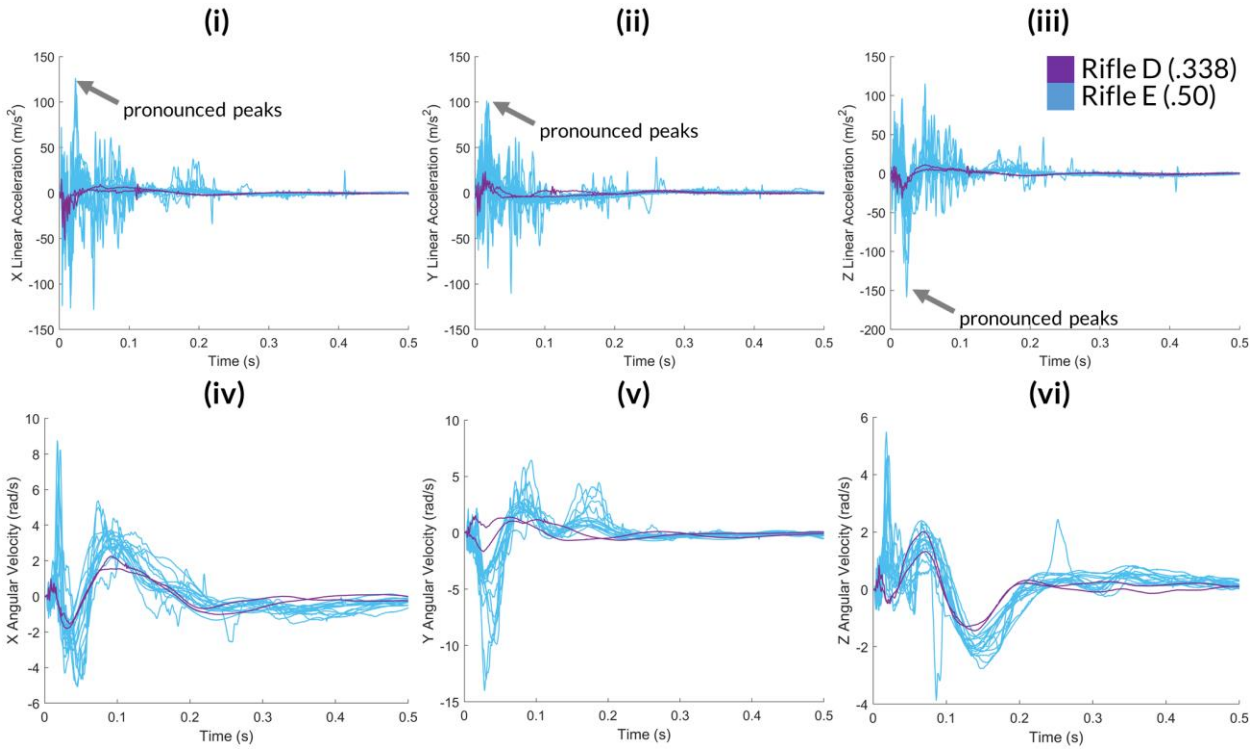
Appendix Figure 56: The head kinematics for Volunteer 3 (from Dataset 1: May 2021), including (i) linear acceleration in X, (ii) linear acceleration in Y, (iii) linear acceleration in Z, (iv) angular velocity in X, (v) angular velocity in Y and (vi) angular velocity in Z for all the shots fired using Rifles A, B and C. Note that the designation in brackets represents the features of each rifle; for example Rifle A (X .50) indicates that Rifle A has Chassis X and is a 50 caliber rifle.



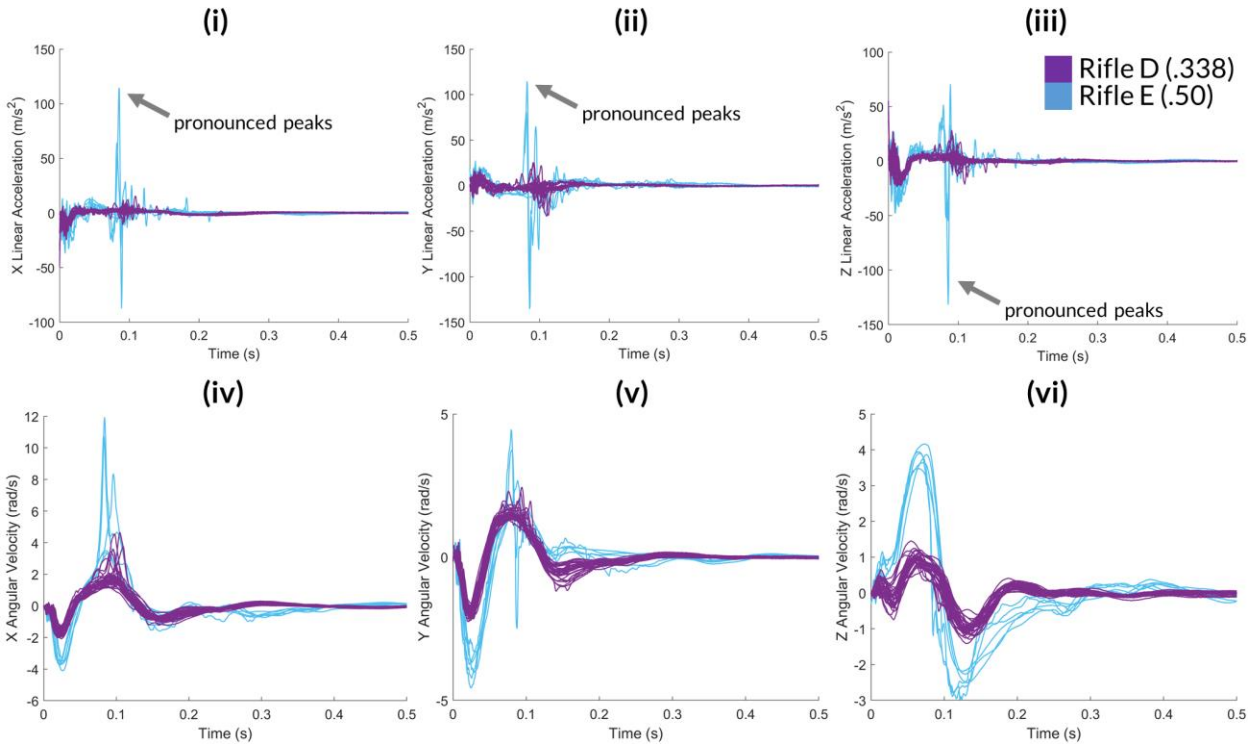
Appendix Figure 57: The head kinematics of Volunteers 1,2 and 3 (from Dataset 1: May 2021) firing Rifle A**,** including (i) linear acceleration in X, (ii) linear acceleration in Y, (iii) linear acceleration in Z, (iv) angular velocity in X, (v) angular velocity in Y and (vi) angular velocity in Z.



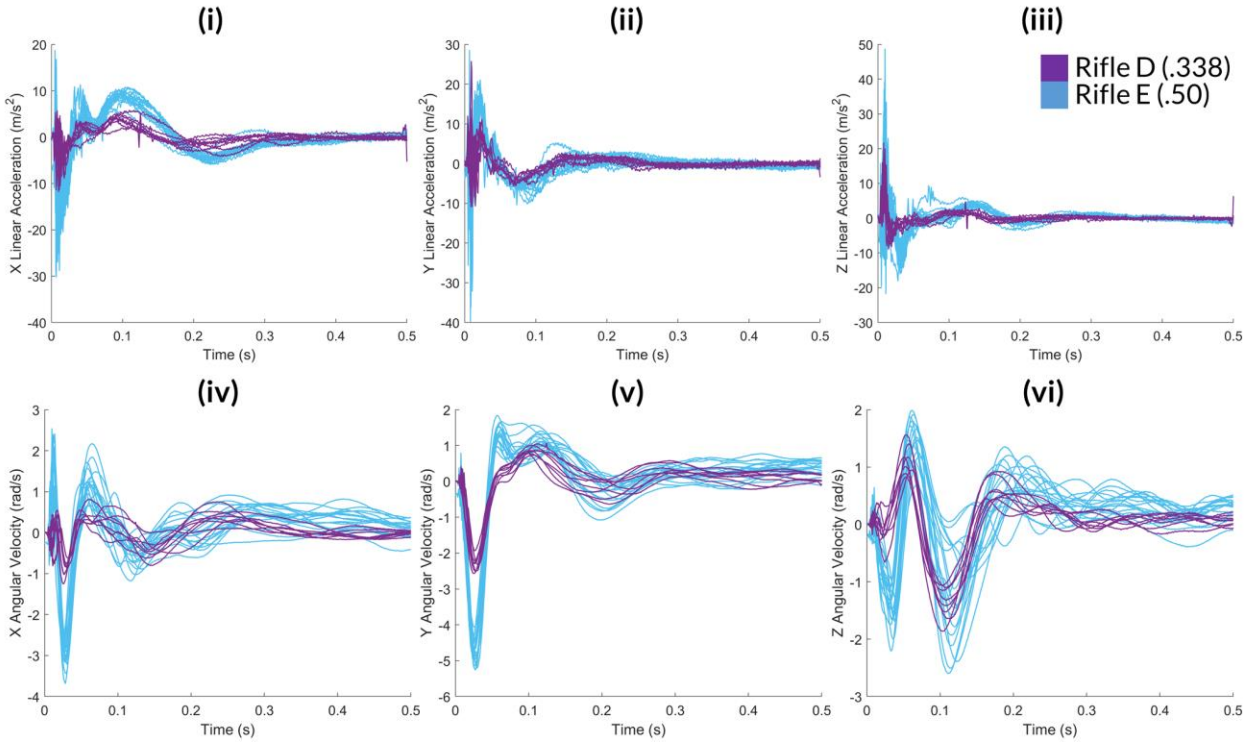
Appendix Figure 58: The head kinematics of Volunteers 1,2 and 3 (from Dataset 1: May 2021) firing Rifle B, including (i) linear acceleration in X, (ii) linear acceleration in Y, (iii) linear acceleration in Z, (iv) angular velocity in X, (v) angular velocity in Y and (vi) angular velocity in Z.



Appendix Figure 59: The head kinematics for Volunteer 5 (from Dataset 2: May 2022), including (i) linear acceleration in X, (ii) linear acceleration in Y, (iii) linear acceleration in Z, (iv) angular velocity in X, (v) angular velocity in Y and (vi) angular velocity in Z for all the shots fired using Rifles D and E. Note that the designation in brackets represents the features of each rifle; for example Rifle A (.338) indicates that Rifle D 338 caliber rifle.



Appendix Figure 60: The head kinematics for Volunteer 6 (from Dataset 2: May 2022), including (i) linear acceleration in X, (ii) linear acceleration in Y, (iii) linear acceleration in Z, (iv) angular velocity in X, (v) angular velocity in Y and (vi) angular velocity in Z for all the shots fired using Rifles D, and E. Note that the designation in brackets represents the features of each rifle; for example Rifle A (.338) indicates that Rifle D 338 caliber rifle.



Appendix Figure 61: The head kinematics for Volunteer 7 (from Dataset 2: May 2022), including (i) linear acceleration in X, (ii) linear acceleration in Y, (iii) linear acceleration in Z, (iv) angular velocity in X, (v) angular velocity in Y and (vi) angular velocity in Z for all the shots fired using Rifles D and E. Note that the designation in brackets represents the features of each rifle; for example Rifle A (.338) indicates that Rifle D 338 caliber rifle.

Appendix B: HIC_{15}

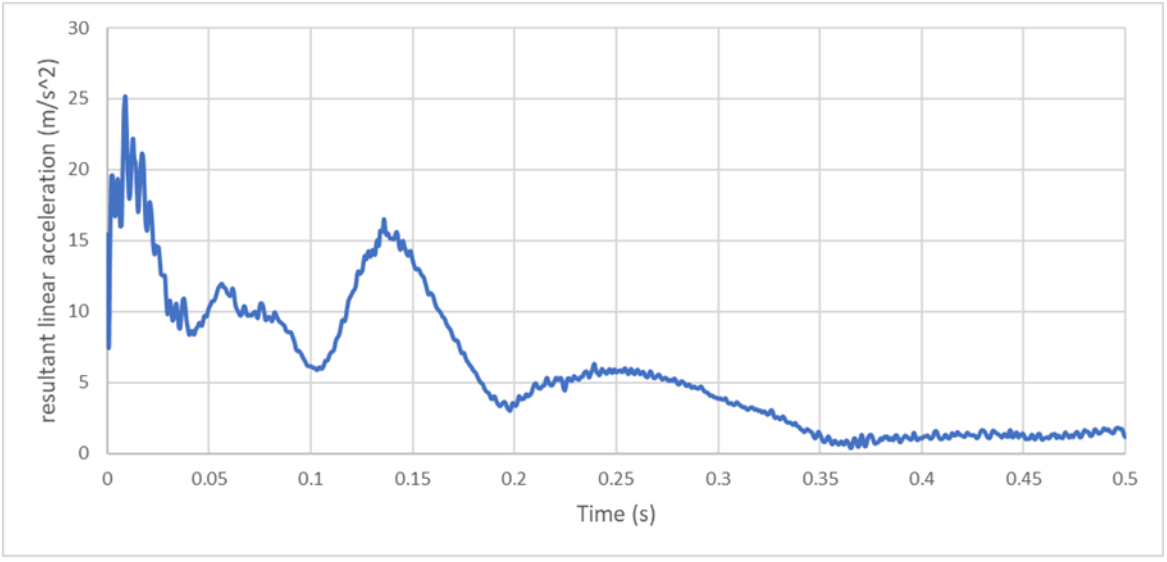
Process to calculate HIC_{15} using MATLAB script

- After filtering using 2023-01-09_UWaterloo_Signal_Processing_Methodology, the processing script outputs a CSV file with all the kinematics for each shot (Appendix Figure 62).

	A	B	C	D	E	F	G	H	I	J	K	L	M	N	O	P	Q
1	Time	LA.X	LA.Y	LA.Z	LA.R	LV.X	LV.Y	LV.Z	LV.R	AA.X	AA.Y	AA.Z	AA.R	AV.X	AV.Y	AV.Z	AV.R
2	(s)	(m/s^2)	(m/s^2)	(m/s^2)	(m/s^2)	(m/s)	(m/s)	(m/s)	(m/s)	(rad/s^2)	(rad/s^2)	(rad/s^2)	(rad/s^2)	(rad/s)	(rad/s)	(rad/s)	(rad/s)
3	0	-13.5834	-0.77897	7.29604	15.43853	-46.998	45.72794	-121.732	138.2694	0.00048	0.000376	-0.00054	0.000815	0.105648	-0.02362	0.077523	0.133152
4	0.000626	-6.45508	-1.02616	-3.4768	7.403324	-111.448	-63.4011	-124.502	178.7207	-0.00598	-0.00069	0.000792	0.006068	0.076819	-0.0308	0.022805	0.085846
5	0.001252	-2.40733	-1.24976	-14.3486	14.6027	-175.897	-172.53	-127.273	277.3172	-0.00942	-9.74E-05	-0.00366	0.010103	-0.02406	-0.08896	-0.08061	0.122433
798																	
799	0.497497	0.710035	-1.40108	0.563235	1.668656	5.939999	2.629391	2.24582	6.873208	0.052205	0.066227	-0.06063	0.10386	-0.02682	-0.3066	0.142986	0.339363
800	0.498123	1.066963	-1.27478	0.33978	1.696737	5.59885	-0.62301	-0.76909	5.685662	0.052777	0.064812	-0.06049	0.103177	-0.02356	-0.30773	0.150304	0.343289
801	0.498748	1.213736	-0.89478	0.351608	1.548356	5.706091	-0.5245	-4.72992	7.430124	0.053703	0.064488	-0.06049	0.103449	-0.01996	-0.31067	0.144231	0.343096
802	0.499374	1.013963	-0.49366	0.500497	1.233821	5.959798	2.071165	-8.44994	10.54564	0.054438	0.064452	-0.0602	0.103642	-0.01641	-0.30985	0.135097	0.338418
803	0.5	0.907148	-0.19491	0.613106	1.112118	6.213504	4.666828	-12.17	14.43935	0.054905	0.063657	-0.05981	0.10317	-0.01257	-0.30718	0.135808	0.336099

Appendix Figure 62: Example of CSV file after data processing for one shot by Volunteer 1. The signal has 800 data points, i.e., data is recorded every 0.000625 s.

- The resultant linear acceleration (Appendix Figure 63) graph can be plotted using columns A and E from the CSV file.



Appendix Figure 63: Example of the resultant linear acceleration plot for one shot of Volunteer 1

- The area under the curve is computed for each 0.015 s interval across 800 data points using the trapezoid rule, starting from t=0s up to the final 15 ms interval (Appendix Figure 64). The interval exhibiting the maximum area is identified as the integration segment in the HIC_{15} equation.

interval 1	interval 2	interval 3
Time	Time	Time
(s)	(s)	(s)
0	0	0
0.000626	0.000626	0.000626
0.001252	0.001252	0.001252
0.001877	0.001877	0.001877
0.002503	0.002503	0.002503
0.003129	0.003129	0.003129
0.003755	0.003755	0.003755
0.00438	0.00438	0.00438
0.005006	0.005006	0.005006
0.005632	0.005632	0.005632
0.006258	0.006258	0.006258
0.006884	0.006884	0.006884
0.007509	0.007509	0.007509
0.008135	0.008135	0.008135
0.008761	0.008761	0.008761
0.009387	0.009387	0.009387
0.010013	0.010013	0.010013
0.010638	0.010638	0.010638
0.011264	0.011264	0.011264
0.01189	0.01189	0.01189
0.012516	0.012516	0.012516
0.013141	0.013141	0.013141
0.013767	0.013767	0.013767
0.014393	0.014393	0.014393
0.015019	0.015019	0.015019
0.015645	0.015645	0.015645
0.01627	0.01627	0.01627
0.016896	0.016896	0.016896

Appendix Figure 64: Example of calculating the area for every 15 ms interval

- After calculating the maximum area, it is then substituted into the HIC_{15} equation to calculate the corresponding HIC_{15} value.
- Process 1 to 4 is performed in MATLAB for every shot fired (Appendix Figure 65).

```
fclose all;
close all;
clear;
clc;

fileNames = dir('E:\05_VRC_trial_V5\09_checkingHIC\*MG41041*');

for j=10

    M = readmatrix(extractBefore(fileNames(j).name,'.')); %reading excel file with all columns

    M1(:,1) = M(:,1); %copy over time column in seconds
    M1(:,2) = M(:,5); %copy over res acc column in m/s2
    M1(:,3) = M(:,5)*0.10197162; %convert m/s2 to G

    %finding t1,t2,area of each interval of 15ms or 0.015s
    %there are 800 data points i.e data recorded every 0.000625 s
    %0.015/0.000625 = 24 i.e there's 24 0.000625 in 0.015s
    %so need to calculate area for every 25 cells
    %800-24 = 776 should be last i value to capture last set of 0.015s
    for i=1:776

        M2(i,1)=M1(i,1); %t1
        M2(i,2)=M1(i+24,1); %t2
        M2(i,3)= M2(i,2) - M2(i,1); %t2-t1, checking if interval is 0.015
        M2(i,4) = trapz(M1(i:i+24,1),M1(i:i+24,3)); %area of each interval, x var is time, y var is res acc in G

    end


    areaWhole = trapz(M1(:,1),M1(:,3));

    [maxIntervalArea, RowmaxIntervalArea] = max(M2(:,4));

    Time1_maxIntervalArea = M2(RowmaxIntervalArea,1);
    Time2_maxIntervalArea = M2(RowmaxIntervalArea,2);

    timeinterval = Time2_maxIntervalArea - Time1_maxIntervalArea;

    HIC_value = (((1/timeinterval)*maxIntervalArea)^2.5)*timeinterval;

    HIC_table{j,1} = extractBefore(fileNames(j).name,'-Processed-HeadCoG'); %filename
    HIC_table{j,2} = areaWhole; %area under whole curve when y axis is in Gs and x axis is in sec
    HIC_table{j,3} = maxIntervalArea; %highest area of 0.015s interval
    HIC_table{j,4} = Time1_maxIntervalArea; %t1 where highest area occurs
    HIC_table{j,5} = Time2_maxIntervalArea; %t2 where highest area occurs
    HIC_table{j,6} = timeinterval; %t2-t1
    HIC_table{j,7} = HIC_value; %HIC15 value

end

% %Exporting data to file
% headers = {'MG ID',...
%     'Area under whole curve', 'highest area of 0.015s interval','t1 where highest area occurs',...
%     't2 where highest area occurs','time interval','HIC15 value'
%  };
%
% ToExport = [headers; HIC_table];
% writecell(ToExport,'41041_HIC.xlsx')
```

Appendix Figure 65: Script used to calculate HIC_{15} for each shot

HIC_{15} for all shots in Dataset 1: May 2021

Inter Rifle

Table 17: Summary of HIC_{15} values in Dataset 1: Volunteers 1,2,3 firing Rifles, A, B, and C

	Volunteer 1 Rifle A	**Volunteer 1 Rifle B**	**Volunteer 1 Rifle C**
shot 1	0.1430	0.0758	0.2324
shot 2	0.1355	0.0982	0.2254
shot 3	0.1635	0.0858	0.1855
shot 4	0.1067	0.0915	0.1260
mean HIC_{15}	**0.1372**	**0.0878**	**0.1923**
Sample standard deviation*	**0.0235**	**0.0095**	**0.0488**
Coefficient of variation (CV) %	**17.12**	**10.82**	**25.38**
	Volunteer 2 Rifle A	**Volunteer 2 Rifle B**	**Volunteer 2 Rifle C**
shot 1	0.3539	0.1138	0.2153
shot 2	0.1485	0.1275	0.2649
shot 3	x	0.1568	0.1748
shot 4	x	0.1516	0.1913
mean HIC_{15}	**0.2512**	**0.1374**	**0.2116**
Sample standard deviation	**0.1452**	**0.0203**	**0.0392**
Coefficient of variation (CV) %	**57.82**	**14.75**	**18.54**
	Volunteer 3 Rifle A	**Volunteer 3 Rifle B**	**Volunteer 3 Rifle C**
shot 1	0.1678	0.1420	0.1381
shot 2	0.2092	0.0706	0.1220
shot 3	0.1649	0.0961	0.1358
mean HIC_{15}	**0.1807**	**0.1029**	**0.1320**
Sample standard deviation	**0.0248**	**0.0362**	**0.0087**
Coefficient of variation (CV) %	**13.73**	**35.17**	**6.63**

*Sample standard deviation = $$\sqrt{\frac{\sum_i^n (x_i - x_{mean})^2}{n-1}}$$

where

x_i = observations in sample

x_{mean} = mean of all observations in sample

n = number of observations

Inter Volunteer

Table 18: Summary of HIC_{15} values in Dataset 1: Volunteers 1,2,3 firing Rifles, A, B, and C

	Volunteer 1 Rifle A	**Volunteer 2 Rifle A**	**Volunteer 3 Rifle A**
shot 1	0.1430	0.3539	0.1678
shot 2	0.1355	0.1485	0.2092
shot 3	0.1635	x	0.1649
shot 4	0.1067	x	x
mean HIC_{15}	**0.1372**	**0.2512**	**0.1807**
Sample standard deviation*	**0.0235**	**0.1452**	**0.0248**
Coefficient of variation (CV) %	**17.12**	**57.82**	**13.73**
	Volunteer 1 Rifle B	**Volunteer 2 Rifle B**	**Volunteer 3 Rifle B**
shot 1	0.0758	0.1138	0.1420
shot 2	0.0982	0.1275	0.0706
shot 3	0.0858	0.1568	0.0961
shot 4	0.0915	0.1516	x
mean HIC_{15}	**0.0878**	**0.1374**	**0.1029**
Sample standard deviation	**0.0095**	**0.0203**	**0.0362**
Coefficient of variation (CV) %	**10.82**	**14.75**	**35.17**
	Volunteer 1 Rifle C	**Volunteer 2 Rifle C**	**Volunteer 3 Rifle C**
shot 1	0.2324	0.2153	0.1381
shot 2	0.2254	0.2649	0.1220
shot 3	0.1855	0.1748	0.1358
shot 4	0.1260	0.1913	x
mean HIC_{15}	**0.1923**	**0.2116**	**0.1320**
Sample standard deviation	**0.0488**	**0.0392**	**0.0087**
Coefficient of variation (CV) %	**25.38**	**18.54**	**6.63**

HIC_{15} for all shots in Dataset 2: May 2022

Inter Rifle

Table 19: Summary of HIC_{15} values in Dataset 2: Volunteers 4,5 firing Rifles D, E

	Volunteer 4 Rifle D	Volunteer 4 Rifle E	Volunteer 5 Rifle D	Volunteer 5 Rifle E
shot 1	0.2666	198.1482	0.2217	0.5455
shot 2	0.2611	0.4487	0.0640	1.0431
shot 3	0.1458	4.9497	x	0.9478
shot 4	0.5689	72.2785	x	0.4898
shot 5	0.5266	4.7602	x	0.7735
shot 6	0.6388	531.2062	x	0.8572
shot 7	0.6881	81.8463	x	0.3468
shot 8	0.4829	72.8167	x	0.5358
shot 9	0.8794	229.8738	x	0.5270
shot 10	0.3139	38.1664	x	5.2673
shot 11	0.1497	43.5698	x	2.9338
shot 12	0.2493	x	x	5.0772
shot 13	0.1912	x	x	2.0935
shot 14	0.5523	x	x	2.4864
shot 15	0.2716	x	x	1.2332
shot 16	0.3250	x	x	x
shot 17	0.1231	x	x	x
shot 18	0.1461	x	x	x
shot 19	0.2199	x	x	x
shot 20	0.1288	x	x	x
shot 21	0.3910	x	x	x
shot 22	0.1439	x	x	x
shot 23	0.1428	x	x	x
shot 24	0.1828	x	x	x
shot 25	0.1202	x	x	x
shot 26	0.1151	x	x	x
shot 27	0.0711	x	x	x
shot 28	0.1990	x	x	x
shot 29	0.1220	x	x	x
shot 30	0.1549	x	x	x
shot 31	0.1406	x	x	x
shot 32	0.2589	x	x	x
shot 33	0.1605	x	x	x
shot 34	0.3469	x	x	x
shot 35	0.7173	x	x	x
shot 36	0.3756	x	x	x

mean HIC_{15}	**0.2992**	**116.1877**	**0.1428**	**1.6772**
Sample standard deviation	**0.2042**	**156.9768**	**0.1115**	**1.6160**
CV (%)	**68.24**	**135.11**	**78.08**	**96.35**

Table 20: Summary of HIC_{15} values in Dataset 2: Volunteer 6 firing Rifles D, E

	Volunteer 6 Rifle D	**Volunteer 6 Rifle E**
shot 1	0.0497	0.3386
shot 2	0.0462	0.2846
shot 3	0.0771	0.3354
shot 4	0.0471	0.4633
shot 5	0.0496	2.0729
shot 6	0.0394	4.7863
shot 7	0.0415	x
shot 8	0.0520	x
shot 9	0.0410	x
shot 10	0.0440	x
shot 11	0.0466	x
shot 12	0.0475	x
shot 13	0.0763	x
shot 14	0.0467	x
shot 15	0.0508	x
shot 16	0.0755	x
shot 17	0.0506	x
shot 18	0.0497	x
shot 19	0.0635	x
shot 20	0.0405	x
shot 21	0.0339	x
shot 22	0.0447	x
shot 23	0.0850	x
shot 24	0.0705	x
shot 25	0.0403	x
shot 26	0.0384	x
shot 27	0.1795	x
shot 28	0.0615	x
shot 29	0.0478	x
shot 30	0.1372	x
shot 31	0.0807	x
shot 32	0.1075	x
shot 33	0.0630	x
mean HIC_{15}	**0.0614**	**1.3802**

Sample standard deviation	**0.0304**	**1.8055**
CV (%)	**49.50**	**130.81**

Table 21: Summary of HIC_{15} values in Dataset 2: Volunteers 7,8 firing Rifles D, E

	Volunteer 7 Rifle D	**Volunteer 7 Rifle E**	**Volunteer 8 Rifle D**	**Volunteer 8 Rifle E**
shot 1	0.0083	0.0926	0.0359	0.1750
shot 2	0.0077	0.0996	0.0370	0.1280
shot 3	0.0156	0.0671	0.0342	0.1145
shot 4	0.0140	0.1119	0.0402	0.1327
shot 5	0.0111	0.0765	0.0355	0.1160
shot 6	0.0164	0.0845	x	0.2172
shot 7	0.0099	0.1065	x	0.1717
shot 8	0.0171	0.0955	x	0.1806
shot 9	x	0.0685	x	0.1549
shot 10	x	0.0782	x	0.1379
shot 11	x	0.0864	x	x
shot 12	x	0.0936	x	x
shot 13	x	0.0914	x	x
shot 14	x	0.0851	x	x
shot 15	x	0.1365	x	x
shot 16	x	0.0764	x	x
shot 17	x	0.1324	x	x
shot 18	x	0.0775	x	x
mean HIC_{15}	**0.0125**	**0.0922**	**0.0366**	**0.1528**
Sample standard deviation	**0.0037**	**0.0195**	**0.0023**	**0.0331**
CV (%)	**29.74**	**21.18**	**6.25**	**21.64**

Inter Volunteer

Table 22: Summary of HIC_{15} values in Dataset 2: Volunteers 4,5,6,7 and 8 firing Rifle D

	Volunteer 4	**Volunteer 5**	**Volunteer 6**	**Volunteer 7**	**Volunteer 8**
shot 1	0.2666	0.2217	0.0497	0.0083	0.0359
shot 2	0.2611	0.0640	0.0462	0.0077	0.0370
shot 3	0.1458	x	0.0771	0.0156	0.0342
shot 4	0.5689	x	0.0471	0.0140	0.0402
shot 5	0.5266	x	0.0496	0.0111	0.0355
shot 6	0.6388	x	0.0394	0.0164	x
shot 7	0.6881	x	0.0415	0.0099	x
shot 8	0.4829	x	0.0520	0.0171	x

shot 9	0.8794	x	0.0410	x	x
shot 10	0.3139	x	0.0440	x	x
shot 11	0.1497	x	0.0466	x	x
shot 12	0.2493	x	0.0475	x	x
shot 13	0.1912	x	0.0763	x	x
shot 14	0.5523	x	0.0467	x	x
shot 15	0.2716	x	0.0508	x	x
shot 16	0.3250	x	0.0755	x	x
shot 17	0.1231	x	0.0506	x	x
shot 18	0.1461	x	0.0497	x	x
shot 19	0.2199	x	0.0635	x	x
shot 20	0.1288	x	0.0405	x	x
shot 21	0.3910	x	0.0339	x	x
shot 22	0.1439	x	0.0447	x	x
shot 23	0.1428	x	0.0850	x	x
shot 24	0.1828	x	0.0705	x	x
shot 25	0.1202	x	0.0403	x	x
shot 26	0.1151	x	0.0384	x	x
shot 27	0.0711	x	0.1795	x	x
shot 28	0.1990	x	0.0615	x	x
shot 29	0.1220	x	0.0478	x	x
shot 30	0.1549	x	0.1372	x	x
shot 31	0.1406	x	0.0807	x	x
shot 32	0.2589	x	0.1075	x	x
shot 33	0.1605	x	0.0630	x	x
shot 34	0.3469	x	x	x	x
shot 35	0.7173	x	x	x	x
shot 36	0.3756	x	x	x	x
mean HIC_{15}	**0.2992**	**0.1428**	**0.0614**	**0.0125**	**0.0366**
std dev	**0.2042**	**0.1115**	**0.0304**	**0.0037**	**0.0023**
CV (%)	**68.24**	**78.08**	**49.50**	**29.74**	**6.25**

Table 23: Summary of HIC_{15} values in Dataset 2: Volunteers 4,5,6,7 and 8 firing Rifle E

	Volunteer 4	**Volunteer 5**	**Volunteer 6**	**Volunteer 7**	**Volunteer 8**
shot 1	198.1482	198.1482	0.3386	0.0926	0.1750
shot 2	0.4487	0.4487	0.2846	0.0996	0.1280
shot 3	4.9497	4.9497	0.3354	0.0671	0.1145
shot 4	72.2785	72.2785	0.4633	0.1119	0.1327
shot 5	4.7602	4.7602	2.0729	0.0765	0.1160
shot 6	531.2062	531.2062	4.7863	0.0845	0.2172

shot 7	81.8463	81.8463	x	0.1065	0.1717
shot 8	72.8167	72.8167	x	0.0955	0.1806
shot 9	229.8738	229.8738	x	0.0685	0.1549
shot 10	38.1664	38.1664	x	0.0782	0.1379
shot 11	43.5698	43.5698	x	0.0864	x
shot 12	x	5.0772	x	0.0936	x
shot 13	x	2.0935	x	0.0914	x
shot 14	x	2.4864	x	0.0851	x
shot 15	x	1.2332	x	0.1365	x
shot 16	x	x	x	0.0764	x
shot 17	x	x	x	0.1324	x
shot 18	x	x	x	0.0775	x
mean HIC_{15}	**116.1877**	**85.9303**	**1.3802**	**0.0922**	**0.1528**
std dev	**156.9768**	**142.4755**	**1.8055**	**0.0195**	**0.0331**
CV (%)	**135.11**	**165.80**	**130.81**	**21.18**	**21.64**

Statistical Analysis for Dataset 1

Inter Rifle (One-way ANOVA)

Table 24: One-Way ANOVA for Volunteer 1

Anova: Single Factor						
SUMMARY						
Groups	*Count*	*Sum*	*Average*	*Variance*		
Volunteer 1 rifle A	4	0.548655748	0.137164	0.000551		
Volunteer 1 rifle B	4	0.351237308	0.087809	9.03E-05		
Volunteer 1 rifle C	4	0.769304803	0.192326	0.002382		
ANOVA						
Source of Variation	*SS*	*df*	*MS*	*F*	*P-value*	*F crit*
Between Groups	0.02187004	2	0.010935	10.85113	**0.003998**	4.256495
Within Groups	0.009069579	9	0.001008			
Total	0.030939619	11				
is p value < 0.05?	Yes					
If yes, reject null hyp	i.e. at least 1 of the means of groups are diff					

Tukey Kramer test	compares the mean between each pairwaise combination of groups					
	step 1	**step 4**	**step 5**			
Comparison	**Abs. Mean Diff**	**Q critical Value**	**Significant?**			
A vs. B	0.04935461	0.062664195	No			
B vs. C	0.104516874	0.062664195	Yes			
A vs. C	0.055162264	0.062664195	No			
step 2						
Find Q critical value						
Q critical value = Q*√(s2pooled / n.)						
Q = Value from Studentized Range Q Table						
s2pooled = Pooled variance across all groups						
n. = Sample size for a given group						
Find Q value from studentized Range q Table						
q(k,df,alpha)						
k = number of groups	3					
df = n-k	9					
Q(3,9,0.05)	3.948					
pooled variance	0.001007731					
step 3						
sample size of each group	4					

Table 25: One-Way ANOVA for Volunteer 2

Anova: Single Factor						
SUMMARY						
Groups	*Count*	*Sum*	*Average*	*Variance*		
Volunteer 2 Rifle A	2	0.502412	0.251206	0.021094		
Volunteer 2 Rifle B	4	0.549787	0.137447	0.000411		
Volunteer 2 Rifle C	4	0.846374	0.211594	0.001539		
ANOVA						
Source of Variation	*SS*	*df*	*MS*	*F*	*P-value*	*F crit*
Between Groups	0.020405	2	0.010202	2.650528	**0.13901**	4.737414
Within Groups	0.026944	7	0.003849			

Total	0.047349	9				

Table 26: One-Way ANOVA for Volunteer 3

Anova: Single Factor						
SUMMARY						
Groups	*Count*	*Sum*	*Average*	*Variance*		
Volunteer 3 rifle A	3	0.541951	0.18065	0.000615		
Volunteer 3 rifle B	3	0.308667	0.102889	0.00131		
Volunteer 3 rifle C	3	0.395919	0.131973	7.65E-05		
ANOVA						
Source of Variation	*SS*	*df*	*MS*	*F*	*P-value*	*F crit*
Between Groups	0.009262	2	0.004631	6.941717	**0.02748**	5.143253
Within Groups	0.004003	6	0.000667			
Total	0.013265	8				
is p value < 0.05?	Yes					
If yes, reject null hyp	i.e. at least 1 of the means of groups are diff					
Tukey Kramer test	compares the mean between each pairwaise combination of groups					
	step 1	**step 4**	**step 5**			
Comparison	**Abs. Mean Diff**	**Q critical Value**	**Significant?**			
A vs. B	0.077761	0.064705	Yes			
B vs. C	0.029084	0.064705	No			
A vs. C	0.048677	0.064705	No			
step 2						
Find Q critical value						
Q critical value = Q*√(s2pooled / n.)						
Q = Value from Studentized Range Q Table						
s2pooled = Pooled variance across all groups						
n. = Sample size for a given group						
Find Q value from studentized Range q Table						

q(k,df,alpha)						
k = number of groups	3					
df = n-k	6					
Q(3,6,0.05)	4.339					
pooled variance	0.000667					
step 3						
sample size of each group	3					

Inter Volunteer (One-way ANOVA)

Table 27: One-Way ANOVA for Rifle A

Anova: Single Factor						
SUMMARY						
Groups	*Count*	*Sum*	*Average*	*Variance*		
Volunteer 1 Rifle A	4	0.548656	0.137164	0.000551		
Volunteer 2 Rifle A	2	0.502412	0.251206	0.021094		
Volunteer 3 Rifle A	3	0.541951	0.18065	0.000615		
ANOVA						
Source of Variation	*SS*	*df*	*MS*	*F*	*P-value*	*F crit*
Between Groups	0.017401	2	0.0087	2.177058	**0.194587**	5.143253
Within Groups	0.023978	6	0.003996			
Total	0.041379	8				

Table 28: One-Way ANOVA for Rifle B

Anova: Single Factor						
SUMMARY						
Groups	*Count*	*Sum*	*Average*	*Variance*		
Volunteer 1 rifle B	4	0.351237	0.087809	9.03E-05		
Volunteer 2 rifle B	4	0.549787	0.137447	0.000411		
Volunteer 3 rifle B	3	0.308667	0.102889	0.00131		
ANOVA						

Source of Variation	*SS*	*df*	*MS*	*F*	*P-value*	*F crit*
Between Groups	0.005135	2	0.002567	4.982217	**0.039328**	4.45897
Within Groups	0.004122	8	0.000515			
Total	0.009257	10				
is p value < 0.05?	Yes					
If yes, reject null hyp	i.e. at least 1 of the means of groups are diff					
Tukey Kramer test	compares the mean between each pairwaise combination of groups					
	step 1	**step 4**	**step 5**			
Comparison	**Abs. Mean Diff**	**Q critical Value**	**Significant?**			
1 vs. 2	0.0496	0.0496	No			
2 vs. 3	0.0346	0.0536	No			
1 vs. 3	0.0151	0.0536	No			
step 2						
Find Q critical value						
Q critical value = Q*√(s2pooled / n.)						
Q = Value from Studentized Range Q Table						
s2pooled = Pooled variance across all groups						
n. = Sample size for a given group						
Find Q value from studentized Range q Table						
q(k,df,alpha)						
k = number of groups	3					
df = n-k	8					
Q(3,8,0.05)	4.041					
pooled variance	0.000604					
step 3 - sample size						
harmonic mean 1,2	4					
harmonic mean 2,3	3.428571					
harmonic mean 1,3	3.428571					

Table 29: One-Way ANOVA for Rifle C

Anova: Single Factor						
SUMMARY						
Groups	*Count*	*Sum*	*Average*	*Variance*		
Volunteer 1 Rifle C	4	0.769305	0.192326	0.002382		
Volunteer 2 Rifle C	4	0.846374	0.211594	0.001539		
Volunteer 3 Rifle C	3	0.395919	0.131973	7.65E-05		
ANOVA						
Source of Variation	*SS*	*df*	*MS*	*F*	*P-value*	*F crit*
Between Groups	0.011429	2	0.005715	3.836657	**0.067876**	4.45897
Within Groups	0.011916	8	0.001489			
Total	0.023345	10				

Statistical Analysis for Dataset 2

Inter Rifle (t-Test)

Table 30: t-Test for Volunteer 4

t-Test: Two-Sample Assuming Unequal Variances		
	Volunteer 4 Rifle D	*Volunteer 4 Rifle E*
Mean	0.299210895	116.1876734
Variance	0.041691963	24641.70058
Observations	36	11
Hypothesized Mean Difference	0	
df	10	
t Stat	-2.448505552	
P(T<=t) one-tail	**0.01717275**	
t Critical one-tail	1.812461123	
P(T<=t) two-tail	0.0343455	
t Critical two-tail	2.228138852	

Table 31: t-Test for Volunteer 5

t-Test: Two-Sample Assuming Unequal Variances		
	Volunteer 5 Rifle D	*Volunteer 5 Rifle E*
Mean	0.142829652	1.677201505
Variance	0.012435589	2.611604951
Observations	2	15

Hypothesized Mean Difference	0	
df	15	
t Stat	-3.613290705	
P(T<=t) one-tail	**0.001277535**	
t Critical one-tail	1.753050356	
P(T<=t) two-tail	0.002555069	
t Critical two-tail	2.131449546	

Table 32: t-Test for Volunteer 6

t-Test: Two-Sample Assuming Unequal Variances		
	Volunteer 6 Rifle D	*Volunteer 6 Rifle E*
Mean	0.061362562	1.380179518
Variance	0.000922584	3.259743184
Observations	33	6
Hypothesized Mean Difference	0	
df	5	
t Stat	-1.789193373	
P(T<=t) one-tail	**0.066801853**	
t Critical one-tail	2.015048373	
P(T<=t) two-tail	0.133603705	
t Critical two-tail	2.570581836	

Table 33: t-Test for Volunteer 7

t-Test: Two-Sample Assuming Unequal Variances		
	Volunteer 7 Rifle D	*Volunteer 7 Rifle E*
Mean	0.012507298	0.092233073
Variance	1.38359E-05	0.000381603
Observations	8	18
Hypothesized Mean Difference	0	
df	20	
t Stat	-16.64945116	
P(T<=t) one-tail	**1.73154E-13**	
t Critical one-tail	1.724718243	
P(T<=t) two-tail	3.46308E-13	
t Critical two-tail	2.085963447	

Table 34: t-Test for Volunteer 8

t-Test: Two-Sample Assuming Unequal Variances		
	Volunteer 8 Rifle D	*Volunteer 8 Rifle E*
Mean	0.036573081	0.152838953
Variance	5.2211E-06	0.001093663
Observations	5	10
Hypothesized Mean Difference	0	
df	9	
t Stat	-11.06488936	
P(T<=t) one-tail	**7.66E-07**	
t Critical one-tail	1.833112933	
P(T<=t) two-tail	1.532E-06	
t Critical two-tail	2.262157163	

Appendix C: BrIC

BrIC for all shots in Dataset 1: May 2021

Inter Rifle

Table 35: Summary of BrIC values in Dataset 1: Volunteers 1,2,3 firing Rifles A, B, and C

	Volunteer 1 Rifle A	**Volunteer 1 Rifle B**	**Volunteer 1 Rifle C**
shot 1	0.1138	0.0940	0.1062
shot 2	0.1233	0.0914	0.1170
shot 3	0.1123	0.1192	0.1315
shot 4	0.1153	0.0984	0.1225
mean BrIC	**0.1162**	**0.1008**	**0.1193**
Sample standard deviation	**0.0049**	**0.0126**	**0.0106**
	Volunteer 2 Rifle A	**Volunteer 2 Rifle B**	**Volunteer 2 Rifle C**
shot 1	0.1815	0.1088	0.1887
shot 2	0.1902	0.1395	0.1915
shot 3	x	0.1860	0.2013
shot 4	x	0.1550	0.2038
mean BrIC	**0.1858**	**0.1474**	**0.1963**
Sample standard deviation	**0.0062**	**0.0321**	**0.0073**
	Volunteer 3 Rifle A	**Volunteer 3 Rifle B**	**Volunteer 3 Rifle C**
shot 1	0.1608	0.1561	0.1516
shot 2	0.1673	0.1497	0.1500
shot 3	0.1568	0.1510	0.1511
mean BrIC	**0.1616**	**0.1523**	**0.1509**
Sample standard deviation	**0.0053**	**0.0034**	**0.0008**

Inter volunteer

Table 36: Summary of BrIC values in Dataset 1: Volunteers 1,2,3 firing Rifles A, B, and C

	Volunteer 1 Rifle A	**Volunteer 2 Rifle A**	**Volunteer 3 Rifle A**
shot 1	0.1138	0.1815	0.1608
shot 2	0.1233	0.1902	0.1673
shot 3	0.1123	x	0.1568
shot 4	0.1153	x	x
mean BrIC	**0.1162**	**0.1858**	**0.1616**
Sample STD Dev	**0.0049**	**0.0062**	**0.0053**
CV	**4.22**	**3.32**	**3.28**

	Volunteer 1 Rifle B	**Volunteer 2 Rifle B**	**Volunteer 3 Rifle B**
shot 1	0.0940	0.1088	0.1561
shot 2	0.0914	0.1395	0.1497
shot 3	0.1192	0.1860	0.1510
shot 4	0.0984	0.1550	x
mean BrIC	**0.1008**	**0.1474**	**0.1523**
Sample STD Dev	**0.0126**	**0.0321**	**0.0034**
CV	**12.54**	**21.81**	**2.21**
	Volunteer 1 Rifle C	**Volunteer 2 Rifle C**	**Volunteer 3 Rifle C**
shot 1	0.1062	0.1887	0.1516
shot 2	0.1170	0.1915	0.1500
shot 3	0.1315	0.2013	0.1511
shot 4	0.1225	0.2038	x
mean BrIC	**0.1193**	**0.1963**	**0.1509**
Sample STD Dev	**0.0106**	**0.0073**	**0.0008**
CV	**8.88**	**3.73**	**0.54**

BrIC for all shots in Dataset 2: May 2022

Inter Rifle

Table 37: Summary of BrIC values in Dataset 2: Volunteers 4,5 firing Rifles D and E

	Volunteer 4 Rifle D	**Volunteer 4 Rifle E**	**Volunteer 5 Rifle D**	**Volunteer 5 Rifle E**
shot 1	0.0538	0.6963	0.0609	0.0990
shot 2	0.0541	0.1002	0.0576	0.1942
shot 3	0.0528	0.1486	x	0.1659
shot 4	0.0618	0.4345	x	0.1071
shot 5	0.0652	0.1161	x	0.1018
shot 6	0.0676	0.6015	x	0.0998
shot 7	0.0716	0.4735	x	0.0943
shot 8	0.0587	0.3833	x	0.0966
shot 9	0.0626	0.4801	x	0.0957
shot 10	0.0584	0.3364	x	0.2866
shot 11	0.0566	0.3963	x	0.2405
shot 12	0.0635	x	x	0.2939
shot 13	0.0582	x	x	0.1241
shot 14	0.0686	x	x	0.1863
shot 15	0.0592	x	x	0.1467
shot 16	0.0604	x	x	x
shot 17	0.0572	x	x	x

shot 18	0.0520	x	x	x
shot 19	0.0543	x	x	x
shot 20	0.0583	x	x	x
shot 21	0.0554	x	x	x
shot 22	0.0466	x	x	x
shot 23	0.0605	x	x	x
shot 24	0.0550	x	x	x
shot 25	0.0509	x	x	x
shot 26	0.0513	x	x	x
shot 27	0.0481	x	x	x
shot 28	0.0521	x	x	x
shot 29	0.0543	x	x	x
shot 30	0.0541	x	x	x
shot 31	0.0545	x	x	x
shot 32	0.0666	x	x	x
shot 33	0.0712	x	x	x
shot 34	0.0657	x	x	x
shot 35	0.0675	x	x	x
shot 36	0.0710	x	x	x
mean HIC_{15}	**0.0589**	**0.3788**	**0.0592**	**0.1555**
Sample standard deviation	**0.0067**	**0.1935**	**0.0023**	**0.0705**

Table 38: Summary of BrIC values in Dataset 2: Volunteer 6 firing Rifles D and E

	Volunteer 6 Rifle D	**Volunteer 6 Rifle E**
shot 1	0.0498	0.1332
shot 2	0.0519	0.1359
shot 3	0.0552	0.1272
shot 4	0.0502	0.1709
shot 5	0.0507	0.2058
shot 6	0.0442	0.2147
shot 7	0.0470	x
shot 8	0.0496	x
shot 9	0.0453	x
shot 10	0.0532	x
shot 11	0.0523	x
shot 12	0.0538	x
shot 13	0.0573	x
shot 14	0.0618	x
shot 15	0.0533	x
shot 16	0.0533	x
shot 17	0.0554	x

shot 18	0.0560	x
shot 19	0.0553	x
shot 20	0.0517	x
shot 21	0.0398	x
shot 22	0.0466	x
shot 23	0.0531	x
shot 24	0.0549	x
shot 25	0.0548	x
shot 26	0.0515	x
shot 27	0.0846	x
shot 28	0.0685	x
shot 29	0.0747	x
shot 30	0.0865	x
shot 31	0.0692	x
shot 32	0.0750	x
shot 33	0.0592	x
mean HIC_{15}	**0.0565**	**0.1646**
Sample standard deviation	**0.0108**	**0.0386**

Table 39: Summary of BrIC values in Dataset 2: Volunteers 7,8 firing Rifles D and E

	Volunteer 7 Rifle D	**Volunteer 7 Rifle E**	**Volunteer 8 Rifle D**	**Volunteer 8 Rifle E**
shot 1	0.0574	0.1090	0.0502	0.1268
shot 2	0.0549	0.1043	0.0476	0.1046
shot 3	0.0546	0.1189	0.0512	0.1151
shot 4	0.0551	0.1181	0.0435	0.1039
shot 5	0.0611	0.1038	0.0412	0.1128
shot 6	0.0549	0.1082	x	0.1261
shot 7	0.0551	0.0974	x	0.1258
shot 8	0.0636	0.1040	x	0.1212
shot 9	x	0.0998	x	0.1166
shot 10	x	0.1056	x	0.1211
shot 11	x	0.1146	x	x
shot 12	x	0.1100	x	x
shot 13	x	0.1117	x	x
shot 14	x	0.1092	x	x
shot 15	x	0.1151	x	x
shot 16	x	0.1126	x	x
shot 17	x	0.1142	x	x
shot 18	x	0.1085	x	x
mean BrIC	**0.0571**	**0.1092**	**0.0468**	**0.1174**
Sample standard deviation	**0.0034**	**0.0060**	**0.0043**	**0.0084**

Inter volunteer

Table 40: Summary of BrIC values in Dataset 2: Volunteers 4,5,6,7 and 8 firing Rifle D

	Volunteer 4	**Volunteer 5**	**Volunteer 6**	**Volunteer 7**	**Volunteer 8**
shot 1	0.0538	0.0609	0.0498	0.0574	0.0502
shot 2	0.0541	0.0576	0.0519	0.0549	0.0476
shot 3	0.0528	x	0.0552	0.0546	0.0512
shot 4	0.0618	x	0.0502	0.0551	0.0435
shot 5	0.0652	x	0.0507	0.0611	0.0412
shot 6	0.0676	x	0.0442	0.0549	x
shot 7	0.0716	x	0.0470	0.0551	x
shot 8	0.0587	x	0.0496	0.0636	x
shot 9	0.0626	x	0.0453	x	x
shot 10	0.0584	x	0.0532	x	x
shot 11	0.0566	x	0.0523	x	x
shot 12	0.0635	x	0.0538	x	x
shot 13	0.0582	x	0.0573	x	x
shot 14	0.0686	x	0.0618	x	x
shot 15	0.0592	x	0.0533	x	x
shot 16	0.0604	x	0.0533	x	x
shot 17	0.0572	x	0.0554	x	x
shot 18	0.0520	x	0.0560	x	x
shot 19	0.0543	x	0.0553	x	x
shot 20	0.0583	x	0.0517	x	x
shot 21	0.0554	x	0.0398	x	x
shot 22	0.0466	x	0.0466	x	x
shot 23	0.0605	x	0.0531	x	x
shot 24	0.0550	x	0.0549	x	x
shot 25	0.0509	x	0.0548	x	x
shot 26	0.0513	x	0.0515	x	x
shot 27	0.0481	x	0.0846	x	x
shot 28	0.0521	x	0.0685	x	x
shot 29	0.0543	x	0.0747	x	x
shot 30	0.0541	x	0.0865	x	x
shot 31	0.0545	x	0.0692	x	x
shot 32	0.0666	x	0.0750	x	x
shot 33	0.0712	x	0.0592	x	x
shot 34	0.0657	x	x	x	x
shot 35	0.0675	x	x	x	x
shot 36	0.0710	x	x	x	x
mean BrIC	**0.0589**	**0.0592**	**0.0565**	**0.0571**	**0.0468**

std dev	**0.0067**	**0.0023**	**0.0108**	**0.0034**	**0.0043**
CV	**11.43**	**3.88**	**19.16**	**5.97**	**9.20**

Table 41: Summary of BrIC values in Dataset 2: Volunteers 4,5,6,7 and 8 firing Rifle E

	Volunteer 4	**Volunteer 5**	**Volunteer 6**	**Volunteer 7**	**Volunteer 8**
shot 1	0.6963	0.0990	0.1332	0.1090	0.1268
shot 2	0.1002	0.1942	0.1359	0.1043	0.1046
shot 3	0.1486	0.1659	0.1272	0.1189	0.1151
shot 4	0.4345	0.1071	0.1709	0.1181	0.1039
shot 5	0.1161	0.1018	0.2058	0.1038	0.1128
shot 6	0.6015	0.0998	0.2147	0.1082	0.1261
shot 7	0.4735	0.0943	x	0.0974	0.1258
shot 8	0.3833	0.0966	x	0.1040	0.1212
shot 9	0.4801	0.0957	x	0.0998	0.1166
shot 10	0.3364	0.2866	x	0.1056	0.1211
shot 11	0.3963	0.2405	x	0.1146	x
shot 12	x	0.2939	x	0.1100	x
shot 13	x	0.1241	x	0.1117	x
shot 14	x	0.1863	x	0.1092	x
shot 15	x	0.1467	x	0.1151	x
shot 16	x	x	x	0.1126	x
shot 17	x	x	x	0.1142	x
shot 18	x	x	x	0.1085	x
mean BrIC	**0.3788**	**0.1555**	**0.1646**	**0.1092**	**0.1174**
std dev	**0.1935**	**0.0705**	**0.0386**	**0.0060**	**0.0084**
CV	**51.08**	**45.32**	**23.46**	**5.46**	**7.16**

Statistical Analysis for Dataset 1

Inter Rifle (One-way ANOVA)

Table 42: One-Way ANOVA for Volunteer 1

Anova: Single Factor						
SUMMARY						
Groups	*Count*	*Sum*	*Average*	*Variance*		
Volunteer 1 Rifle A	4	0.464706	0.116176	2.4E-05		
Volunteer 1 Rifle B	4	0.403139	0.100785	0.00016		
Volunteer 1 Rifle C	4	0.477142	0.119285	0.000112		
ANOVA						

Source of Variation	*SS*	*df*	*MS*	*F*	*P-value*	*F crit*
Between Groups	0.000785	2	0.000393	3.978829	**5.78E-02**	4.256495
Within Groups	0.000888	9	9.87E-05			
Total	0.001673	11				

Table 43: One-Way ANOVA for Volunteer 2

Anova: Single Factor						
SUMMARY						
Groups	*Count*	*Sum*	*Average*	*Variance*		
Volunteer 2 rifle A	2	0.371652	0.185826	3.81E-05		
Volunteer 2 rifle B	4	0.589413	0.147353	0.001033		
Volunteer 2 rifle C	4	0.785305	0.196326	5.36E-05		
ANOVA						
Source of Variation	*SS*	*df*	*MS*	*F*	*P-value*	*F crit*
Between Groups	0.00511	2	0.002555	5.424553	**3.78E-02**	4.737414
Within Groups	0.003297	7	0.000471			
Total	0.008407	9				
is p value < 0.05?	Yes					
If yes, reject null hyp	i.e. at least 1 of the means of groups are diff					
Tukey Kramer test	compares the mean between each pairwaise combination of groups					
	step 1	**step 4**	**step 5**			
Comparison	**Abs. Mean Diff**	**Q critical Value**	**Significant?**			
A vs. B	0.038473	0.0494	No			
B vs. C	0.048973	0.0403	Yes			
A vs. C	0.0105	0.0494	No			
step 2						
Find Q critical value						
Q critical value = Q*√(s2pooled / n.)						
Q = Value from Studentized Range Q Table						

s2pooled = Pooled variance across all groups						
n. = Sample size for a given group						
Find Q value from studentized Range q Table						
q(k,df,alpha)						
k = number of groups	3					
df = n-k	7					
Q(3,7,0.05)	4.165					
pooled variance	0.000375					
step 3						
harmonic mean A,B	2.666667					
harmonic mean B,C	4					
harmonic mean A,C	2.666667					

Table 44: One-Way ANOVA for Volunteer 3

Anova: Single Factor						
SUMMARY						
Groups	*Count*	*Sum*	*Average*	*Variance*		
Volunteer 3 rifle A	3	0.484844	0.161615	2.8E-05		
Volunteer 3 rifle B	3	0.45677	0.152257	1.14E-05		
Volunteer 3 rifle C	3	0.452748	0.150916	6.54E-07		
ANOVA						
Source of Variation	*SS*	*df*	*MS*	*F*	*P-value*	*F crit*
Between Groups	0.000204	2	0.000102	7.636536	**2.24E-02**	5.143253
Within Groups	8.01E-05	6	1.33E-05			
Total	0.000284	8				
is p value < 0.05?	Yes					
If yes, reject null hyp	i.e. at least 1 of the means of groups are diff					
Tukey Kramer test	compares the mean between each pairwaise combination of groups					
	step 1	**step 4**	**step 5**			

Comparison	Abs. Mean Diff	Q critical Value	Significant?			
A vs. B	0.009358	0.009151	Yes			
B vs. C	0.001341	0.009151	No			
A vs. C	0.010698	0.009151	Yes			
step 2						
Find Q critical value						
Q critical value = Q*√(s2pooled / n.)						
Q = Value from Studentized Range Q Table						
s2pooled = Pooled variance across all groups						
n. = Sample size for a given group						
Find Q value from studentized Range q Table						
q(k,df,alpha)						
k = number of groups	3					
df = n-k	6					
Q(3,6,0.05)	4.339					
pooled variance	1.33E-05					
step 3						
sample size of each group	3					

Inter Volunteer (One-way ANOVA)

Table 45: One-Way ANOVA for Rifle A

Anova: Single Factor						
SUMMARY						
Groups	*Count*	*Sum*	*Average*	*Variance*		
Volunteer 1 rifle A	4	0.464706	0.116176	2.4E-05		
Volunteer 2 rifle A	2	0.371652	0.185826	3.81E-05		
Volunteer 3 rifle A	3	0.484844	0.161615	2.8E-05		
ANOVA						
Source of Variation	*SS*	*df*	*MS*	*F*	*P-value*	*F crit*
Between Groups	0.007455721	2	0.003728	134.5991	**1.04E-05**	5.143253

Within Groups	0.000166176	6	2.77E-05			
Total	0.007621897	8				
is p value < 0.05?	Yes					
If yes, reject null hyp	i.e. at least 1 of the means of groups are diff					
Tukey Kramer test	compares the mean between each pairwaise combination of groups					
	step 1	**step 4**	**step 5**			
Comparison	**Abs. Mean Diff**	**Q critical Value**	**Significant?**			
1 vs. 2	0.0696	0.0146	Yes			
2 vs. 3	0.0242	0.0154	Yes			
1 vs. 3	0.0454	0.0128	Yes			
step 2						
Find Q critical value						
Q critical value = Q*√(s2pooled / n.)						
Q = Value from Studentized Range Q Table						
s2pooled = Pooled variance across all groups						
n. = Sample size for a given group						
Find Q value from studentized Range q Table						
q(k,df,alpha)						
k = number of groups	3					
df = n-k	6					
Q(3,6,0.05)	4.339					
pooled variance	3.00366E-05					
step 3 - sample size						
harmonic mean 1,2	2.666666667					
harmonic mean 2,3	2.4					
harmonic mean 1,3	3.428571429					

Table 46: One-Way ANOVA for Rifle B

Anova: Single Factor						
SUMMARY						
Groups	*Count*	*Sum*	*Average*	*Variance*		
Volunteer 1 rifle B	4	0.403139	0.100785	0.00016		
Volunteer 2 rifle B	4	0.589413	0.147353	0.001033		
Volunteer 3 rifle B	3	0.45677	0.152257	1.14E-05		
ANOVA						
Source of Variation	*SS*	*df*	*MS*	*F*	*P-value*	*F crit*
Between Groups	0.006071	2	0.003035	6.745026	**1.92E-02**	4.45897
Within Groups	0.0036	8	0.00045			
Total	0.009671	10				
is p value < 0.05?	Yes					
If yes, reject null hyp	i.e. at least 1 of the means of groups are diff					
Tukey Kramer test	compares the mean between each pairwaise combination of groups					
	step 1	**step 4**	**step 5**			
Comparison	**Abs. Mean Diff**	**Q critical Value**	**Significant?**			
1 vs. 2	0.0466	0.0405	Yes			
2 vs. 3	0.0049	0.0437	No			
1 vs. 3	0.0515	0.0437	Yes			
step 2						
Find Q critical value						
Q critical value = Q*√(s2pooled / n.)						
Q = Value from Studentized Range Q Table						
s2pooled = Pooled variance across all groups						
n. = Sample size for a given group						
Find Q value from studentized Range q Table						
q(k,df,alpha)						
k = number of groups	3					

df = n-k	8					
Q(3,8,0.05)	4.041					
pooled variance	0.000401					
step 3 - sample size						
harmonic mean 1,2	4					
harmonic mean 2,3	3.428571					
harmonic mean 1,3	3.428571					

Table 47: One-Way ANOVA for Rifle C

Anova: Single Factor						
SUMMARY						
Groups	*Count*	*Sum*	*Average*	*Variance*		
Volunteer 1 rifle C	4	0.477142	0.119285	0.000112		
Volunteer 2 rifle C	4	0.785305	0.196326	5.36E-05		
Volunteer 3 rifle C	3	0.452748	0.150916	6.54E-07		
ANOVA						
Source of Variation	*SS*	*df*	*MS*	*F*	*P-value*	*F crit*
Between Groups	0.011974	2	0.005987	96.07107	**2.55E-06**	4.45897
Within Groups	0.000499	8	6.23E-05			
Total	0.012473	10				
is p value < 0.05?	Yes					
If yes, reject null hyp	i.e. at least 1 of the means of groups are diff					
Tukey Kramer test	compares the mean between each pairwaise combination of groups					
	step 1	**step 4**	**step 5**			
Comparison	**Abs. Mean Diff**	**Q critical Value**	**Significant?**			
1 vs. 2	0.0770	0.0150	Yes			
2 vs. 3	0.0454	0.0163	Yes			
1 vs. 3	0.0316	0.0163	Yes			

step 2						
Find Q critical value						
Q critical value = Q*√(s2pooled / n.)						
Q = Value from Studentized Range Q Table						
s2pooled = Pooled variance across all groups						
n. = Sample size for a given group						
Find Q value from studentized Range q Table						
q(k,df,alpha)						
k = number of groups	3					
df = n-k	8					
Q(3,8,0.05)	4.041					
pooled variance	5.55E-05					
step 3 - sample size						
harmonic mean 1,2	4					
harmonic mean 2,3	3.428571					
harmonic mean 1,3	3.428571					

Statistical Analysis for Dataset 2

Inter Rifle (t-Test)

Table 48: t-Test for Volunteer 4

t-Test: Two-Sample Assuming Unequal Variances		
	Volunteer 4 Rifle D	*Volunteer 4 Rifle E*
Mean	0.058889421	0.378803482
Variance	4.52827E-05	0.037441533
Observations	36	11
Hypothesized Mean Difference	0	
df	10	
t Stat	-5.482424095	
P(T<=t) one-tail	**1.34E-04**	
t Critical one-tail	1.812461123	
P(T<=t) two-tail	0.000268328	
t Critical two-tail	2.228138852	

Table 49: t-Test for Volunteer 5

t-Test: Two-Sample Assuming Unequal Variances		
	Volunteer 5 Rifle D	*Volunteer 5 Rifle E*
Mean	0.05922731	0.155497155
Variance	5.28463E-06	0.004965608
Observations	2	15
Hypothesized Mean Difference	0	
df	14	
t Stat	-5.270154588	
P(T<=t) one-tail	**5.92E-05**	
t Critical one-tail	1.761310136	
P(T<=t) two-tail	0.000118421	
t Critical two-tail	2.144786688	

Table 50: t-Test for Volunteer 6

t-Test: Two-Sample Assuming Unequal Variances		
	Volunteer 6 Rifle D	*Volunteer 6 Rifle E*
Mean	0.056529037	0.16461815
Variance	0.000117304	0.001491155
Observations	33	6
Hypothesized Mean Difference	0	
df	5	
t Stat	-6.807886165	
P(T<=t) one-tail	**5.21E-04**	
t Critical one-tail	2.015048373	
P(T<=t) two-tail	0.001041703	
t Critical two-tail	2.570581836	

Table 51: t-Test for Volunteer 7

t-Test: Two-Sample Assuming Unequal Variances		
	Volunteer 7 Rifle D	*Volunteer 7 Rifle E*
Mean	0.057094566	0.10916636
Variance	1.162E-05	3.54762E-05
Observations	8	18
Hypothesized Mean Difference	0	
df	22	
t Stat	-28.14319	

P(T<=t) one-tail	**4.78E-19**	
t Critical one-tail	1.717144374	
P(T<=t) two-tail	9.56741E-19	
t Critical two-tail	2.073873068	

Table 52: t-Test for Volunteer 8

t-Test: Two-Sample Assuming Unequal Variances		
	Volunteer 8 Rifle D	*Volunteer 8 Rifle E*
Mean	0.046766998	0.117400434
Variance	1.8494E-05	7.06973E-05
Observations	5	10
Hypothesized Mean Difference	0	
df	13	
t Stat	-21.52445641	
P(T<=t) one-tail	**7.50E-12**	
t Critical one-tail	1.770933396	
P(T<=t) two-tail	1.50044E-11	
t Critical two-tail	2.160368656	

Inter Volunteer (One-way ANOVA)

Table 53: One-Way ANOVA for Rifle D

Anova: Single Factor						
SUMMARY						
Groups	*Count*	*Sum*	*Average*	*Variance*		
Volunteer 4	36	2.120019	0.058889	4.53E-05		
Volunteer 5	2	0.118455	0.059227	5.28E-06		
Volunteer 6	33	1.865458	0.056529	0.000117		
Volunteer 7	8	0.456757	0.057095	1.16E-05		
Volunteer 8	5	0.233835	0.046767	1.85E-05		
ANOVA						
Source of Variation	*SS*	*df*	*MS*	*F*	*P-value*	*F crit*
Between Groups	0.000669	4	0.000167	2.402276	**5.67E-02**	2.487366
Within Groups	0.005499	79	6.96E-05			
Total	0.006168	83				

Table 54: One-Way ANOVA for Rifle E

Anova: Single Factor						
SUMMARY						
Groups	*Count*	*Sum*	*Average*	*Variance*		
Volunteer 4	11	4.166838	0.378803	0.037442		
Volunteer 5	15	2.332457	0.155497	0.004966		
Volunteer 6	6	0.987709	0.164618	0.001491		
Volunteer 7	18	1.964994	0.109166	3.55E-05		
Volunteer 8	10	1.174004	0.1174	7.07E-05		
ANOVA						
Source of Variation	*SS*	*df*	*MS*	*F*	*P-value*	*F crit*
Between Groups	0.574172	4	0.143543	17.44225	**2.7E-09**	2.539689
Within Groups	0.452629	55	0.00823			
Total	1.026801	59				
is p value < 0.05?	Yes					
If yes, reject null hyp	i.e. at least 1 of the means of groups are diff					
Tukey Kramer test	compares the mean between each pairwaise combination of groups					
	step 1	**step 4**	**step 5**			
Comparison	**Abs. Mean Diff**	**Q critical Value**	**Significant?**			
4 vs. 5	0.223306	0.0895	Yes			
4 vs. 6	0.214185	0.1144	Yes			
4 vs. 7	0.269637	0.0863	Yes			
4 vs. 8	0.261403	0.0985	Yes			
5 vs. 6	0.009121	0.1089	No			
5 vs. 8	0.038097	0.0921	No			
6 vs. 7	0.0555	0.1063	No			
6 vs. 8	0.0472	0.1164	No			
7 vs. 8	0.0082	0.0889	No			
step 2						
Find Q critical value						

Q critical value = Q*√(s2pooled / n.)						
Q = Value from Studentized Range Q Table						
s2pooled = Pooled variance across all groups						
n. = Sample size for a given group						
Find Q value from studentized Range q Table						
q(k,df,alpha)						
k = number of groups	5					
df = n-k	55					
Q(3,55,0.05)	3.399	closest to Q(3,60,0.05)				
pooled variance	0.008801					
step 3 - harmonic means						
4 vs. 5	12.69231					
4 vs. 6	7.764706					
4 vs. 7	13.65517					
4 vs. 8	10.47619					
5 vs. 6	8.571429					
5 vs. 8	12					
6 vs. 7	9					
6 vs. 8	7.5					
7 vs. 8	12.85714					

Appendix D: MPS_{95}

MPS_{95} for all shots in Dataset 1: May 2021

Inter Rifle

Table 55: Summary of MPS_{95} values in Dataset 1: Volunteers 1,2,3 firing Rifles A, B, and C

	Volunteer 1 Rifle A	**Volunteer 1 Rifle B**	**Volunteer 1 Rifle C**
shot 1	0.0348	0.0322	0.0388
shot 2	0.0375	0.0284	0.0389
shot 3	0.0367	0.0375	0.0417
shot 4	0.0378	0.0327	0.0404
mean MPS_{95}	**0.0367**	**0.0327**	**0.0399**
Sample standard deviation	**0.0013**	**0.0037**	**0.0014**
	Volunteer 2 Rifle A	**Volunteer 2 Rifle B**	**Volunteer 2 Rifle C**
shot 1	0.0750	0.0301	0.0856
shot 2	0.0654	0.0357	0.0761
shot 3	x	0.0552	0.0668
shot 4	x	0.0409	0.0800
mean MPS_{95}	**0.0702**	**0.0405**	**0.0771**
Sample standard deviation	**0.0068**	**0.0107**	**0.0079**
	Volunteer 3 Rifle A	**Volunteer 3 Rifle B**	**Volunteer 3 Rifle C**
shot 1	0.0549	0.0532	0.0518
shot 2	0.0624	0.0498	0.0517
shot 3	0.0561	0.0518	0.0571
mean MPS_{95}	**0.0578**	**0.0516**	**0.0535**
Sample standard deviation	**0.0040**	**0.0017**	**0.0031**

Inter Volunteer

Table 56: Summary of MPS_{95} values in Dataset 1: Volunteers 1,2,3 firing Rifles A, B, and C

	Volunteer 1 Rifle A	**Volunteer 2 Rifle A**	**Volunteer 3 Rifle A**
shot 1	0.0348	0.0750	0.0549
shot 2	0.0375	0.0654	0.0624
shot 3	0.0367	x	0.0561
shot 4	0.0378	x	x
mean MPS_{95}	**0.0367**	**0.0702**	**0.0578**
Sample STD Dev	**0.0013**	**0.0068**	**0.0040**
CV	**3.61**	**9.70**	**6.93**
	Volunteer 1 Rifle B	**Volunteer 2 Rifle B**	**Volunteer 3 Rifle B**

shot 1	0.0322	0.0301	0.0532
shot 2	0.0284	0.0357	0.0498
shot 3	0.0375	0.0552	0.0518
shot 4	0.0327	0.0409	x
mean MPS_{95}	**0.0327**	**0.0405**	**0.0516**
Sample STD Dev	**0.0037**	**0.0107**	**0.0017**
CV	**11.39**	**26.56**	**3.33**
	Volunteer 1 Rifle C	**Volunteer 2 Rifle C**	**Volunteer 3 Rifle C**
shot 1	0.0388	0.0856	0.0518
shot 2	0.0389	0.0761	0.0517
shot 3	0.0417	0.0668	0.0571
shot 4	0.0404	0.0800	x
mean MPS_{95}	**0.0399**	**0.0771**	**0.0535**
Sample STD Dev	**0.0014**	**0.0079**	**0.0031**
CV	**3.54**	**10.25**	**5.76**

MPS_{95} for all shots in Dataset 2: May 2022

Inter Rifle

Table 57: Summary of MPS_{95} values in Dataset 2: Volunteers 4,5 firing Rifles D and E

	Volunteer 4 Rifle D	**Volunteer 4 Rifle E**	**Volunteer 5 Rifle D**	**Volunteer 5 Rifle E**
shot 1	0.0228	0.2897	0.0208	0.0451
shot 2	0.0233	0.0376	0.0200	0.0754
shot 3	0.0221	0.0536	x	0.0771
shot 4	0.0210	0.2003	x	0.0393
shot 5	0.0280	0.0497	x	0.0353
shot 6	0.0291	0.2191	x	0.0383
shot 7	0.0286	0.1695	x	0.0358
shot 8	0.0217	0.1430	x	0.0355
shot 9	0.0263	0.1883	x	0.0344
shot 10	0.0235	0.1317	x	0.1232
shot 11	0.0241	0.1306	x	0.0901
shot 12	0.0238	x	x	0.1256
shot 13	0.0234	x	x	0.0571
shot 14	0.0255	x	x	0.0778
shot 15	0.0240	x	x	0.0619
shot 16	0.0224	x	x	x
shot 17	0.0224	x	x	x
shot 18	0.0210	x	x	x

shot 19	0.0244	x	x	x
shot 20	0.0249	x	x	x
shot 21	0.0240	x	x	x
shot 22	0.0198	x	x	x
shot 23	0.0245	x	x	x
shot 24	0.0218	x	x	x
shot 25	0.0209	x	x	x
shot 26	0.0215	x	x	x
shot 27	0.0182	x	x	x
shot 28	0.0226	x	x	x
shot 29	0.0233	x	x	x
shot 30	0.0234	x	x	x
shot 31	0.0227	x	x	x
shot 32	0.0253	x	x	x
shot 33	0.0278	x	x	x
shot 34	0.0258	x	x	x
shot 35	0.0274	x	x	x
shot 36	0.0262	x	x	x
mean MPS_{95}	**0.0238**	**0.1466**	**0.0204**	**0.0635**
Sample standard deviation	**0.0025**	**0.0783**	**0.0005**	**0.0310**

Table 58: Summary of MPS_{95} values in Dataset 2: Volunteers 6 firing Rifles D and E

	Volunteer 6 Rifle D	**Volunteer 6 Rifle E**
shot 1	0.0195	0.0442
shot 2	0.0200	0.0441
shot 3	0.0220	0.0420
shot 4	0.0204	0.0650
shot 5	0.0208	0.0787
shot 6	0.0180	0.0884
shot 7	0.0192	x
shot 8	0.0205	x
shot 9	0.0192	x
shot 10	0.0214	x
shot 11	0.0213	x
shot 12	0.0222	x
shot 13	0.0228	x
shot 14	0.0228	x
shot 15	0.0213	x
shot 16	0.0230	x
shot 17	0.0235	x
shot 18	0.0225	x

shot 19	0.0206	x
shot 20	0.0204	x
shot 21	0.0175	x
shot 22	0.0196	x
shot 23	0.0209	x
shot 24	0.0218	x
shot 25	0.0202	x
shot 26	0.0199	x
shot 27	0.0279	x
shot 28	0.0243	x
shot 29	0.0232	x
shot 30	0.0271	x
shot 31	0.0222	x
shot 32	0.0239	x
shot 33	0.0233	x
mean MPS_{95}	**0.0216**	**0.0604**
Sample standard deviation	**0.0023**	**0.0201**

Table 59: Summary of MPS_{95} values in Dataset 2: Volunteers 7,8 firing Rifles D and E

	Volunteer 7 Rifle D	**Volunteer 7 Rifle E**	**Volunteer 8 Rifle D**	**Volunteer 8 Rifle E**
shot 1	0.0221	0.0486	0.0171	0.0381
shot 2	0.0217	0.0437	0.0197	0.0316
shot 3	0.0214	0.0455	0.0197	0.0359
shot 4	0.0198	0.0480	0.0185	0.0363
shot 5	0.0228	0.0453	0.0155	0.0379
shot 6	0.0214	0.0438	x	0.0425
shot 7	0.0195	0.0448	x	0.0413
shot 8	0.0216	0.0453	x	0.0398
shot 9	x	0.0441	x	0.0382
shot 10	x	0.0486	x	0.0401
shot 11	x	0.0498	x	x
shot 12	x	0.0483	x	x
shot 13	x	0.0506	x	x
shot 14	x	0.0490	x	x
shot 15	x	0.0519	x	x
shot 16	x	0.0481	x	x
shot 17	x	0.0526	x	x
shot 18	x	0.0482	x	x
mean MPS_{95}	**0.0213**	**0.0476**	**0.0181**	**0.0382**
Sample standard deviation	**0.0011**	**0.0027**	**0.0018**	**0.0031**

Inter Volunteer

Table 60: Summary of MPS_{95} values in Dataset 2: Volunteers 4,5,6,7 and 8 firing Rifle D

	Volunteer 4	**Volunteer 5**	**Volunteer 6**	**Volunteer 7**	**Volunteer 8**
shot 1	0.0228	0.0208	0.0195	0.0221	0.0171
shot 2	0.0233	0.0200	0.0200	0.0217	0.0197
shot 3	0.0221	x	0.0220	0.0214	0.0197
shot 4	0.0210	x	0.0204	0.0198	0.0185
shot 5	0.0280	x	0.0208	0.0228	0.0155
shot 6	0.0291	x	0.0180	0.0214	x
shot 7	0.0286	x	0.0192	0.0195	x
shot 8	0.0217	x	0.0205	0.0216	x
shot 9	0.0263	x	0.0192	x	x
shot 10	0.0235	x	0.0214	x	x
shot 11	0.0241	x	0.0213	x	x
shot 12	0.0238	x	0.0222	x	x
shot 13	0.0234	x	0.0228	x	x
shot 14	0.0255	x	0.0228	x	x
shot 15	0.0240	x	0.0213	x	x
shot 16	0.0224	x	0.0230	x	x
shot 17	0.0224	x	0.0235	x	x
shot 18	0.0210	x	0.0225	x	x
shot 19	0.0244	x	0.0206	x	x
shot 20	0.0249	x	0.0204	x	x
shot 21	0.0240	x	0.0175	x	x
shot 22	0.0198	x	0.0196	x	x
shot 23	0.0245	x	0.0209	x	x
shot 24	0.0218	x	0.0218	x	x
shot 25	0.0209	x	0.0202	x	x
shot 26	0.0215	x	0.0199	x	x
shot 27	0.0182	x	0.0279	x	x
shot 28	0.0226	x	0.0243	x	x
shot 29	0.0233	x	0.0232	x	x
shot 30	0.0234	x	0.0271	x	x
shot 31	0.0227	x	0.0222	x	x
shot 32	0.0253	x	0.0239	x	x
shot 33	0.0278	x	0.0233	x	x
shot 34	0.0258	x	x	x	x
shot 35	0.0274	x	x	x	x
shot 36	0.0262	x	x	x	x
mean MPS_{95}	**0.0238**	**0.0204**	**0.0216**	**0.0213**	**0.0181**
std dev	**0.0025**	**0.0005**	**0.0023**	**0.0011**	**0.0018**

CV	**10.49**	**2.50**	**10.42**	**5.21**	**10.04**

Table 61: Summary of MPS_{95} values in Dataset 2: Volunteers 4,5,6,7 and 8 firing Rifle E

	Volunteer 4	**Volunteer 5**	**Volunteer 6**	**Volunteer 7**	**Volunteer 8**
shot 1	0.2897	0.0451	0.0442	0.0486	0.0381
shot 2	0.0376	0.0754	0.0441	0.0437	0.0316
shot 3	0.0536	0.0771	0.0420	0.0455	0.0359
shot 4	0.2003	0.0393	0.0650	0.0480	0.0363
shot 5	0.0497	0.0353	0.0787	0.0453	0.0379
shot 6	0.2191	0.0383	0.0884	0.0438	0.0425
shot 7	0.1695	0.0358	x	0.0448	0.0413
shot 8	0.1430	0.0355	x	0.0453	0.0398
shot 9	0.1883	0.0344	x	0.0441	0.0382
shot 10	0.1317	0.1232	x	0.0486	0.0401
shot 11	0.1306	0.0901	x	0.0498	x
shot 12	x	0.1256	x	0.0483	x
shot 13	x	0.0571	x	0.0506	x
shot 14	x	0.0778	x	0.0490	x
shot 15	x	0.0619	x	0.0519	x
shot 16	x	x	x	0.0481	x
shot 17	x	x	x	0.0526	x
shot 18	x	x	x	0.0482	x
mean MPS_{95}	**0.1466**	**0.0635**	**0.0604**	**0.0476**	**0.0382**
std dev	**0.0783**	**0.0310**	**0.0201**	**0.0027**	**0.0031**
CV	**53.38**	**48.87**	**33.20**	**5.74**	**8.15**

Statistical Analysis for Dataset 1

Inter Rifle (One-way ANOVA)

Table 62: One-Way ANOVA for Volunteer 1

Anova: Single Factor						
SUMMARY						
Groups	*Count*	*Sum*	*Average*	*Variance*		
Volunteer 1 rifle A	4	0.146799	0.0367	1.75E-06		
Volunteer 1 rifle B	4	0.130903	0.032726	1.39E-05		
Volunteer 1 rifle C	4	0.159762	0.039941	1.99E-06		

ANOVA						
Source of Variation	*SS*	*df*	*MS*	*F*	*P-value*	*F crit*
Between Groups	0.000104	2	5.22E-05	8.883444	**7.41E-03**	4.256495
Within Groups	5.29E-05	9	5.88E-06			
Total	0.000157	11				
is p value < 0.05?	Yes					
If yes, reject null hyp	i.e. at least 1 of the means of groups are diff					
Tukey Kramer test	compares the mean between each pairwaise combination of groups					
	step 1	**step 4**	**step 5**			
Comparison	**Abs. Mean Diff**	**Q critical Value**	**Significant?**			
A vs. B	0.003974	0.004787	No			
B vs. C	0.007215	0.004787	Yes			
A vs. C	0.003241	0.004787	No			
step 2						
Find Q critical value						
Q critical value = Q*√(s2pooled / n.)						
Q = Value from Studentized Range Q Table						
s2pooled = Pooled variance across all groups						
n. = Sample size for a given group						
Find Q value from studentized Range q Table						
q(k,df,alpha)						
k = number of groups	3					
df = n-k	9					
Q(3,9,0.05)	3.948					
pooled variance	5.88E-06					
step 3						
sample size of each group	4					

Table 63: One-Way ANOVA for Volunteer 2

Anova: Single Factor						
SUMMARY						
Groups	*Count*	*Sum*	*Average*	*Variance*		
Volunteer 2 rifle A	2	0.140331	0.070166	4.63E-05		
Volunteer 2 rifle B	4	0.161896	0.040474	0.000116		
Volunteer 2 rifle C	4	0.308499	0.077125	6.25E-05		
ANOVA						
Source of Variation	*SS*	*df*	*MS*	*F*	*P-value*	*F crit*
Between Groups	0.002893	2	0.001447	17.45146	**1.91E-03**	4.737414
Within Groups	0.00058	7	8.29E-05			
Total	0.003474	9				
is p value < 0.05?	Yes					
If yes, reject null hyp	i.e. at least 1 of the means of groups are diff					
Tukey Kramer test	compares the mean between each pairwaise combination of groups					
	step 1	**step 4**	**step 5**			
Comparison	**Abs. Mean Diff**	**Q critical Value**	**Significant?**			
A vs. B	0.0297	0.0221	Yes			
B vs. C	0.0367	0.0180	Yes			
A vs. C	0.0070	0.0221	No			
step 2						
Find Q critical value						
Q critical value = Q*√(s2pooled / n.)						
Q = Value from Studentized Range Q Table						
s2pooled = Pooled variance across all groups						
n. = Sample size for a given group						
Find Q value from studentized Range q Table						
q(k,df,alpha)						
k = number of groups	3					

df = n-k	7					
Q(3,7,0.05)	4.165					
pooled variance	7.48E-05					
step 3 -harmonic mean						
A vs. B	2.666667					
B vs. C	4					
A vs. C	2.666667					

Table 64: One-Way ANOVA for Volunteer 3

Anova: Single Factor						
SUMMARY						
Groups	*Count*	*Sum*	*Average*	*Variance*		
Volunteer 3 Rifle A	3	0.173428	0.057809	1.61E-05		
Volunteer 3 Rifle B	3	0.154778	0.051593	2.96E-06		
Volunteer 3 Rifle C	3	0.160631	0.053544	9.52E-06		
ANOVA						
Source of Variation	*SS*	*df*	*MS*	*F*	*P-value*	*F crit*
Between Groups	6.06E-05	2	3.03E-05	3.188547	**1.14E-01**	5.143253
Within Groups	5.71E-05	6	9.51E-06			
Total	0.000118	8				

Inter Volunteer (One-way ANOVA)

Table 65: One-Way ANOVA for Rifle A

Anova: Single Factor						
SUMMARY						
Groups	*Count*	*Sum*	*Average*	*Variance*		
Volunteer 1 rifle A	4	0.146799	0.0367	1.75E-06		
Volunteer 2 rifle A	2	0.140331	0.070166	4.63E-05		
Volunteer 3 rifle A	3	0.173428	0.057809	1.61E-05		
ANOVA						
Source of Variation	*SS*	*df*	*MS*	*F*	*P-value*	*F crit*
Between Groups	0.001691	2	0.000846	60.6291	**1.05E-04**	5.143253

Within Groups	8.37E-05	6	1.39E-05			
Total	0.001775	8				
is p value < 0.05?	Yes					
If yes, reject null hyp	i.e. at least 1 of the means of groups are diff					
Tukey Kramer test	compares the mean between each pairwaise combination of groups					
	step 1	**step 4**	**step 5**			
Comparison	**Abs. Mean Diff**	**Q critical Value**	**Significant?**			
1 vs. 2	0.0335	0.0123	Yes			
2 vs. 3	0.0124	0.0129	No			
1 vs. 3	0.0211	0.0108	Yes			
step 2						
Find Q critical value						
Q critical value = Q*√(s2pooled / n.)						
Q = Value from Studentized Range Q Table						
s2pooled = Pooled variance across all groups						
n. = Sample size for a given group						
Find Q value from studentized Range q Table						
q(k,df,alpha)						
k = number of groups	3					
df = n-k	6					
Q(3,6,0.05)	4.339					
pooled variance	2.14E-05					
step 3 - sample size						
harmonic mean 1,2	2.666667					
harmonic mean 2,3	2.4					
harmonic mean 1,3	3.428571					

Table 66: One-Way ANOVA for Rifle B

Anova: Single Factor						

SUMMARY						
Groups	*Count*	*Sum*	*Average*	*Variance*		
Volunteer 1 rifle B	4	0.130903	0.032726	1.39E-05		
Volunteer 2 rifle B	4	0.161896	0.040474	0.000116		
Volunteer 3 rifle B	3	0.154778	0.051593	2.96E-06		
ANOVA						
Source of Variation	*SS*	*df*	*MS*	*F*	*P-value*	*F crit*
Between Groups	0.000611	2	0.000305	6.195439	**2.37E-02**	4.45897
Within Groups	0.000394	8	4.93E-05			
Total	0.001005	10				
is p value < 0.05?	Yes					
If yes, reject null hyp	i.e. at least 1 of the means of groups are diff					
Tukey Kramer test	compares the mean between each pairwaise combination of groups					
	step 1	**step 4**	**step 5**			
Comparison	**Abs. Mean Diff**	**Q critical Value**	**Significant?**			
1 vs. 2	0.0077	0.0134	No			
2 vs. 3	0.0111	0.0145	No			
1 vs. 3	0.0189	0.0145	Yes			
step 2						
Find Q critical value						
Q critical value = Q*√(s2pooled / n.)						
Q = Value from Studentized Range Q Table						
s2pooled = Pooled variance across all groups						
n. = Sample size for a given group						
Find Q value from studentized Range q Table						
q(k,df,alpha)						
k = number of groups	3					
df = n-k	8					
Q(3,8,0.05)	4.041					
pooled variance	4.41E-05					

step 3 - sample size						
harmonic mean 1,2	4					
harmonic mean 2,3	3.428571					
harmonic mean 1,3	3.428571					

Table 67: One-Way ANOVA for Rifle C

Anova: Single Factor						
SUMMARY						
Groups	*Count*	*Sum*	*Average*	*Variance*		
Volunteer 1 rifle C	4	0.159762	0.039941	1.99E-06		
Volunteer 2 rifle C	4	0.308499	0.077125	6.25E-05		
Volunteer 3 rifle C	3	0.160631	0.053544	9.52E-06		
ANOVA						
Source of Variation	*SS*	*df*	*MS*	*F*	*P-value*	*F crit*
Between Groups	0.00282	2	0.00141	53.10633	**2.41E-05**	4.45897
Within Groups	0.000212	8	2.65E-05			
Total	0.003032	10				
is p value < 0.05?	Yes					
If yes, reject null hyp	i.e. at least 1 of the means of groups are diff					
Tukey Kramer test	compares the mean between each pairwaise combination of groups					
	step 1	**step 4**	**step 5**			
Comparison	**Abs. Mean Diff**	**Q critical Value**	**Significant?**			
1 vs. 2	0.0372	0.0100	Yes			
2 vs. 3	0.0236	0.0108	Yes			
1 vs. 3	0.0136	0.0108	Yes			
step 2						
Find Q critical value						
Q critical value = Q*√(s2pooled / n.)						
Q = Value from Studentized Range Q Table						

s2pooled = Pooled variance across all groups						
n. = Sample size for a given group						
Find Q value from studentized Range q Table						
q(k,df,alpha)						
k = number of groups	3					
df = n-k	8					
Q(3,8,0.05)	4.041					
pooled variance	2.47E-05					
step 3 - sample size						
harmonic mean 1,2	4					
harmonic mean 2,3	3.428571					
harmonic mean 1,3	3.428571					

Statistical Analysis for Dataset 2

Inter Rifle (t-Test)

Table 68: t-Test for Volunteer 5

t-Test: Two-Sample Assuming Unequal Variances		
	Volunteer 5 Rifle D	*Volunteer 5 Rifle E*
Mean	0.020393832	0.063455245
Variance	2.59297E-07	0.000961826
Observations	2	15
Hypothesized Mean Difference	0	
df	14	
t Stat	-5.372137048	
P(T<=t) one-tail	**4.92E-05**	
t Critical one-tail	1.761310136	
P(T<=t) two-tail	9.84367E-05	
t Critical two-tail	2.144786688	

Table 69: t-Test for Volunteer 6

t-Test: Two-Sample Assuming Unequal Variances		
	Volunteer 6 Rifle D	*Volunteer 6 Rifle E*
Mean	0.02161443	0.060416792
Variance	5.07595E-06	0.00040231
Observations	33	6
Hypothesized Mean Difference	0	
df	5	
t Stat	-4.733212889	
P(T<=t) one-tail	**2.59E-03**	
t Critical one-tail	2.015048373	
P(T<=t) two-tail	0.00518127	
t Critical two-tail	2.570581836	

Table 70: t-Test for Volunteer 7

t-Test: Two-Sample Assuming Unequal Variances		
	Volunteer 7 Rifle D	*Volunteer 7 Rifle E*
Mean	0.021283421	0.047565966
Variance	1.22888E-06	7.46672E-06
Observations	8	18
Hypothesized Mean Difference	0	
df	24	
t Stat	-34.86018592	
P(T<=t) one-tail	**2.26E-22**	
t Critical one-tail	1.71088208	
P(T<=t) two-tail	4.52825E-22	
t Critical two-tail	2.063898562	

Table 71: t-Test for Volunteer 8

t-Test: Two-Sample Assuming Unequal Variances		
	Volunteer 8 Rifle D	*Volunteer 8 Rifle E*
Mean	0.0180919	0.038165897
Variance	3.30185E-06	9.66355E-06
Observations	5	10
Hypothesized Mean Difference	0	
df	12	
t Stat	-15.7389853	

P(T<=t) one-tail	**1.12E-09**	
t Critical one-tail	1.782287556	
P(T<=t) two-tail	2.23971E-09	
t Critical two-tail	2.17881283	

Inter Volunteer (One-way ANOVA)

Table 72: One-Way ANOVA for Rifle D

Anova: Single Factor						
SUMMARY						
Groups	*Count*	*Sum*	*Average*	*Variance*		
Volunteer 4	36	0.857573	0.023821	6.25E-06		
Volunteer 5	2	0.040788	0.020394	2.59E-07		
Volunteer 6	33	0.713276	0.021614	5.08E-06		
Volunteer 7	8	0.170267	0.021283	1.23E-06		
Volunteer 8	5	0.090459	0.018092	3.3E-06		
ANOVA						
Source of Variation	*SS*	*df*	*MS*	*F*	*P-value*	*F crit*
Between Groups	0.000203	4	5.07E-05	9.941636	**1.44E-06**	2.487366
Within Groups	0.000403	79	5.1E-06			
Total	0.000606	83				
is p value < 0.05?	Yes					
If yes, reject null hyp	i.e. at least 1 of the means of groups are diff					
Tukey Kramer test	compares the mean between each pairwaise combination of groups					
	step 1	**step 4**	**step 5**			
Comparison	**Abs. Mean Diff**	**Q critical Value**	**Significant?**			
4 vs. 5	0.003428	0.0031	Yes			
4 vs. 6	0.002207	0.0010	Yes			
4 vs. 7	0.002538	0.0017	Yes			
4 vs. 8	0.00573	0.0020	Yes			
5 vs. 6	0.001221	0.0031	No			
5 vs. 8	0.002302	0.0036	No			

6 vs. 7	0.0003	0.0017	No			
6 vs. 8	0.0035	0.0021	Yes			
7 vs. 8	0.0032	0.0024	Yes			
step 2						
Find Q critical value						
Q critical value = Q*√(s2pooled / n.)						
Q = Value from Studentized Range Q Table						
s2pooled = Pooled variance across all groups						
n. = Sample size for a given group						
Find Q value from studentized Range q Table						
q(k,df,alpha)						
k = number of groups	5					
df = n-k	79					
Q(3,79,0.05)	3.377	closest to Q(3,80,0.05)				
pooled variance	3.22E-06					
step 3 - harmonic means						
4 vs. 5	3.789474					
4 vs. 6	34.43478					
4 vs. 7	13.09091					
4 vs. 8	8.780488					
5 vs. 6	3.771429					
5 vs. 8	2.857143					
6 vs. 7	12.87805					
6 vs. 8	8.684211					
7 vs. 8	6.153846					

Table 73: One-Way ANOVA for Rifle E

Anova: Single Factor						
SUMMARY						
Groups	*Count*	*Sum*	*Average*	*Variance*		
Volunteer 4	11	1.613119	0.146647	0.006128		
Volunteer 5	15	0.951829	0.063455	0.000962		
Volunteer 6	6	0.362501	0.060417	0.000402		
Volunteer 7	18	0.856187	0.047566	7.47E-06		
Volunteer 8	10	0.381659	0.038166	9.66E-06		

ANOVA						
Source of Variation	*SS*	*df*	*MS*	*F*	*P-value*	*F crit*
Between Groups	0.084989	4	0.021247	15.18272	**2.01E-08**	2.539689
Within Groups	0.076969	55	0.001399			
Total	0.161959	59				
is p value < 0.05?	Yes					
If yes, reject null hyp	i.e. at least 1 of the means of groups are diff					
Tukey Kramer test	compares the mean between each pairwaise combination of groups					
	step 1	**step 4**	**step 5**			
Comparison	**Abs. Mean Diff**	**Q critical Value**	**Significant?**			
4 vs. 5	0.083192	0.0370	Yes			
4 vs. 6	0.08623	0.0473	Yes			
4 vs. 7	0.099081	0.0356	Yes			
4 vs. 8	0.108481	0.0407	Yes			
5 vs. 6	0.003038	0.0450	No			
5 vs. 8	0.025289	0.0380	No			
6 vs. 7	0.0129	0.0439	No			
6 vs. 8	0.0223	0.0481	No			
7 vs. 8	0.0094	0.0367	No			
step 2						
Find Q critical value						
Q critical value = Q*√(s2pooled / n.)						
Q = Value from Studentized Range Q Table						
s2pooled = Pooled variance across all groups						
n. = Sample size for a given group						
Find Q value from studentized Range q Table						
q(k,df,alpha)						
k = number of groups	5					
df = n-k	55					
Q(3,55,0.05)	3.399	closest to Q(3,60,0.05)				
pooled variance	0.001502					

step 3 - harmonic means						
4 vs. 5	12.69231					
4 vs. 6	7.764706					
4 vs. 7	13.65517					
4 vs. 8	10.47619					
5 vs. 6	8.571429					
5 vs. 8	12					
6 vs. 7	9					
6 vs. 8	7.5					
7 vs. 8	12.85714					

Appendix E: A_{CSV}

A_{CSV} for all shots in Dataset 1: May 2021

Inter Rifle

Table 74: Summary of area under cumulative strain-volume curves (A_{CSV}) values in Dataset 1: Volunteers 1,2,3 firing Rifles A, B, and C

	Volunteer 1 Rifle A	**Volunteer 1 Rifle B**	**Volunteer 1 Rifle C**
shot 1	0.0225	0.0193	0.0237
shot 2	0.0235	0.0181	0.0245
shot 3	0.0231	0.0235	0.0257
shot 4	0.0234	0.0204	0.0247
mean A_{csv}	**0.0231**	**0.0203**	**0.0246**
Sample standard deviation	**0.0005**	**0.0023**	**0.0008**
	Volunteer 2 Rifle A	**Volunteer 2 Rifle B**	**Volunteer 2 Rifle C**
shot 1	0.0449	0.0182	0.0492
shot 2	0.0387	0.0222	0.0450
shot 3	x	0.0329	0.0399
shot 4	x	0.0261	0.0467
mean A_{csv}	**0.0418**	**0.0249**	**0.0452**
Sample standard deviation	**0.0044**	**0.0063**	**0.0040**
	Volunteer 3 Rifle A	**Volunteer 3 Rifle B**	**Volunteer 3 Rifle C**
shot 1	0.0350	0.0344	0.0324
shot 2	0.0379	0.0314	0.0330
shot 3	0.0341	0.0320	0.0367
mean A_{csv}	**0.0357**	**0.0326**	**0.0341**
Sample standard deviation	**0.0019**	**0.0016**	**0.0023**

Inter volunteer

Table 75: Summary of area under cumulative strain-volume curves (A_{CSV}) values in Dataset 1: Volunteers 1,2,3 firing Rifles A, B, and C

	Volunteer 1 Rifle A	**Volunteer 2 Rifle A**	**Volunteer 3 Rifle A**
shot 1	0.0225	0.0449	0.0350
shot 2	0.0235	0.0387	0.0379
shot 3	0.0231	x	0.0341
shot 4	0.0234	x	x
mean A_{CSV}	**0.0231**	**0.0418**	**0.0357**
Sample standard deviation	**0.0005**	**0.0044**	**0.0019**
	Volunteer 1 Rifle B	**Volunteer 2 Rifle B**	**Volunteer 3 Rifle B**

shot 1	0.0193	0.0182	0.0344
shot 2	0.0181	0.0222	0.0314
shot 3	0.0235	0.0329	0.0320
shot 4	0.0204	0.0261	x
mean A_{CSV}	**0.0203**	**0.0249**	**0.0326**
Sample standard deviation	**0.0023**	**0.0063**	**0.0016**
	Volunteer 1 Rifle C	**Volunteer 2 Rifle C**	**Volunteer 3 Rifle C**
shot 1	0.0237	0.0492	0.0324
shot 2	0.0245	0.0450	0.0330
shot 3	0.0257	0.0399	0.0367
shot 4	0.0247	0.0467	x
mean A_{CSV}	**0.0246**	**0.0452**	**0.0341**
Sample standard deviation	**0.0008**	**0.0040**	**0.0023**

A_{CSV} for all shots in Dataset 2: May 2022

Inter Rifle

Table 76: Summary of area under cumulative strain-volume curves (A_{CSV}) values in Dataset 2: Volunteers 4,5 firing Rifles D and E

	Volunteer 4 Rifle D	**Volunteer 4 Rifle E**	**Volunteer 5 Rifle D**	**Volunteer 5 Rifle E**
shot 1	0.0138	0.1653	0.0134	0.0289
shot 2	0.0145	0.0237	0.0129	0.0468
shot 3	0.0141	0.0352	x	0.0458
shot 4	0.0131	0.1164	x	0.0238
shot 5	0.0173	0.0323	x	0.0228
shot 6	0.0180	0.1279	x	0.0241
shot 7	0.0180	0.1020	x	0.0218
shot 8	0.0135	0.0874	x	0.0223
shot 9	0.0162	0.1062	x	0.0220
shot 10	0.0149	0.0837	x	0.0769
shot 11	0.0149	0.0830	x	0.0609
shot 12	0.0156	x	x	0.0805
shot 13	0.0148	x	x	0.0369
shot 14	0.0164	x	x	0.0525
shot 15	0.0148	x	x	0.0424
shot 16	0.0147	x	x	x
shot 17	0.0140	x	x	x
shot 18	0.0136	x	x	x
shot 19	0.0154	x	x	x
shot 20	0.0159	x	x	x

shot 21	0.0156	x	x	x
shot 22	0.0125	x	x	x
shot 23	0.0156	x	x	x
shot 24	0.0137	x	x	x
shot 25	0.0134	x	x	x
shot 26	0.0138	x	x	x
shot 27	0.0115	x	x	x
shot 28	0.0139	x	x	x
shot 29	0.0145	x	x	x
shot 30	0.0146	x	x	x
shot 31	0.0148	x	x	x
shot 32	0.0161	x	x	x
shot 33	0.0175	x	x	x
shot 34	0.0161	x	x	x
shot 35	0.0173	x	x	x
shot 36	0.0166	x	x	x
mean A_{csv}	**0.0150**	**0.0875**	**0.0132**	**0.0406**
Sample standard deviation	**0.0015**	**0.0435**	**0.0003**	**0.0200**

Table 77: Summary of area under cumulative strain-volume curves (A_{CSV}) values in Dataset 2: Volunteers 6 firing Rifles D and E

	Volunteer 6 Rifle D	**Volunteer 6 Rifle E**
shot 1	0.0118	0.0274
shot 2	0.0121	0.0280
shot 3	0.0134	0.0256
shot 4	0.0124	0.0412
shot 5	0.0125	0.0518
shot 6	0.0110	0.0581
shot 7	0.0117	x
shot 8	0.0125	x
shot 9	0.0118	x
shot 10	0.0129	x
shot 11	0.0129	x
shot 12	0.0134	x
shot 13	0.0138	x
shot 14	0.0140	x
shot 15	0.0129	x
shot 16	0.0137	x
shot 17	0.0141	x
shot 18	0.0137	x
shot 19	0.0126	x

shot 20	0.0123	x
shot 21	0.0111	x
shot 22	0.0122	x
shot 23	0.0128	x
shot 24	0.0132	x
shot 25	0.0125	x
shot 26	0.0122	x
shot 27	0.0177	x
shot 28	0.0150	x
shot 29	0.0153	x
shot 30	0.0174	x
shot 31	0.0138	x
shot 32	0.0151	x
shot 33	0.0143	x
mean A_{csv}	**0.0133**	**0.0387**
Sample standard deviation	**0.0015**	**0.0139**

Table 78: Summary of area under cumulative strain-volume curves (A_{CSV}) values in Dataset 2: Volunteers 7,8 firing Rifles D and E

	Volunteer 7 Rifle D	**Volunteer 7 Rifle E**	**Volunteer 8 Rifle D**	**Volunteer 8 Rifle E**
shot 1	0.0137	0.0291	0.0106	0.0239
shot 2	0.0135	0.0269	0.0116	0.0201
shot 3	0.0134	0.0275	0.0117	0.0227
shot 4	0.0128	0.0293	0.0111	0.0225
shot 5	0.0149	0.0279	0.0095	0.0241
shot 6	0.0136	0.0277	x	0.0269
shot 7	0.0123	0.0275	x	0.0260
shot 8	0.0139	0.0280	x	0.0251
shot 9	x	0.0269	x	0.0243
shot 10	x	0.0294	x	0.0256
shot 11	x	0.0303	x	x
shot 12	x	0.0293	x	x
shot 13	x	0.0312	x	x
shot 14	x	0.0302	x	x
shot 15	x	0.0320	x	x
shot 16	x	0.0291	x	x
shot 17	x	0.0328	x	x
shot 18	x	0.0297	x	x
mean A_{csv}	**0.0135**	**0.0292**	**0.0109**	**0.0241**
Sample standard deviation	**0.0008**	**0.0017**	**0.0009**	**0.0020**

Inter Volunteer

Table 79: Summary of MPS_{95} values in Dataset 2: Volunteers 4,5,6,7 and 8 firing Rifle D

	Volunteer 4 Rifle D	**Volunteer 5 Rifle D**	**Volunteer 6 Rifle D**	**Volunteer 7 Rifle D**	**Volunteer 8 Rifle D**
shot 1	0.0138	0.0134	0.0118	0.0137	0.0106
shot 2	0.0145	0.0129	0.0121	0.0135	0.0116
shot 3	0.0141	x	0.0134	0.0134	0.0117
shot 4	0.0131	x	0.0124	0.0128	0.0111
shot 5	0.0173	x	0.0125	0.0149	0.0095
shot 6	0.0180	x	0.0110	0.0136	x
shot 7	0.0180	x	0.0117	0.0123	x
shot 8	0.0135	x	0.0125	0.0139	x
shot 9	0.0162	x	0.0118	x	x
shot 10	0.0149	x	0.0129	x	x
shot 11	0.0149	x	0.0129	x	x
shot 12	0.0156	x	0.0134	x	x
shot 13	0.0148	x	0.0138	x	x
shot 14	0.0164	x	0.0140	x	x
shot 15	0.0148	x	0.0129	x	x
shot 16	0.0147	x	0.0137	x	x
shot 17	0.0140	x	0.0141	x	x
shot 18	0.0136	x	0.0137	x	x
shot 19	0.0154	x	0.0126	x	x
shot 20	0.0159	x	0.0123	x	x
shot 21	0.0156	x	0.0111	x	x
shot 22	0.0125	x	0.0122	x	x
shot 23	0.0156	x	0.0128	x	x
shot 24	0.0137	x	0.0132	x	x
shot 25	0.0134	x	0.0125	x	x
shot 26	0.0138	x	0.0122	x	x
shot 27	0.0115	x	0.0177	x	x
shot 28	0.0139	x	0.0150	x	x
shot 29	0.0145	x	0.0153	x	x
shot 30	0.0146	x	0.0174	x	x
shot 31	0.0148	x	0.0138	x	x
shot 32	0.0161	x	0.0151	x	x
shot 33	0.0175	x	0.0143	x	x
shot 34	0.0161	x	x	x	x
shot 35	0.0173	x	x	x	x
shot 36	0.0166	x	x	x	x
mean ACSV	**0.0150**	**0.0132**	**0.0133**	**0.0135**	**0.0109**
Std dev	**0.0015**	**0.0003**	**0.0015**	**0.0008**	**0.0009**
CV (%)	**10.25**	**2.54**	**11.57**	**5.77**	**8.20**

Table 80: Summary of MPS_{95} values in Dataset 2: Volunteers 4,5,6,7 and 8 firing Rifle E

	Volunteer 4 Rifle E	**Volunteer 5 Rifle E**	**Volunteer 6 Rifle E**	**Volunteer 7 Rifle E**	**Volunteer 8 Rifle E**
shot 1	0.1653	0.0289	0.0274	0.0291	0.0239
shot 2	0.0237	0.0468	0.0280	0.0269	0.0201
shot 3	0.0352	0.0458	0.0256	0.0275	0.0227
shot 4	0.1164	0.0238	0.0412	0.0293	0.0225
shot 5	0.0323	0.0228	0.0518	0.0279	0.0241
shot 6	0.1279	0.0241	0.0581	0.0277	0.0269
shot 7	0.1020	0.0218	x	0.0275	0.0260
shot 8	0.0874	0.0223	x	0.0280	0.0251
shot 9	0.1062	0.0220	x	0.0269	0.0243
shot 10	0.0837	0.0769	x	0.0294	0.0256
shot 11	0.0830	0.0609	x	0.0303	x
shot 12	x	0.0805	x	0.0293	x
shot 13	x	0.0369	x	0.0312	x
shot 14	x	0.0525	x	0.0302	x
shot 15	x	0.0424	x	0.0320	x
shot 16	x	x	x	0.0291	x
shot 17	x	x	x	0.0328	x
shot 18	x	x	x	0.0297	x
mean ACSV	**0.0875**	**0.0406**	**0.0387**	**0.0292**	**0.0241**
Std dev	**0.0435**	**0.0200**	**0.0139**	**0.0017**	**0.0020**
CV	**49.72**	**49.24**	**35.94**	**5.87**	**8.15**

Statistical Analysis for Dataset 1

Inter Rifle (One-way ANOVA)

Table 81: One-Way ANOVA for Volunteer 1

Anova: Single Factor						
SUMMARY						
Groups	*Count*	*Sum*	*Average*	*Variance*		
Volunteer 1 rifle A	4	0.092563	0.023141	2.14E-07		
Volunteer 1 rifle B	4	0.081306	0.020326	5.47E-06		
Volunteer 1 rifle C	4	0.098562	0.024641	6.43E-07		
ANOVA						
Source of Variation	*SS*	*df*	*MS*	*F*	*P-value*	*F crit*

Between Groups	3.84E-05	2	1.92E-05	9.096062	**6.90E-03**	4.256495
Within Groups	1.9E-05	9	2.11E-06			
Total	5.74E-05	11				
is p value < 0.05?	Yes					
If yes, reject null hyp	i.e. at least 1 of the means of groups are diff					
Tukey Kramer test	compares the mean between each pairwaise combination of groups					
	step 1	**step 4**	**step 5**			
Comparison	**Abs. Mean Diff**	**Q critical Value**	**Significant?**			
A vs. B	0.002814	0.002867	No			
B vs. C	0.004314	0.002867	Yes			
A vs. C	0.0015	0.002867	No			
step 2						
Find Q critical value						
Q critical value = Q*√(s2pooled / n.)						
Q = Value from Studentized Range Q Table						
s2pooled = Pooled variance across all groups						
n. = Sample size for a given group						
Find Q value from studentized Range q Table						
q(k,df,alpha)						
k = number of groups	3					
df = n-k	9					
Q(3,9,0.05)	3.948					
pooled variance	2.11E-06					
step 3						
sample size of each group	4					

Table 82: One-Way ANOVA for Volunteer 2

Anova: Single Factor						
SUMMARY						
Groups	*Count*	*Sum*	*Average*	*Variance*		
Volunteer 2 rifle A	2	0.08365	0.041825	1.91E-05		
Volunteer 2 rifle B	4	0.099444	0.024861	3.95E-05		
Volunteer 2 rifle C	4	0.180761	0.04519	1.57E-05		
ANOVA						
Source of Variation	*SS*	*df*	*MS*	*F*	*P-value*	*F crit*
Between Groups	0.000901	2	0.00045	17.04923	**2.04E-03**	4.737414
Within Groups	0.000185	7	2.64E-05			
Total	0.001085	9				
is p value < 0.05?	Yes					
If yes, reject null hyp	i.e. at least 1 of the means of groups are diff					
Tukey Kramer test	compares the mean between each pairwaise combination of groups					
	step 1	**step 4**	**step 5**			
Comparison	**Abs. Mean Diff**	**Q critical Value**	**Significant?**			
A vs. B	0.0170	0.0127	Yes			
B vs. C	0.0203	0.0104	Yes			
A vs. C	0.0034	0.0127	No			
step 2						
Find Q critical value						
Q critical value = Q*√(s2pooled / n.)						
Q = Value from Studentized Range Q Table						
s2pooled = Pooled variance across all groups						
n. = Sample size for a given group						
Find Q value from studentized Range q Table						
q(k,df,alpha)						
k = number of groups	3					

df = n-k	7					
Q(3,7,0.05)	4.165					
pooled variance	2.48E-05					
step 3 - harmonic mean						
A vs. B	2.666667					
B vs. C	4					
A vs. C	2.666667					

Table 83: One-Way ANOVA for Volunteer 3

Anova: Single Factor						
SUMMARY						
Groups	*Count*	*Sum*	*Average*	*Variance*		
Volunteer 3 Rifle A	3	0.106999	0.035666	3.77E-06		
Volunteer 3 Rifle B	3	0.097829	0.03261	2.52E-06		
Volunteer 3 Rifle C	3	0.102172	0.034057	5.31E-06		
ANOVA						
Source of Variation	*SS*	*df*	*MS*	*F*	*P-value*	*F crit*
Between Groups	1.4E-05	2	7.01E-06	1.81289	**2.42E-01**	5.143253
Within Groups	2.32E-05	6	3.87E-06			
Total	3.72E-05	8				

Inter volunteer (One-way ANOVA)

Table 84: One-Way ANOVA for Rifle A

Anova: Single Factor						
SUMMARY						
Groups	*Count*	*Sum*	*Average*	*Variance*		
Volunteer 1 rifle A	4	0.092563	0.023141	2.14E-07		
Volunteer 2 rifle A	2	0.08365	0.041825	1.91E-05		
Volunteer 3 rifle A	3	0.106999	0.035666	3.77E-06		
ANOVA						
Source of Variation	*SS*	*df*	*MS*	*F*	*P-value*	*F crit*
Between Groups	0.000545	2	0.000272	59.88285	**1.09E-04**	5.143253

Within Groups	2.73E-05	6	4.55E-06			
Total	0.000572	8				
is p value < 0.05?	Yes					
If yes, reject null hyp	i.e. at least 1 of the means of groups are diff					
Tukey Kramer test	compares the mean between each pairwaise combination of groups					
	step 1	**step 4**	**step 5**			
Comparison	**Abs. Mean Diff**	**Q critical Value**	**Significant?**			
1 vs. 2	0.0187	0.0074	Yes			
2 vs. 3	0.0062	0.0078	No			
1 vs. 3	0.0125	0.0065	Yes			
step 2						
Find Q critical value						
Q critical value = Q*√(s2pooled / n.)						
Q = Value from Studentized Range Q Table						
s2pooled = Pooled variance across all groups						
n. = Sample size for a given group						
Find Q value from studentized Range q Table						
q(k,df,alpha)						
k = number of groups	3					
df = n-k	6					
Q(3,6,0.05)	4.339					
pooled variance	7.7E-06					
step 3 - sample size						
harmonic mean 1,2	2.666667					
harmonic mean 2,3	2.4					
harmonic mean 1,3	3.428571					

Table 85: One-Way ANOVA for Rifle B

Anova: Single Factor						
SUMMARY						
Groups	*Count*	*Sum*	*Average*	*Variance*		
Volunteer 1 rifle B	4	0.081306	0.020326	5.47E-06		
Volunteer 2 rifle B	4	0.099444	0.024861	3.95E-05		
Volunteer 3 rifle B	3	0.097829	0.03261	2.52E-06		
ANOVA						
Source of Variation	*SS*	*df*	*MS*	*F*	*P-value*	*F crit*
Between Groups	0.00026	2	0.00013	7.423754	**1.50E-02**	4.45897
Within Groups	0.00014	8	1.75E-05			
Total	0.0004	10				
is p value < 0.05?	Yes					
If yes, reject null hyp	i.e. at least 1 of the means of groups are diff					
Tukey Kramer test	compares the mean between each pairwaise combination of groups					
	step 1	**step 4**	**step 5**			
Comparison	**Abs. Mean Diff**	**Q critical Value**	**Significant?**			
1 vs. 2	0.0045	0.0080	No			
2 vs. 3	0.0077	0.0087	No			
1 vs. 3	0.0123	0.0087	Yes			
step 2						
Find Q critical value						
Q critical value = Q*√(s2pooled / n.)						
Q = Value from Studentized Range Q Table						
s2pooled = Pooled variance across all groups						
n. = Sample size for a given group						
Find Q value from studentized Range q Table						
q(k,df,alpha)						
k = number of groups	3					

df = n-k	8					
Q(3,8,0.05)	4.041					
pooled variance	1.58E-05					
step 3 - sample size						
harmonic mean 1,2	4					
harmonic mean 2,3	3.428571					
harmonic mean 1,3	3.428571					

Table 86: One-Way ANOVA for Rifle C

SUMMARY						
Groups	*Count*	*Sum*	*Average*	*Variance*		
Volunteer 1 rifle C	4	0.098562	0.024641	6.43E-07		
Volunteer 2 rifle C	4	0.180761	0.04519	1.57E-05		
Volunteer 3 rifle C	3	0.102172	0.034057	5.31E-06		
ANOVA						
Source of Variation	*SS*	*df*	*MS*	*F*	*P-value*	*F crit*
Between Groups	0.000846	2	0.000423	56.71746	**1.88E-05**	4.45897
Within Groups	5.97E-05	8	7.46E-06			
Total	0.000906	10				
is p value < 0.05?	Yes					
If yes, reject null hyp	i.e. at least 1 of the means of groups are diff					
Tukey Kramer test	compares the mean between each pairwaise combination of groups					
	step 1	**step 4**	**step 5**			
Comparison	**Abs. Mean Diff**	**Q critical Value**	**Significant?**			
1 vs. 2	0.0205	0.0054	Yes			
2 vs. 3	0.0111	0.0059	Yes			
1 vs. 3	0.0094	0.0059	Yes			

step 2						
Find Q critical value						
Q critical value = Q*√(s2pooled / n.)						
Q = Value from Studentized Range Q Table						
s2pooled = Pooled variance across all groups						
n. = Sample size for a given group						
Find Q value from studentized Range q Table						
q(k,df,alpha)						
k = number of groups	3					
df = n-k	8					
Q(3,8,0.05)	4.041					
pooled variance	7.22E-06					
step 3 - sample size						
harmonic mean 1,2	4					
harmonic mean 2,3	3.428571					
harmonic mean 1,3	3.428571					

Statistical Analysis for Dataset 2

Inter Rifle (t-Test)

Table 87: t-Test for Volunteer 4

t-Test: Two-Sample Assuming Unequal Variances		
	Volunteer 4 Rifle D	*Volunteer 4 Rifle E*
Mean	0.015029316	0.087549998
Variance	2.37173E-06	0.001895099
Observations	36	11
Hypothesized Mean Difference	0	
df	10	
t Stat	-5.524071535	
P(T<=t) one-tail	**1.27E-04**	
t Critical one-tail	1.812461123	
P(T<=t) two-tail	0.000253107	
t Critical two-tail	2.228138852	

Table 88: t-Test for Volunteer 5

t-Test: Two-Sample Assuming Unequal Variances		
	Volunteer 5 Rifle D	*Volunteer 5 Rifle E*
Mean	0.013163648	0.040564488
Variance	1.11535E-07	0.000398916
Observations	2	15
Hypothesized Mean Difference	0	
df	14	
t Stat	-5.307792587	
P(T<=t) one-tail	**5.53E-05**	
t Critical one-tail	1.761310136	
P(T<=t) two-tail	0.000110594	
t Critical two-tail	2.144786688	

Table 89: t-Test for Volunteer 6

t-Test: Two-Sample Assuming Unequal Variances		
	Volunteer 6 Rifle D	*Volunteer 6 Rifle E*
Mean	0.013285766	0.03869576
Variance	2.36243E-06	0.000193384
Observations	33	6
Hypothesized Mean Difference	0	
df	5	
t Stat	-4.470830587	
P(T<=t) one-tail	**3.29E-03**	
t Critical one-tail	2.015048373	
P(T<=t) two-tail	0.006574206	
t Critical two-tail	2.570581836	

Table 90: t-Test for Volunteer 7

t-Test: Two-Sample Assuming Unequal Variances		
	Volunteer 7 Rifle D	*Volunteer 7 Rifle E*
Mean	0.013501202	0.02916183
Variance	6.07213E-07	2.93014E-06
Observations	8	18
Hypothesized Mean Difference	0	
df	24	
t Stat	-32.05489941	

P(T<=t) one-tail	**1.63E-21**	
t Critical one-tail	1.71088208	
P(T<=t) two-tail	3.25595E-21	
t Critical two-tail	2.063898562	

Table 91: t-Test for Volunteer 8

t-Test: Two-Sample Assuming Unequal Variances		
	Volunteer 8 Rifle D	*Volunteer 8 Rifle E*
Mean	0.010911033	0.024115004
Variance	8.01028E-07	3.86372E-06
Observations	5	10
Hypothesized Mean Difference	0	
df	13	
t Stat	-17.85988567	
P(T<=t) one-tail	**7.88E-11**	
t Critical one-tail	1.770933396	
P(T<=t) two-tail	1.57604E-10	
t Critical two-tail	2.160368656	

Inter Volunteer (One-way ANOVA)

Table 92: One-Way ANOVA for Rifle D

Anova: Single Factor						
SUMMARY						
Groups	*Count*	*Sum*	*Average*	*Variance*		
Volunteer 4 rifle D	36	0.541055	0.015029	2.37E-06		
Volunteer 5 rifle D	2	0.026327	0.013164	1.12E-07		
Volunteer 6 rifle D	33	0.43843	0.013286	2.36E-06		
Volunteer 7 rifle D	8	0.10801	0.013501	6.07E-07		
Volunteer 8 rifle D	5	0.054555	0.010911	8.01E-07		
ANOVA						
Source of Variation	*SS*	*df*	*MS*	*F*	*P-value*	*F crit*
Between Groups	0.000105	4	2.63E-05	12.52478	**6.13E-08**	2.487366
Within Groups	0.000166	79	2.1E-06			
Total	0.000272	83				

is p value < 0.05?	Yes					
If yes, reject null hyp	i.e. at least 1 of the means of groups are diff					
Tukey Kramer test	compares the mean between each pairwaise combination of groups					
	step 1	**step 4**	**step 5**			
Comparison	**Abs. Mean Diff**	**Q critical Value**	**Significant?**			
4 vs. 5	0.001866	0.0019	No			
4 vs. 6	0.001744	0.0006	Yes			
4 vs. 7	0.001528	0.0010	Yes			
4 vs. 8	0.004118	0.0013	Yes			
5 vs. 6	0.000122	0.0019	No			
5 vs. 8	0.002253	0.0022	Yes			
6 vs. 7	0.0002	0.0011	No			
6 vs. 8	0.0024	0.0013	Yes			
7 vs. 8	0.0026	0.0015	Yes			
step 2						
Find Q critical value						
Q critical value = Q*√(s2pooled / n.)						
Q = Value from Studentized Range Q Table						
s2pooled = Pooled variance across all groups						
n. = Sample size for a given group						
Find Q value from studentized Range q Table						
q(k,df,alpha)						
k = number of groups	5					
df = n-k	79					
Q(3,79,0.05)	3.377	closest to Q(3,80,0.05)				
pooled variance	1.25E-06					
step 3 - harmonic means						
4 vs. 5	3.789474					
4 vs. 6	34.43478					
4 vs. 7	13.09091					
4 vs. 8	8.780488					
5 vs. 6	3.771429					
5 vs. 8	2.857143					
6 vs. 7	12.87805					

6 vs. 8	8.684211					
7 vs. 8	6.153846					

Table 93: One-Way ANOVA for Rifle E

Anova: Single Factor						
SUMMARY						
Groups	*Count*	*Sum*	*Average*	*Variance*		
Volunteer 4 rifle E	11	0.96305	0.08755	0.001895		
Volunteer 5 rifle E	15	0.608467	0.040564	0.000399		
Volunteer 6 rifle E	6	0.232175	0.038696	0.000193		
Volunteer 7 rifle E	18	0.524913	0.029162	2.93E-06		
Volunteer 8 rifle E	10	0.24115	0.024115	3.86E-06		
ANOVA						
Source of Variation	*SS*	*df*	*MS*	*F*	*P-value*	*F crit*
Between Groups	0.029043	4	0.007261	15.60724	**1.36E-08**	2.539689
Within Groups	0.025587	55	0.000465			
Total	0.054631	59				
is p value < 0.05?	Yes					
If yes, reject null hyp	i.e. at least 1 of the means of groups are diff					
Tukey Kramer test	compares the mean between each pairwaise combination of groups					
	step 1	**step 4**	**step 5**			
Comparison	**Abs. Mean Diff**	**Q critical Value**	**Significant?**			
4 vs. 5	0.046986	0.0213	Yes			
4 vs. 6	0.048854	0.0272	Yes			
4 vs. 7	0.058388	0.0205	Yes			
4 vs. 8	0.063435	0.0235	Yes			
5 vs. 6	0.001869	0.0259	No			
5 vs. 8	0.016449	0.0219	No			
6 vs. 7	0.0095	0.0253	No			
6 vs. 8	0.0146	0.0277	No			
7 vs. 8	0.0050	0.0212	No			
step 2						

Find Q critical value						
Q critical value = Q*√(s2pooled / n.)						
Q = Value from Studentized Range Q Table						
s2pooled = Pooled variance across all groups						
n. = Sample size for a given group						
Find Q value from studentized Range q Table						
q(k,df,alpha)						
k = number of groups	5					
df = n-k	55					
Q(3,55,0.05)	3.399	closest to Q(3,60,0.05)				
pooled variance	0.000499					
step 3 - harmonic means						
4 vs. 5	12.69231					
4 vs. 6	7.764706					
4 vs. 7	13.65517					
4 vs. 8	10.47619					
5 vs. 6	8.571429					
5 vs. 8	12					
6 vs. 7	9					
6 vs. 8	7.5					
7 vs. 8	12.85714					

Appendix F: Individual Brain Regions

A_{CSV} for all shots in Dataset 1: May 2021

Inter Rifle

Table 94: Mean A_{CSV} of each individual brain region when Volunteers 1,2 and 3 fired Rifle A, B and C

Volunteer 1 mean A_{CSV}					
				RMS effect	**chassis effect**
Brain Region	**Rifle A**	**Rifle B**	**Rifle C**	**% diff b/w A and B**	**% diff b/w A and C**
Cerebrum Gray	0.0256	0.0219	0.0264	-14.5	3.0
Cerebellum	0.0112	0.0103	0.0133	-8.3	18.6
Corpus Callosum	0.0313	0.0278	0.0360	-11.2	15.0
Thalamus	0.0250	0.0229	0.0297	-8.5	18.8
Brainstem Midbrain	0.0321	0.0269	0.0349	-16.2	8.6
brainstem	0.0156	0.0131	0.0173	-16.0	11.1
basal ganglia	0.0280	0.0231	0.0307	-17.4	9.8
cerebrum white	0.0249	0.0223	0.0265	-10.6	6.5
Volunteer 2 mean A_{CSV}					
				RMS effect	**chassis effect**
Brain Region	**Rifle A**	**Rifle B**	**Rifle**	**% diff b/w A and B**	**% diff b/w A and C**
Cerebrum Gray	0.0432	0.0267	0.0469	-38.2	8.6
Cerebellum	0.0243	0.0135	0.0252	-44.3	3.7
Corpus Callosum	0.0573	0.0361	0.0625	-37.0	9.0
Thalamus	0.0503	0.0311	0.0569	-38.3	13.1
Brainstem Midbrain	0.0450	0.0353	0.0486	-21.6	7.9
brainstem	0.0261	0.0163	0.0248	-37.4	-5.1
basal ganglia	0.0499	0.0307	0.0531	-38.6	6.3
cerebrum white	0.0473	0.0268	0.0517	-43.4	9.2
Volunteer 3 mean A_{CSV}					
				RMS effect	**chassis effect**
Brain Region	**Rifle A**	**Rifle B**	**Rifle C**	**% diff b/w A and B**	**% diff b/w A and C**
Cerebrum Gray	0.0382	0.0344	0.0358	-10.0	-6.2
Cerebellum	0.0211	0.0181	0.0197	-14.1	-6.3
Corpus Callosum	0.0566	0.0534	0.0534	-5.7	-5.7
Thalamus	0.0458	0.0433	0.0445	-5.6	-2.9
Brainstem Midbrain	0.0571	0.0511	0.0524	-10.5	-8.3
brainstem	0.0285	0.0227	0.0252	-20.4	-11.5

basal ganglia	0.0476	0.0436	0.0442	-8.5	-7.2
cerebrum white	0.0371	0.0346	0.0363	-6.7	-2.2

Inter Volunteer

Table 95: Mean A_{CSV} of each individual brain region when Volunteers 1,2 and 3 fired Rifle A, B and C

	Rifle A mean A_{CSV}		
Brain Region	**Volunteer 1**	**Volunteer 2**	**Volunteer 3**
Cerebrum Gray	0.0256	0.0432	0.0382
Cerebellum	0.0112	0.0243	0.0211
Corpus Callosum	0.0313	0.0573	0.0566
Thalamus	0.0250	0.0503	0.0458
Brainstem Midbrain	0.0321	0.0450	0.0571
brainstem	0.0156	0.0261	0.0285
basal ganglia	0.0280	0.0499	0.0476
cerebrum white	0.0249	0.0473	0.0371
min	**0.0112**	**0.0243**	**0.0211**
max	**0.0321**	**0.0573**	**0.0571**
range	**0.0209**	**0.0331**	**0.0361**
	Rifle B mean A_{CSV}		
Brain Region	**Volunteer 1**	**Volunteer 2**	**Volunteer 3**
Cerebrum Gray	0.0219	0.0267	0.0344
Cerebellum	0.0103	0.0135	0.0181
Corpus Callosum	0.0278	0.0361	0.0534
Thalamus	0.0229	0.0311	0.0433
Brainstem Midbrain	0.0269	0.0353	0.0511
brainstem	0.0131	0.0163	0.0227
basal ganglia	0.0231	0.0307	0.0436
cerebrum white	0.0223	0.0268	0.0346
min	**0.0103**	**0.0135**	**0.0181**
max	**0.0278**	**0.0361**	**0.0534**
range	**0.0175**	**0.0226**	**0.0353**
	Rifle C mean A_{CSV}		
Brain Region	**Volunteer 1**	**Volunteer 2**	**Volunteer 3**
Cerebrum Gray	0.0264	0.0469	0.0358
Cerebellum	0.0133	0.0252	0.0197
Corpus Callosum	0.0360	0.0625	0.0534

Thalamus	0.0297	0.0569	0.0445
Brainstem Midbrain	0.0349	0.0486	0.0524
brainstem	0.0173	0.0248	0.0252
basal ganglia	0.0307	0.0531	0.0442
cerebrum white	0.0265	0.0517	0.0363
min	**0.0133**	**0.0248**	**0.0197**
max	**0.0360**	**0.0625**	**0.0534**
range	**0.0227**	**0.0377**	**0.0337**

A_{CSV} for all shots in Dataset 2: May 2022

Inter Rifle

Table 96: Mean A_{CSV} of each individual brain region when Volunteers 4,5,6,7 and 8 fired Rifle D and E

Volunteer 4 mean A_{CSV}			
Brain Region	**Rifle D**	**Rifle E**	**% diff b/w D and E**
Cerebrum Gray	0.0159	0.0856	439.3
Cerebellum	0.0095	0.1051	1008.4
Corpus Callosum	0.0188	0.1249	565.7
Thalamus	0.0156	0.1064	581.7
Brainstem Midbrain	0.0192	0.1526	696.4
brainstem	0.0130	0.1361	943.9
basal ganglia	0.0172	0.0996	477.5
cerebrum white	0.0165	0.0768	365.8
Volunteer 5 mean A_{CSV}			
Brain Region	**Rifle D**	**Rifle E**	**% diff b/w D and E**
Cerebrum Gray	0.0136	0.0425	212.5
Cerebellum	0.0083	0.0335	305.8
Corpus Callosum	0.0194	0.0544	180.3
Thalamus	0.0157	0.0455	189.2
Brainstem Midbrain	0.0177	0.0615	247.0
brainstem	0.0098	0.0435	343.6
basal ganglia	0.0162	0.0489	202.9
cerebrum white	0.0142	0.0408	187.6
Volunteer 6 mean A_{CSV}			

Brain Region	Rifle D	Rifle E	% diff b/w D and E
Cerebrum Gray	0.0144	0.0405	181.3
Cerebellum	0.008	0.0282	252.5
Corpus Callosum	0.0194	0.0586	202.1
Thalamus	0.0156	0.0483	209.6
Brainstem Midbrain	0.0201	0.0565	181.1
brainstem	0.0113	0.0342	202.7
basal ganglia	0.017	0.0498	192.9
cerebrum white	0.0139	0.0398	186.3
Volunteer 7 mean A_{csv}			
Brain Region	**Rifle D**	**Rifle E**	**% diff b/w D and E**
Cerebrum Gray	0.0147	0.0316	114.5
Cerebellum	0.0081	0.0182	124.8
Corpus Callosum	0.0162	0.0396	144.7
Thalamus	0.0139	0.0317	127.3
Brainstem Midbrain	0.0179	0.0428	138.5
brainstem	0.0116	0.0259	124.0
basal ganglia	0.0156	0.0355	127.9
cerebrum white	0.0144	0.0309	114.5
Volunteer 8 mean A_{csv}			
Brain Region	**Rifle D**	**Rifle E**	**% diff b/w D and E**
Cerebrum Gray	0.0114	0.0260	128.7
Cerebellum	0.0068	0.0137	103.1
Corpus Callosum	0.0142	0.0327	130.3
Thalamus	0.0124	0.0277	123.8
Brainstem Midbrain	0.0134	0.0330	145.8
brainstem	0.0082	0.0190	130.9
basal ganglia	0.0117	0.0284	143.3
cerebrum white	0.0122	0.0259	112.3

Inter Volunteer

Table 97: Mean A_{CSV} of each individual brain region when Volunteers 4,5,6,7 and 8 fired Rifle D and E

Rifle D			Rifle E		
	REGION	**Acsv**		**REGION**	**Acsv**
Volunteer 4	Brainstem Midbrain	0.0192	**Volunteer 4**	Brainstem Midbrain	0.1526
	Corpus Callosum	0.0188		Brainstem	0.1361

	Basal Ganglia	0.0172		Corpus Callosum	0.1249
	Cerebrum White	0.0165		Thalamus	0.1064
	Cerebrum Gray	0.0159		Cerebellum	0.1051
	Thalamus	0.0156		Basal Ganglia	0.0996
	Brainstem	0.0130		Cerebrum Gray	0.0856
	Cerebellum	0.0095		Cerebrum White	0.0768
min		**0.0095**	**min**		**0.0768**
max		**0.0192**	**max**		**0.1526**
difference		**0.0097**	**difference**		**0.0758**
Volunteer 5	Corpus Callosum	0.0194	**Volunteer 5**	Brainstem Midbrain	0.0615
	Brainstem Midbrain	0.0177		Corpus Callosum	0.0544
	Basal Ganglia	0.0162		Basal Ganglia	0.0489
	Thalamus	0.0157		Thalamus	0.0455
	Cerebrum White	0.0142		Brainstem	0.0435
	Cerebrum Gray	0.0136		Cerebrum Gray	0.0425
	Brainstem	0.0098		Cerebrum White	0.0408
	Cerebellum	0.0083		Cerebellum	0.0335
min		**0.0083**	**min**		**0.0335**
max		**0.0194**	**max**		**0.0615**
difference		**0.0111**	**difference**		**0.0280**
Volunteer 6	Brainstem Midbrain	0.0201	**Volunteer 6**	Corpus Callosum	0.0586
	Corpus Callosum	0.0194		Brainstem Midbrain	0.0565
	Basal Ganglia	0.017		Basal Ganglia	0.0498
	Thalamus	0.0156		Thalamus	0.0483
	Cerebrum Gray	0.0144		Cerebrum Gray	0.0405
	Cerebrum White	0.0139		Cerebrum White	0.0398
	Brainstem	0.0113		Brainstem	0.0342
	Cerebellum	0.008		Cerebellum	0.0282
min		**0.0080**	**min**		**0.0282**
max		**0.0201**	**max**		**0.0586**
difference		**0.0121**	**difference**		**0.0304**
Volunteer 7	Brainstem Midbrain	0.0179	**Volunteer 7**	Brainstem Midbrain	0.0428
	Corpus Callosum	0.0162		Corpus Callosum	0.0396
	Basal Ganglia	0.0156		Basal Ganglia	0.0355
	Cerebrum Gray	0.0147		Thalamus	0.0317
	Cerebrum White	0.0144		Cerebrum Gray	0.0316
	Thalamus	0.0139		Cerebrum White	0.0309
	Brainstem	0.0116		Brainstem	0.0259
	Cerebellum	0.0081		Cerebellum	0.0182
min		**0.0081**	**min**		**0.0182**

max		**0.0179**	**max**		**0.0428**
difference		**0.0098**	**difference**		**0.0246**
Volunteer 8	Corpus Callosum	0.0142	**Volunteer 8**	Brainstem Midbrain	0.0330
	Brainstem Midbrain	0.0134		Corpus Callosum	0.0327
	Thalamus	0.0124		Basal Ganglia	0.0284
	Cerebrum White	0.0122		Thalamus	0.0277
	Basal Ganglia	0.0117		Cerebrum Gray	0.0260
	Cerebrum Gray	0.0114		Cerebrum White	0.0259
	Brainstem	0.0082		Brainstem	0.0190
	Cerebellum	0.0068		Cerebellum	0.0137
min		**0.0068**	**min**		**0.0137**
max		**0.0142**	**max**		**0.0330**
difference		**0.0074**	**difference**		**0.0192**